Australian Centre for Advanced Photovoltaics

UNSW SYDNEY

Annual Report 2022

acap.org.au

Acknowledgements

Written and compiled by
Australian Centre for Advanced Photovoltaics

Edited by

Richard Corkish, Martin Green, Robert Largent

PP1: Kean Chern Fong, Moonyong Kim

PP2: Tian Zhang, Anthony Chesman, Jianjun Li, David Jones

PP3: Paul Shaw

PP4: Nathan Chang, Rong Deng

PP5: Anthony Chesman, Robert Largent, Richard Corkish

Photos, figures and graphs
Courtesy of Centre staff and students

Cover image

Dr Chandany Sen at the Loana Solar Cell Analysis System in the Solar Industrial Research Facility, UNSW

Contract Number - 2013/ASI015
Project title - UNSW, Photovoltaic Strategic Research Initiative, Australian Centre for Advanced Photovoltaics (ACAP) Project
Submission date (12 May 2023)

CRICOS Provider Code: 00098G

TABLE OF CONTENTS

ACAP
DIRECTOR'S REPORT

Solar photovoltaics involves the generation of electricity directly from sunlight when this light shines upon solar cells packaged into a solar module. Silicon is the most common material used to make these photovoltaic cells, similarly to its predominant role in microelectronics, although several other photovoltaic materials are being actively investigated.

Despite the ongoing impact of the Coronavirus pandemic, 2022 was another exciting year both for ACAP and the national and international photovoltaic industry. The pace of solar adoption accelerated with over 250 gigawatts of photovoltaic systems installed globally, the equivalent in capacity to 250 large nuclear or coal-fired plants. Australia reinforced its position as the largest user per capita, with over 25-gigawatts accumulated installations, the first country surpassing an installed capacity of 1,000 watts/capita. Solar's contribution to electricity generation in the Australian National Electricity Market and the South West Interconnected System increased to 14.7%, averaged over 2022.

The marked change in attitude to solar by international authorities, noted in the 2020 and 2021 reports, was reinforced by further support during 2022 for the role solar can play in climate change mitigation. The Intergovernmental Panel on Climate Change (IPCC) released a report in April 2022, titled Climate Change 2022: Mitigation of Climate Change, that included an overview of mitigation options and their estimated ranges of costs and potential for 2030 impact. Solar was found to provide the best option for large, near-term carbon emission reduction at zero or negative costs, closely followed by wind. These results have since been incorporated into the IPCC's sixth assessment report released in March 2023.

During the year, the Australian conceived and developed PERC technology, with PERC standing for "passivated emitter and rear cell", maintained its market dominance with circa 90% global market share. PERC's main contender is commonly known as TOPCon, an acronym for "tunnel-oxide passivated contact", an approach also first conceived and demonstrated at UNSW. TOPCon is also known as "PERT with passivated contact" (PERT/PC), where PERT is a PERC variant with the "T" representing the rear being totally diffused. Australia, through ACAP, is well positioned to accelerate the further development and commercialisation of these high-efficiency technologies; also to exploit the lower electricity costs so enabled.

This is the tenth annual ACAP report, with ACAP activities supported by the Australian Government through the Australian Renewable Energy Agency (ARENA). ACAP aims to significantly accelerate photovoltaic development by leveraging development of "over the horizon" photovoltaic technology, providing a pipeline of improved technology for increased performance and ongoing cost reduction. A second aim is to provide high quality training opportunities for the next generation of photovoltaic researchers, with one targeted outcome being to consolidate Australia's position as the photovoltaic research and educational hub of the Asia-Pacific manufacturing region. In achieving these aims, ACAP works with a wide range of both local and international partners.

In June 2022, the Australian Federal Minister for Climate Change and Energy, Chris Bowen, announced $45 million in funding to extend ACAP operations to 2030 "to help develop better and cheaper solar technologies that will help cut energy costs and reduce emissions". For this second, ACAP2.0 phase of activity, I will hand over ACAP Directorship to Professor Renate Egan, who has led activities at ACAP's UNSW node since 2015. In recognition of her outstanding contributions to solar research, industry development advocacy and communications, Renate was inducted into the "Australian Solar Hall of Fame" by the Smart Energy Council in 2022. She is an ATSE Fellow, the longstanding chair of the Australian PV Institute, the co-founder of Solar Analytics and has been recognised as one of the Eight Great Women in the Business of Science and Solar internationally by Renewable Energy World.

ACAP1.0 came into being on 1 February 2013 after the signing of a Head Agreement between the University of New South Wales (UNSW) and ARENA. During 2013, related Collaboration Agreements were signed between UNSW and the other ACAP nodes: Australian National University (ANU), University of Melbourne (UoM), Monash University, University of Queensland (UQ) and CSIRO (Manufacturing, Melbourne) and, additionally, with the ACAP industrial partners, Suntech Research and Development, Australia (SRDA) (partnership now transferred to Wuxi Suntech Power Co., Ltd.), Trina Solar Ltd, BlueScope Steel, PV Lighthouse and BT Imaging; subsequently with RayGen Resources Pty Ltd, Microsolar, SunDrive, Tindo Operations, 5B, Evolving Energy and Sun Cable. Our major international partners include the NSF-DOE Engineering Research Center for Quantum Energy and Sustainable Solar Technologies (QESST), based at Arizona State University, and the US National Renewable Energy Laboratory (NREL), as well as the Molecular Foundry, Berkeley, Stanford University, the Korean Green Energy Institute and the University of Sydney. For ACAP2.0, the University of Sydney and CSIRO (Energy Centre, Newcastle) will be integrated as ACAP nodes.

This report covers the period from 1 January to 31 December 2022. Over its first ten years, ACAP has moved effectively to establish a high profile within the international research community. This is evidenced by the string of independently confirmed world records for energy conversion efficiency in efforts led by different nodes and for several different technologies since ACAP's commencement. These include records for rear-junction silicon cells (ANU: 24.4%, 2013), overall sunlight to electricity conversion (UNSW: 40.4%, 2014; 40.6%, 2016), one-sun mini-module (UNSW: 34.5%, 2016), small-area "thin-film" CZTS (Cu_2ZnSnS_4) cells (UNSW: 9.5%, 2016; 11.0%, 2017), for >1 cm² CZTS cells (UNSW: 10.0%, 2017), perovskite mini-modules (UNSW: 11.5%,

2016), for >1 cm² perovskite cells (UNSW: 18.0%, 2016; 19.6%, 2017; ANU: 21.6%, 2019; 22.6%, 2020) and for III-V tandem cells (NREL/UNSW: 32.9%, 2021). In 2022, SunDrive, an ACAP Industrial Partner comprised mostly of UNSW node graduates, achieved a world record 25.54% efficiency for commercial sized M6 HJT cells.

This tradition of international impact was continued into 2022 with key developments during the year summarised in the highlight pages immediately following this report. Particularly significant was the continued high level of recognition of ACAP's impact through major local and international awards.

Associate Professor Brett Hallam from the UNSW node was awarded the 2022 Prime Minister's Prize for New Innovators for his work in commercialising innovative technology that has greatly improved the performance of solar cells. His discoveries have resulted in a 10% increase in the efficiency of solar cells, representing a significant achievement in the field. The Prime Minister's Prize for New Innovators recognises outstanding achievements in the field of innovation, particularly in the commercialisation of research. Associate Professor Hallam's work represents an important contribution to the ongoing development and adoption of solar energy technologies, and his recognition as a prize winner highlights the importance of continued investment in renewable energy research and development.

Professors Xiaojing Hao (UNSW node) and Kylie Catchpole (ANU node) have been inducted as Fellows of the Australian Academy of Technological Sciences and Engineering (ATSE) in recognition of achievements for individuals who have made significant contributions to technological sciences and engineering. Fellows of the ATSE are recognised for their excellence in their respective fields and for their significant impact on industry, government and academia. As Fellows, they will provide strategic advice and engage in discussions on how technological sciences and engineering can be used to address Australia's most pressing challenges.

Dr AnYao Liu (ANU node) has been awarded the prestigious Ulrich Gösele Young Scientist Award for her groundbreaking work on improving the efficiency of silicon solar cells. The prestigious award pays tribute to the late Professor Gösele, who was one of the two founders of the Max Planck Institute for Microstructure Physics and acknowledges the exceptional research achievements of young scientists who are making significant contributions to the field of silicon research. Dr Liu's research has focused on using deposited thin films and high temperature processes to remove metallic impurities from silicon solar cells, a process known as impurity gettering. By removing these impurities, the efficiency of the cells can be increased, making solar electricity more cost-effective.

Dr Nguyen Trong Hieu (ANU node), was among ten outstanding young people honoured at a ceremony held by the Ho Chi Minh Communist Youth Union (HCYU) Central Committee in March 2022. The Vietnam Young Talent Fund organised the ceremony in Hanoi, which was attended by President Nguyen Xuan Phuc. From 138 candidates, Dr Hieu was chosen for his achievements in scientific research. The committee recognised his excellent performance in this area, along with nine other exceptional young talents, who were selected for their contributions to various fields such as sports, culture, art and social activities. Dr Hieu has made impressive contributions to the development of advanced characterisation techniques for photovoltaic devices.

I personally was delighted to be awarded, in April 2022 in the presence of the Emperor and Empress, the 2021 Japan Prize in the category of Resources, Energy, Environment, Social Infrastructure in recognition of my more than four decades of research at UNSW. In October 2022, I was similarly delighted to be awarded the 2022 Millennium Technology Prize in Helsinki, considered to be one of the world's most prestigious science and technology prizes, by the President of Finland for my conception and leadership in the development of the Passivated Emitter and Rear Cell (PERC).

The work resulting in these outcomes and many more high quality results are described in the body of this 2022 Annual Report and contributed to making 2022, once again, an extremely successful year for ACAP.

I would like to thank ARENA for its ongoing financial support and also for the very effective involvement of ARENA personnel in supporting the ACAP program, both informally and via the ACAP National Steering Committee and the International Advisory Committee. I would additionally like to thank, in particular, all researchers affiliated with ACAP for their contributions to the broad range of progress reported in the following pages.

Finally, I am pleased to be able to report that ACAP has taken another major step towards attaining its significant long-term objectives by achieving its key tenth-year milestones. I look forward to seeing similar progress in 2023 and subsequent years, albeit more from the sideline.

SCIENTIA PROFESSOR MARTIN GREEN

Director, ACAP

2022
HIGHLIGHTS

HIGH IMPACT PAPERS

Papers published under the ACAP program since ACAP's formation in 2013 have already been recognised as making a large impact at the international level. A total of 79 of these have been classified as "Highly Cited Papers", based on their ranking within the top 1% in their field. Nearly half of these, 36 in total, earned the additional distinction of being identified as "Hot Papers", within the top 0.1% in their field. This is a disproportionately high number relative to the total number of ACAP publications and reflects the impact and high international standing of ACAP research.

Eleven additional papers have been recognised as "Highly Cited Papers" with two, the first two listed below, of these additionally being identified as "Hot Papers", within the top 0.1% in the field.

- Gharibzadeh, S., Fassl, P., Hossain, I. M., Rohrbeck, P., Frericks, M., Schmidt, M., Duong, T., Khan, M. R., Abzieher, T., Nejand, B. A., Schackmar, F., Almora, O., Feeney, T., Singh, R., Fuchs, D., Lemmer, U., Hofmann, J. P., Weber, S. A. L. & Paetzold, U. W. (2021). Two birds with one stone: dual grain-boundary and interface passivation enables > 22% efficient inverted methylammonium-free perovskite solar cells. *Energy & Environmental Science* 14, 5875-5893.
- Hu, L., Zhao, Q., Huang, S. J., Zheng, J. H., Guan, X. W., Patterson, R., Kim, J., Shi, L., Lin, C. H., Lei, Q., Chu, D. W., Tao, W., Cheong, S. S., Tilley, R. D., Ho-Baillie, A. W. Y., Luther, J. M., Yuan, J. Y. & Wu, T. (2021). Flexible and efficient perovskite quantum dot solar cells via hybrid interfacial architecture. *Nature Communications* 12.
- Ballif, C., Haug, F. J., Boccard, M., Verlinden, P. J. & Hahn, G. (2022). Status and perspectives of crystalline silicon photovoltaics in research and industry. *Nature Reviews Materials* 7, 597-616.
- Chang, L. C., Sheng, M., Duan, L. P. & Uddin, A. (2021). Ternary organic solar cells based on non-fullerene acceptors: A review. *Organic Electronics* 90.
- Gan, Z. X., Cheng, Y. C., Chen, W. J., Loh, K. P., Jia, B. H. & Wen, X. M. (2021). Photophysics of 2D Organic-Inorganic Hybrid Lead Halide Perovskites: Progress, Debates, and Challenges. *Advanced Science* 8.
- Green, M. A., Dunlop, E. D., Hohl-Ebinger, J., Yoshita, M., Kopidakis, N., Bothe, K., Hinken, D., Rauer, M. & Hao, X. J. (2022). Solar cell efficiency tables (Version 60). *Progress in Photovoltaics* 30, 687-701.
- Li, W., Rothmann, M. U., Zhu, Y., Chen, W. J., Yang, C. Q., Yuan, Y. B., Choo, Y. Y., Wen, X. M., Cheng, Y. B., Bach, U. & Etheridge, J. (2021). The critical role of composition-dependent intragrain planar defects in the performance of MA(1)(-)(x)FA(x)PbI(3) perovskite solar cells. *Nature Energy* 6, 624-632.
- Peng, J., Kremer, F., Walter, D., Wu, Y. L., Ji, Y., Xiang, J., Liu, W. Z., Duong, T., Shen, H. P., Lu, T., Brink, F., Zhong, D. Y., Li, L., Lem, O. L. C., Liu, Y., Weber, K. J., White, T. P. & Catchpole, K. R. (2022). Centimetre-scale perovskite solar cells with fill factors of more than 86 per cent. *Nature* 601, 573.
- Xi, F. S., Li, S. Y., Ma, W. H., Chen, Z. J., Wei, K. X. & Wu, J. J. (2021). A review of hydrometallurgy techniques for the removal of impurities from metallurgical-grade silicon. *Hydrometallurgy* 201.
- Xue, J. J., Wang, R., Chen, X. H., Yao, C. L., Jin, X. Y., Wang, K. L., Huang, W. C., Huang, T. Y., Zhao, Y. P., Zhai, Y. X., Meng, D., Tan, S., Liu, R. Z., Wang, Z. K., Zhu, C. H., Zhu, K., Beard, M. C., Yan, Y. F. & Yang, Y. (2021). Reconfiguring the band-edge states of photovoltaic perovskites by conjugated organic cations. *Science* 371, 636.
- Zhu, C., Meng, L., Zhang, J. Y., Qin, S. C., Lai, W. B., Qiu, B. B., Yuan, J., Wan, Y., Huang, W. C. & Li, Y. F. (2021). A Quinoxaline-Based D-A Copolymer Donor Achieving 17.62% Efficiency of Organic Solar Cells. *Advanced Materials* 33.

A set of 2022 papers was selected as sufficiently timely and interesting to provide the cover illustration for some of the field's most prestigious journals. One article, from the CSIRO node team, led by Fei Zheng, reported that Brownian tree-shaped dendrites found in quasi-2D perovskite films are beneficial to cell performance. (Zheng, F., Angmo, D., Hall, C. R., Rubanov, S., Yuan, F., Laird, J. S., Gao, M., Smith, T. A. & Ghiggino, K. P. (2022). Brownian Tree-Shaped Dendrites in Quasi-2D Perovskite Films and Their Impact on Photovoltaic Performance (Adv. Mater. Interfaces 13/2022). Advanced Materials Interfaces 9, 2270071 (Figure 2.1(a).)

In another, (Figure 2.1(b)) an ANU PhD student Mike Tebyetekerwa, Dr Hieu Nguyen (ANU) and Dr Jian Zhang (Shenzhen University), reported the introduction of chromium germanium telluride quantum dots (CGT QDs) beneath the transition metal dichalcogenides (TMDs) to control light-matter interactions in their heterostructures, depending on the QDs thickness. With CGT QDs (either high or low density), the researchers could simultaneously control the photoluminescence emission and electronic properties of monolayer TMDs. The paper was selected as a cover of Journal of Colloid and Interface Science. (Zhang, J., Tebyetekerwa, M. & Nguyen, H. T. (2022). Interfacing transition metal dichalcogenides with chromium germanium telluride quantum dots for controllable light-matter interactions. Journal of Colloid and Interface Science 611, 432-440.)

Another from a CSIRO team led by Leonard W. T. NG, described new organic photovoltaics with non-fullerene acceptors (NFAs) that have enabled a new breakthrough photovoltaic conversion efficiency approaching 20%, close to that of perovskites. (NG, L. W. T., Lee, S. W., Chang, D. W., Hodgkiss, J. M. & Vak, D. (2022). Organic Photovoltaics' New Renaissance: Advances Toward Roll-to-Roll Manufacturing of Non-Fullerene Acceptor Organic Photovoltaics (Adv. Mater. Technol. 10/2022). Advanced Materials Technologies 7, 2270066) (Figure 2.1(c).)

A fourth cover, celebrating a paper from UNSW led by Dr Germain Rey, presented a method to extend photoluminescence (PL) imaging to field-deployed solar modules in full sunlight. The method takes advantage of sunlight absorption in the Earth's atmosphere in a narrow spectral range and recent developments in ultra-narrow bandpass optical filter technology. The method lays the foundations for PL imaging, a powerful inspection method for the PV industry and research, to be applied to routine high-volume inspection of PV modules on large-scale solar power plants. (Rey, G., Kunz, O., Green, M. & Trupke, T. (2022). Luminescence imaging of solar modules in full sunlight using ultranarrow bandpass filters. Progress in Photovoltaics: Research and Applications 30, 1115-1121) (Figure 2.1(d)).

Shuai Nie et al. from UNSW had a cover (Figure 2.1(e)) for their work on photoluminescence imaging, which is a powerful inspection technique for research laboratories and photovoltaic production lines. They presented an imaging system that is not affected by two common limitations: (a) due to the non-uniformities of the measured samples, the acquired images are affected by lateral carrier flow, resulting in inaccurate lifetime analysis and image blurring; (b) samples' non-uniformities are measured at locally different injection levels. (Nie, S., Zhu, Y., Kunz, O., Trupke, T. & Hameiri, Z. (2022). Advanced photoluminescence imaging using non-uniform excitation. Progress in Photovoltaics: Research and Applications 30, 349-359.)

A sixth cover illustrated the work of Dongchen Lan and Martin Green from the UNSW node shown in Figure 2.1(f) reporting on "Combatting temperature and reverse-bias challenges facing perovskite solar cells" in Joule 6(8), 1782-1797.

(e) Figure 2.1 (a–f): Cover illustrations for ACAP publication in some of the field's most prestigious journals.

MINISTER CHRIS BOWEN ANNONCES $45 MILLION IN FUNDING FOR ACAP

Figure 2.2: Minister for Climate Change and Energy Chris Bowen announced $45 million in new funding for ACAP.

The Australian Centre for Advanced Photovoltaics (ACAP) has been awarded a $45 million grant by the Australian Government to fund its groundbreaking solar photovoltaic (PV) research until 2030. ACAP comprises research groups from several Australian universities, commercial entities, the CSIRO and international partners. The funding will keep Australia at the forefront of innovation in solar PV. The research program aims to develop "over the horizon" PV technology to create a pipeline of improved technology for increased performance and ongoing cost reduction, supporting the ARENA goal of achieving 30% solar PV cell efficiency and reducing the cost of installation of solar modules to 30 cents a watt by 2030.

ACAP's research also supports ARENA's focus on supporting ultra-low-cost generation, which is aimed at realising the opportunity for further step-change innovation in PV. ACAP has a strong track record of industry partnerships, which has led to the spin-out of Australian companies such as Open Instruments, Solar Visionand SunDrive. The funding will ensure that ACAP remains one of the world's top research centres for innovation in solar energy and solar PV technology, helping to underpin education and training, and keep Australia at the forefront of the PV industry well into the future.

SCIENTIA PROFESSOR MARTIN GREEN AWARDED THE MILLENNIUM TECHONOLGY PRIZE

Figure 2.3: Scientia Professor Martin Green (left) receiving the Millennium Technology Prize from the President of the Republic of Finland, Sauli Niinistö (right).

Scientia Professor Martin Green has been awarded the 2022 Millennium Technology Prize for his leadership in the development of the Passivated Emitter and Rear Cell (PERC) – the world's most commercially viable and efficient silicon solar cell technology. The Prize, presented by Technology Academy Finland, highlights the impact of science and innovation on society and is considered to be one of the most prestigious science and technology prizes in the world. The President of Finland Sauli Niinistö, conferred the prize upon Professor Green at a ceremony in Helsinki.

Professor Green's work has resulted in a significant transformation of the global energy sector and has accelerated the fight against climate change. The development of the PERC technology has helped increase the conversion efficiency of commercial solar cells by over 50% in relative terms from 16.5% in the early 1980s to 25% in the early 2000s. As a result, PERC cells currently account for over 91% of the worldwide production of silicon solar modules. Solar energy is now considered instrumental in the global transition to renewable energy and decarbonisation.

In his acceptance speech, Professor Green said that the Millennium Technology Prize not only recognises his contribution to photovoltaics, but also the achievements of his students and research colleagues at the University of New South Wales and ACAP, as well as those of the broader photovoltaic research and commercial community. He stated that the pace of change is accelerating, that the world will shift to solar and wind energy over the coming decade and that a huge transformation of historic significance is underway.

Professor Green and his teams at UNSW and ACAP are now working on combining cell technologies to reach 40% solar cell efficiency by exploring options such as stacking cells on top of each other. He noted that solar cells are increasingly being used to replace large power stations that use fossil fuels. In 2021, 20 countries or regions, including Australia, Chile, Germany, Greece, Italy, Netherlands, Spain, Vietnam and California, generated between 8% and 25% of their total electricity supply from solar energy.

The Millennium Technology Prize produced a video featuring Professor Green which can be viewed at the following url:

Passivated Emitter and Rear Cell (PERC) – Winner innovation of the 2022 Millennium Technology Prize

https://youtu.be/WzgJfXPKcYQ

SCIENTIA PROFESSOR MARTIN GREEN RECEIVES THE WCPEC AWARD

Figure 2.4: Professor Green receiving the 2022 WCPEC Award from conference chair, Dr Alessandra Scognamiglio (right).

The 2022 WCPEC Award was presented to Scientia Professor Martin Green. The WCPEC Award is a recognition given to exceptional individuals who have contributed significantly to the advancement of photovoltaic science and technology. This award is presented every four years during the World Conference on Photovoltaic Energy Conversion, a major event that brings together the three main conferences in the field.

The WCPEC committee stated that Professor Green has made outstanding, internationally recognised contributions to the development of photovoltaics. One of his major contributions is the development of PERC cells, which are now widely used in the PV industry. He also co-invented "buried-contact" cells with his colleague Professor Stuart Wenham, which were the most efficient commercially available solar cells for most of the 1990s. Professor Green has continuously worked to improve the efficiency of silicon cells, achieving a >50% increase since 1983, from 16.5% to 25%, through 18 successive improvements.

In addition to his contributions to PV device development, Professor Green has also played a significant role in the development of the PV industry and sector. He established Asian manufacturing by training scientists and engineers, which triggered dramatic cost reductions in the last decade. Professor Green has also provided important leadership in the field by sharing his vision for the development of PV and the global PV sector through his textbooks and by establishing the world's first undergraduate degree in PV Engineering in 2000 and by establishing the UNSW School of Photovoltaic and Renewable Energy Engineering.

Professor Green received the WCPEC Award for his exceptional contributions to photovoltaic science and technology, his leadership, and his vision for the future of the global PV sector.

Further information about the prize can be found at the following url:

WCPEC Award Winner!

https://www.wcpec-8.com/index.php/programme-2022-1/prizesawards-2022-1?view=article&id=107&catid=15

ASSOCIATE PROFESSOR BRETT HALLAM AWARDED THE PRIME MINISTER'S PRIZE FOR SCIENCE

Figure 2.5: Professor Brett Hallam received the Prime Minister's Prize for New Innovators.

Associate Professor Brett Hallam from the University of New South Wales (UNSW) and ACAP has won the 2022 Prime Minister's Prize for New Innovators for his work in commercialising innovative technology that has greatly improved the performance of solar cells. His discoveries have resulted in a 10% increase in the efficiency of solar cells, representing a significant achievement in the field.

The technologies founded by Associate Professor Hallam have also provided benefits to Australian consumers of around $500 million in 2021 alone, while the global benefits were estimated at $17 billion. These figures are expected to continue increasing as the solar industry continues to expand.

Associate Professor Hallam's research has played a crucial role in boosting the performance of the global energy economy by making solar energy more efficient and cost-effective. His work has contributed to the growing momentum towards renewable energy sources and reducing reliance on fossil fuels.

The Prime Minister's Prize for New Innovators recognises outstanding achievements in the field of innovation, particularly in the commercialisation of research. Associate Professor Hallam's work represents an important contribution to the ongoing development and adoption of solar energy technologies, and his recognition as a prize winner highlights the importance of continued investment in renewable energy research and development.

Further information about the prize can be found at the following url:

PM's 2022 Prize for New Innovators

https://www.industry.gov.au/publications/prime-ministers-prizes-science-2022/2022-prize-new-innovators

PROFESSOR XIAOJING HAO & PROFESSOR KYLIE CATCHPOLE BECOME ATSE FELLOWS

Figure 2.6: Professor Xiaojing Hao FTSE (left) and Professor Kylie Catchpole FTSE (right) inducted as Fellows of the Australian Academy of Technological Science and Engineering.

Professor Xiaojing Hao (UNSW) and Professor Kylie Catchpole (ANU) have been inducted as Fellows of the Australian Academy of Technological Sciences and Engineering (ATSE) in recognition of achievements for individuals who have made significant contributions to technological sciences and engineering. Fellows of the ATSE are recognised for their excellence in their respective fields and for their significant impact on industry, government and academia. As Fellows, they will provide strategic advice and engage in discussions on how technological sciences and engineering can be used to address Australia's most pressing challenges.

Professor Xiaojing Hao FTSE is a world-renowned expert in solar technology and has made significant contributions to the field. She has helped establish Australia's global leadership in solar energy through her pioneering research in thin-film solar cells using kesterite materials. Her innovative work has set five world records for solar cell efficiency and has been instrumental in the development of new materials for solar energy conversion. Professor Hao's research has the potential to provide a cost-effective solution for large-scale solar energy deployment in regions where silicon-based solar panels are not practical.

Professor Kylie Catchpole FTSE is a global expert in solar energy, and her contributions to the field have been recognised internationally. Her pioneering work in increasing the efficiency of solar cells and solar hydrogen technology has led to significant breakthroughs in the field. Professor Catchpole has led teams that have achieved world record solar cell efficiencies and has played a significant role in shaping Australia's hydrogen strategy. Her work in solar hydrogen technology was named a top 10 innovation in 2020 by the Japanese Government's Innovations for a Cool Earth Forum, further highlighting the significant impact of her research. Professor Catchpole's contributions to the field of solar energy have the potential to provide a sustainable and cost-effective solution to meet the world's growing energy demands while reducing carbon emissions.

Further information can be found at the following urls:

Xiaojing Hao FTSE – https://www.atse.org.au/our-fellows/2022-new-fellows/Xiaojing-Hao-ftse/

Kylie Catchpole FTSE – https://www.atse.org.au/our-fellows/2022-new-fellows/kylie-catchpole-ftse/

DR ANYAO LIU AWARDED THE ULRICH GOSELE YOUNG SCIENTIST AWARD

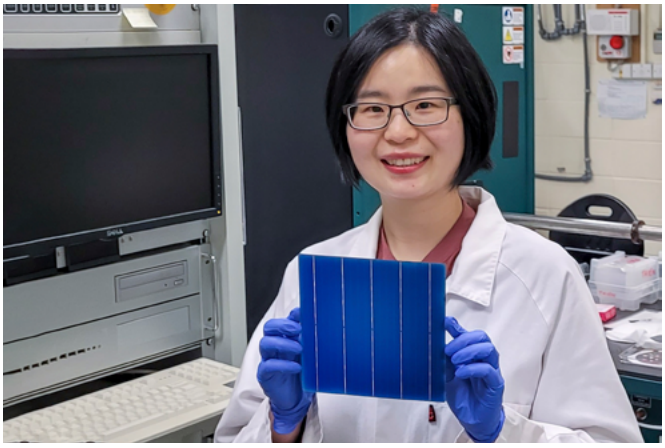

Figure 2.7: Dr AnYao Liu, shown in her lab, has received the Ulrich Gösele Young Scientist Award.

Dr AnYao Liu (ANU) has been awarded the prestigious Ulrich Gösele Young Scientist Award for her groundbreaking work on improving the efficiency of silicon solar cells.

The prestigious award pays tribute to the late Professor Gösele, who was one of the two founders of the Max Planck Institute for Microstructure Physics and acknowledges the exceptional research achievements of young scientists who are making significant contributions to the field of silicon research.

One of the main challenges of silicon solar cells is the presence of impurities, such as metallic elements, which can reduce the efficiency of the cells and increase the cost of solar electricity. Dr Liu's research has focused on using deposited thin films and high temperature processes to remove metallic impurities from silicon solar cells, a process known as impurity gettering. By removing these impurities, the efficiency of the cells can be increased, making solar electricity more cost-effective.

Her work has contributed significantly to the field of silicon research and has the potential to make solar energy more accessible and cost-effective.

Further information can be found at the following url:

Dr Liu awarded for her ground-breaking research in solar cell technologies – https://cecc.anu.edu.au/news/dr-liu-awarded-her-ground-breaking-research-solar-cell-technologies

DR HIEU NGUYEN RECEIVES VIETNAM'S TEN OUTSTANDING YOUNG FACES AWARD

Figure 2.8: Top: Image of Dr Hieu Nguyen shown during Vietnam's "ten outstanding young people" ceremony. Bottom: Dr Hieu Nguyen in his lab.

Dr Dr Hieu Nguyen (ANU), was among ten outstanding young people honoured at a ceremony held by the Ho Chi Minh Communist Youth Union (HCYU) Central Committee in March 2022. The Vietnam Young Talent Fund organised the ceremony in Hanoi, which was attended by President Nguyen Xuan Phuc.

Out of 138 candidates, Dr Nguyen was chosen for his achievements in scientific research. The committee recognised his excellent performance in this area, along with nine other exceptional young talents, who were selected for their contributions to various fields such as sports, culture, art and social activities.

During the ceremony, President Phuc commended the HCYU for identifying and nurturing young talents through effective activities like the Vietnam Outstanding Young Face Award. He emphasised the government's commitment to developing high quality human resources and attracting talents to contribute to national development and defence.

President Phuc also expressed that more talented individuals will be developed among Vietnamese youth, and that they will continue to make significant contributions to the nation and the community. Dr Nguyen's recognition as an outstanding young talent is seen as a testament to the potential and abilities of young Vietnamese researchers and their promising future in the field of scientific research.

Further information can be found at the following url:

Outstanding young faces in Vietnam honoured for 2021 – https://en.vietnamplus.vn/outstanding-young-faces-in-vietnam-honoured-for-2021/235139.vnp

SCIENTIA PROFESSOR MARTIN GREEN RECEIVES THE JAPAN PRIZE (COVID DELAYED)

Figure 2.9: Professor Martin Green (left) and the Emperor and Empress of Japan (right) at his Japan Prize Ceremony.

Australian Scientia Professor Martin Green has been awarded the 2021 Japan Prize in the field of "Resources, Energy, Environment, Social Infrastructure" for his groundbreaking work in the field of photovoltaics. The prize, which recognises scientific contributions to the fields of science and technology worldwide, is one of the world's most prestigious awards. Professor Green's work has led to significant advances in photovoltaic technology, which now contributes to global decarbonisation efforts. His record-breaking achievements, including the invention of the PERC solar cell, have led to enormous reductions in the costs of photovoltaic solar systems.

The Japan Prize Foundation awards a monetary prize along with a diploma and commemorative medal to each laureate. Although awarded in 2021, the ceremony was delayed due to COVID-19 travel restrictions and was held in 2022, officiated by the Emperor and Empress of Japan.

POFESSOR THORSTEN TRUPKE RECEIVES 2021 IEEE WILLIAM R. CHERRY AWARD (COVID DELAYED)

Figure 2.10: Professor Thorsten Trupke receiving the 2021 IEEE William R. Cherry Award.

In 2022, Professor Thorsten Trupke was officially presented with the 2021 IEEE William R. Cherry Award, an honour given to individuals who have devoted their professional lives to the advancement of the science and technology of photovoltaic energy conversion. The ceremony had been delayed due to travel restrictions caused by the COVID-19 pandemic.

Professor Trupke's pioneering work in photovoltaics as a semiconductor scientist led to the development of photoluminescence (PL) imaging technology. This breakthrough innovation has allowed for the quick detection of hidden faults and defects in wafers, solar cells and modules without the need for electrical connection. The technology has now been universally adopted in the PV manufacturing industry, serving as an essential diagnostic and production tool.

The impact of Professor Trupke's work is immense. The use of PL imaging has not only improved the efficiency and reliability of PV technology, but it has also helped to reduce manufacturing costs and waste. Through his dedication and commitment to the field, Professor Trupke has not only made significant contributions to photovoltaic energy conversion but also to sustainable energy production as a whole.

Further information can be found at the following url:

https://ieee-pvsc.org/PVSC48/awards-cherry.php

POFESSOR RENATE EGAN INDUCTED INTO THE SMART ENERGY COUNCIL AUSTRALIAN SOLAR HALL OF FAME

Figure 2.11: Professor Renate Egan was added into the Smart Energy Council's Australian Solar Hall of Fame.

In recognition of her outstanding contributions to solar research, industry development advocacy and communications, Professor Renate Egan was added to the "Australian Solar Hall of Fame" by the Smart Energy Council in 2022.

Professor Egan, the leader of ACAP's UNSW node, has career-long accomplishments that have led to her induction into the Solar Hall of Fame.

Renate is an ATSE Fellow, the current secretary of the Australian PV Institute, the co-founder of Solar Analytics and has been recognised as one of the Eight Great Women in the Business of Science and Solar internationally by Renewable Energy World.

Through her involvement as Director and CTO of CSG Solar AG and Managing Director of Suntech R&D Australia, she was responsible for the development of energy technologies in Australia, Germany and China. Professor Egan is considered to be a leading authority on manufacturing, costing and technology transfer.

VISITORS AND TOURS

Figure 2.12: Top: Alice Lang from 5B giving one of the presentations to the Diplomatic Community. Bottom: Professor Bram Hoex speaking about the Atomic Layer Deposition system in SIRF.

18 May 2022

Event for the Sydney Diplomatic Community: The Department of Foreign Affairs and Trade (DFAT) requested UNSW to host a visit to the School of Photovoltaics and Renewable Energy (SPREE), inviting the diplomatic community to see the cutting-edge photovoltaic technology developed through the SPREE and ACAP. The objective was to let governments know about PV technology and its potential to help address the world's growing energy demands.

The DFAT-invited diplomatic community consisted of several Consul-Generals, including those from Singapore, France, the United Kingdom, Spain, Germany, the United States, India, Indonesia, Japan and Canada. The visit included presentations by ACAP members, including Professors Alistair Sproul, Renate Egan and Bram Hoex. They discussed Australia's role in the development of photovoltaic technology, the latest technology developments and how PV can help reduce carbon emissions and promote sustainable energy.

In addition to the presentations by the ACAP team, Mr David Griffin, Founder and CEO of Sun Cable, presented on his company's project to supply solar electricity to Singapore, and Alison Lang from 5B presented on rapid-deployment PV technology for solar farms.

The visit presented an opportunity to exhibit the latest advancements in photovoltaic technology to the diplomatic community, highlighting PV's technical capabilities and feasibility.

Additionally, it served as a platform to introduce the diplomatic community to ACAP partners participating in future and current sustainable energy solutions as with Sun Cable's "This is what we plan to do" and 5B's "This is how we do it".

Figure 2.13: Bottom left image (L to R): Hon. Chris Bowen MP, Hon Raj Kumar Singh (India) and Professor Martin Green in the SIRF.

13 July 2022

Ministers from Australia and India: The Minister for Climate Change and Energy, Chris Bowen, with Indian Minister of Power and Indian Minister of New and Renewable Energy, Raj Kumar Singh and Hon. Matt Thistlethwaite, MP visited the Solar Industrial Research Facility (SIRF) at UNSW.

During the visit, the ministers were shown advanced solar technology at the facility. Minister Singh expressed India's interest in developing a partnership with the university to embrace solar technology. Minister Bowen highlighted that both India and Australia have incredible potential to be big global players in solar and clean energy technologies.

Figure 2.14: Top: (L to R) Professor Renate Egan, Dr Edwin Schlossberg, Professor Martin Green, Ambassador Caroline Kennedy, Professor Alistair Sproul and Professor Attila Brungs at the Solar Industrial Research Facility.

16 August 2022

US Ambassador Caroline Kennedy visited the Solar Industrial Research Facility with Professor Martin Green speaking with her about the latest advances in solar energy technology and how the SIRF is a world-class photovoltaic pilot line manufacturing facility that enables the development of silicon solar cell technologies from laboratory processes to factory-ready industrial processes. Ambassador Kennedy saw innovative research being conducted at the facility and heard about how Australian-designed solar technology is already providing clean, sustainable energy around the world.

In discussions, it was noted that both Australia and the United States are committed to reducing greenhouse gas emissions by transitioning to renewable energy sources and that over 90% of commercial silicon solar cells use technology that was designed at UNSW.

Figure 2.15: Top: (L to R): Dr Henner Kampwerth (UNSW), Dr Oliver Kuntz (UNSW), Mr Reinhard Bütikofer MEP and Professor Renate Egan (UNSW) during a tour and discussion at the Solar Industrial Research Facility.

19 August 2022

Mr Reinhard Bütikofer MEP visited Australia as part of the Australian Government's Special Visits Program (SVP), which hosts influential figures who are relevant to Australian foreign policy interests. As a member of the European Parliament for the German Green party and co-Chair of the European Green Party, Mr Bütikofer has a keen interest in the climate agenda.

During his visit, one of the key objectives was to promote the understanding of Australia's policies on climate change, clean energy transition and the environment, as well as the actions taken by businesses in Australia. This was aimed at increasing European/German cooperation with Australia as well as raising awareness of Australia's value as a partner in the transition to net-zero emissions.

Professor Renata Egan led the tour showing Mr Bütikofer the Solar Industrial Research Facility and highlighted equipment developed by BT Imaging, a spin-off company that developed and manufactures commercial photoluminescence (PL) PV imaging systems.

Figure 2.16: (Top) Professor Martin Green (left) showing the European Parliamentary Delegation BT Imaging's M1 photoluminescence module tester and (bottom) showing silicon cells.

20 September 2022

European Union: UNSW ACAP hosted a delegation from the European Union Parliament, which included representatives from Germany, Sweden, Ireland, Portugal, Belgium, Italy and Czechia. The group consisted of 17 EU members and was led by Professor Martin Green, who provided a tour of the Solar Industrial Research Facility, showcasing the manufacturing and testing equipment used for solar cells. During their visit, the delegates engaged in discussions on renewable energy, CO_2 reduction, energy security and battery storage.

CONFERENCE AWARDS

49th IEEE PHOTOVOLTAIC SPECIALIST CONFERENCE

Figure 2.17: Zubair Abdullah-Vetter was awarded the Best Poster Award at the 49th IEEE PVSC.

Zubair Abdullah-Vetter (UNSW) received the Best Poster Award at the 49th IEEE Photovoltaics Specialist Conference for his work "Using machine learning to predict the complete degradation of accelerated damp heat testing in just 10% of testing time" – Area 8: PV Materials and Module Durability and Accelerated Testing Methods.

7 June 2022

8th WORLD CONFERENCE ON PHOTOVOLTAIC ENERGY

Figure 2.18: Shuai Nie was awarded a Student Award at WCPEC-8.

Shuai Nie (UNSW) received a Student Award at WCPEC-8 for her work "Photoluminescence Imaging Using Non-Uniform Excitation: Recent Progress".

WCPEC Student Awards were delivered in recognition of the most remarkable and outstanding research work in the field of PV.

30 September 2022

BORLAND FORUM 2022

Figure 2.19: Luke Sutherland (right) receiving the 2022 Borland award for his presentation on efficient production of Perovskite Solar Cells.

Luke Sutherland (Monash) was presented with the 2022 Borland Award as best speaker for his presentation "Highly Efficient and Roll-To-Roll Processable Perovskite Solar Cells Incorporating Printed Electrodes."

At the Borland Forum, outstanding postgraduate students who have been selected by their tertiary institutions present their materials-related research projects through short presentations. The 2022 event had presentations delivered by students from the University of Melbourne, Swinburne University of Technology, Monash University, Deakin University and RMIT University.

October 2022

INTERNATIONAL PHOTOVOLTAIC SCIENCE AND ENGINEERING CONFERENCE – 33

Figure 2.20: Yiyu (Felix) Zeng was awarded a Poster Award at PVSEC-33.

Yiyu (Felix) Zeng (UNSW) received a Poster Award at PVSEC-33, Nagoya for his work "Comparative durability study of commercial inner-pore antireflection coatings and alternative dense coatings", in Area 2: Advanced Application and core technologies for massive installation.

17 November 2022

ACAP ANNUAL CONFERENCE 2022

Figure 2.21: Jiali Wang was awarded Best Oral Presentation at the ACAP Annual Conference.

Jiali Wang – Received the ACAP Award for best oral presentation: "Inkjet printing for boron-doped polycrystalline silicon passivating contacts".

1 December 2022

Figure 2.22: Luke Sutherland received the award for Best Poster Presentation at the ACAP Annual Conference.

Luke Sutherland received the ACAP award for Best Poster Presentation: "R2R Perovskite Solar Cells With Solvent-free Printed Electrodes"

1 December 2022

ASIA-PACIFIC SOLAR RESEARCH CONFERENCE 2022

Philipe Gunawan received the Wal Read Memorial Award for best student oral presentation:

"Hybrid PV-CSP for heat and hydrogen production: Study case iron-making industry"

1 December 2022

Shayan Naderi received the John Ballinger Prize for best student buildings-related oral presentation:

"Solar pre-cooling with different tariff structures and household time of use patterns"

1 December 2022

Ashleigh Nicholls received the Muriel Watt Prize for best female student oral presentation:

"Opportunities for flexible resources to improve transmission utilisation in Renewable Energy Zones"

1 December 2022

Figure 2.23: Ning Song received the Energy Advances Award at the APSRC 2022.

Ning Song received the Energy Advances Award for Outstanding Poster in PV Device Research:

"Multifunctional multilayer antireflection coatings for solar module glass"

1 December 2022

Figure 2.24: Grace Dansoa Tabi received the Monica Oliphant award at the APSRC 2022.

Grace Dansoa Tabi received the Monica Oliphant Prize for best female student poster:

"Simulation of nanohole point contacts for perovskite solar cells with insulating passivation layers"

1 December 2022

Guoliang Wang received the Wal Read Memorial Award for best student poster:

"Hole-selective contact engineering for perovskite single-junction and tandem solar cell"

1 December 2022

AUCAOS SYMPOSIUM 2022

The Australasian Community for Advanced Organic Semiconductors (AUCAOS) Symposium (ACAP is a Platinum Sponsor) convened the organic semiconductor research community of Australia and New Zealand, providing a platform to discuss the latest advancements in computation/theory, the chemistry of novel materials, including processing, film morphology, and spectroscopy, along with device physics, and device fabrication/manufacturing/testing.

Figure 2.25: Plenary Speaker Christine Luscombe (left) presented AUCAOS awards to the winners (or to the winner's representative).

AUCAOS awards from left to right:

- Christine Luscombe, Okinawa Institute of Science and Technology. (Plenary Speaker, presenting awards)
- Calvin Lee (ACAP, UoM), The University of Melbourne (Poster presentation award winner. 2nd prize)
- David Jones (ACAP, UoM) receiving on behalf of Gagandeep Ahluwalia (ACAP, UoM), The University of Melbourne (Poster presentation award winner. 3rd prize)
- Jessie Posar, University of Sydney (ECR presentation award winner)
- William Pappas, University of New South Wales (PhD presentation award winner)
- Paul Burn (ACAP, UQ) receiving on behalf of Audrey Sanzogni, The University of Queensland (Poster presentation award winner. 1st prize).

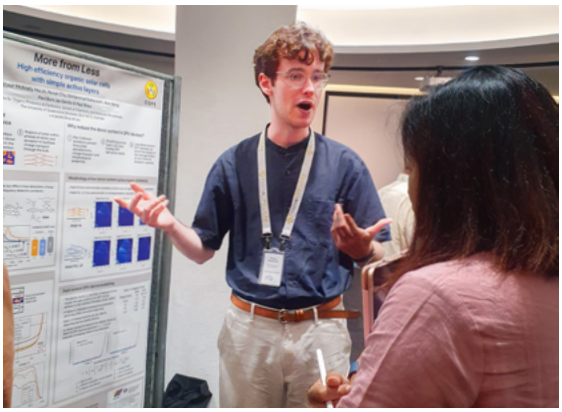

Figure 2.26: PhD Student Shaun McAnally (ACAP, UQ) presented his poster "More from Less: High efficiency organic solar cells with simple active layers" at AUCAOS.

AUCAOS was held over 7–9 December 2022.

FACULTY OF ENGINEERING AWARD

Figure 2.27: Dr Arman Mahboubi Soufiani shows Professor Hameiri's groups Equity, Diversity & Inclusion Award.

Professor Ziv Hameiri's ACDC Group (Artificial intelligence | Characterisation Defects | Contacts) at UNSW SPREE were¬ awarded the UNSW Faculty of Engineering Excellence Award 2022 for Equity, Diversity & Inclusion.

The members of the team awarded are Priya Dwivedi, Ziv Hameiri, Shuai Nie, John Rodriguez, Arman Mahboubi Soufiani and Brendan Wright.

7 December 2022

UNSW RESEARCH TRANSLATION EXPO

The University of New South Wales (UNSW) hosted the 2022 UNSW Research Translation Expo. The event aimed to increase both internal and external awareness of successful research translation. The Expo featured over 50 exhibitions and posters from UNSW spin-offs, start-ups, and other staff and affiliates engaged in research translation and was attended by over 300 people. The event featured a panel discussion with leading innovators from UNSW across multiple disciplines.

Figure 2.28: Professor Renate Egan staffing the ACAP booth at the UNSW Research Translation Expo.

One of the main objectives of the event was to connect UNSW staff interested in research translation with relevant support teams within the Division of Research and Enterprise. The expo also served as a campaign launch for the Powered by UNSW Innovation Community.

ORGANISATIONAL STRUCTURE AND RESEARCH OVERVIEW

The Australian Centre for Advanced Photovoltaics (ACAP) was established in 2013 to develop the next generations of photovoltaic technology and to provide a pipeline of opportunities for performance increase and cost reduction. The Australian partners in ACAP are

the University of New South Wales (UNSW), the Australian National University (ANU), the University of Melbourne (UoM), Monash University, the University of Queensland (UQ) and CSIRO, plus our industrial partners Wuxi Suntech Power Co. Ltd, Trina Solar Ltd, BlueScope Steel, BT Imaging, PV Lighthouse, RayGen Resources, Tindo Operations, 5B, Sun Cable, SunDrive and Microsolar Energy. ACAP also links with research institute partners, specifically the National Science Foundation and Department of Energy–supported Engineering Research Center for Quantum Energy and Sustainable Solar Technologies (QESST), based at Arizona State University, the National Renewable Energy Laboratory (NREL), Lawrence Berkeley National Laboratory (LBNL), Stanford University, the Green Energy Institute (GEI), based in South Korea, and the University of Sydney. These national and international research collaborations provide a pathway for highly visible, structured photovoltaic research collaboration between Australian and international researchers, research institutes and agencies, with significant joint programs based on the clear synergies between the participating bodies.

ACAP is driving significant acceleration of photovoltaic development beyond that achievable by partners acting individually, with significant leveraging of past and current funding. This program is supported by the Australian Government through the Australian Renewable Energy Agency (ARENA). The Australian Government, through ARENA, is supporting Australian research and development in solar photovoltaic and solar thermal technologies to help solar power become cost competitive with other energy sources. (The views expressed herein are not necessarily the views of the Australian Government, and the Australian Government does not accept responsibility for any information or advice contained within this report.)

ACAP's organisational chart is shown in Figure 3.1. International activities are coordinated by an International Advisory Committee with membership drawn from ARENA, researcher representatives from several countries, a representative nominated by major industry partners, and the Director of ACAP. The International Advisory

Committee is also charged with identifying, developing and monitoring progress in areas where synergies exist between Australian and international nodes that can be exploited and also monitors joint collaborative projects with existing and new partners. Some examples of current international activities, many arising from competitive ACAP Collaboration Grants, are reported in Chapter 6 and in the Appendix to this report.

As well as these collaborative activities, the major partners, ACAP, QESST and NREL, conduct their own largely independent research programs meeting the specific research and training objectives of their major supporters and sponsors. In the case of ACAP, research is milestone driven with annual milestone targets established through each year's Action Plan, in accordance with the Funding Agreement with ARENA.

ACAP's National Steering Committee comprises a representative of ARENA, industrial and academic representatives, and the node directors. It is charged with overseeing these nationally based activities with the more granular operation of ACAP managed by a Management Committee, which consists of the node leaders or delegates from each of the nodes.

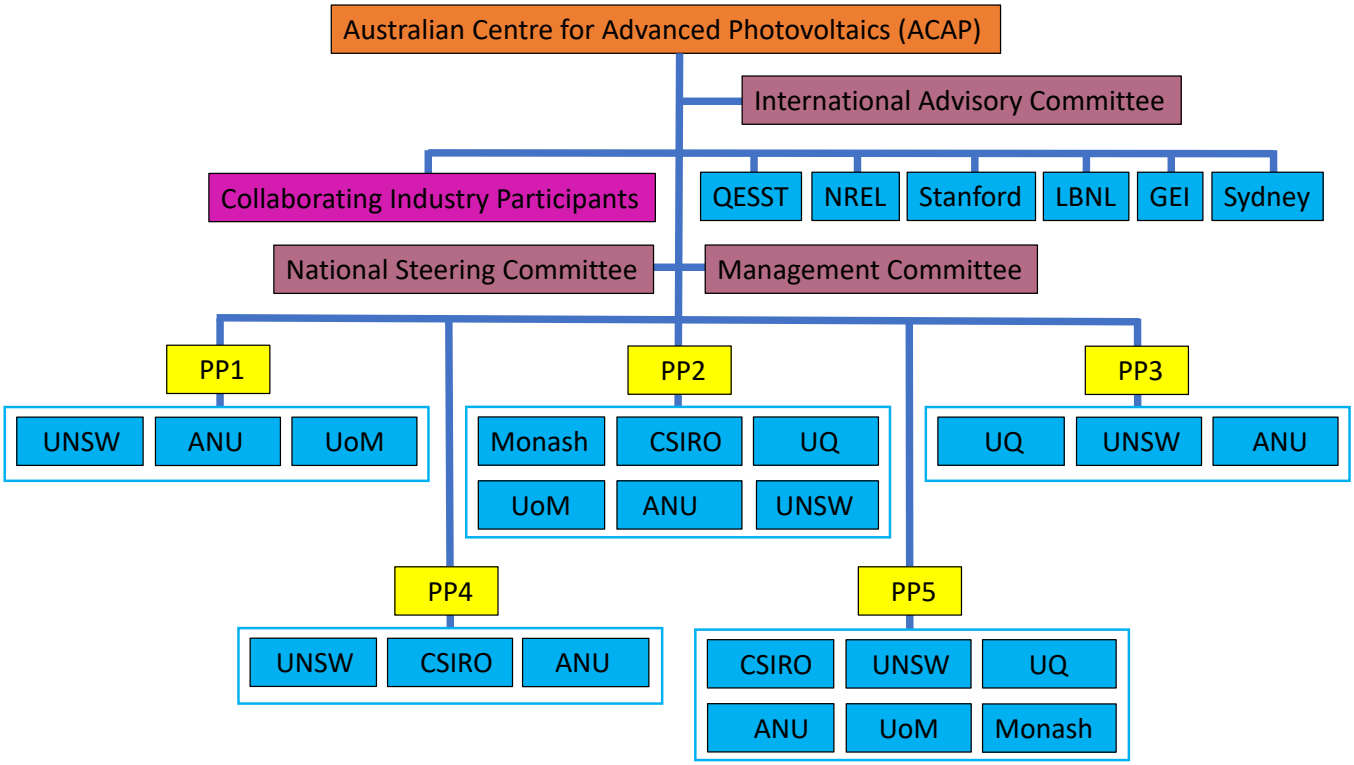

Figure 3.1: Organisational chart. Collaborating industry participants are involved in collaborative research as well as in the Advisory and Steering Committees.

As indicated in Figure 3.1, the ACAP program is organised under five Program Packages (PP1–PP5), each supported by multiple nodes. PP1 deals with silicon wafer–based cells, by far the dominant photovoltaic technology commercially, and likely to remain so for at least the next 10 years. Here the challenge is to continue to reduce manufacturing costs and extend operational lifetimes beyond the presently warranted 25–30 years, while improving energy conversion efficiency. PP1 focuses on three main areas: cells made from solar-grade silicon, rear contact cells and silicon-based tandem cells, both monolithic and mechanically stacked.

PP2 involves collaborative research into a range of organic, organic-inorganic hybrid cells and "Earth-abundant" thin-film materials, including Si and CuZnSnS (CZTS), as well as more futuristic "third generation" approaches. Since ACAP's inception, the relatively new photovoltaic material, the organic-inorganic perovskites, has been included within the scope of this Program Package and additional funding was provided from 2016 to 2020 to expand and intensify the research on these materials and devices. The program had the overall goal of demonstrating high efficiencies for these new thin-film cells of above 1 cm² area and of demonstrating manufacturability.

PP3 "Optics and Characterisation", targets development of general techniques to improve the optical performance of solar cells and for allowing improved insight into cell operating characteristics, irrespective of cell technology in both cases.

PP4 "Manufacturing Issues", aims at delivery of a substantiated methodology for assessing life cycle costs of the different technologies under investigation by ACAP. The original overall cost target was to undercut the US Government's SunShot targets, for one or more of the technologies, in at least one major SunShot targeted application, as deduced by a substantiated costing methodology. Environmental costs are also considered in this Program Package, through rigorous life cycle assessment and evaluation of end-of-life options.

PP5 involves education, training and outreach. ACAP monitors the number of researchers in different categories benefiting from the support it provides, as well as outreach activities, including public lectures on material relevant to ACAP activities, newspaper and magazine articles, responses to governmental calls for submissions, visits by policy developers and their advisors, information papers and presentations to both policy developers and their advisors.

Targets for PP1–PP5 are established through the Activity Plan for each year.

AFFILIATED
STAFF AND STUDENTS

UNIVERSITY OF NEW SOUTH WALES

Green, Martin (Centre Director)

Corkish, Richard (Centre Chief Operating Officer)

Academic Staff and Senior Researchers

Egan, Renate (Node Leader)

Abbott, Malcolm (p/t)

Bilbao, Jose (p/t)

Bremner, Stephen

Bruce, Anna

Chan, Catherine Emily

Conibeer, Gavin

Ekins-Daukes, Nicholas

Hallam, Brett

Hameiri, Ziv

Hao, Xiaojing

Ho-Baillie, Anita (Adjunct)

Hoex, Bram

Ji, Jingjia

Kampwerth, Henner

Kay, Merlinde

Keevers, Mark

Kunz, Oliver

Lennon, Alison (adjunct from March 2022)

Perez-Wurfl,

Ivan Passey,Rob

Rougieux, Fiacre

Shrestha, Santosh

Tayebjee, Murad

Trupke, Thorsten (p/t)

Uddin, Ashraf

Young, Trevor

ECR and Postdoctoral Fellows

Bahl, Prateek

Bany Mousa, Osama

Borojevic, Nino

Chang, Nathan

Chen, Ran

Chen, Weijian

Ciesla, Alison

Cui, Xin

Deng, Rong

Dias, Pablo Ribeiro (until Feb 2022)

Dwivedi, Priya

Fletcher,Jack

Haghdadi, Navid

Hamer, Phillip

He, Mingrui

Heslop, Simon Francis

Hossain, Md. Anower

Hsiao, Pei-Chieh

Huang, Jialiang

Jiang, Yajie

Kim, Moonyong (from Jun 2021)

Kuczyńska-Łażewska, Anna (from Jul – Nov 2022)

Lee Chin,Robert

Li, Jianjun

Liu, Xu

Liu, Ziheng

Makarowsky, Alex

Mahboubi Soufiani, Arman

Monteiro Lunardi, Marina (P/T)

Nielsen, Michael

atterson, Robert

Payne, David (Adjunct)

Pollard, Michael

Prasad,Abhnil

Pusch, Andreas

Rahimpour, Zahra

Roberts, Michael Benedict

Roemer, Udo

Soeriyadi, Anastasia Hertanti (until Nov 2022)

Song, Ning

Sun, Kaiwen

Suryawanshi, Mahesh Pralhad

Teymouri, Arastoo

Vaqueiro Contreras, Michelle

Wang, Li

Wang, Sisi

Wright, Brendan

Wright, Matthew

Yan, Chang

Yi, Chuqi

Yildiz, Baran

Zeng, Yiyu

Zhou, Zibo

Zhu, Yan

PhD Students

Abdullah-Vetter, Zubair

Al Kiyumi, Lamees

Yaqoob Mubarak

Baldacchino, Alexander

Buratti, Yoann

Cai, Yalun

Choi, Eunyoung

Cong, Jialin

Dehghanimadvar, Mohammad

Dipta, Shahriyar Safat

Dubajic, Milos

Feng, Ziyue

Gorman, Nicholas

Guo, Xinyao

Hall, Ryan

Hanif, Muhammad

Hosseinabadi, Parisa

Howlader, Ashraful Hossain

Javier, Gaia Maria

Kaleem, Akasha

Kasim, Samsudeen

Khan, Muhammad Umair

Khoo, Kean Thong

Kim, Eui Ho

Le, Anh

Lehmann, Alex

Leyton, David

Li, Caixia

Li, Guo

Lim, Jihoo

Liu, Mengdi

Madumelu, Chukwuka

Mo, Alvin

Mungra, Mreedula

Mussakhanuly, Nursultan

N Radhwi, Haytham

Nie, Shuai

Oestroem, Ina

Phua, Benjamin

Poddar, Shukla

Poduval, Geedhika

Qian, Chen

Sakib, Syed Nazmus

Samadi, Aref

Sang, Borong

Sazzad, Muhammad Hasnan

Sharma, Abhinav

Shim, Hongjae

Sun, Zhenyu

Tarique, Walia

Teh, Zhi Li

Thomas, Ian

Wang, Ao

Wang, Haoran

Wang, Liping

Wang, Ruimeng

Wang, Shaozhou

Wang, Yansong

Wang, Yihao

Wang, Zhimeng

Wu, Qiyuan

Wu, Xinyuan

Xie, Tong

Yang, Zhen

Yuan, Xiaojie

Zandi, Soma

Zhang, Meng Fei

Zhang, Xueyun

Zhang, Yu

Zhang, Yuchao

Zhou, Zhuangyi

Masters Students

Dandekar, Pranav

Deng, Kun

Fan, Jiahao

Fan, Kenneth

Htun, Kyaw Zin

Jia, Guoyu

Katyarmal, Aditi Ajay

Liu, Anthony

Ren, Ruiyan

Runkai, Liu

Wang, Xutao

Xie, Rui

Xu, Yaqing

Yao, Weiran

Yen, Ruiyan

Yerbulatkyzy, Gaukhar

Zhang, Haotian

Zhang, Weiyi

Zhang, Yijia

Zhong, Haoyu Zhu, Xiaohu

Zhou, Yiliao

Zhu, Evelyn

Honours Students

Aarons, Benjamin

Alhoweidi, Mohammed

Basuki, Kenny

Bowen, Olivia Grace

Chong, Elvis

Dillon, Michael

Drury, Storm

Estoque, Joshua

Fan, Atkins De Hua

Fan, Kenneth De Cheng

Gardner, Ryan

Hadley, Tristan

Hassaan, Ibrahim

Ho, Christopher

Jayasimha, Rohan

Ketmontri, Ketti

Lan, Jerry

Li, Zeyu

Li, Zonglin

Lima, Marcel Valencia

Meers, Clement

Mellon, Toby

Ngo, Albert

Nowrungsah, Nichil

Ow, Zhong Ming

Rafique, Araz

Raju, Aravind

Rusli, Priscilla

Scott, Alexander

Tan, Verity

Thapar, Esha

Thompson, Drew

Tran, Benjamin Dai

Wallace, Hugh

Wang, Sijin

Webster, Jasper

Whitehouse, Peter

Wikramanayake, Jasmin

Won,Chanhe

Wormleaton, Jasmine

Wu, Zixi

Youn, Jon

Yuan, Minghao

Zhang, Weiyi

AUSTRALIAN NATIONAL UNIVERSITY

Academic Staff and Senior Researchers

Blakers, Andrew (Node Leader)

Black, Lachlan

Catchpole, Kylie

Chern Fong, Kean

Duong, The

Liu, Anyao

Macdonald, Daniel

Nguyen, Hieu

Phang, Pheng

Shen, Heping

Walter, Daniel

Weber, Klaus

ECR and Postdoctoral Fellows

Ahmad, Viqar

Basnet, Rabin

Cheng, Cheng

Duan, Leiping

Ernst, Marco

Kang, Di

Kho, Teng

Lu, Bin

Mayon, Yahuitl Osorio

Nadolny, Anna

Sio, Hang Cheong

Surve, Sachin

Tong, Jingnan

Truong, Thien

Weber, Tim

Wensheng, Liang

Zhang, Hualin

PhD

Bartholazzi, Gabriel

Broadhurst, Glenn

Bui, Anh

Chang, Li-Chun

Cheng, Cheng

Ilkhechi, Noushin

Huang, Keqing

Ismael, Mohamed

Le, Tien

Li, Zhuofeng

Nguyen, Khao

Nguyen, Thuan

Sabah, Sanjida

Silalahi, David

Siriwardhana, Manjula

Tabi, Grace

Wang, Jiali

Yang, Zhongshu

MPhil Students

Runkai, Liu

Wibowo, Ary

CSIRO MANUFACTURING

Academic Staff and Senior Researchers

Chesman, Anthony (Node Leader)

Chantler, Régine

Faulks, Chloe

Gao, Mei

Scully, Andrew

Vak, Doojin

Weerasinghe, Hasitha

ECR and Postdoctoral Fellows

Angmo, Dechan

Hongyan, Huang

Kim, Juengeun (visiting)

Ng, Leonard

Zheng, Fei (Visiting)

PhD Students

An, Na Gyeong

Sutherland, Luke

UNIVERSITY OF MELBOURNE

Academic Staff and Senior Researchers

Ghiggino, Ken (Node Leader)

Jones, David (Node Leader)

Bullock, James

Smith, Trevor

ECR and Postdoctoral Fellows

Ahluwalia, Gagandeep

Jameel, Mohamed

Lee, Calvin

Masoomi-Godarzi-Saghar

Seyyedhamzeh, Mozdeh

Subbiah, Jegadesian

PhD Students

Fischer, Karen (joint with KIT)

Kheirabadi, Hamoon

Novakovic, Sacha

Saker-Neto, Nicolau

Masters Students

Lin, Jianchao

Nalenan, Marissa

Ruoxuan Shi

Yanlin Wang

MONASH UNIVERSITY

Academic Staff and Senior Researchers

Bach, Udo (Node Leader)

Jasieniak, Jacek

Simonov, Alexandr

ECR and Postdoctoral Fellows

Fürer, Sebastian

Rietwyk, Kevin

Surmiak, Adam

Zhang, Tian

PhD Students

Deng, Siqi

Eskandarian, Masoomeh

Guo, Qianying

Jie, Zhao

Nurrosyid, Naufan

Rodriguez, Juan

Benitez

Zhao, Boya

UNIVERSITY OF QUEENSLAND

Academic Staff and Senior Researchers

Burn, Paul (Node Leader)

Shaw, Paul (Node Leader)

ECR and Postdoctoral Fellows

Babazadeh, Mohammad

Bati, Abdulaziz

Chen, Peng Jun

Gao, Mile

Hao, Mengmeng

Jiang, Wei

Jin, Hellen

Mallo, Neil

McAnally, Shaun

Rashid, Rashid

Raynor, Aaron

Stroet, Martin

Wallwork, Nicholle

PhD Students

Chu, Ronan

Feng, Yaomiao

Gupta, Satakshi

Li, Hui

McAnally, Shaun

Packman, Lachlan

Honours Students

McGoldrick, Stephanie

Smyth, James

QESST

Augusto, André

Bowden, Stuart

Honsberg, Christiana

King, Richard

Teng, Mao

NATIONAL RENEWABLE ENERGY LABORATORY

Al-Jassim, Mowafak

Friedman, Daniel

Heath, Garvin

Kopidakis, Nikos

Levi, Dean

Reid, Obadiah

Woodhouse, Michael

WUXI SUNTECH POWER CO. LTD

Chen, Rulong

TRINA SOLAR

Feng, Zhiqiang

BT IMAGING

Bardos, Robert

Trupke, Thorsten

BLUESCOPE STEEL

Zappacosta, Dion

PV LIGHTHOUSE

Abbott, Malcolm

McIntosh, Keith

Sudbury, Ben

RAYGEN

Lasich, John

Thomas, Ian

Modra, Danny

GREEN ENERGY INSTITUTE

Park, Jongsung

TINDO SOLAR

Jaenisch, Shayne

Sporne, Robert

5B AUSTRALIA

Evans, Rhett

Monteiro Lunardi, Marina

Turner, Adrian

EVOLVING ENERGY

Sturch, James

MICROSOLAR

Xue, Chaowei

SUN Cable

Griffin, David

Marshall, Luke

SUNDRIVE SOLAR

Allen, Vincent

Hu, David

Lennon, Alison

THE UNIVERSITY OF SYDNEY

Ho-Baillie, Anita

AUSTRALIAN PHOTOVOLTAICS INSTITUTE

Wilson, Chris

CUBIC PV

Van Mierlo, Frank

NEOEN AUSTRALIA

Cheylus, Jean-Christophe

ONE STOP WAREHOUSE

Ye, Leo

Xi, Jack

SCIPHER TECHNOLOGIES

Sayers, Chris

Stanfield, James

PP1
SILICON SOLAR CELLS

OVERVIEW

Silicon-based solar cells make up more than 95% of commercial solar products worldwide. The continuous decline in costs, improved efficiencies and highly advanced and matured industrial processes indicate that this share would potentially increase further in the upcoming time. Despite tremendous growth in the past few decades, the industry continues to focus on making cheaper and more efficient solar cells. ACAP's Program Package 1 (PP1) supports the fundamental research leading towards better, cheaper and more efficient cells. In particular, it focuses on areas of low-cost solar-grade silicon material, rear-contact high efficiency cells, passivated contacts, and silicon tandem structures.

PP1.1 SOLAR-GRADE SILICON

Utilising low-cost silicon material is one way to further reduce the cost of industrial solar cells. Solar-grade silicon material offers one such alternative to expensive electronic-grade silicon. The research focusing on upgraded metallurgical-grade (UMG) silicon material is carried out at ANU and UNSW in collaboration with Apollon Solar (UMG silicon wafer provider). With the development of a pre-treatment step of Tabula-Rasa, ANU was successful in achieving a world record efficiency of 22.6% (certified) on a 2 cm × 2 cm cell fabricated at ANU on an n-type Cz-grown UMG wafer supplied by Apollon Solar. Recent work at ANU on oxygen-related ring defects in solar-grade silicon wafers has demonstrated new methods to reduce the impact of these unwanted defects, which could also be useful for standard electronic-grade wafers.

PP1.2A REAR CONTACT CELLS

Rear contact solar cells inherently possess high efficiency architecture by allowing greater photon collection ability and negligible front optical losses. This project aims at making high efficiency interdigitated back contact (IBC) solar cells and bifacial cells using industrially feasible processes. ANU has produced a record single-junction device with an efficiency of 25 ± 0.6% using their oxide-nitride-oxide (ONO) dielectric structure, and bifacial cells with 29% BiFi20 (20% rear albedo) effective efficiency.

The ongoing work demonstrates the integration of doped polySi passivated contact structures towards further improvements in the device efficiency, and novel polySi/heterocontact hybrid IBC device designs towards significantly simplifying its fabrication processes. IBC cells integrating doped polysilicon passivated contacts attained efficiencies of ~23%. This project has also demonstrated a working prototype hybrid-IBC design featuring SiOx/polySi(n+)/MoOx/Al stack, with a measured efficiency of 14%. Loss analysis of both device designs have provided clear indications of areas of improvement and optimisation towards subsequent improvements.

PP1.2B PASSIVATED CONTACTS

One of the prominent loss channels in current industrial cells is the contacts at the metal/silicon interface. Passivated contacts provide a solution to this problem by reducing recombination at the contacts, while still allowing current to flow through them. We have explored in depth several approaches to achieving such passivated contacts, including high temperature methods based on doped poly-silicon films, and low temperature approaches using metal oxides. A key outcome has been a series of world record full-sized n-type silicon solar cells featuring doped poly-silicon passivated contacts on the rear side, fabricated at Jinko Solar, through an ongoing collaboration with the team at ANU. These devices were produced using industrially viable equipment and techniques, and included a 25.4% device certified at ISFH CalTeC in October 2021, and 26.4% in December 2022.

PP1.3C TANDEM CELLS

In the case of mechanically stacked GaAs tandems, ANU has developed and fully characterised a III-V/Si tandem featuring bifacial capabilities with front side efficiency of 33% and a potential effective bifacial efficiency of 38.6% with 200W m-2 rear illumination.

PP1.1 SOLAR-GRADE SILICON

PP1.1A SOLAR-GRADE SILICON CELLS

ANU Team

Prof. Dan Macdonald, Dr Rabin Basnet, Dr AnYao Liu, Dr Sieu Pheng Phang

ANU Students

Mr Tien Le, Mr Zhongshu Yang

Partners

Arizona State University (ASU)
Apollon Solar (France)

Funding Support

ACAP, ARENA, ARC, ANU

Aims

The use of low-cost solar-grade silicon materials has the potential to contribute to further reductions in the cost and embodied energy of photovoltaic modules. However, to enable the widespread industrial application of such solar-grade materials, it is necessary to demonstrate that the cell efficiency and stability is comparable to standard electronic-grade silicon wafers. This requires the development of techniques to remove and mitigate performance-limiting defects in solar-grade silicon materials, either during the ingot growth stage, or during subsequent cell processing. Impurity gettering and defect hydrogenation are two critical steps to achieve this. This project aims to develop effective and practical gettering and hydrogenation techniques and apply them to the fabrication of solar cells made with solar-grade wafers, ultimately aiming for device efficiencies above 23%.

Progress

As reported previously, in 2019 we achieved a world record efficiency of 22.6% (certified) on a 2 cm × 2 cm cell fabricated at ANU on an n-type Cz-grown upgraded metallurgical-grade (UMG) solar-grade wafer supplied by our partners Apollon Solar. The rear side of the cell featured a full-area thin tunnelling oxide with an overlying phosphorus-doped polysilicon layer, to form a high quality passivated contact. This simple rear-side structure allows for high efficiency devices while retaining a low thermal budget, and provides outstanding impurity gettering.

However, these devices are often affected by oxygen-related ring defects that form within the solar-grade wafers during cell fabrication. In 2022 we developed new mitigation strategies for these ring defects, which are also important in electronic-grade wafers grown by the Czochralski process. Previously, we have shown that hydrogenation can passivate some of these ring defects in solar-grade silicon (Basnet et al. 2018). With the objective of achieving a greater degree of defect passivation, we have recently investigated alternative passivating agents for ring defects in solar-grade silicon. Fluorine has previously been used as a passivating agent in silicon microelectronic devices. Recently, Sio et al.. (2021) demonstrated passivation of defects more relevant to silicon solar cells, such as the boron-oxygen defect, grain boundaries, and interfaces in polysilicon passivating contacts, using MgF and LiF films. We therefore investigated the potential for MgF films to passivate ring defects, and compared the outcomes with the conventional hydrogenation method using SiN films (Basnet et al. 2022). The effectiveness of the passivation of ring defects using MgF and SiN as a function of annealing temperature, for an annealing time of 5 minutes, is shown in the PL images in Figure PP1.1A.1. The PL images show that neither the SiN nor MgF films resulted in the passivation of ring defects at 400°C in the solar-grade samples. At higher temperatures, the passivation of ring defects in the MgF-coated samples is fully activated at 600°C, whereas hydrogenation is already activated at 500°C. We have also shown that fluorinated defects are more resistant to subsequent annealing steps, potentially providing increased flexibility in device processing.

We have also continued to improve our understanding of impurity gettering of unwanted metal impurities in silicon wafers via doped poly-silicon films. Recent work has provided, for the first time, a detailed understanding of the gettering mechanisms in poly-silicon films both with and without pinholes. These insights allow poly-silicon contact processes with optimised gettering efficiency to be developed for a given silicon material and/or thermal budget.

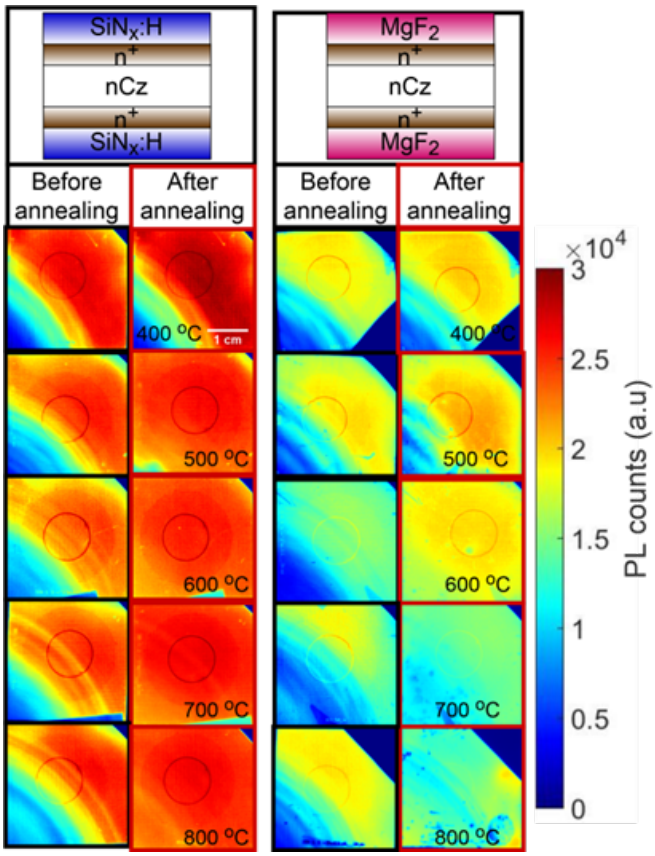

Figure PP1.1A.1: Uncalibrated PL images of samples coated with the SiN (left) and MgF (right) films before and after annealing at temperatures from 400–800°C for 5 minutes in a nitrogen ambient environment. The PL images were captured under 0.87-sun illumination and with an exposure time of 5 seconds. Note the circle in the middle of the PL images is the reflection of an inductive coil from the PL system.

References

Basnet, R., Rougieux, F. E., Sun, C., Phang, S. P., Samundsett, C., Einhaus, R., Degoulange, J. & Macdonald, D. (2018). Methods to Improve Bulk Lifetime in n-Type Czochralski-Grown Upgraded Metallurgical-Grade Silicon Wafers. IEEE Journal of Photovoltaics 8, 990-996.

Basnet, R., Sio, H. C., Sun, C., Nguyen, H. T. & Macdonald, D. (2022). Passivation of Ring Defects in Czochralski-Grown Silicon Using Magnesium Fluoride Films. ACS Applied Energy Materials 5, 9877-9884.

Sio, H. C., Kang, D., Liu, R., Stuckelberger, J., Samundsett, C. & Macdonald, D. (2021). Fluorine Passivation of Defects and Interfaces in Crystalline Silicon. ACS Applied Materials & Interfaces 13, 32503-32509.

PP1.2A REAR CONTACT

ANU Team

Dr Kean Chern Fong, Dr Matthew Stocks, Dr Teng Choon Kho, Dr Wensheng Liang, Dr Jingnan Tong, Dr Marco Ernst, Dr Parvathala Narangari, Mr Stephane Armand, Prof. Andrew Blakers

Academic Partners

PV Lighthouse

Funding Support

ARENA, ANU

Aims

The objectives of PP1.2A are twofold: to develop very high efficiency laboratory-based silicon solar cells; and, in parallel, to develop cell fabrication techniques and processes compatible with industrially feasible low-cost implementation of interdigitated back contact (IBC) solar cells. IBC cells, by their very nature, are both inherently capable of very high efficiencies owing to superior optics compared to conventional cell architectures and owing to an improved ability to tailor fabrication processes to meet specific goals of cell features. However, such cells are also characterised by more complex and expensive fabrication processes. The target for the end of the program is to fabricate cells using any techniques with efficiencies of 26% or above, and in parallel to produce cells using industrially applicable techniques, and by doing so meeting an internal efficiency target of 25% or above.

Progress

This project has so far successfully demonstrated independently measured device efficiencies of 25% ± 0.6% for a single-junction IBC solar cell featuring novel oxide-nitride-oxide (ONO) passivation, and a 24.3% rear-junction bifacial cell with a 96.3% bifacial factor, with an effective BiFi20 efficiency of 29.0% featuring laser processed contacts.

In 2022, this project focused on the development of polysilicon IBC solar cells, and hybrid heterocontact-polysilicon IBC devices, with the goal of attaining higher device efficiencies with a simplified fabrication procedure. We successfully demonstrated polysilicon-contacted IBC solar cells building upon previous 25% ONO IBC architecture, inheriting key features of having ONO on both the front and rear passivation, with the addition of phosphorus-doped polysilicon on chemically grown tunnel-oxide for the n-type contacts. The champion cell structure and IV curve are as presented in Figure PP1.2A.1, demonstrating a V_{OC} of 701 mV, with an efficiency of 23.0%, and a pseudo efficiency of 23.8%. Improvements to the device design are being developed by improvements to the tunnel oxide growth and polysilicon doping process.

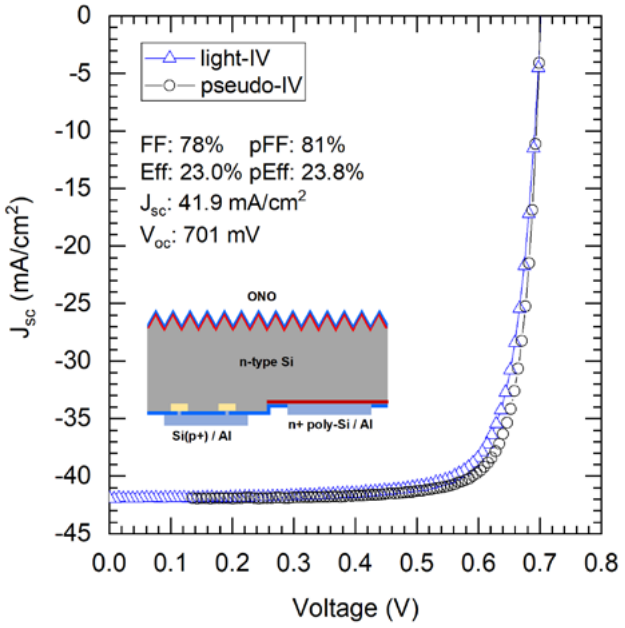

Figure PP1.2A.1: Design of polysilicon passivated contact IBC solar cell (inset), and the measured IV and pseudo-IV curve.

We have also demonstrated a novel device concept combining n-type polySi and MoO_x layers to form a hybrid IBC design with significant simplification to the fabrication process by implementing a tunnel-junction contact. Development of the tunnel-junction contact on test structures has demonstrated fully ohmic n-type contacts are possible with this stack and are capable of very low contact resistivity, limited to only the contact resistivity of the underlying polysilicon layers where the addition of the MoO_x layer did not have a discernible effect on the overall contact resistivity. An SEM image of this stack is as presented in Figure PP1.2A.2, which shows the cross-section of the Si/SiO_x/poly-Si(n+)/MoO_x/Al stack (from left to right), measured to have a fully ohmic contact.

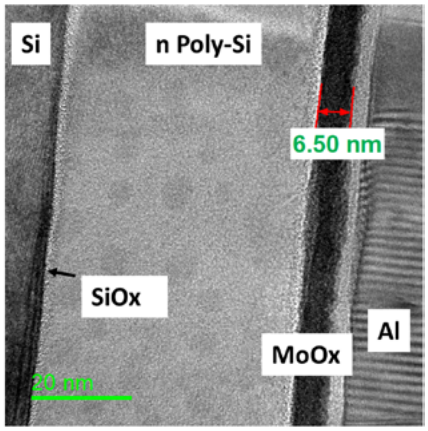

Figure PP1.2A.2: SEM image showing the cross-section of the SiO_x/polySi(n+)/MoO_x/Al tunnel-junction contact.

We successfully integrated the implementation of this tunnel-junction contact in a working hybrid-IBC prototype, as illustrated in Figure PP1.2A.3 and with a measured efficiency of 14% with a pseudo-efficiency of 18.5%. The prototype device demonstrated the feasibility of this design, where analysis of the electrical characteristics now offers insight into key areas of improvement and process optimisation necessary for progression towards high efficiencies.

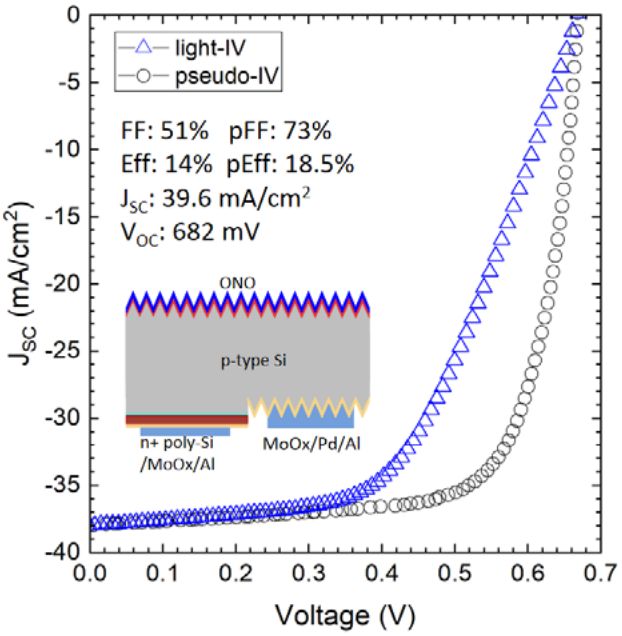

Figure PP1.2A.3: Design of the hybrid-IBC cell (inset), and the measured IV and pseudo-IV curve.

References

Fong, K.C. (2021). "Public Dissemination Report: Next Generation Industrial Bifacial Silicon Solar Cell" ARENA.

Kho, T. C., Fong, K. C., Stocks, M., McIntosh, K., Franklin, E., Phang, S. P., Liang, W. S. & Blakers, A. (2020). Excellent ONO passivation on phosphorus and boron diffusion demonstrating a 25% efficient IBC solar cell. Progress in Photovoltaics 28, 1034-1044.

Wensheng, L., Jingnan, T., Teng Choon, K., Rabin, B., Thien, T., Parvathala, N. et al. (2022). Hybrid IBC Solar cells with poly-Si and metal oxide passivating contacts. 2022 Asia-Pacific Solar Research Conference, Newcastle.

PP1.2B PASSIVATED CONTACTS

ANU Team

Prof. Dan Macdonald, Dr Pheng Phang, Dr Josua Stuckelberger, Dr Lachlan Black, Dr Eric Wang

ANU Students

Mr Mohamed Ismael, Mr Gabriel Carvalho, Ms Jiali Wang, Mr Thien Truong, Ms Di Kang

Academic Partners

EPFL/CSEM Switzerland, University of Melbourne

Funding Support

ARENA, ANU

Aims

The most advanced silicon solar cells use "passivated contacts" to selectively transport electrons and holes towards the cell terminals, while minimising recombination at the metal/silicon interfaces. This project aims to help bring such passivated contacts to the broader PV industry, by developing low-cost and simple approaches to creating such contacting schemes. The first strand of our work is based on the proven high temperature approach of depositing doped silicon films onto an ultra-thin dielectric layer, usually silicon oxide. A second class of low temperature approaches is also being explored, based on depositing dopant-free materials that have either a very high or a very low work function, together with a suitable bandgap, which makes them selective to the transport of holes or electrons, respectively.

Progress

In 2022 we continued to make significant contributions to the development and commercialisation of high temperature doped polysilicon passivating contacts. The most significant of these achievements was the fabrication of full-sized n-type solar cells with rear-side polysilicon passivating contacts at Jinko Solar, supported by an ongoing collaboration with both UNSW and ANU, culminating in a world record device of 26.4% in December 2022.

For the low temperature passivated contact route, we have continued to make good progress in 2022. We have continued the development of hole- and electron-selective contacting schemes based on copper oxide / molybdenum oxide and titanium oxide films respectively, both with and without thin tunnelling interlayers. These films allow simple fabrication of solar cells with no patterning steps required for the rear side, with a low thermal budget. In 2021 we reported on excellent results obtained with stacked films of Al-doped and undoped layers of titanium oxide. These electron-selective contacts have yielded low contact resistances (<20 mΩ.cm^2) and very low surface recombination current densities (J_0 < 2 fA cm^{-2}), leading to small-area n-type solar cells fabricated at ANU with efficiencies of up to 21.9%. A cross-sectional transmission electron microscopy image and associated elemental profile of this contact structure is shown in Figure PP1.2B.1. In 2022 we published these results (Shehata et al. 2022), and further improved upon them by introducing an additional transparent conductive oxide layer in the stack, resulting in a reduction of the contact resistivity to ~3 mΩ.cm^2 while maintaining J_0 < 3 fA cm^{-2}. These new results will be published in 2023. The lower contact resistivity of these stacks is expected to enable partial-area contact structures, which should allow efficiencies above 24% for this technology.

For hole-selective contacts, in 2022 we developed an atomic layer deposition process for copper oxide films with suitable properties for hole-selective contacts. Our publication on these results is currently under review and will be published in 2023. Our next step will be to investigate the addition of different dopant elements to improve the contact properties. We have also obtained promising results on the use of oxide interlayers to improve passivation of copper oxide and molybdenum oxide hole-selective contacts, in the best case obtaining J_0 ~ 80 fA cm^{-2} together with contact resistivity <100 mΩ cm^2, which exceeds the best previous results for this material without the use of (more optically absorbing) amorphous silicon interlayers. These results will be published in 2023.

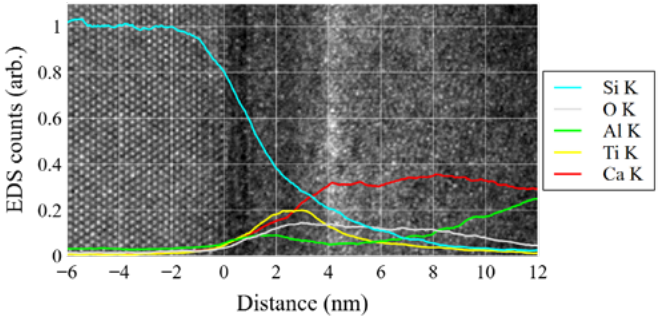

Figure PP1.2B.1: Cross-sectional TEM image and corresponding EDS elemental map of electron-selective contact structure formed by stacked Al-doped / undoped TiOx films on Si.

References

Shehata, M. M., Phang, P., Basnet, R., Yin, Y., Kremer, F., Bartholazzi, G., Andersson, G. G., Macdonald, D. H. & Black, L. E. (2022). Outstanding surface passivation for highly efficient silicon solar cells enabled by innovative AlyTiOx/TiOx electron-selective contact stack. Solar RRL 6 (10), 2200550.

PP1.3 SILICON TANDEM CELLS

PP1.3BC MECHANICALLY STACKED GALLIUM ARSENIDE TANDEMS

ANU Team

Professor Andrew Blakers, Dr Osorio Mayon, Christopher Jones, Dr Kean Chern Fong, Dr Marco Ernst, Dr Wensheng Liang, Dr Teng Choon Kho, Dr Jingnan Tong, Mr Stephane Armand

Academic Partner

NREL, MicroLink Devices, USA

Funding Support

ACAP, ARENA

Aims

The ultimate aim of this project is to deliver a mechanically stacked tandem III-V cell with 32% efficiency. This is being pursued with gallium arsenide (GaAs) top cells with the precursors grown by NREL and MicroLink Devices, with GaAs and silicon bottom cells processed at ANU.

Progress

The Australian National University (ANU) has successfully processed dual-junction (2J) III-V tandem solar cells from epitaxial layers sourced from MicroLink Devices, USA. The 2J III-V cells are a monolithic III-V tandem composed of current-matching GaInP (top cell) and GaAs (bottom cell). These cells were bonded to a glass handle and have an open rear electrode (metal fingers) to allow the non-absorbed light to pass through to the bottom silicon cell. In addition, the cells have a front anti-reflection coating (ARC) to minimise the reflection of light and a rear ARC to maximise the transmission of light to the bottom silicon cell. The solar cell parameters of these cells are shown in Table 1. The champion cell efficiency was 27.4%. All measurements were performed according to standard test conditions, at a cell temperature of 25°C and under illumination of 1000 W m^{-2}, with AM1.5G spectrum from a Wavelabs LED solar simulator c alibrated to a reference cell.

Table PP1.3C.1. Measured 2J III-V solar cell parameters.

	V_{oc} (mV)	J_{sc} (mAcm^{-2})	FF (%)	Efficiency (%)
Average 4 cells	2.309 ± 0.01	13.9 ± 0.2	84.1 ± 0.4	27.0 ± 0.4
Champion cell	2.315	14.1	84.0	27.4

The 2J III-V cells were used in mechanically stacked tandem configuration with monofacial and bifacial silicon cells fabricated at ANU. The monofacial silicon cell is a passivated emitter with a rear locally diffused cell (PERL) fabricated using an n-type wafer. The efficiency of the 2J III-V cells in tandem with the monofacial silicon cell is 33.3%. As the bottom cell, the monofacial silicon cell contributed with 5.9% efficiency to the total tandem efficiency (Figure PP1.3C.1). The following figures show the measured EQE, reflectance and IV curves of the 2J III-V in tandem with the monofacial silicon cell.

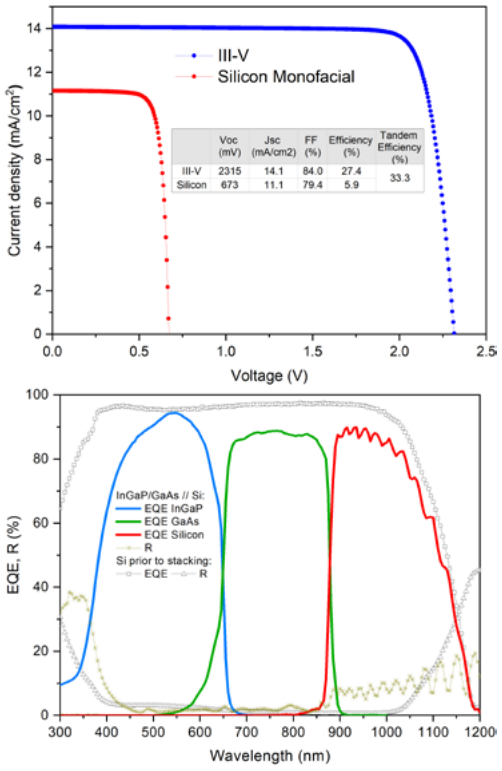

Figure PP1.3C.1: Measured EQE, reflectance and IV curves of the 2J III-V/silicon (monofacial) cell tandem fabricated at ANU.

The bifacial silicon cell has a bifacial factor of nearly 1 that means it has nearly symmetrical power generation capacity on both sides (front and rear) of the device. Laser-doping was used to locally increase the electrical conductivity of the bifacial cell. The 2J III-V cells in tandem with the bifacial silicon cell without illuminating the rear side of the bifacial cell had an efficiency of 33.6%. However, when the rear illumination to the bifacial silicon cell is 100 W/m2 the effective tandem efficiency is 36%. Furthermore, with a rear illumination of 200 W/m2 the effective tandem efficiency is 38.6%. The illumination to the rear side of the bifacial cell, also called back normal irradiance (BNI), was from another solar simulator calibrated with a silicon reference cell. The following figures show the measured EQE, reflectance and IV curves of the 2J III-V in tandem with the bifacial silicon cell.

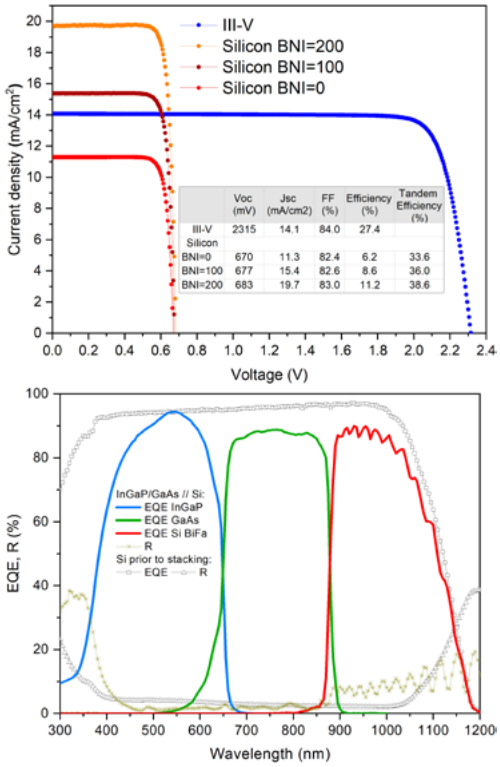

Figure PP1.3C.2: Measured EQE, reflectance and IV curves of the 2J III-V/silicon (bifacial) cell tandem fabricated at ANU. Back normal irradiance (BNI) is the irradiance in W m^{-2} on the rear side of the bifacial silicon cell.

Highlights

- 33.3% III-V/silicon tandem efficiency with monofacial silicon cell.
- 33.6% to 38.6% III-V/silicon effective tandem efficiency with bifacial silicon cell.

Future Work

- Further improvement of III-V/silicon tandem cell efficiency.
- Develop large-area III-V/silicon tandems.
- Develop hybrid CPV/PV 2J III-V/Si tandem module.

PP2
THIN-FILM, THIRD GENERATION AND HYBRID DEVICES

OVERVIEW

Program Package 2 (PP2) encompasses research into a range of next generation cell technologies with the overall goals of demonstrating efficiency above 16% for cells of greater than 1 cm2 area across this range and of demonstrating the feasibility of significantly reduced costs. The current program is divided into tasks to address the key materials groups: organic photovoltaics (OPV), "Earth-abundant" inorganic thin-film materials and the hot topic of organic-inorganic perovskites. Good progress has again been made in 2022 in all target areas.

PP2.1 ORGANIC PHOTOVOLTAIC DEVICES

The thin-film organic photovoltaics task (PP2.1) aims to identify and address roadblocks in organic photovoltaics to enable cost-effective, mass manufacture of modules using this technology. The research targets lower-cost materials and/or processes compared to those of conventional cells or, alternatively, applications such as flexible or partly transparent cells for which conventional cells are not well suited. Organic photovoltaic (OPV) devices have a theoretical power conversion efficiency (PCE) of >20%, with single-junction cells now reported with PCEs of over 19%. There is still considerable scope to molecularly engineer organic semiconductor materials. In addition, they can be solution processed, leading to the possibility of low embedded energy manufacturing. In 2022, the team demonstrated the first application of machine-learning-assistance to achieve the highest PCE from roll-to-roll (R2R) fabricated OPV. Specific outstanding results for the year included:

- The highest PCE (10.2 %) for R2R fabricated flexible OPV (0.1 cm^2 device)
- Development of globally unique high-throughput automatic PV research platform
- Demonstration of high-throughput fabrication of 11,800 OPV research cells in a day and testing all cells in 18 hours.

PP2.2 CZTS SOLAR CELLS

Thin films of the compound semiconductor Cu_2ZnSnS_4 (CZTS) are the focus of PP2.2. In 2022 UNSW has achieved the following highlight outcomes on the path to stable, low-cost, low-toxicity thin films:

- A moisture-assisted post-deposition annealing (MAPDA) treatment is introduced to control the local chemical composition and regulate the defects properties.
- A heterojunction annealing is combined with moisture-assisted post-deposition annealing (MAPDA) treatment to further supress the interfacial and bulk recombination in CZTS solar cells.
- A liquid-phase-assisted grain growth strategy is introduced to supress the detrimental grain boundaries and improve the carrier collection efficiency.
- A Ge incorporation process is developed for defect engineering and phase evolution intervention.
- High efficiency CZTS solar cell with in-house measurement over 11% efficiency is achieved.
- Baseline process and efficiency has been established for wide bandgap CIGS solar cells.
- ZnSnO buffer layer has been carefully tuned for achieving 14% efficient Cd-free CIGS solar cells.

PP2.5 PEROVSKITES

A new work program was started in 2016 to advance organohalide perovskite technologies, namely by improving device performance, durability and scale. Since metal halide perovskite semiconductors were first identified as a new class of optoelectronic material with immense potential for high performance photovoltaic (PV) cells, the record efficiency for these devices has continued to increase at an unprecedented rate. The physical properties of perovskite thin films, coupled with their ability to be produced cheaply at a large scale, has earmarked them as a technology that has the potential to greatly disrupt the PV marketplace.

A significant effort has been initiated internationally on this materials class, and ACAP has several unique advantages that place the proposed activities at the forefront of these efforts. Foremost among these advantages are the different perspectives that ACAP is able to offer, given the expertise within different ACAP groups on the dye-sensitised, organic photovoltaics, inorganic thin-film, silicon cell and module areas, as well as strong contacts to the commercial sector. To capture these research efforts within ACAP, a new program package for Perovskite Solar Cells under PP2 Thin-Film, Third Generation and Hybrid Devices was established to carry out focused and highly collaborative Australian research and industry efforts in perovskite photovoltaics.

In 2022, the teams developed new solution-based fabrication methods by controlling crystallisations, morphology and composition homogeneity through precursor engineering and additive engineering. There was extensive exploration of passivation strategies and a deeper understanding of the underlying passivation mechanisms by 2D Ruddlesden–Popper (RPs), organic additives and HTL/ETL interface. With the further development of techniques and materials, large-area devices and modules produced by scalable fabrication methods based on roll-to-roll and blade coating were realised. In addition, high device performances were achieved, which include a reverse-scanned efficiency of 24.6% with significantly mitigated hysteresis, record fill factors over 85%, and notable ambient stability of unencapsulated devices over 2800 hours retaining 95% of their initial efficiency.

PP2.1 ORGANIC PHOTOVOLTAIC DEVICES

Research Team

Academic/ Postdoctoral
University of Queensland: Prof. Paul Burn, Dr Paul Shaw, Dr Hui Jin, Dr Wei Jiang, Dr Neil Mallo

University of Melbourne: A/Prof. David Jones, Prof. Ken Ghiggino, Prof. Trevor Smith, Dr Jegadesan Subbiah, Dr Calvin Lee, A/Prof. Wallace Wong, Dr Valerie Mitchell, Dr James Bullock, Dr Saghar Masoomi-Godarzi, Dr Gagandeep Ahluwalia

UNSW: A/Prof. Ashraf Uddin, Prof. Gavin Conibeer, Prof. Bram Hoex, Dr Anower Hossain, Dr Matthew Wright, A/Prof. John Stride, Prof. Mahbub Hassan

CSIRO: Dr Anthony Chesman, Dr Mei Gao, Dr Doojin Vak, Dr Hasitha Weerasinghe, Dr Leonard WT Ng
Monash University: Dr Na Gyeong An, Prof. Udo Bach

Research Students

University of Queensland: Shaun McAnally, Ronan Chu, Satakshi Gupta, James Smyth, Stephanie McGoldrick

University of Melbourne: Hamoon Kheirabadi

UNSW: Leiping Duan, Habibur Rahman, Shahriyar Safat Dipta, Walia Binte Tarique, Ashraful Hossain Howlader, Yanxiang Wang, Jiawei Hu

Academic Partners

Prof. Ian Gentle (University of Queensland); Prof. Jinhong Du (Institute of Metal Research, Chinese Academy of Sciences); Dr Alexander Colsmann, Mr Philipp Marlow, Mr Lorenz Graf von Reventlow, Karen Fischer (Karlsruhe Institute of Technology, Germany); Prof. Paul Meredith, Dr Ardalan Armin, Oskar J. Sandberg, Nasim Zarrabi (Swansea University, UK); Prof. Mukundan Thelakkat, Prof. Anna Köhler, Julian Hugenberg, Sebastian Pallasch (University of Bayreuth, Germany); Prof. Jin Young Kim, Dr Na Gyeong An (UNIST, Korea); Prof Dong Wook Chang, Seok Woo Lee (Pukyong National University, Korea); Prof Yinhua Zhou, Yang Liu (Huazhong University of Science and Technology, China); Dr Leonard WT Ng (Nanyang Technological University, Singapore); Prof Jin Young Kim (Ulsan National Institute of Science and Technology, Korea)

Funding Support

ACAP, UQ, UoM, CSIRO

The continued research and development of Organic Photovoltaic (OPV) devices has led to materials with better absorption and donor-acceptor energy offsets, which has resulted in record power conversion efficiencies (PCEs) reported as >19% under laboratory conditions (Ng et al. 2022). This achievement mainly relies on using high performance non-fullerene acceptors (NFA). Due to the rapid development of new molecules and the variety of their chemical structures, understanding how the different dielectric constant NFA materials affect optoelectronic and device properties is far from complete and is primarily explored in this scheme. Simplifying the synthesis of polymeric donors and NFAs provides an effective channel for scaling up future materials. Using industrially relevant solvents to fabricate OPV devices would reduce production costs and provide a clear pathway towards commercialisation. Finally, the innovative use of digital research methods to fabricate and test solar cells will enable the rapid exploration of OPV technologies from lab-to-fab in the future.

For ease of reading, this program has been divided into four broad sections: Materials, Device Architecture, Printing and Scale-up, and Applications.

Aims

The materials development program has had the following aims:

- Development of donors and non-fullerene materials for bulk heterojunction active layers.
- Creation and understanding of the properties of organic semiconductor materials designed to have a high dielectric constant.
- Controlling morphology development through materials design.
- Third generation solar cells.
- Establish structure-function relationships between molecular geometry, dipole moment and dielectric constant.
- Determine the optoelectronic properties of the materials.

Progress

Materials

Block copolymer for efficient, thermally stable organic photovoltaic devices deposited from industrially relevant solvents

Block copolymers (BCP) are envisaged to offer control over domain size and the interfacial angle between the donor/acceptor block, inhibiting macro phase separation and delivering long-term structural and thermodynamic stability to the morphology. In addition, the ease of tunability of energy levels and processing solvent by modifying the conjugated backbone and sidechains on either block in BCPs makes them a promising single-component active layer material. However, the device efficiencies of such block copolymers are lagging behind those based on a blended active layer due to non-ideal morphological issues and a lack of new BCP materials. In this work, UOM researchers design and synthesise a new BCP containing push-pull conjugated copolymer blocks (BCP4) using naphthalene-bithiophene (N2200) an acceptor polymer block and benzodithiophene-benzothiadiazole (CP3) as a donor block (Figure PP2.1.1).

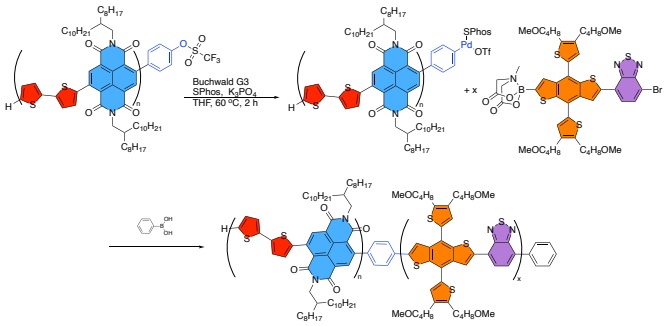

Figure PP2.1.1: Synthetic route to fully conjugated di-block copolymer BCP4. The asymmetrically functionalised push-pull monomers for N2200 (n-type polymer) were added followed by the asymmetrically functionalised push-pull monomer for CP3 (p-type polymer).

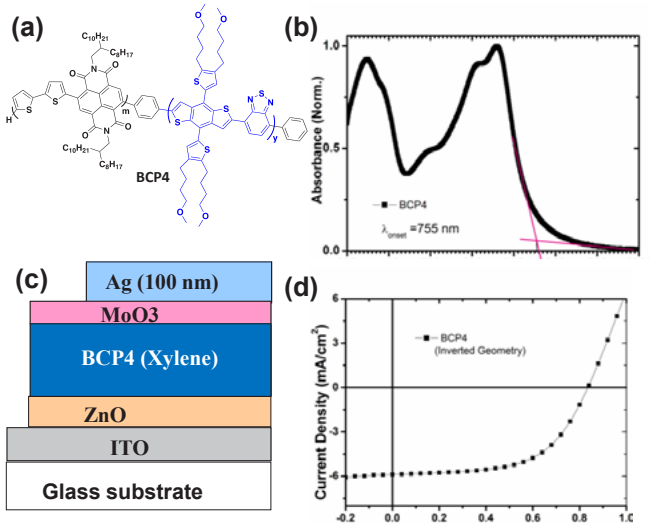

Figure PP2.1.2: (a) Chemical structure and (b) solid-state UV/vis absorption spectrum of block copolymer (BCP4). (c) Schematic diagram, and (d) J-V characteristics of OPV devices.

The chemical structure and absorption spectrum of BCP4 are shown in Figure PP2.1.2 (a) and (b). The bandgap of BCP4 is measured as 1.64 eV with a photon harvesting range from 300 to 790 nm. The schematic diagram of the inverted device geometry and J-V characteristics of the OPV device is shown in Figure PP2.1.2 (c) and (d) respectively. We also studied the device performance using regular geometry (ITO/PEDOT): PSS/BCP4/PFN-Br/Ag), and the device performance parameters are summarised in Table PP2.1.1. The OPV device with inverted geometry shows the best PCE of 2.9%, and the nanostructure morphology of BCP4 was investigated using tapping mode AFM. As shown in the AFM morphology (Figure PP2.1.3), the di-block copolymer (BCP4) was self-assembled to form nanoscale morphology with spontaneous phase separation into well-defined, linear domains.

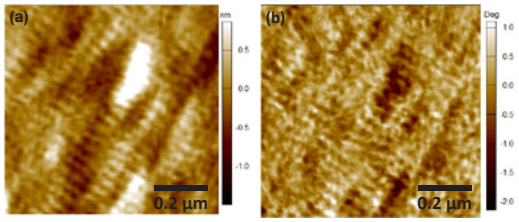

Figure PP2.1.3: (a) AFM height, and (b) phase images of BCP4.

Table PP2.1.1: Photovoltaic performance of organic solar cell using BCP4 with conventional and inverted geometry.

Devicel Geometry/ Annealing	J_{SC} (mAcm^{-2})	V_{OC} (mV)	FF (%)	PCE (%)
BCP4 - 150°C (Conventional Geometry)	0.74	5.65	54	2.25
BCP4 - 150°C (Inverted Geometry)	0.80	5.9	60	2.90

Improving the efficiency of bulk heterojunctions with novel non-fullerene acceptors

The 2021 report described a series of novel small molecule materials with relatively high electron affinities that showed promising results when used as acceptors in bulk heterojunction devices. Initial devices showed power conversion efficiencies (PCEs) of up to 5.7%. Further work has been undertaken to optimise the device architecture to maximise the PCE. A number of donor polymers were investigated and through energy-level matching, the wide bandgap donor polymer, poly[(thiophene)-alt-(6,7-difluoro-2-(2-hexyldecyloxy)-3-methylquinoxaline] (PTQ11), was chosen as the partner material for the acceptor materials. Both standard and inverted device structures were considered, with the latter architecture of ITO/ZnO/bulk heterojunction/ MoO_x/Ag showing a doubling of the PCE at 11.7%

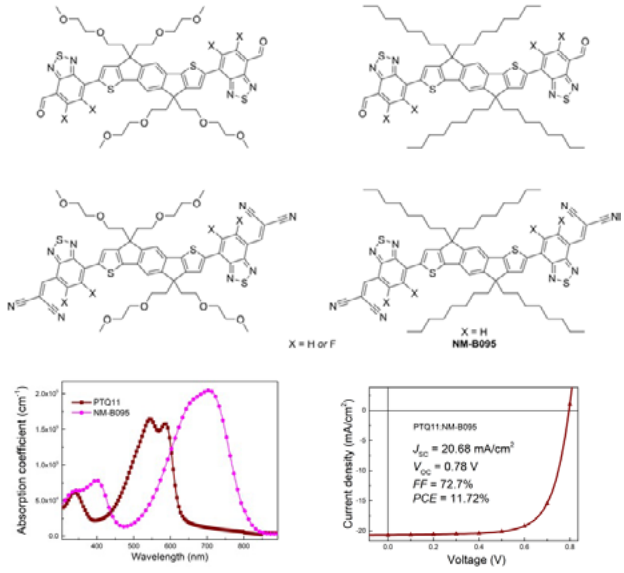

Figure PP2.1.4: The chemical structures of the indacenodithiophene series used for studying the influence of solubilising group (glycol or n-octyl), acceptor substitution (protonated or fluorinated) and endcap (aldehyde or dicyanovinyl) on bulk heterojunction devices (top). The absorption spectra of the materials used in the optimised bulk heterojunction device and its current density-voltage plot with the performance parameters as an inset (bottom).

Investigation of the effect of the dipole moment of a material on their dielectric constant.

One of the limiting factors in organic photovoltaics is the high exciton binding energy of the organic semiconductor materials, which reduces the direct formation of free charge carriers. The exciton binding energy is inversely proportional to the dielectric constant of the material, and it has been postulated that an organic semiconductor with a dielectric constant of ~10 would result in the spontaneous formation of free charges (Koster et al. 2012).

However, the dielectric constant of a material is frequency-dependent, and there is an ongoing debate as to which frequency range is important for exciton dissociation. The relatively small number of studies on engineering dielectric constants have focused on the kHz to MHz range, where dipolar effects play a significant role (Sami et al. 2022).

In previous work on developing materials to increase the dielectric constant (with a key focus on the optical frequency), the activities centred on symmetric materials that had no net molecular dipole moment. During the program of work this year, three structural isomers were investigated and compared, with a view to increasing the molecular dipole moment, namely materials that were linear, banana or horseshoe shaped (Figure PP2.1.5). The three families were composed of similar acceptor end functionality with the shape introduced via the donor component. That is, the compounds all contained benzothiadiazole (BT) acceptors that were either protonated (x = H) or fluorinated (x = F). Furthermore, the compounds all had the same *n*-octyl solubilising groups. The ground-state configurations of the six compounds were determined using density functional theory calculations, which showed that in all cases the compounds were near coplanar. The linear analogue had no net dipole moment as a result of the symmetry. With the increased curvature of the core, the molecular dipole increased to 15 debye for the banana-shaped analogue and 18 debye for the horseshoe-shaped molecules. Changing the shape of the central aromatic ring had a significant effect on the absorption properties of the materials. With increased curvature, the absorbance shifted to shorter wavelengths, and there was a decrease in the extinction coefficient. Fluorination of the BT resulted in a further blue-shift of the absorption, with only a small effect on the extinction coefficient.

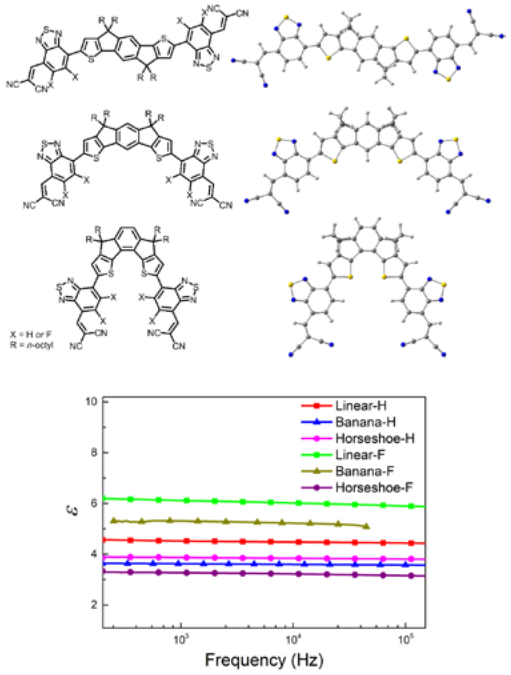

Figure PP2.1.5: The chemical structures (top left) and optimised ground-state configurations (top right) of the compounds of this study. The linear configuration (top structure) has no net dipole moment. The banana-shaped analogue (middle structure) has a dipole moment of 15 debye, while the horseshoe-shaped analogue (bottom structure) has a dipole moment of 18 debye. The dielectric constants of the chemicals in the kHz to MHz range are shown.

It was found that there was no correlation of the net molecular dipole moment on the kHz – MHz range dielectric constant (see Figure PP2.1.5) nor was there a significant effect on the optical frequency dielectric constants.

Table PP2.1.2: Film mass densities and measured charge mobilities of the compounds in Figure PP2.1.5

Core	x	Density ($g\ cm^{-3}$)	μ_e ($\times 10^{-6}$ $cm^2V^{-1}s^{-1}$)	μ_h ($\times 10^{-6}$ cm^2V^{-}
Linear	H	1.12	53.3±6.6	10.2±0.9
	F	1.15	8.4±1.7	6.1±0.8
Banana	H	1.19	9.8±1.1	5.3±0.7
	F	1.21	8.6±0.9	0.6±0.1
Horseshoe	H	1.12	21.2±0.1	5.8±0.1
	F	1.18	5.2±0.1	--

It was interesting to note that the film mass density was not strongly dependent on the shape of the compound. The banana-shaped analogues were found to have a slightly higher mass density and the fluorinated derivatives all had higher mass densities than their protonated counterparts. In contrast, core shape and halogenation had a significant effect on the charge mobility. The fluorinated analogues were found to have lower electron mobilities than their non-fluorinated counterparts, and the hole mobility of the banana-shaped analogue

was an order of magnitude smaller compared to the linear analogue. We were unable to measure a hole mobility for the fluorinated horseshoe material. The H analogues showed more balanced electron and hole mobilities. The linear analogue was found to have the highest mobility, with the banana-shaped analogue the lowest. The relatively low mobilities for the banana-shaped material could be the result of the break in the pi-orbital delocalisation due to the substitution pattern on the central aromatic ring.

Tuning the optical frequency dielectric constant through endcap engineering

The optical frequency dielectric constant of a material may have the largest effect on the magnitude of the exciton binding energy. Modification of the electron acceptor and/or donor component in a molecule can affect the electronic polarisation, which in turn affects the dielectric constant. A key result from the program this year has been identifying the effect of the acceptor on the optical-frequency dielectric constant. In the study, the donor component of the materials was kept the same (cyclopentadithiophene (CPDT)) and the high electron affinity end groups changed from dicyanovinyl (DCV) to benzothiadiazole (BT), difluorobenzodithiazole (DFBT), 3-(1,1-dicyanomethylene)indanone (INCN), 3-(1,1-dicyanomethylene)-5,6-dichloroindanone (INCN-2Cl) and 3-(1,1-dicyanomethylene)-5,6-dichloroindanone (INCN-2F) (Figure PP2.1.6). To the best of our knowledge the highest previously reported optical frequency dielectric constant value was 4.60. The novel materials with INCN acceptor end groups were found to have optical frequency dielectric constants of up to a remarkable 6.57.

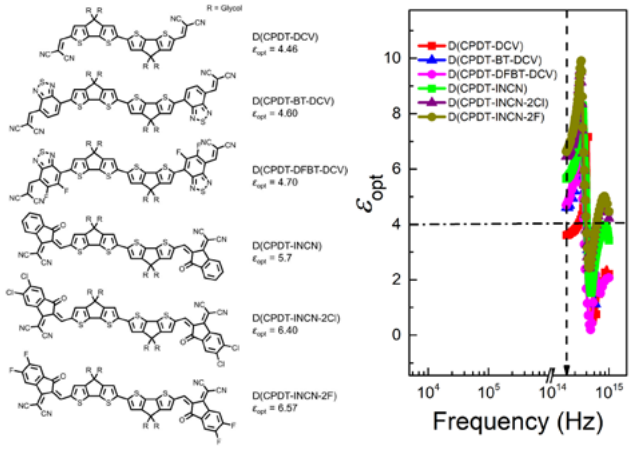

Figure PP2.1.6: The chemical structures of the compounds developed to understand the effect of the acceptor groups on the optical-frequency dielectric constant. The dielectric constants in the optical frequency range is shown on the right.

The materials with INCN acceptor groups, which have the higher dielectric constants, also have a more red-shifted absorbance and higher molar extinction coefficient compared to their BT-based analogues [D(CPDT-BT-DCV) and D(CPDT-DFBT-DCV)]. The combination of these properties makes these materials promising candidates for homojunction devices.

The three materials with the highest optical-frequency dielectric constants (5.70–6.57) were used as the photoactive layer in both conventional and inverted homojunction devices. It was found that the device performance improved with increasing dielectric constant of the material. In particular, the devices all showed a sharp increase in the external quantum efficiency (EQE) near the optical gap of the material where there is no excess energy to facilitate exciton separation (Figure PP2.1.7). The best EQE was almost 10% near 1000 nm, which was around double that previously reported. At this stage the best performing device had a PCE of 0.58%, which is still significantly lower than the best bulk heterojunction devices but a step forward on what has been previously reported.

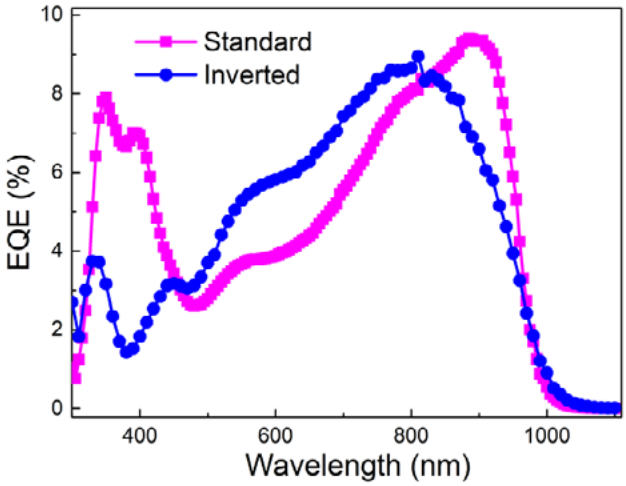

Figure PP2.1.7: The EQE of homojunction devices with the best performing material show a sharp onset near the optical gap, which is consistent with spontaneous charge generation

Finally, we developed a series of asymmetrically substituted material based on the compounds in Figure PP2.1.6 and are currently studying their properties.

Highlights

- Bulk heterojunction devices containing novel non-fullerene acceptors have been optimised to give a PCE of 11.7%.
- Twenty-five new compounds have been prepared to explore the factors that affect the dielectric constants of organic semiconductor materials. These include:
  - A series of materials of different shapes designed to have different and large dipole moments.
  - A study on the effect of end groups, which has led to an optical-frequency dielectric constant of 6.57.
- Homojunction OPV devices prepared with these materials had EQEs close to 10% at a wavelength of near 1000 nm.

Future Work

- Continue to explore the acceptor materials in bulk heterojunction solar cells, with a focus on ternary blends.
- Elucidate the factors that affect the optoelectronic properties of the materials, and in particular, the dielectric constants.
- Use the knowledge gained to synthesise the next generation of high dielectric constant materials.
- Determine the factors limiting the PCEs of homojunction devices

Singlet fission materials – toward generation 3 devices

A curious feature in some organic semiconductor materials is that when a single photon of high energy is absorbed two or more excited states at lower energy are created, a process called multiple exciton generation (MEG). In special organic semiconductors this process is called singlet fission and leads to two new excited states. It has been shown that we can create charge from each of these new excited states potentially doubling the power output of a solar cell for absorbed yellow, green or blue light, or increasing the potential theoretical efficiency of a solar cell from 32% to 44%. Even a 4–5% absolute increase in solar cell efficiency could lead to a significant 20% reduction in cost per watt of delivered power. This would lead to a step change in the efficiency of solar cells.

Singlet fission needs two closely interacting molecules, and UoM has previously developed new classes of bridged materials where the two molecules are linked allowing control of intra-molecular interactions, enhancing SF.

Now UoM have been developing a screening process to enable rapid development of new materials. By collecting data on fluorescence decay rates, and ground state bleach recovery potential SF can be identified. Although these two properties are necessary for SF, they are not sufficient to confirm SF, and this must be done using ultrafast laser spectroscopy. UoM has purchased an Edinburgh Instruments FS5 fitted with two pulsed light sources, enabling fluorescent decay rates to be determined. Addition of a Magnitude Instruments nano-second transient absorption spectrometer allows determination of ground-state bleach recovery. This allows rapid determination of potential SF materials for detailed study, or feedback into the materials design process (Figure PP2.1.8)

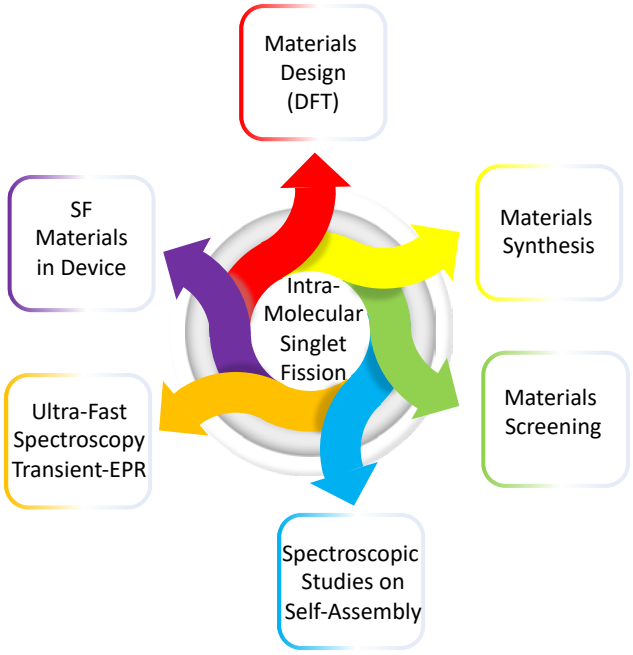

Figure PP2.1.8: Materials development flowchart used in the synthesis of new singlet fission materials. A new materials screening process will allow rapid materials discovery.

Highlights

- Screening of new materials has started using fluorescent decay rates.
- New TA spectrometer has been installed and commissioned.
- Screening on 10–-15 potential SF materials is underway.

Future Work

- Identify potential SF materials for detailed study using ultra-fast spectroscopy.
- Incorporate SF materials into devices

Devices

Aims

- To fabricate high performance OPV devices.
- Tuning of bulk heterojunction nanoscale morphology using volatile solid additives.
- Interface energetics studies of organic semiconductor and doped electron transport layer using UPS. •
- Thermally stable organic solar cell using block copolymer.

Fluorine functionalised solid additives for high efficiency organic solar cells

Nanoscale morphology control of the bulk heterojunction (BHJ) active layer in organic solar cells (OSCs) is one of the key approaches to improve device efficiencies. Among various approaches to tune the active layer morphology, the solid additive is proposed as a simple and efficient way to enable morphology tuning. In this work, the UoM researcher successfully adopted phosphine-based fluorinated materials as an additive (TPFPP, Figure PP2.1.1(a)) to fine-tune the BHJ morphology at the nanoscale and improve device efficiency. Using the solid additive TPFPP, the organic photovoltaic (OPV) device made with a PM6:BTP-eC9-based active layer reached an efficiency of 16.9% along with the simultaneous increase of short-circuit current (Jsc) and fill factor (FF)

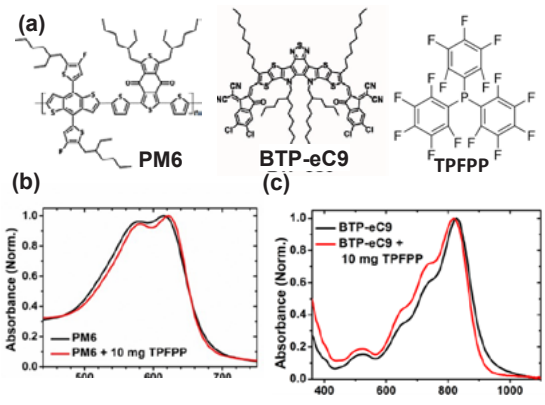

Figure PP2.1.9: (a) The molecular structures of PM6, BTP-eC9, and TPFPP; (b) UV-Vis absorption spectra of PM6 film; and (c) BTP-eC9 film with and without 10 mg/ml of TPFPP.

Table PP2.1.3: Photovoltaic performance of organic solar cell (PM6:BTP-eC9) with different concentrations of TPFPP.

Active Layer (PM6:BTP-eC9)	J_{sc} (mA cm^{-2})	V_{oc} (V)	FF (%)	PCE (%)
TPFPP (0mg)	24.2	0.82	74	15.1
TPFPP (5mg)	25.5	0.80	78	16.2
TPFPP (10mg)	25.9	0.80	80	16.9
TPFPP (20mg)	24.1	0.78	75	15.3

The chemical structures of PM6, Y6 and TPFPP are shown in Figure PP2.1.9(a). The UV-vis spectra of PM6 neat films processed with and without additives (TPFPP) are plotted in Figure PP2.1.9(b). Compared to the pristine PM6 film, the absorption spectra of the film with TPFPP additives exhibit a red-shift around 5 nm, which could be ascribed to the enhanced intermolecular pi–pi interactions among PM6. And the acceptor BTP-Ec9 film with additive shows a slightly broadened spectrum with blue-shift compared to the film without additive (Figure PP2.1.9(c)), which is attributed to H-type π-π stacking of BTP-eC9 molecules. To fabricate OPV devices, conventional device geometry of ITO/PEDOT;PSS/PM6:BTP-eC9/PFN-Br/Ag was used as shown in Figure PP2.1.10(a). The current density-voltage (J-V) curves of the device with various additive concentrations of the active layer are shown in Figure PP2.1.10(b), and the device performance parameters are summarised in Table PP2.1.10. The device without TPFPP shows a PCE of 15.1%. With the increase of TPFPP additive content, the PCE of the device improved and achieved a maximum value at 10 mg/ml additive content, exhibiting a V_{oc} value of 0.80 V, a J_{sc} value of 25.9 mA cm^{-2}, an FF value of 80%, and a PCE of 16.9%, which is a significant improvement compared to OPV devices without TPFPP additive.

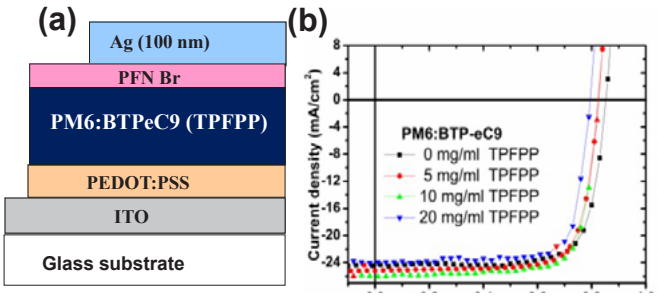

Figure PP2.1.10: (a) Schematic diagram of conventional device geometry; and (b) J-V curves of the OPV devices with various concentrations of TPFPP additives.

The influence of additives in the morphology of PM6:BTP-eC9 films was studied using atomic force microscopy (AFM). As shown in Figure PP2.1.11, the active layer films show enhanced aggregation morphology with the addition of TPFPP additive, which confirms the interaction of additives with the photoactive layer blend. At higher additive content (10 and 20 mg/ml) the surfaces exhibit excessive holes or clusters due to the evaporation of additives, And average root-mean-square (RMS) roughness increased from 0.75 nm to 4.3 nm.

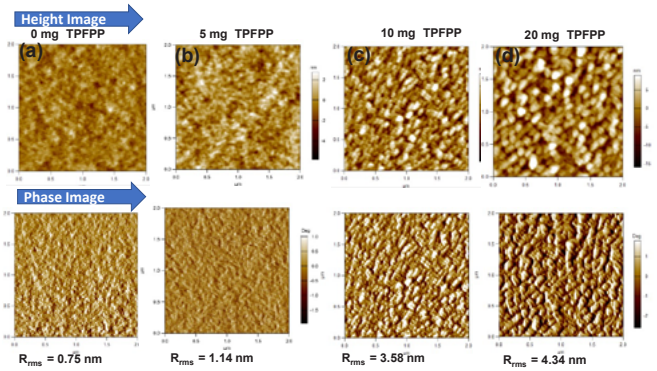

Figure PP2.1.11: AFM height (top) and phase (bottom) images of PM6:BTP-eC9 films with various concentrations of TPFPP additives (a) 0 mg/ml, (b) 5 mg/ml, (c) 10 mg/ml, and (d) 20 mg/ml.

To confirm the evaporation of TPFPP additive from the active layer upon annealing at 100°C, X-ray photoelectron spectroscopy (XPS) measurement and XPS depth-profile analysis were performed. High-resolution XPS spectra of F1s and P2p elements (Figure PP2.1.12(a), (b)) showed the absence of TPFPP peak in both annealed and non-annealed films. As shown in Figures PP2.1.12(a), (b) and (c), both XPS and depth profile analysis confirms the absence of a phosphorus P2p signal in both films. However, the absence of a P2p signal in the non-annealed film might be due to the removal of volatile additives during the ultra-high vacuum process during XPS characterisation.

To investigate the molecular interaction of TPFPP with an active layer blend, ATR-FTIR measurements were performed on the active layer blend films with and without TPFPP additives processed at RT and thermal annealing (100°C) conditions. It is known that the halogen atom in TPFPP can interact with active layer molecules containing S, N or O atoms through the formation of halogen bonding. As shown in Figure PP2.1.12(d), the peaks at 1430 and 1650 cm^{-1} are assigned to the C-C and C=0 stretching. ATR-FTIR spectra of films without TPFPP and with TPFPP processed at 100°C are identical, confirming the removal of solid additive upon thermal annealing. The blend film with TPFPP additives processed without annealing exhibits a peak shift from 1650 to 1640 cm^{-1} and 1540 to 1530 cm^{-1}, suggesting the interaction of TPFPP with the photoactive layer.

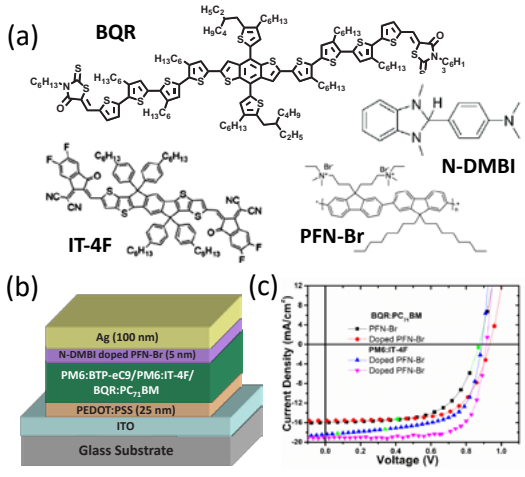

Figure PP2.1.12: High-resolution XPS spectra of (a) F1s, (b) P2p, (c) XPS-depth profile analysis of active layer with 10 mg TPFPP, and (d) ATR-FTIR spectra of PM6:BTP-eC9 films with and without TPFPP.

Interface energetics of doped electron transport layer (ETL) for efficient organic solar cells

Interface engineering of organic semiconductors is a promising strategy to improve the performance of organic photovoltaic (OPV) devices by efficient charge extraction from the photoactive layer through favourable energy-level alignment at the organic/metal interface. In addition, doping of electrode interlayer materials can be used to tune the electronic properties of the ETL layer, which can effectively suppress the recombination of carriers at the interface and improve the ohmic contact between the active layer and the electrodes. In this work, the UOM researcher adopted n-dopant materials (n-DMBF) to dope PFN-Br ETL materials to investigate the interface energetics between the photoactive layer and doped ETL layer using ultraviolet photoelectron spectroscopy (UPS) (Figure PP2.1.13).

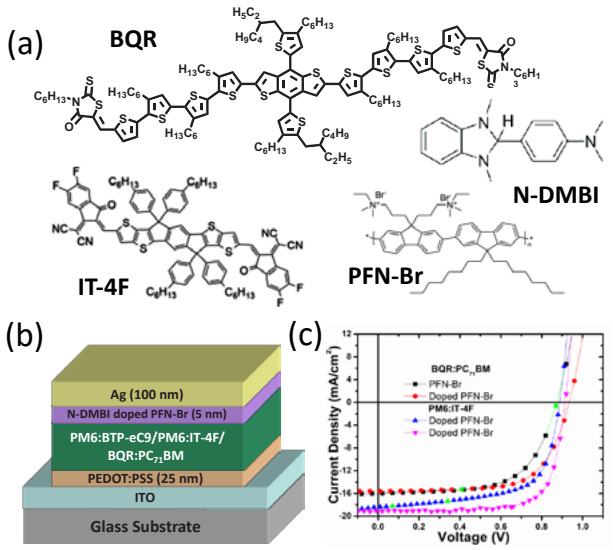

Figure PP2.1.13: (a) The molecular structures of BQR, IT-4F, PFN-Br and N-DMBI. (b) Schematic diagram of conventional device geometry. (c) Photovoltaic characteristics of the OSC with and without doping of ETL layer.

Table PP2.1.4: Photovoltaic performance of organic solar cell with and without N-DMBI doped PFN-Br ETL layer.

Active Layer	ETL Layer	J_{sc} (mAcm^{-2})	V_{oc} (mV)	FF (%)	PCE (%)
PM6:BTP-eC9	PFN-Br	24.4	0.81	78	15.5
	PFN-Br +0.05% N-DMBF	25.9	0.85	81	17.6
PM6:IT-4F	PFN-Br	18.2	0.87	68	10.7
	PFN-Br +0.05% N-DMBF	19.0	0.89	75	12.8
PM6:Pc&1BM	PFN-Br	15.9	0.86	64	8.7
	PFN-Br +0.05% N-DMBF	15.6	0.90	70	9.8

The chemical structures of BQR, IT-4F, PFN-Br and n-DMBF are shown in Figure PP2.1.13(a). To investigate the effect of the doped ETL layer on the device performance, we have used a conventional device geometry as shown in Figure PP2.1.13(b). Through optimisation, we found that 0.05 wt% doping of N-DBMI material with respect to PFN-Br shows optimum performance, and the J-V curves for the OPV devices fabricated using PM6:IT-4F, BQR: $PC_{71}BM$ and PM6:BTP-ec9 active layers are shown in Figure PP2.1.13(c). As shown in Table PP2.1.4, the OPV device performances are significantly enhanced with the doped-PFN layer and the best efficiency of 17.6%, 12.8% and 9.8% were achieved for the devices with active layer PM6:BTP-eC9, PM6:IT-4F and BQR-$PC_{71}BM$ respectively.

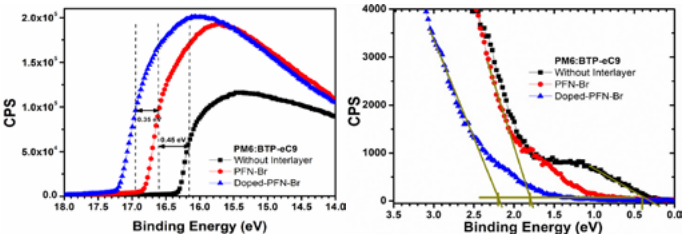

Figure PP2.1.14: UPS spectra of PM6:BTP-eC9 layer with and without ETL.

To Investigate the effect of doping the ETL layer, UPS measurements were carried out to determine the work function (WF) as well as valence band energy levels of the photoactive layer with and without the doped ETL layer. As shown in Figure PP2.1.4(a), the shift in the secondary electron cut-off (E_f) of the UPS spectrum reveals the interfacial dipole induced by the ETL layer and work function is significantly reduced from 5.07 to 4.27 eV for n-DMBI doped PFN-Br film and to 4.62 eV for the undoped ETL layer, resulting in enhanced performance of OPV devices. The change in work function causes the vacuum level shift at the interface, which facilitates the ohmic contact and efficient electron extraction at the interface as shown in Figure PP2.1.15.

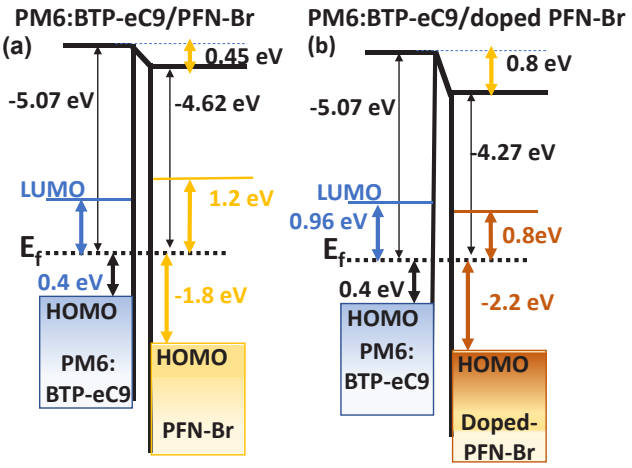

Figure PP2.1.15: Energy diagrams near the PM6:BTP-eC9/ETL interface in the vacuum level alignment (a) with PFN-Br, and (b) doped PFN-Br.

Interface engineering: atomic layer deposited zirconium-doped zinc oxide ETL

Organic solar cells (OSCs) are promising photovoltaic devices and zinc oxide (ZnO) is a commonly used electron transport layer (ETL) in OSCs. However, the conventional spin-coating ZnO layer is currently limiting its efficiency potential. For the first time we have performed

atomic layer deposition (ALD) of ZnO, which allows for controlled thin-film growth with atomic-scale control, and can effectively be used to optimise the ZnO for non-fullerene OSCs. First, density functional theory (DFT) calculations have shown the impact of doping ZnO with zirconium (Zr) on its density of states and details the synthesis of Zr doped ZnO films by ALD using a supercycle approach (Figure PP2.1.16). A 2.4% Zr concentration is found to be optimal in terms of optoelectronic properties and sufficiently low defect density. This improvement is attributed to a lower series resistance, a suppressed surface recombination, and an enhanced current extraction resulting from the Zr-doped ZnO. This work demonstrates the potential of atomic-scale engineering afforded by ALD towards achieving the ultimate efficiency of OSCs.

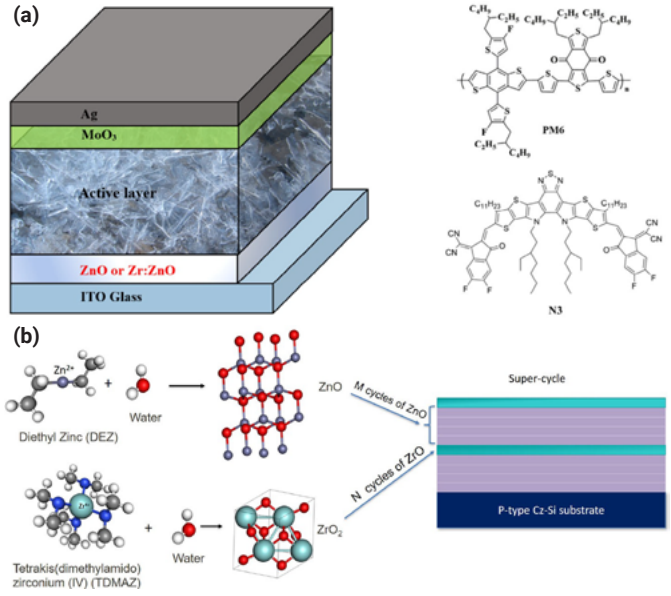

Figures PP2.1.16: (a) Schematic diagram of the inverted OSC device structure. Chemical structure of the PM6 and N3 compounds used in the active layer. (b) Pictorial representation of the supercycle process of the ALD growth of Zr-doped ZnO on a p-type Cz Si substrate. The substrate thickness to film thickness is not to scale.

Interface modification by atomic layer deposited titanium oxide

The modification of the interface layer plays a significant role in achieving performance enhancement in OSCs. The use of the atomic layer deposition (ALD) ultra-thin TiO_x to modify the interface layer in OSCs is reported. The modification with only two TiO_x ALD cycles not only effectively passivates the interface between the ZnO electron transport layer (ETL) and the active layer, but also reduces the series resistance and improves the charge transport process in the device (Figure PP2.1.17). Semitransparent OSCs are also fabricated by applying this interface modification strategy. The modification with two TiO_x ALD cycles increases the electrical device performance without affecting the optical properties of the semitransparent device. An average PCE of 10.46% with an average visible transmittance (AVT) of 19.61% and a colour rendering index (CRI) close to 100 is demonstrated for the fabricated semitransparent device with the modification (Figure PP2.1.17). The ALD-assisted interface modification provides a straightforward way to realise high performance semitransparent OSCs.

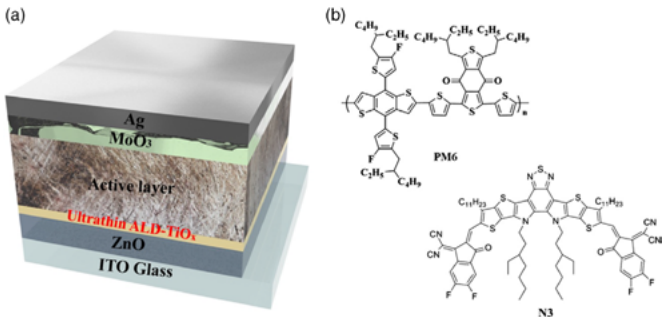

Figure PP2.1.17: (a) Schematic diagram of the OSC with the ultra-thin ALD TiOx passivation layer. (b) Chemical structure diagrams of donor material PM6 and acceptor material N3.

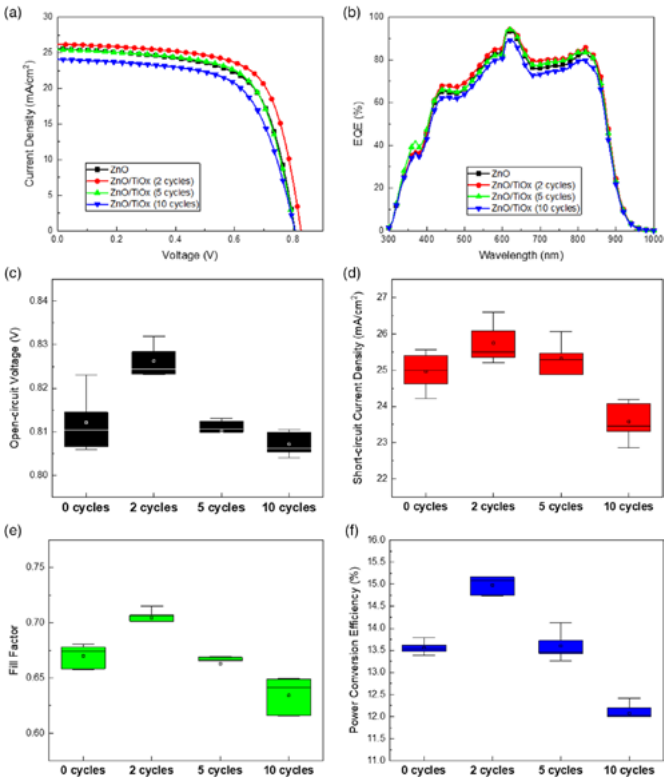

Figure PP2.1.18: (a) Current density as a function of voltage (J-V) of OSCs with a different number of TiO_x ALD cycles in between the ETL and the active layer. Measurements were done at room temperature under one-sun test conditions (AM 1.5G illumination at 100 $mWcm^{-2}$). (b) EQE spectrum as a function of wavelength for the OSCs modified with a different number of TiO_x ALD cycles. Box plot of the corresponding photovoltaic parameters including (c) open-circuit voltage (V_{OC}), (d) short-circuit current density (J_{SC}), (e) FF, and (f) power conversion versus the number of TiO_x ALD cycles.

Control of the molecular morphology in the active layer

The performance of non-fullerene, polymer bulk heterojunction (BHJ) organic photovoltaic devices has a significant correlation with the molecular morphology of the donor and acceptor. The small organic molecules coordinated to a metal oxide, an electron transport seed layer (ETSL), can profoundly modify the donor:acceptor molecular morphology of inverted organic photovoltaic (OPV) devices. Using grazing incidence wide angle X-ray scattering (GIWAXS), we have shown that a PTB7-Th:IEICO-4F BHJ active layer has a higher degree of face on molecular alignment on ETSL-1 (biphenyl-4,40 -dicarboxylic acid, coordinated to ZnO), while for naphthalene-2,6-dicarboxylic acid

coordinated to ZnO (ETSL-2), it is reduced (Figure PP2.1.20). Devices of PTB7-Th:IEICO-4F BHJ prepared on ETSL-1 had a 19.91% increase in the average power conversion efficiency (PCE), a 1.56% increase in the fill factor (FF), and a 16.66% enhancement in the short-circuit current density. The observed improvements are believed to be due to significant modifications to the oxide-BHJ interfacial region of ETSL-1, namely the elimination of nano-ridges and defect centres, along with an enhanced wettability. These factors can be correlated with the enhanced device performances, leading to the conclusion that the modulation of the molecular morphology of donor:acceptor blends by ETSL-1 has a broad impact on improving OPV cell efficiencies.

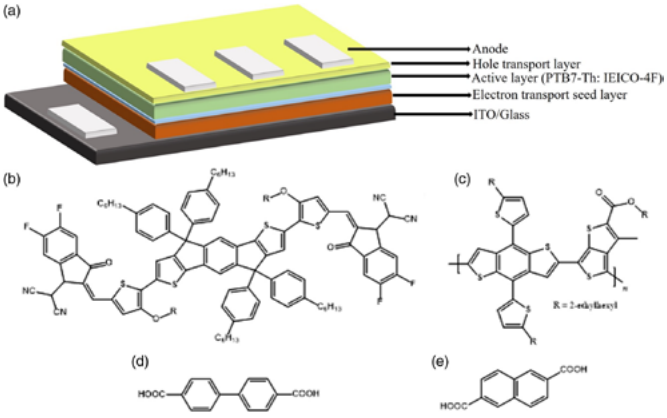

Figure PP2.1.19: (a) Device schematic of glass/ITO (cathode)/ETSL (electron transport seed layer)/PTB7-Th:IEICO-4F (BHJ)/MoO_3 (hole transport layer)/Ag (anode) inverted OPV device, (b) non-fullerene acceptor (IEICO-4F), (c) chemical structure of the donor (PTB7-Th), (d) biphenyl dicarboxylic acid (BPDC), and (e) naphthalene dicarboxylic acid (NDC).

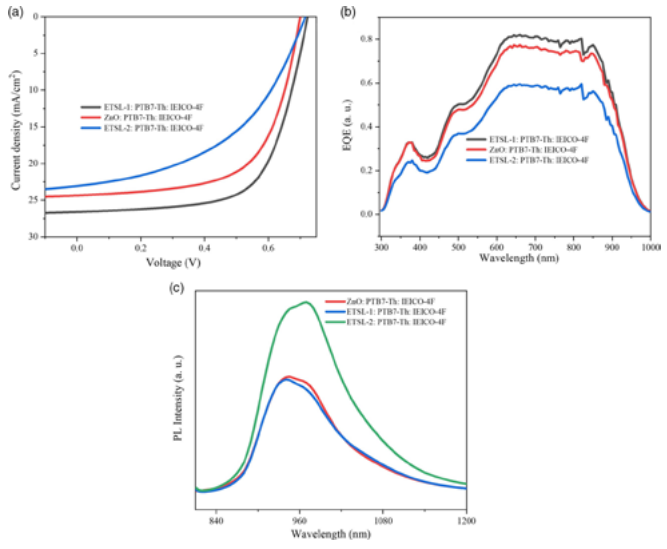

Figure PP2.1.20: (a) J-V analysis, (b) EQE analysis, and (c) PL spectrum analysis of ZnO/PTB7-Th:IEICO-4F (CN additive), ETSL-1/PTB7-Th:IEICO-4F (CN additive), and ETSL-2/PTB7-Th:IEICO-4F (CN additive).

Highlights

- Organic solar cell with PCE 17.6% was achieved.
- Interface energetics of the doped interlayer was explored using UPS.
- Thermally stable block copolymer was synthesised, and its photovoltaic properties and morphology of the film were investigated.

Future Work

- Continue to investigate the optimum doping of the ETL layer for thickness-independent interlayer.
- Explore the functional additive materials for the fabrication of highly stable organic solar cells.
- Incorporation of singlet fission materials for efficient OPV device.
- Explore new acceptor materials and device optimisation for high performance OPV devices over 18%.

PRINTING AND SCALE-UP

Aims

The ultimate aim of this activity within ACAP is the development of low-cost printing-based upscaling technologies for the fabrication of OPV. In 2022, this research focused on further progressing the digital transformation of OPV research methods that would enable the rapid optimisation of OPV technologies, thereby accelerating the translation from lab-to-fab. This program has the following aims:

- Development of a digital-technology-assisted research protocol for high-throughput fabrication of OPV and semi-automatic data analysis.
- Further development of an automatic roll-to-roll PV tester for digitalisation of optical and electrical properties of PV.
- Development of high performance and high-accuracy machine learning (ML) models to predict manufacturing parameter-dependent OPV performance.
- Demonstration of high performance printed OPV.

Progress

The record PCE for OPV has been rising rapidly since the discovery of high performance non-fullerene acceptors (NFA) and has reached almost 20% PCE (Ng et al. 2022). This rapid increase has largely been attributed to the progress in materials engineering for new acceptor materials, but process engineering has also contributed to efficiency improvements.

The key challenge in printing-based scale-up is that such laboratory technologies are typically not applicable to industrial manufacturing processes. Therefore, there has been a significant efficiency gap between printed cells and state-of-the-art laboratory cells, as the development of printing technologies for new materials requires significant time and effort.
To address this upscaling lag issue, the CSIRO team has been focusing on developing a whole new digital-technology-assisted research approach rather than making steady improvements in manufacturing processes. An automatic high-throughput fabrication and testing system, called MicroFactory, has been developed and used with digital technologies, such as machine learning (ML). ML models with various algorithms have been developed for printed OPV and the performance of each model with optimised hyperparameters has been assessed for digital PV research in the future. New materials were introduced in printed OPV and quickly optimised with the MicroFactory platform to demonstrate a record efficiency for fully roll-to-roll fabricated OPV.

MicroFactory: High-throughput PV research platform

The purpose of the MicroFactory PV research platform was to automatically fabricate and test printed PV. The platform mimics the manufacturing process and utilises a factory-like progression, with materials sequentially introduced, modified and tested on a continuous production line at a desktop scale. The high-throughput research platform enabled the fabrication and testing of over 10,000 cells/day rather than the typical 10–30 cells/day, allowing researchers to explore numerous manufacturing parameters in a day. Figure PP2.1.21(a) shows the automatic fabrication system with an industry-compatible slot-die coater and programmable syringe pumps. With this in situ formulation capability, the system can produce numerous unique cells.

The platform was first developed in 2020 and has been further developed for improved reliability and capability. The key improvement in 2022 was the introduction of a fibre-based spectrometer in the roll-to-roll tester, as shown in Figure PP2.1.21(b). The system measures not only J-V characteristics but also the absorption spectra of each cell. The input port for the spectrometer is located near the J-V testing station and the light from the solar simulator is used as a light source for the absorption measurement. The data acquisition time for the diode-array-based spectrometer is shorter than for J-V scans. Therefore, the optical characterisation of PV devices can be done without compromising the throughput (over 10,000 tests/day) of the automatic roll-to-roll tester.

Figure PP2.1.21(c) shows a screenshot of the custom software running the automatic roll-to-roll tester collecting J-V curves and UV/vis absorption spectra at the same time. The system is network-connected and all test results are digitalised and saved in an online database to be used with digital technologies.

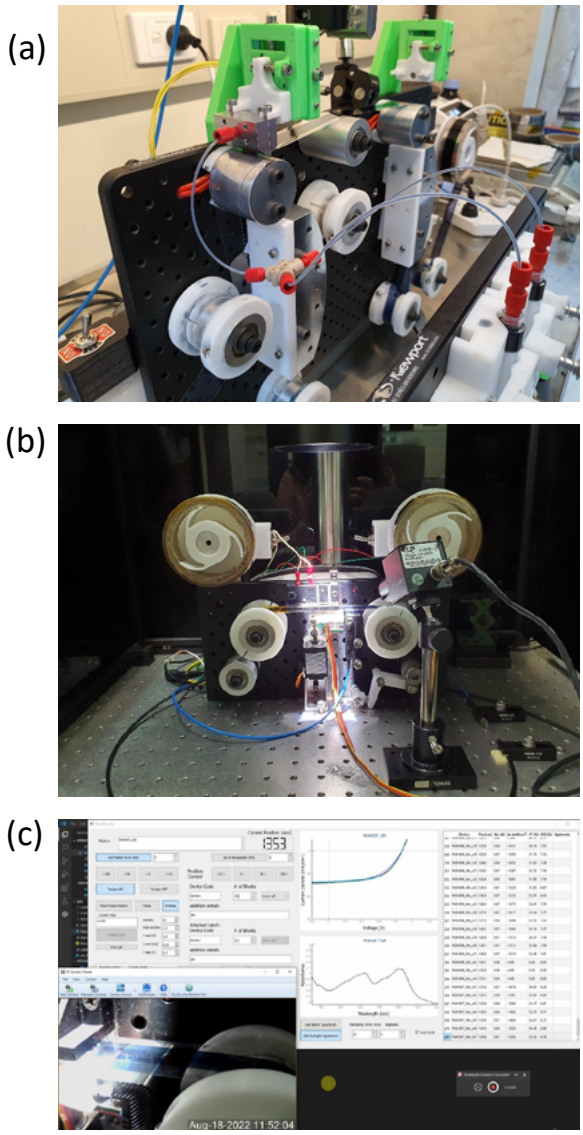

Figure PP2.1.21: Custom-built ultra-high-throughput roll-to-roll PV research platform. (a) A programmable automatic roll-to-roll slot-die coater with in situ formulator; (b) an upgraded roll-to-roll solar tester with an integrated fibre-based spectrometer; and (c) a screenshot of roll-to-roll tester showing measurements of J-V curves and UV/vis absorption spectra at the same time at >10,000 cells/day speed.

The Introduction of the spectrometer enabled verification of the composition of the roll-to-roll slot-die coated films. To demonstrate the roll-to-roll optical characterisation capability, an in situ formulation experiment was performed with three OPV materials as shown in Figure PP2.1.22. The materials have been used in a three-component photoactive layer to demonstrate colour-tuned semitransparent OPV (An et al. 2021b)The material system was chosen due to its distinctive absorption peaks. While materials with similar spectra can also be quantitively analysed via a proper spectrum analysis, the material combination was preferred for demonstration purposes. Figure PP2.1.22(d) shows the absorption spectra of a slot-die coated film with a gradient composition along the 6 m-long film. Twelve thousand spectra were obtained from the film, but only every fifth spectrum is shown for visibility. The figure clearly shows a gradually changing composition. The data has been used to quantitively analyse the composition of films and will be used as training data for ML in the future.

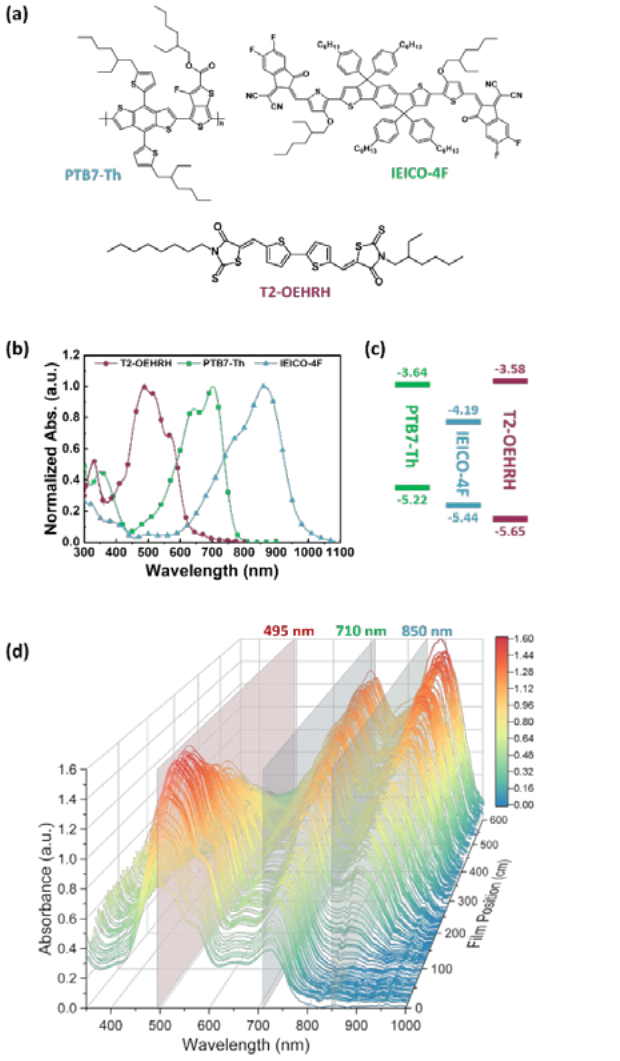

Figure PP2.1.22: An example of in situ formulated slot-die coating and roll-to-roll spectrum measurement. (a) Molecular structures, (b) absorption spectra, and (c) energy levels of donor and acceptor materials used to demonstrate colourful semitransparent OPV. (d) Absorption spectra depending on the film position of roll-to-roll slot-die coated film with a gradient composition along the 6 m-long film.

Machine learning and deep learning for OPV research

Digital technology has been introduced in printed OPV research. The first example was demonstrated by the CSIRO team in collaboration with Ulsan National Institute of Science & Technology (UNIST) (An et al. 2021a). In the first ML-assisted OPV research, ML models were developed based on a simple data set with three features. The low dimensionality was deliberately chosen to enable adequate visualisation of all parameter-dependent PCEs made by ML models. Therefore, three key fabrication parameters (the absolute quantities of three photoactive materials), were varied while keeping all other fabrication parameters constant. While the work demonstrated significant progress towards the digital transformation of PV research, it relied heavily on manual fabrication and data preparation. The project took about 10 months to produce 2218 composition-dependent PCE data sets as training data for ML.

The innovative MicroFactory platform significantly shortened the time required to produce the training data. As reported in the 2021 ACAP report, the CSIRO team produced 11,800 cells in a day and tested all of them the following day. All fabrication and performance parameters were digitalised and saved in a cloud database for ML, as well as manual data analysis. With the significantly improved data generation capability, the next important challenge was identified to be exploring various ML algorithms, including deep learning (DL), to develop high performance ML models for OPV. Therefore, the data set was used to explore ML algorithms.

The first step was exploratory data analysis (EDA) to gain insight from the features, as shown in Figure PP2.1.23. Unlike manually controlled and recorded features in the first demonstration, the MicroFactory platform records a large number of manufacturing parameters, including ambient conditions during the fabrication process. Some parameters may or may not influence the device performance, but all possible parameters are recorded to be used as features of training data for ML.

In the single-batch experiment with 11,800 cells, composition parameters were scanned from one end to the other to generate poor devices, as well as high performance devices. The low-performance device data is also important for training purposes. ML models need to learn what makes a device fail. Therefore, devices with a broad PCE range were deliberately produced. As an example, PCEs of devices depending on two key features, donor fraction and total deposition density (TDD in μg/cm², total solid contents in the unit area that is linearly related with the film thickness) are shown in Figure PP2.1.23(b). The relationship between each feature and PCE as a Pearson correlation coefficient, also known as Pearson's r, is shown in Figure PP2.1.23(c). While some features such as the humidity during a certain layer are currently not so meaningful as the data was collected from only one batch, ongoing automatic experiments will accumulate such data and further analysis with forthcoming big data will enable the identification of important manufacturing parameters

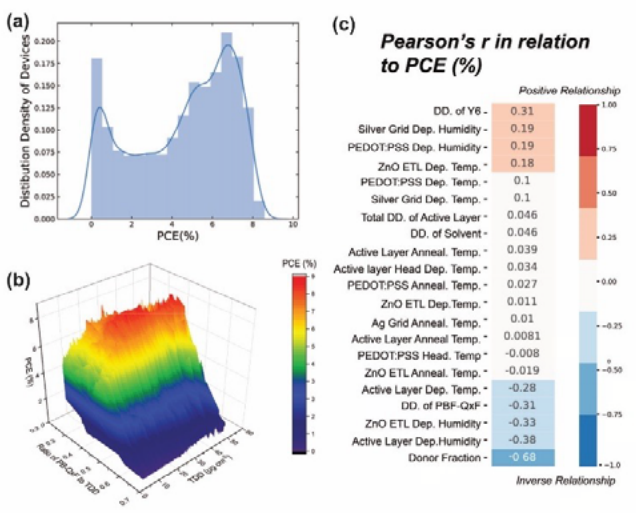

Figure PP2.1.23: Exploratory data analysis of automatically roll-to-roll fabricated OPV at 11,800 cells/day fabrication speed. (a) PCE distribution of the OPV, (b) an example of fabrication parameter-dependent PCE, and (c) the relationships between fabrication/environmental parameters and PCEs of fully roll-to-roll fabricated OPV.

ML models were then developed using freely available open-source libraries, including the widely used Scikit-Learn, TensorFlow and a relatively new eXtreme Gradient Boosting (XGBoost). Before model training, the data set was divided into three groups, i.e. training, data and validation sets. A commonly used five-fold cross-validation protocol was engaged to develop and evaluate ML models. Eighty per cent of the data sets was used for training the models and 12% of the data set was used as a test set, which is required during the training of DL (ANN algorithm) models. Eight per cent of the data sets was unseen by ML models and were used to assess the performance of each model.

All non-ANN models were optimised via GridSearchCV, Scikit-Learn's exhaustive grid search library for hyperparameters of ML models. ANN models can be designed with unlimited possibilities. Therefore, relatively simple models were designed to have a fixed number of nodes in each layer and only the number of hidden layers was varied to find the best model. Rectified linear units (ReLU) were used for all ANN models as an activation function.

The performance of all ML models is evaluated and summarised in Figure PP2.1.24(c). The R^2 score, also known as the coefficient of determination, is one of the performance evaluation measures for regression-based ML models. It represents the difference between the actual values in the data set and predictions made by the model. "1" is a perfect match and lowers the poorer performance of the model. The ML models were sorted by the R^2 score obtained from the validation set, i.e. unseen data during the training.

As expected, basic regularised regressions showed poor performance and were found not suitable for PV research. Random Forest and XGBoost, widely used ML algorithms, showed high performance with R^2 for the validation data as good as that of the best ANN model. However, the ML models show significantly better R^2 value for the training data in the figure meaning overfitting. Overfitted models work well only with training data but may fail to predict future observations reliably. Considering this fact, the five-layer ANN model showed the overall best performance. The ANN models were then used to predict optimum fabrication parameters and the parameters have been used to produce improved OPV with up to 9.35% PCE.

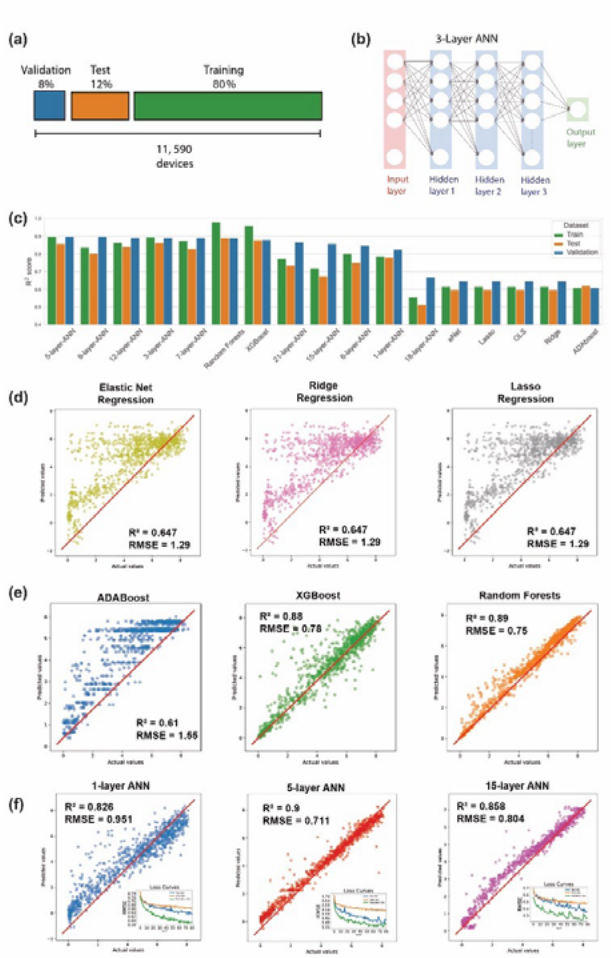

Figure PP2.1.24: Development and evaluation of ML models with various algorithms. (a) Train, test and validation split of the cleaned 11,590 device data. (b) A schematic illustration of the three-layer artificial neural network (ANN) model as an example. All layers except the output layer have 36 nodes and the number of nodes was kept constant for all ANN models. (c) R^2, one of the performance evaluation measures for regression-based machine learning models, of various ML models for training, test and validation data sets. (d)–(f) Experimental PCEs of validation data sets versus predicted PCEs by ML models with (d) regularised regressions, (e) ensemble regressions, and (f) deep learning (DL) regressions.

Rapid technology translation

The MicroFactory platform was designed to mimic the industrial fabrication process but at a significantly small scale. Therefore, the manufacturing process with newly developed materials can be developed without needing to upscale the synthesis of materials. Upscaling material synthesis has been a critical challenge to develop manufacturing technologies for OPV. When new materials are developed in research laboratories, the quantities are typically much less than 1 g. It requires significant effort and time to upscale material synthesis for conventional printing trials in research labs. Moreover, some materials are not suitable for printing due to the requirements of printing processes and upscaled high performance materials are not guaranteed to improve the performance of printed OPV. Therefore, it is very important to verify the printability of new materials before upscaling the material synthesis.

MicroFactory has played a critical role in the discovery of printable materials by screening newly developed materials with extremely low material usage. In principle, slot-die is a lossless deposition method. Therefore, the film can be fabricated with the minimal amount of precursor materials. By automatically controlling deposition parameters, it can screen various conditions with the quantity that would be used for one cell in typical research laboratories for spin-coating. As an example, the demonstration of the fabrication of 11,800 cells in a day used only 85 mg of the donor polymer. The material consumption depends on the target thickness of the photoactive layer of OPV, but 10 mg of donor polymer can produce typically 500–1000 cells. By manipulating the deposition condition during continuous fabrication, devices with various conditions can be fabricated. As a result, new materials can be screened at the very early stage of development with the MicroFactory platform. This capability has been accelerating printing-based OPV technologies and will shorten the "scaling lag".

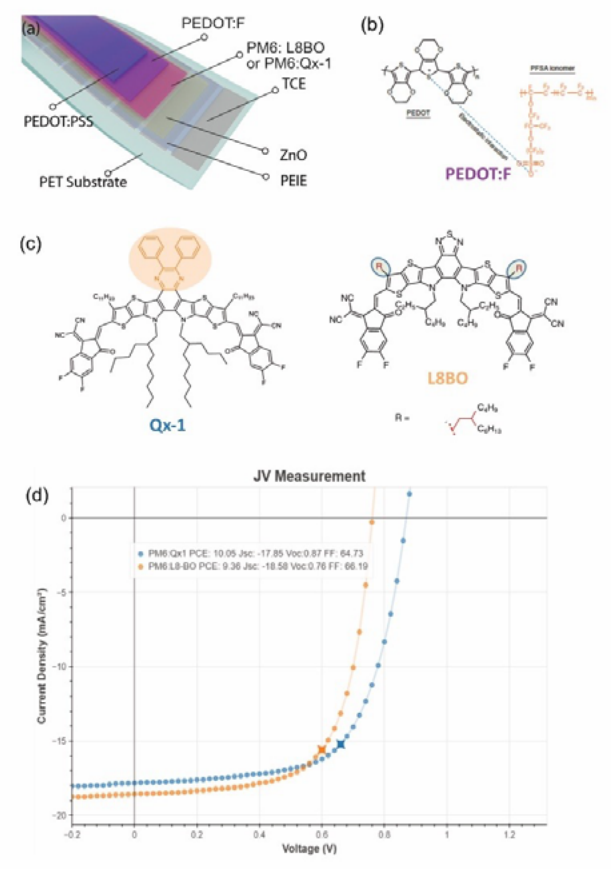

Figure PP2.1.25: Roll-to-roll printing trial of newly developed high performance materials and the first demonstration of over 10% PCE from fully roll-to-roll printed OPV. (a) The device configuration of fully roll-to-roll fabricated OPV, (b) PEDOT:F, a printable high work-function HTL, (c) newly developed high performance non-fullerene acceptors, and (d) J-V curves of fully roll-to-roll fabricated OPV with a record efficiency in its kind.

Figure PP2.1.25 shows an example of the development of high performance printed OPV using the MicroFactory platform. Qx-1 (Shi et al. 2022) and L8BO (Li et al. 2021) are new high performance NFAs. The CSIRO team acquired the materials and quickly optimised the printing parameters. PEDOT:F was also developed recently and published in Nature Energy in 2022 (Jiang et al. 2022). Through a collaboration with Huazhong University of Science and Technology (HUST, China), a small quantity of the new material PEDOT:F was received and applied to printed OPV to demonstrate 10% PCE from fully roll-to-roll fabricated OPV for the first time. Despite the rapid progress of small cell efficiencies attributed to breakthroughs in material discovery, the progress of fully roll-to-roll fabricated OPV has lagged far behind mostly due to the already explained scaling lag issue. Not including CSIRO's internal records, the highest reported PCE has been only about 7% (Carlé et al. 2017). This new development shows a leap in the record efficiency of roll-to-roll printed OPV. Considering the recent rapid progress facilitated by significantly improved research capacity via automation and the introduction of digital technologies, it is expected to continue to produce world-leading OPV technologies for commercial production.

Highlights

- Achieved 10% PCE from vacuum-free roll-to-roll fabricated flexible OPV cells for the first time.
- Further development of a globally unique high-throughput automatic PV research platform for systematic digital data generation.
- Development of high performance machine learning and deep learning models for OPV research.

Applications

Potential of semitransparent organic solar cells in agro-photovoltaic greenhouses

Agro-photovoltaics is a considerably new solar sharing concept between photovoltaic energy generation and agricultural production (Figure PP2.1.26). Agro-photovoltaic aims to promote solar energy while producing crops on the same land. Currently, agro-photovoltaics employ conventional silicon solar cells at a high cost. However, organic PV offers convenient features like panel flexibility, semitransparency, and an easier fabrication route at a lower price (Figure PP2.1.27). This work assesses and analyses the potential for semitransparent organic solar cells in agro-photovoltaic greenhouses. Semitransparent solar cells transform agro-photovoltaics from a solar sharing technology to selective solar spectrum utilisation. Organic semitransparent cells with 9.4% power conversion efficiency and 24.6% average visible transmittance are employed to design the greenhouse. For evaluation, a 3D greenhouse model is designed to simulate and compare light interaction and crop growth with both traditional and semitransparent technologies. This case study used ground-measured weather data from Geraldton (Australia), a tomato growth model, and transmittance data from a semitransparent organic solar cell having PTB7-Th: IEICO-4F as the active layer. The simulation results show a 46% increase in dry ground weight of tomato crops with the semitransparent organic solar cell compared to the conventional silicon cell agro-photovoltaic greenhouse. The simulation model shows reasonable coherence when implemented for two other locations. A thorough model analysis with economic sensitivity is performed to assess the potential usage of semitransparent solar cells in a greenhouse to yield better crop growth.

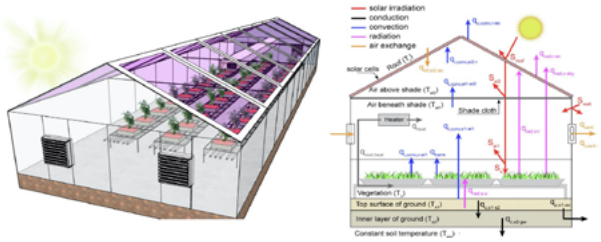

Figure PP2.1.26: Dynamic STOSCs greenhouse model. Reprinted with permission from reference 6.

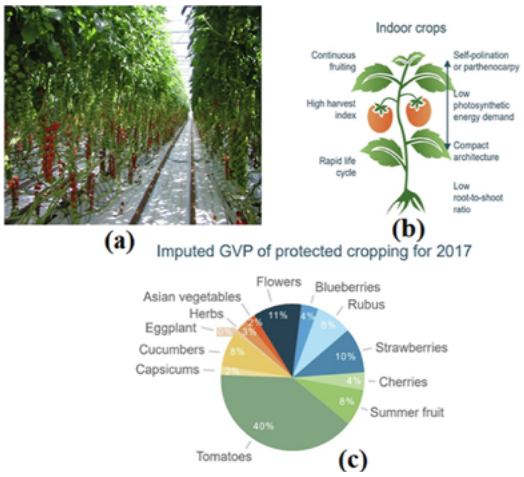

Figure PP2.1.27: (a) An image of a commercial tomato greenhouse. (b) The specifications of an indoor crop. (c) The estimated gross value of production of crops under protected cropping in Australia in 2017.

OPV for IoT application

Gestures, being regarded as one of the most natural ways for humans to communicate with anyone or anything, have sparked the integration of gesture recognition to consumer electronics. To recognise human gestures, various sensors and modalities, such as WiFi (electromagnetic), camera (image), microphone (acoustic), accelerometer (motion) and light sensor (ambient light), have been investigated and validated. These modalities, either deployed in the environment (e.g., WiFi, camera), or implemented on the device itself (e.g. microphone, accelerometer, light sensor), can achieve great gesture recognition performance in certain conditions.

UNSW have designed a system, SolarGest, which can recognise hand gestures near an organic solar-powered device by analysing the patterns of the photocurrent (Figure PP2.1.28). SolarGest is based on the observation that each gesture interferes with incident light rays on the solar panel in a unique way, leaving its discernible signature in harvested photocurrent. Using solar energy harvesting laws, we develop a model to optimise design and usage of SolarGest. To further improve the robustness of SolarGest under non-deterministic operating conditions, we combine dynamic time warping with Z-score transformation in a signal processing pipeline to pre-process each gesture waveform before it is analysed for classification. We evaluate SolarGest with both conventional opaque solar cells as well as emerging see-through transparent cells. Our experiments demonstrate that SolarGest achieves 99% for six gestures with a single cell and 95% for 15 gestures with 2 × 2 solar cell arrays. The power measurement study suggests that SolarGest consume 44% less power compared to light sensor–based systems (Figure PP2.1.29).

Figure PP2.1.28: Illustration of a transparent solar powered smartwatch with solar-based gesture recognition.

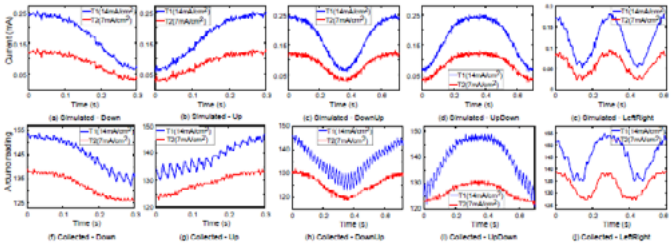

Figure PP2.1.29: Comparison of simulated gesture signal with the signal generated by solar cells.

Highlights

- Morphology control of donor and acceptor systems for different donor/acceptor based OPV devices.
- Understanding the mechanism of initial photo-degradation of OPV devices.
- Improved the OPV device efficiency and stability by interface engineering of buffer layers.
- Developed highly efficient semitransparent OPV devices with colour rendering index and transparency.

Future Work

- Continued investigation into morphology control of donor/acceptor materials in bulk heterojunction solar cells.
- Extended lifetimes study and degradation mechanism in OPV devices.Develop high efficiency ternary blend OPV devices.
- Develop highly efficient semitransparent OPV devices with high AVT for window and agro-photovoltaic applications.
- Develop high efficiency organic-organic and organic-perovskite tandem solar cells.

References

An, N. G., Kim, J. Y. & Vak, D. (2021a). Machine learning-assisted development of organic photovoltaics via high-throughput in situ formulation. Energy & Environmental Science. Royal Society of Chemistry 14, 3438-3446.

An, N. G., Lee, T., Heo, J., Kim, J. W., Song, S., Lee, W., Walker, B., Lim, E. & Kim, J. Y. (2021b). Exploiting Ternary Blends to Accurately Control the Coloration of Semitransparent, Non-Fullerene, Organic Solar Cells. Solar RRL. John Wiley & Sons, Ltd 5, 2000742.

Carlé, J. E. et al. (2017). Overcoming the Scaling Lag for Polymer Solar Cells. Joule 274-289.

Jiang, Y. et al. (2022). An alcohol-dispersed conducting polymer complex for fully printable organic solar cells with improved stability. Nature Energy.

Koster, L. J. A., Shaheen, S. E. & Hummelen, J. C. (2012) Pathways to a New Efficiency Regime for Organic Solar Cells Adv. Energy Mater. 2, 1246.

Li, C. et al. (2021). Non-fullerene acceptors with branched side chains and improved molecular packing to exceed 18% efficiency in organic solar cells. Nature Energy. Springer US 6, 605-613.

Ng, L. W. T., Woo, S., Dong, L., Chang, W., Hodgkiss, J. M. & Vak, D. (2022). OPVs New Renaissance : Advances toward roll-to-roll manufacturing of Non-fullerene Acceptor OPVs. Advanced Materials Technologies In press.

Sami, S., Alessandri, R., Wijaya, J. B. W., Grünewald, F., de Vries, A. H., Marrink, S. J., Broer, R. & Havenith, R. W. A. (2022) Strategies for Enhancing the Dielectric Constant of Organic Materials J. Phys. Chem. C 126, 19462.

Shi, Y. et al. (2022). Small reorganization energy acceptors enable low energy losses in non-fullerene organic solar cells. Nature Communications. Springer US 13, 1-10.

PP2.2 CZTS SOLAR CELLS

Lead Partner
UNSW

UNSW Team
Prof. Xiaojing Hao, Scientia Prof. Martin Green, Prof. Nicholas (Ned) Ekins-Daukes, Dr Jialiang Huang, Dr Chang Yan, Dr Kaiwen Sun, Dr Jianjun Li, Dr Xin Cui, Dr Mingrui He

UNSW Students
Heng Sun, Xiaojie Yuan, Ao Wang, Guojun He, Jialin Cong

Industry Partner
Baosteel

Other Partners
Catalonia Institute for Energy Research (IREC), LONGi Solar, IBM, NTU, NREL, Corning Research & Development Corp., University of Sydney, Tsinghua University, Chonnam National University, East China Normal University

Funding Support
ARENA, ACAP, ARC, Baosteel

Aims

All successfully commercialised non-concentrating photovoltaic technologies to date are based on silicon or chalcogenides (semiconductors containing Group VI elements, specifically Te, Se and S). The successful chalcogenide semiconductor materials, CdTe and $Cu(In,Ga)Se_2$ (CIGS), can be regarded as "synthetic silicon" where the balance between atoms in these materials provides the same average number of valence band electrons as in silicon, resulting in the same tetrahedral coordination (Figure PP2.2.1) (Walsh et al. 2012).

Cd is toxic while Te and In are among the 12 most scarce elements in Earth's crust. These factors would seem to clearly limit the long-term potential of the established chalcogenide technologies. By delving more deeply into the Periodic Table, an alternative option can be uncovered with the same number of valence band electrons on average but involving only Earth-abundant, non-toxic elements.

A kesterite Cu_2ZnSnS_4 (CZTS) compound semiconductor has emerged based on such reasoning, as a promising candidate for thin-film solar cells. Analogous to the chalcopyrite structure of CIGS, CZTS shares similar optical and electrical properties. CZTS has a bandgap of around 1.5 eV, and a large absorption coefficient of over 10^4 cm^{-1}. Notable is that the bandgap of the CZTS family can be tuned to span a wide range beyond 2.25 eV, even above the accessible range of the highest efficiency III-V cells. This makes the material suitable for tandem cells. For thin-film solar cells, energy conversion efficiencies up to 13% and 11% have been achieved so far for CZTSSe and CZTS solar cells by Nanjing University of Posts and Telecommunications and UNSW, respectively (Green et al., 2023).

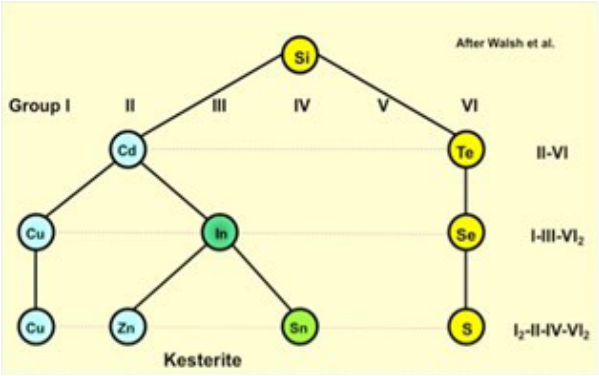

Figure PP2.2.1: The schematic of "Synthetic Si" showing how the CZTS is derived.

ACAP's work in the CZTS area takes the sputtering fabrication direction, a low-cost, high-throughput and up-scalable manufacturing process which has been used in the commercialised high performance CIGS solar cells. In this regard, CZTS offers a realistic potential to achieve the efficiency levels required for transferring lab-scale processes to commercialisation in the short term as being fully compatible with current CIGS production lines. Using kesterite materials less than two microns thick, cells can be light and flexible if grown on a flexible substrate, which has the wide applications in areas such as building integrated photovoltaics (BIPV), transport vehicles, unmanned aerial vehicles (UAVs), and Internet of Things (IoT), harvesting light and reducing greenhouse gas emissions. Work in this strand includes the development of high efficiency CZTS solar cells on soda–lime glass and flexible stainless steel.

Progress

Suppressing non-radiative recombination with a novel moisture-assisted post-deposition annealing

The performance of kesterite Cu_2ZnSnS_4 (CZTS) solar cells is known to be severely limited by the non-radiative recombination near the heterojunction interface and within the bulk of the CZTS absorber resulting from abundant deep-level defects. Herein, an effective defect engineering approach for CZTS solar cells using a newly invented moisture-assisted post-deposition annealing (MAPDA) treatment is introduced (Sun et al. 2022b). This treatment modifies the local chemical composition within the heterojunction and CZTS grain boundaries and enhances the incorporation of Cd within the CZTS layer during CdS deposition (Figure PP2.2.2). Cd not only accumulates at the grain boundaries, but it also presents in grain interiors where it occupies Cu lattice sites (Figure PP2.2.3). The overall modification of the local chemical environment suppresses deep level defects and activates relatively shallow acceptor Cu_{Zn} antisites and Cu vacancies (Figure PP2.2.4), giving rise to remarkably improved device performance (Figure PP2.2.5). The improvement is particularly significant at the heterointerface with a reduction of heterointerface defect density over one order, contributing to the suppression of SRH recombination at the heterojunction region and thereby improvement of device performance. This work opens a new direction for defect engineering of kesterite materials, which may also be applicable to other thin-film semiconductors.

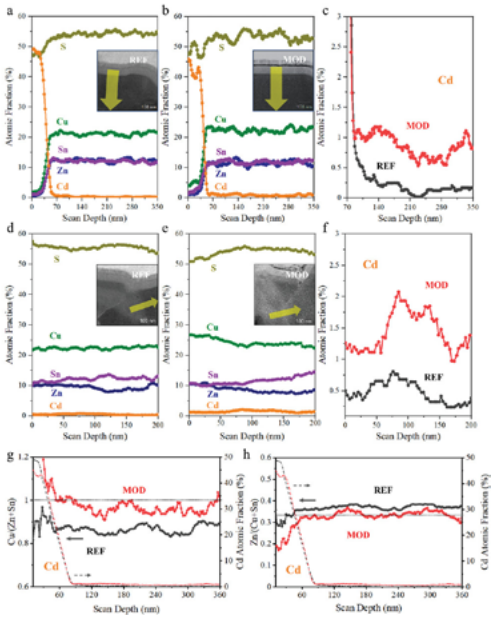

Figure PP2.2.2: (a)–(c) TEM-EDS line scans of atomic fractions of the constituent elements across the heterojunctions from the surface of CdS until 300 nm deep into the CZTS bulk; and (d)–(f) the CZTS grain boundaries from the adjacent grain interiors. The inset TEM images show the line scan directions and areas for analyses. The comparisons of trace element Cd concentrations are displayed in (c) and (f) for the heterojunctions and the CZTS grain boundaries, respectively. (g), (h) Cation ratios in the control device (REF) and the device with moisture-assisted post-deposition annealing (MAPDA) at 350°C (MOD) derived from TEM-EDS line scans shown in (a) and (b), respectively: (g) Cu/(Zn+Sn), (h) Zn/(Cu+Sn). The ideal stoichiometric ratios are shown by horizontal dashed lines.

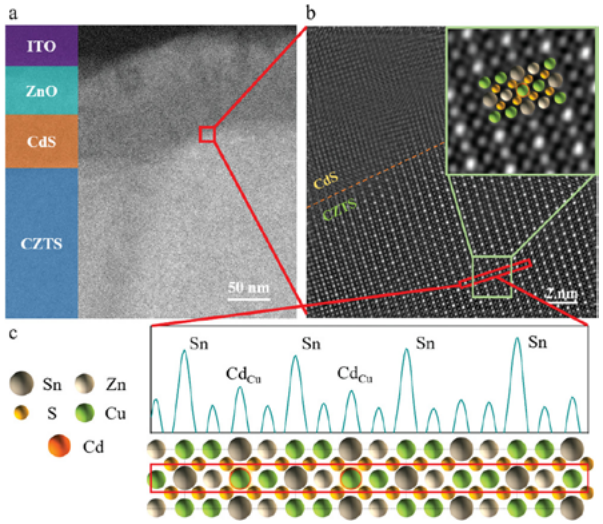

Figure PP2.2.3: (a) Bright-field TEM image of cross-sectional CZTS device using the moisture-assisted post-deposition annealing (MAPDA) treatment, with the layer identification shown schematically at left. (b) Filtered atomic resolution HAADF image of a region near the CdS/CZTS heterointerface. (c) The intensity profile of a row of cations marked by the red rectangle shows the cation exchange (Cd occupying Cu sites), with respect to the kesterite structure depicted in the bottom schema.

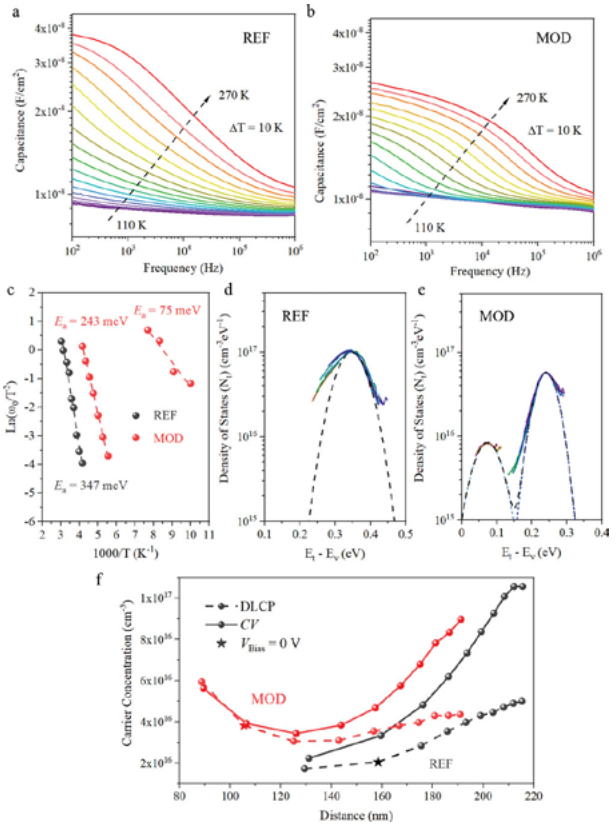

Figure PP2.2.4: Defect study through admittance spectroscopy for the control device (REF) and the device with MAPDA treatment at 350°C (MOD). (a) Admittance (C–f–T) spectra of REF. (b) Admittance (C–f–T) spectra of MOD. (c) Arrhenius plots obtained from admittance spectra. (d) Energy-resolved defect profiles of REF. (e) Energy-resolved defect profiles of MOD. (f) Carrier concentration profiles measured by C–V (solid lines) and DLCP (broken lines) at 10 kHz from +0.2 to −1.6 V DC bias.

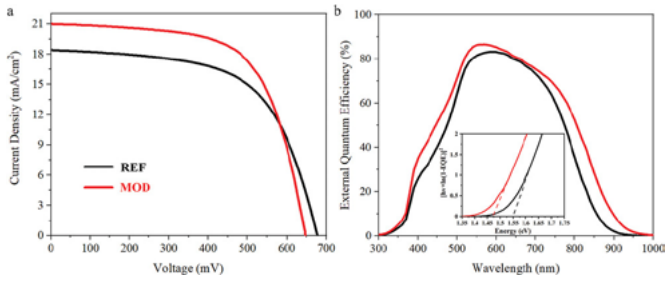

Figure PP2.2.5: (a) J–V characteristics of the control device (REF) and the device with moisture-assisted post-deposition annealing (MAPDA) at 350°C (MOD). (b) EQE spectra of these same cells. The inset image shows the [hv ×ln(1–EQE)]2 plots to determine bandgaps of the CZTS absorbers.

Furthermore, the MAPDA treatment is combined with a subsequent heterojunction heat treatment to manipulate the local distribution of Na and Cd (Sun et al. 2022a). The MAPDA treatment facilitates the controllable reduction of the Na concentration, thus promoting the spontaneous diffusion of Cd into the heterojunction region (Figures PP2.2.6 and PP2.2.7). A subsequent 150°C low-temperature heterojunction heat treatment after MAPDA treatment enables further modification of Cd and Na distributions (Figure PP2.2.8), leading to significantly enhanced optoelectronic properties at the CZTS/CdS heterojunction and greatly improved device performance with a peak conversion efficiency of 9.40% (Figure PP2.2.9). The modified heterojunction significantly improves quasi-Fermi-level splitting under low-photon injection (Figure PP2.2.10), making CZTS solar cells more feasible in low-light applications.

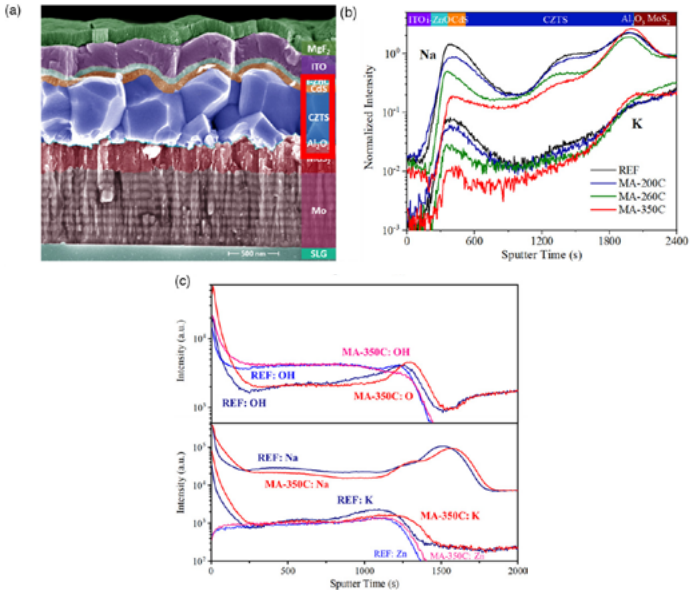

Figure PP2.2.5: Statistical data of V_{OC} (a), J_{SC} (b), fill factor (c), and efficiency (d) of the devices fabricated with Sample B (lower carrier density) and Sample C (higher carrier density). Seventeen and 13 devices are included for Sample B and Sample C, respectively. The devices with unordinary poor performance severely affected by side effects are omitted.

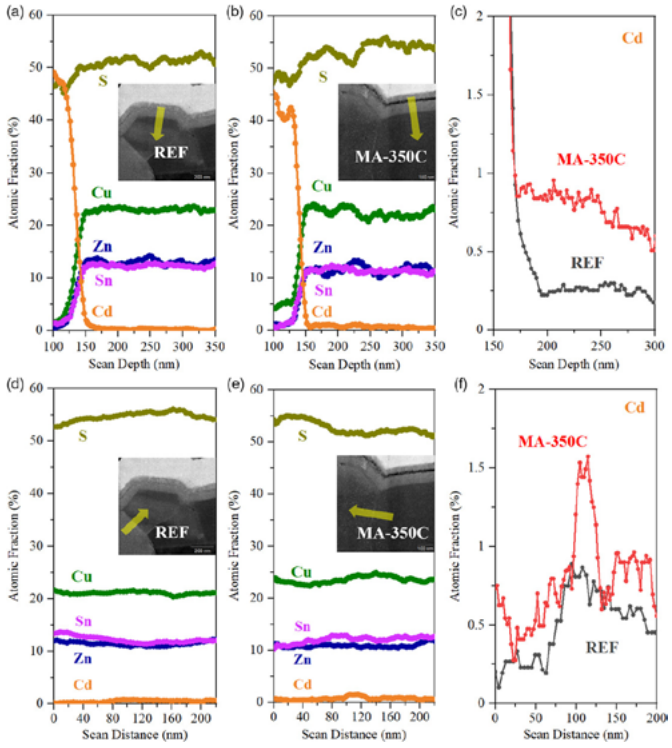

Figure PP2.2.7: Constituent elemental distributions extracted from TEM–EDS line scan (a) across a CdS/CZTS heterojunction region of the control device (REF), (b) across the heterojunction region of the device with MAPDA treatment at 350°C for 5 min (MA-350C), (c) enlarged Cd distributions from (a) and (b), (d) across the GB region of REF, (e) across a GB region of MA-350C, and (f) enlarged Cd distributions from (d) and (e).

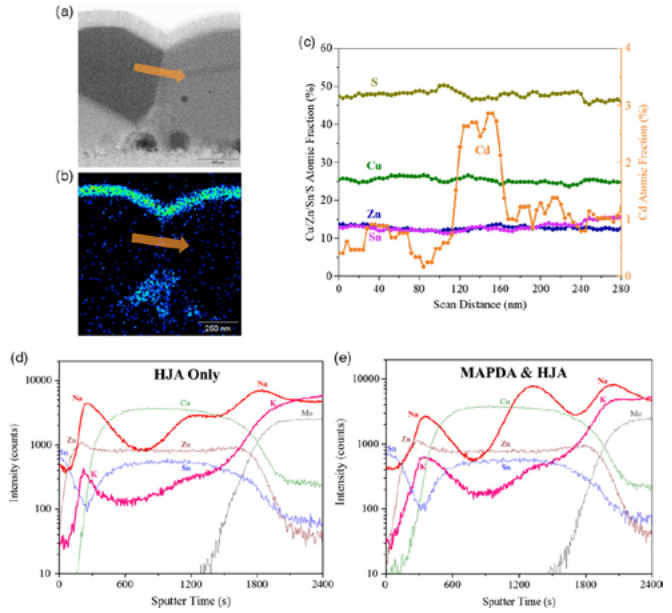

Figure PP2.2.8: TEM results for the device with combined treatments of MAPDA and HJA. Arrows indicate the direction of a line scan across a GB. (a) TEM image, (b) EDS map of Cd, and (c) line scan profiles. ToF-SIMS depth profiles from the bottom of ITO to the surface of MoS2 for devices with (d) HJA treatment only and (e) the combined MAPDA and HJA treatment.

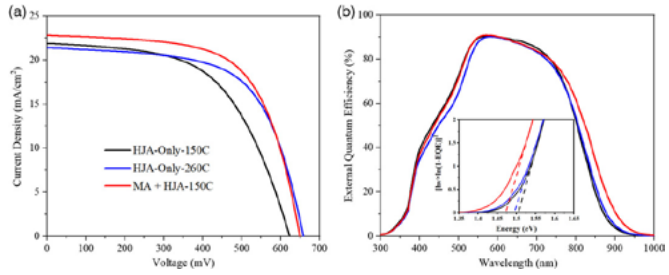

Figure PP2.2.9: Photovoltaic performance curves for the devices with HJA at 150 and 260°C and with the combined treatments of MAPDA at 350°C plus HJA at 150°C. (a) J–V characteristics of the best cells. (b) EQE spectra of the corresponding cells in (a).

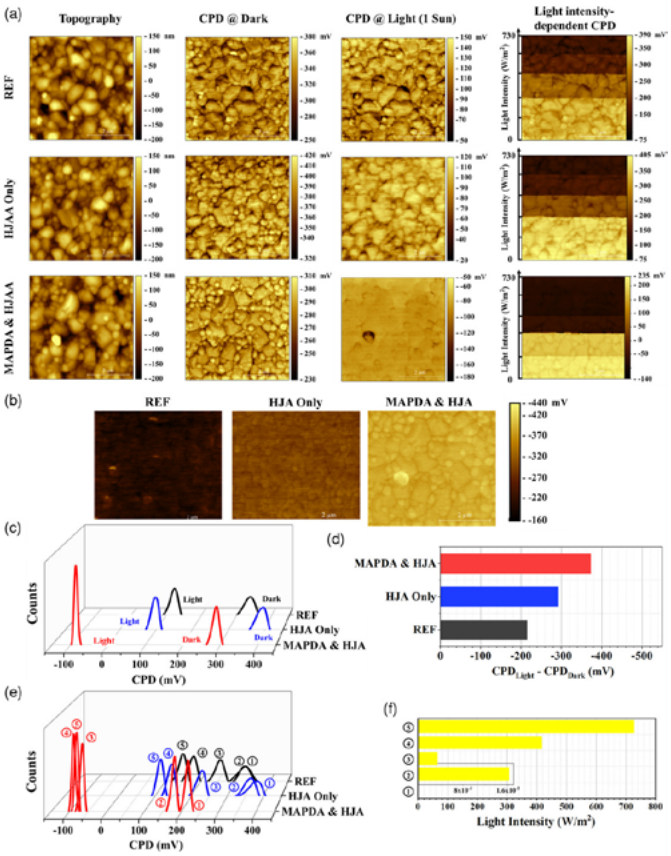

Figure PP2.2.10: KPFM measurement for CdS-coated samples: the control sample, REF, sample with HJA treatment only, and sample with the combined MAPDA and HJA treatments. (a) Raw images including topography maps and CPD maps measured in the dark, under illumination at ≈1000 W m^{-2}, and with variations in light intensity. The same scale range was used for light intensity–dependent CPD maps, providing direct visual contrast of the CPD change. The intensity values can be seen in (f). (b) Open-circuit voltage (V_{OC}) variation maps with nanoscale resolution, obtained from CPD @Light–CPD @Dark. (c) CPD distributions extracted from CPD maps measured in the dark and under illumination at ≈1000 W m^{-2}. (d) The bar chart displays the corresponding SPV values in (c). (e) The CPD distributions at each light intensity. The numbers represent the corresponding light intensity shown in (f) where a 750 nm excitation wavelength was used for all light measurements in this figure.

Liquid-phase promoted grain growth for high efficient Cu_2ZnSnS_4 solar cells

Small grain size and near-horizontal grain boundaries are known to be detrimental to the carrier collection efficiency and device performance of pure-sulfide Cu_2ZnSnS_4 (CZTS) solar cells. However, forming large grains spanning the absorber layer while maintaining high electronic quality is challenging particularly for pure sulfide CZTS. Herein, a liquid-phase-assisted grain growth (LGG) model that enables the formation of large grains spanning across the CZTS absorber without compromising the electronic quality is demonstrated (Yuan et al.). By introducing a Ge-alloyed CZTS (CZTGS) nanoparticle layer at the bottom of the sputtered precursor (Figure PP2.2.11), a Cu-rich and Sn-rich liquid phase forms at the high temperature sulfurisation stage (Figure PP2.2.12), which can effectively remove the detrimental near-horizontal grain boundaries and promote grain growth (Figure PP2.2.13), thus greatly improving the carrier collection efficiency and reducing nonradiative recombination. The remaining liquid phase layer at the rear interface shows a high work function, acting as an effective hole transport layer. The modified morphology greatly increases the short-circuit current density and fill factor, enabling 10.3% efficient green Cd-free CZTS devices (Figure PP2.2.15). This work unlocks a grain growth mechanism, advancing the morphology control of sulfide-based kesterite solar cells.

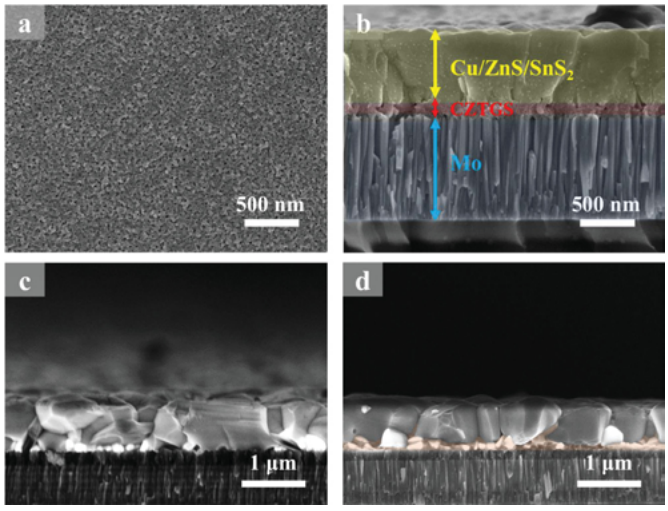

Figure PP2.2.11: (a) Top-view SEM image of the CZTGS nanoparticle layer. (b) Cross-sectional SEM image of the co-sputtered Cu/ZnS/SnS_2 precursor layer on spin-coated CZTGS layer before sulfurization annealing, and (c) the reference CZTS and (d) CZTGS-modified CZTS after sulfurization annealing. The reference CZTS film shows some near-horizontal grain boundaries in the CZTS layer, while the CZTGS-modified CZTS film shows large grains spanning the CZTS layer. A dense layer underneath the CZTS grains of the CZTGS-modified sample is colour-coded as transparent orange.

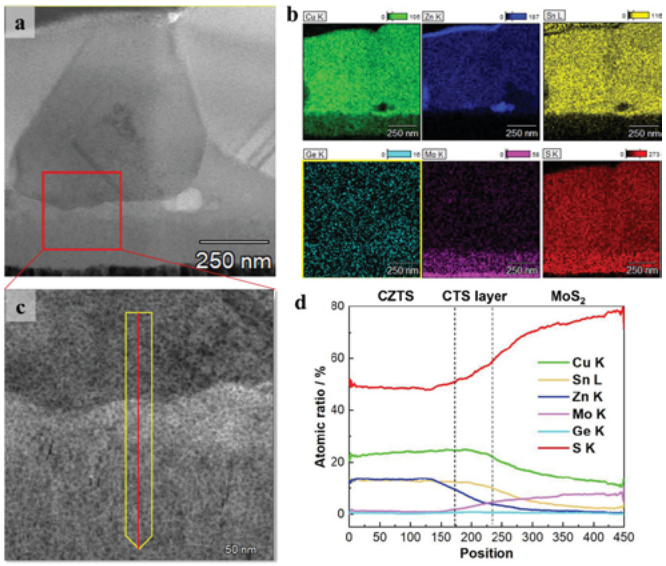

Figure PP2.2.12: (a) Cross-sectional HADDF-TEM image and (b) corresponding EDS elemental mapping of CZTGS-modified device. (c) The magnified HADDF image of a selected area [red square in (a)], and (d) the elemental line-scan EDS across the Zn-poor bottom layer (L-CTS layer) as depicted in (c). The Ge concentration was below the EDS detection limit.

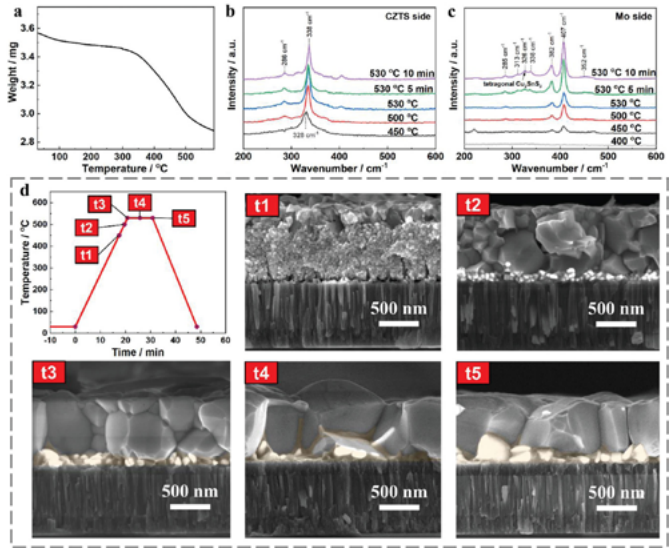

Figure PP2.2.13: (a) TGA curve of CZTGS nanoparticle film measured under N_2 atmosphere and Raman spectra of exfoliated CZTGS-modified samples at different sulfurization stages on (b) CZTS side and (c) Mo-side. Two additional peaks are marked with dash lines on Mo-side. (d) Cross-sectional SEM images of CZTGS-modified samples at different sulfurization stages. For these samples, the annealing was interrupted and cooled down to room temperature at different times t1 (450°C), t2 (500°C), t3 (530°C), t4 (530°C 5 min), and t5 (530°C 10 min), as marked in the annealing profile. A liquid-like bottom layer (orange area) forms between t3 and t5 and a reduction in the number of near-horizontal grain boundaries can be observed.

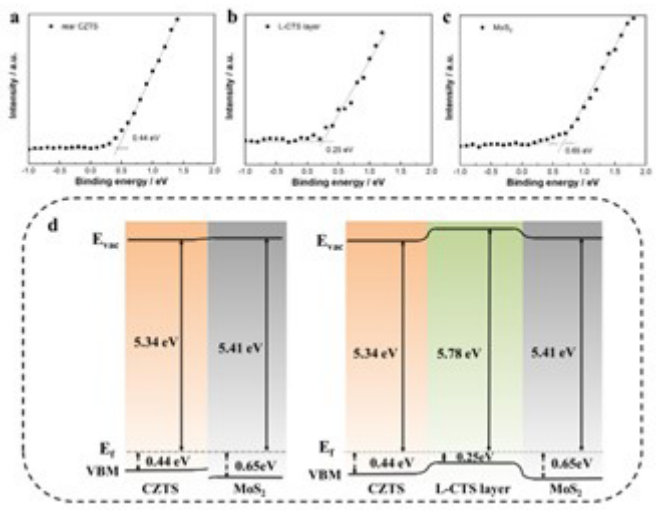

Figure PP2.2.14: XPS valence band data on (a) rear CZTS, (b) L-CTS layer and (c) MoS2. Solid straight lines are linear fits near the Fermi level (Ef) of the measured samples. The valence band maximum (VBM) can be obtained from the value of the intercept with the energy baseline (horizontal lines). (d) band structure near the rear interface of the device without (left) and with CTS layer (right).

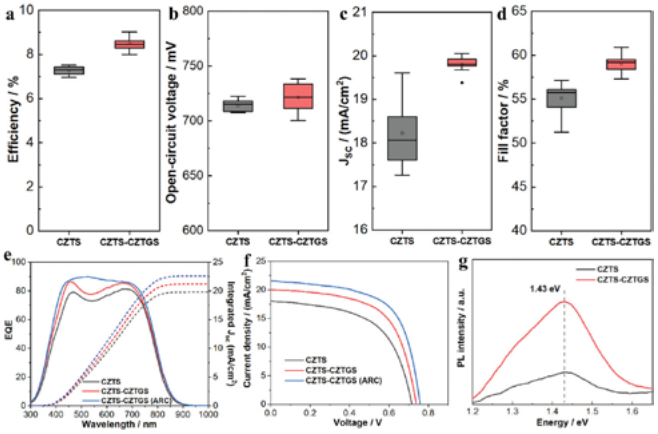

Figure PP2.2.15: Comparison of the statistical distribution of the device performances between reference CZTS and CZTGS-modified devices: (a) efficiency, (b) V_{OC}, (c) J_{SC}, (d) FF. The sample size is 12 cells for both samples which are measured based on total area device. (e) EQE curves with integrated J_{SC} (active area), and (f) light J-V curves (total area, under AM 1.5G) of the typical reference CZTS (black), CZTGS-modified CZTS without (red), and with ARC layer (blue). The integrated J_{SC} was calculated from the EQE curves and AM 1.5G spectrum. (g) PL spectra of reference CZTS and CZTGS-modified CZTS devices. The centre of the peak is marked with a dashed line.

Ge incorporation for defect engineering and phase evolution intervention

To suppress the non-radiative V_{OC} loss by engineering defect states and manipulating the phase evolution during the critical kesterite phase formation stage, a novel strategy is used by introducing a Ge cap layer on the CZTS precursor. With this Ge cap layer, CZTS grain formation is delayed at low temperatures, leading to fewer nuclear centres at the initial crystallisation stage (Figures PP2.2.16 and PP2.2.17). Consequently, the final film exhibits less unfavourable grain boundaries and enhanced grain interior quality. The remaining Ge in the absorber is also expected to reduce the detrimental

deep-level defects concentration, further contributing to improved defect states (Figure PP2.2.18). As a result, a remarkably high V_{OC} beyond 800 mV (63.2% Shockley-Queisser limit) is achieved with an efficiency of 10.7% (Figures PP2.2.19 and PP2.2.20), indicating the non-radiative recombination is effectively inhibited (Figure PP2.2.21).

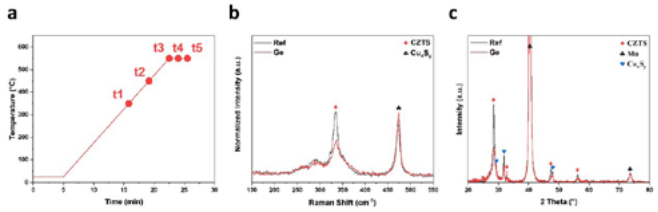

Figure PP2.2.16: (a) Annealing profiles for both Ref and Ge samples. The critical time points are t1 (350°C), t2 (450°C), t3 (550°C), t4 (550°C after 1.5 min), and t5 (550°C after 3 min). Samples are cooled down and taken out for characterisation after reaching the targeted time. (b) Normalised Raman spectra and (c) XRD patterns of Ref and Ge samples at t1.

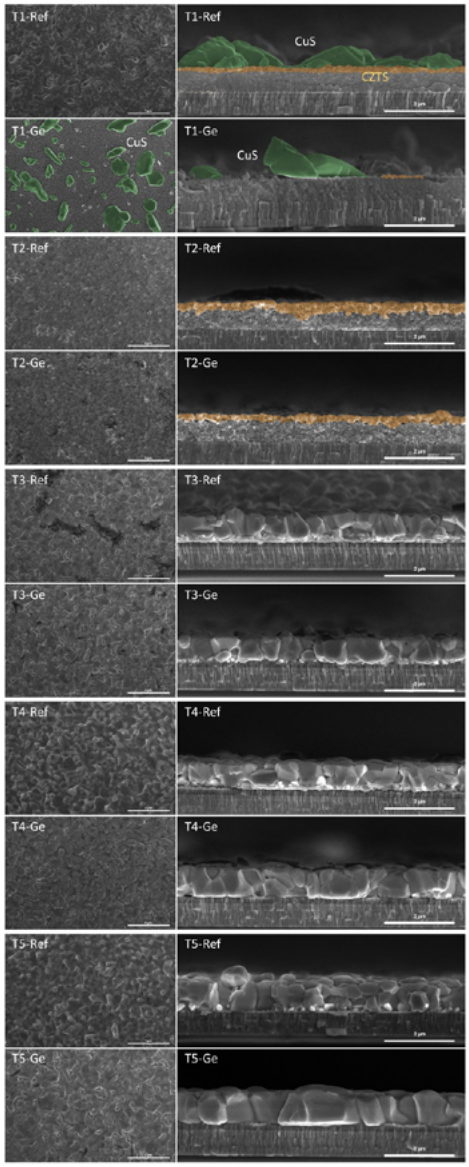

Figure PP2.2.17: Cross-section and plane-view SEM images of Ref and Ge samples from t1 to t5.

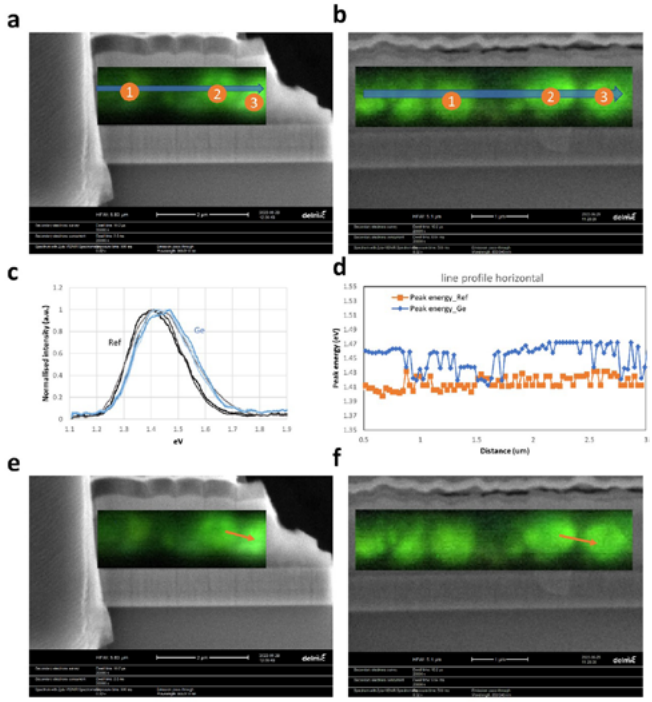

Figure PP2.2.18: CL mapping of (a) Ref and (b) Ge device with three grains of interest are marked. CL lines scan were implemented in the direction indicated by arrows. (c) CL spectra of three marked grains in Ref and Ge. (d) CL peak energy line-scan from grain 1 to 3 for two samples. Representative grain boundaries of (e) Ref and (f) Ge samples for CL signal contrast analysis.

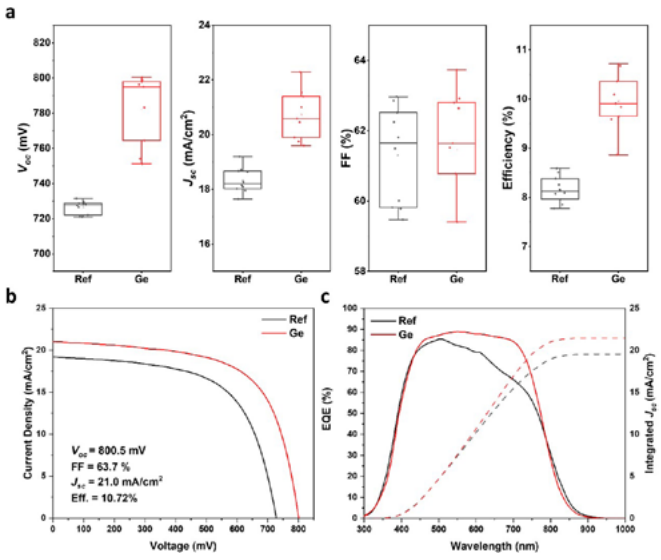

Figure PP2.2.19: (a) Statistic performance distribution of Ref and Ge solar cells on each 2.5 x 2.5 cm² sample. (b) Current density-voltage (J-V) curves of the most efficient Ref and Ge device. The photovoltaic parameters of the champion Ge solar cell are indicated. (c) EQE spectra of Ref and Ge cell with integrated J_{SC} curves. The integrated J_{SC} is slightly higher than the measured value from J-V due to the absence of metal grid shading.

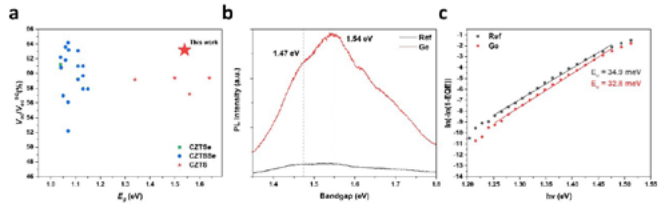

Figure PP2.2.20: (a) V_{OC} deficit determined by $V_{OC}/V_{OC}SQ$ for reported high-performance kesterite solar cells. (b) Room-temperature PL spectra of Ref and Ge device. (c) Urbach tail energy EU of Ref and Ge cell derived from EQE.

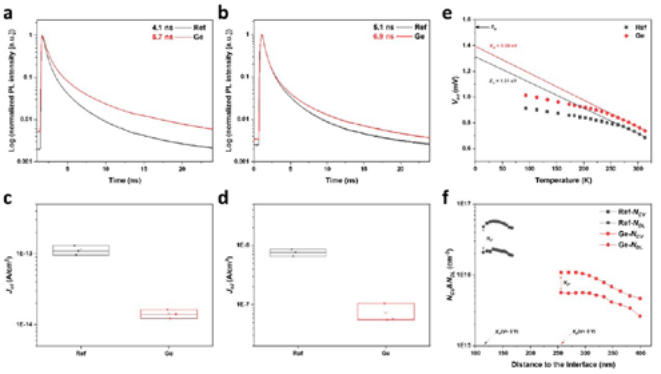

Figure PP2.2.21: Normalised TRPL measurement of Ref and Ge solar cells with a laser excitation wavelength of (a) 470 nm and (b) 630 nm. Fitted recombination current density (c) J_{01} and (d) J_{02} of Ref and Ge solar cells from Suns-V_{OC} measurement. Three representative cells on each sample are presented. (d) Temperature-dependent V_{OC} curves and fitted activation energy EA of Ref and Ge solar cells. The bandgap of 1.54 eV for the Ge cell is indicated. (f) CV and DLCP profiles of Ref and Ge solar cells. The depletion width Xd is obtained from where V = 0, and the interface defect density NIT is calculated from the difference between carrier density results from CV and DLCP at this point.

Identify the dominant microscale carrier loss mechanisms in state-of-the-art CZTSe solar cells

Understanding carrier loss mechanisms at microscopic regions is imperative for the development of high-performance polycrystalline inorganic thin-film solar cells. Despite the progress achieved for kesterite, a promising environmentally benign and Earth-abundant thin-film photovoltaic material, the microscopic carrier loss mechanisms and their impact on device performance remain largely unknown. Herein, we unveil these mechanisms in state-of-the-art (12.5%) $Cu_2ZnSnSe_4$ (CZTSe) solar cells using a framework that integrates multiple microscopic and macroscopic characterisations with three-dimensional device simulations (Figure PP2.2.20). The results indicate the CZTSe films have a relatively long intragrain electron lifetime of 10–30 ns and small recombination losses through bandgap and/or electrostatic potential fluctuations (Figure PP2.2.21). We identify that the effective minority carrier lifetime of CZTSe is dominated by a large grain boundary recombination velocity (~10^4 cm s−1, estimated using CL mapping and TRPL measurements, PP2.2.22), which is the major limiting factor of present device performance. These findings and the framework can greatly advance the research of kesterite and other emerging photovoltaic materials. This work has been published in Nature Energy (Li et al. 2022)

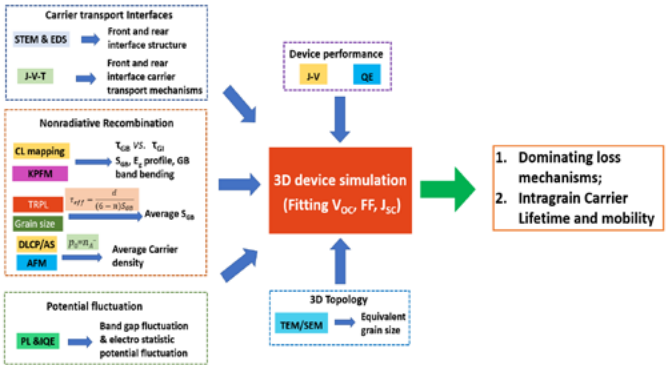

Figure PP2.2.20: The schematic diagram of the framework that linksmicroscale and macroscale loss analysis technologies using 3D device simulations.

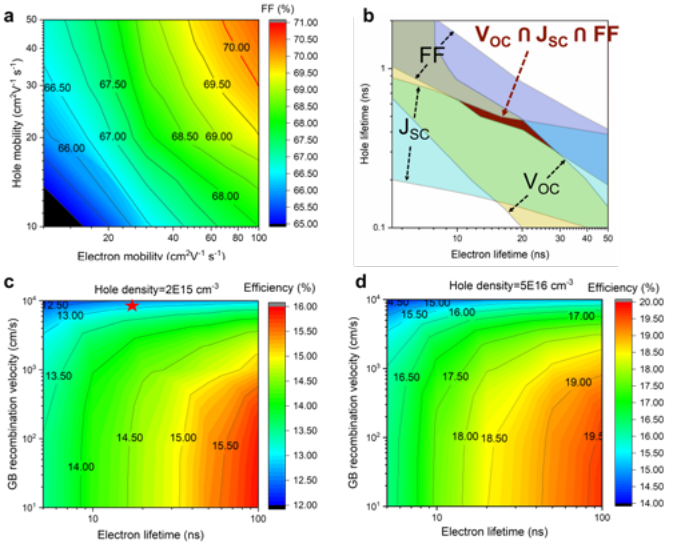

Figure PP2.2.21: Device simulations for CZTSe solar cells. (a) The simulated contour of FF versus electron and hole mobilities under fixed electron and hole lifetime of 15 ns and 0.3 ns, respectively, which are obtained from fitting J-V and EQE curves. (b) Simulated V_{OC} (light yellow), FF (light purple) and J_{SC} (light blue) versus electron and hole lifetimes within ±1% deviation compared with the experimental baseline. The overlapped region coloured in dark brown indicates where the electron and hole lifetime can well fit experimental V_{OC}, FF and J_{SC} simultaneously. The other overlapped regions indicate where V_{OC} and J_{SC} (green), J_{SC} and FF (dark blue) and V_{OC} and FF (military green) are well fitted. (c), (d) Simulated contours of efficiency against carrier lifetime and grain boundary recombination velocity under hole density of 2×10^{15} cm^{-3} (c) and 5×10^{16} cm^{-3} (d), respectively. The red star in (c) indicates the current state-of-the-art CZTSe cells. The optical loss is reduced in (d) to an extent that maximum J_{SC} can achieve 40 mA cm^{-2}.

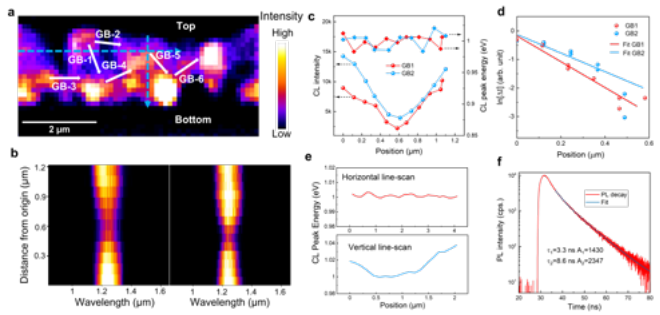

Figure PP2.2.22: CL and PL analysis. (a) Hyperspectral and intensity-combined CL map acquired at 10 keV from an FIB-prepared cross-sectional sample of a CZTSe absorber. The white arrows labelled with grain boundary numbers are where CL profiles are extracted for further analysis. The horizontal and vertical blue dash arrows indicate where line scans are taken. (b) Spectro-, spatial- and intensity-resolved CL maps of the two representative grain boundaries indicated in (a). (c) Extracted CL intensity and peak energy profiles across the two grain boundaries. (d) ln[ΔI] plots of the CL intensity profiles of GB1 and GB2 for positive distance values. The red and blue solid lines are linear regressions. (e) Extracted CL peak energy profiles along the horizontal and vertical blue dashed arrows indicated in (a). (f) TRPL measured with a 532 nm laser and its corresponding double exponential decay fit. The unit cps. means count per second.

Fabrication of a CZTSe absorber with larger grain size and high bulk-quality

Detailed microscopic loss analysis has unveiled that the grain boundaries in CZTSe are the main non-radiative recombination channels. While the strategies to passivate grain boundaries are not available, it is apparent that increasing grain size is critical for improving device performance, especially for improving the J_{SC}. We have developed a growth method to fabricate a large-grain spanning CZTSe absorber (Li et al. 2021). However, the bulk quality is reduced mainly because the top of the CZTSe absorber is no longer Zn-rich in local composition. Here, we developed a new growth method for a large-grain CZTSe absorber. By modifying the annealing procedure, a Zn-rich local composition at the top of the absorber is realised in these large-grain spanning absorbers (Figure PP2.2.23), which greatly improves the J_{SC} while remaining high V_{oc} and high efficiency (Figure PP2.2.24). The bulk quality of the large grain absorber has been improved as the Urbach tail energy reduces. However, compared to our record efficiency CZTSe, there is still room to improve (Figure PP2.2.25). On the other hand, as the J_{SC} has been improved to ~40 mA/cm^2, the electrical energy loss in the TCO emitter layer and the metal fingers significantly increases, which greatly limited the FF devices (upper limit of FF is 71% given a PFF of 79% measured using Suns-V_{OC}). Therefore, the pattern of the metal fingers is redesigned to reduce the total optical loss and electrical loss, which enables an upper limit FF of 76% given a PFF of 79% (Figure PP2.2.26). With these modifications, we can expect that the baseline efficiency can be improved to 13.5–14%. This part of the work is ongoing.

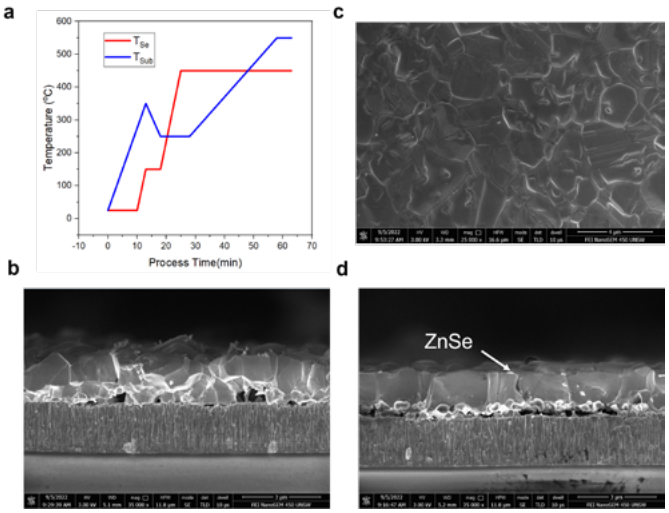

Figure PP2.2.23: (a) The annealing profile of the new growth process for a large-grain CZTSe absorber. (b) The plan-view SEM image of the large-grain CZTSe absorber. (c) and (d) The cross-section SEM images of the reference CZTSe absorber and the new large-grain absorber respectively.

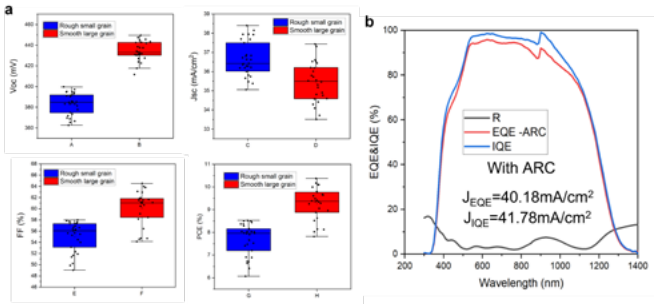

Figure PP2.2.24: (a) Statistical photovoltaic performance parameters of the reference cells and the large-grain cells. (b) The EQE and IQE of a representative large-grain cell with ARC coating.

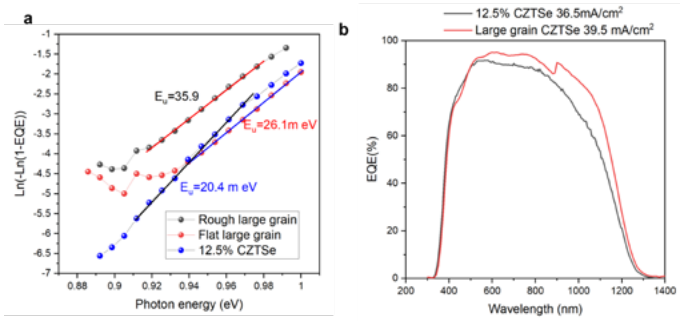

Figure PP2.2.25: (a) The fitted Urbach Energy of the reference cells and the large-grain cells, in comparison with our record 12.5% CZTSe cell. (b) The EQE curves of the large-grain cells and the 12.5% record CZTSe cell.

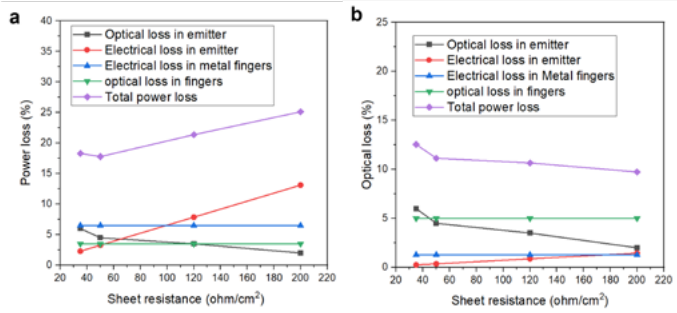

Figure PP2.2.26: The calculated optical and electrical power losses in emitter and metal fingers of the previous (a) and new (b) metal finger designs.

Highlighted progress for high bandgap chalcogenide $CuInGaS_2$ solar cells

In addition to conducting the research on CZTS solar cells, we further expanded our research capabilities to high bandgap $CuInGaS_2$ solar cells due to their promising PV properties and similar process strategies to CZTS. Pure sulfide $Cu(In,Ga)S_2$ (CIGS) is an excellent light-absorbing energy material for thin-film solar cells due to its suitable optical and electrical properties. The bandgap of CIGS can be readily adjusted from 1.5 eV to 2.4 eV by altering the Ga/(In+Ga) (GGI) ratio, making it one of the most promising upper cell candidates for the top cells in tandem solar cells. In this report, we will also include some highlighted progress on the development of this material. Our team has developed a KCN-free and H_2S-free process baseline for sulfide CIGS (He et al. 2020). This year, we further investigated the Cd-free ZnSnO (ZTO) buffer layers on CIGS and their effects on the device performance. The devices show that ZTO 2:1 contributes to better performance (Figure PP2.2.27) because of its better band alignment with the CIGS as well as less non-radiative recombination characterised by PL (Figure PP2.2.28). The temperature-dependent V_{OC} measurement shows that the recombination in our CIGS solar cells is bulk-dominated rather than interface-dominated (Figure PP2.2.29). Finally, a champion CIGS solar cell with efficiency over 14% is achieved (Figure PP2.2.30).

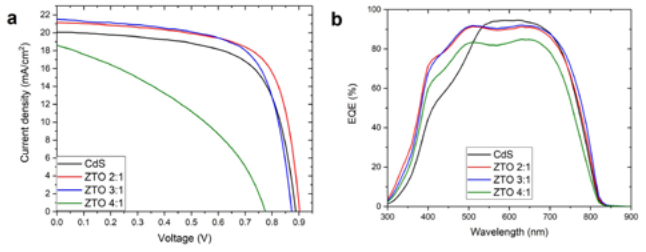

Figure PP2.2.27: (a) Current density-voltage (J-V) curves; and (b) EQE spectra of the most efficient CIGS device with different buffer layers.

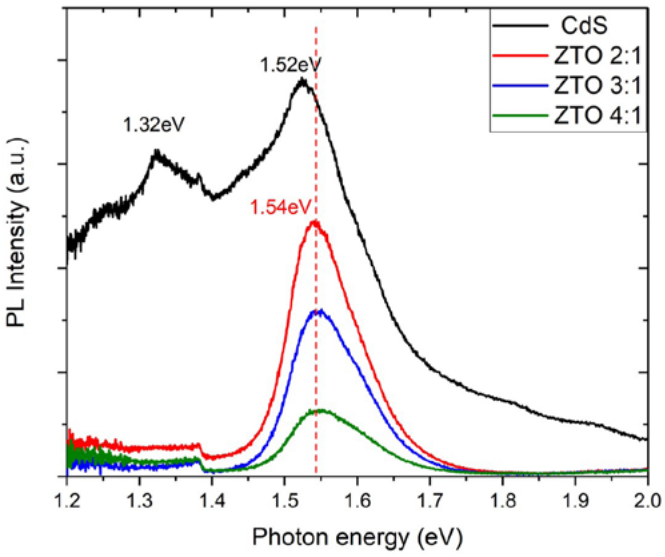

Figure PP2.2.28: PL spectra of CIGS device with different buffer layers.

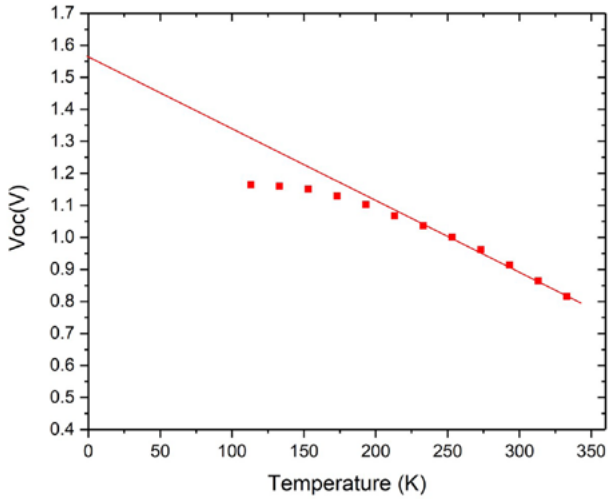

Figure PP2.2.29: Temperature-dependent Voc curves and fitted activation energy EA of champion CIGS solar cells.

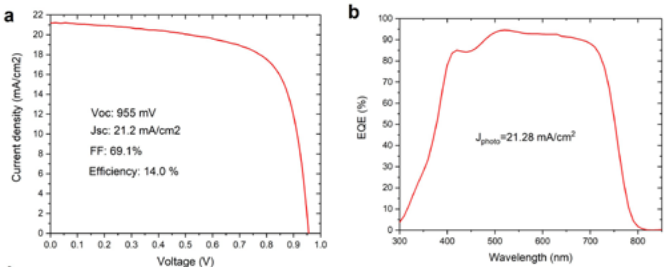

Figure PP2.2.30: (a) Current density-voltage (J-V) curves; and (b) EQE spectra of the highest CIGS device in UNSW lab.

Highlights

- A moisture-assisted post-deposition annealing (MAPDA) treatment is introduced to control the local chemical composition and regulate the defects' properties.
- A heterojunction annealing is combined with moisture-assisted post-deposition annealing (MAPDA) treatment to further suppress the interfacial and bulk recombination in CZTS solar cells.
- A liquid-phase-assisted grain growth strategy is introduced to suppress the detrimental grain boundaries and improve the carrier collection efficiency.
- A Ge incorporation process is developed for defect engineering and phase evolution intervention.
- High efficiency CZTS solar cell with in-house measurement over 11% efficiency is achieved.
- Baseline process and efficiency has been established for wide bandgap CIGS solar cells.
- ZnSnO buffer layer has been carefully tuned for achieving 14% efficient Cd-free CIGS solar cells.
- Dominant microscopic carrier loss mechanisms in state-of-the-art CZTSe cells are unveiled.
- A framework that can be used to dynamically analysis the dominant carrier loss mechanisms in thin-film solar cells has been established.
- A new growth process has been developed to fabricate a large-grain CZTSe absorber which greatly improves the J_{SC} without sacrificing V_{oc} and FF. The record efficiency of CZTSe is expected to be improved to a higher level (~14%) soon with the optimisation of metal fingers.

Future Work

Future work in 2023 will be focused on the integration of our recently developed effective strategies, including defect control in bulk and surface of kesterite absorber, bandgap grading using gradient of Ag, S and Ge substitutions, which is expected to further improve the device performance. Strategies for back surface field and hole transporting layers will be further investigated.

References

Green, M. A., Dunlop, E. D., Siefer, G., Yoshita, M., Kopidakis, N., Bothe, K. & Hao, X. 2023. Solar cell efficiency tables (Version 61). Progress in Photovoltaics: Research and Applications, 31, 3-16.

He, G., Yan, C., Li, J., Yuan, X., Sun, K., Huang, J., Sun, H., He, M., Zhang, Y., Stride, J. A., Green, M. A. & Hao, X. 2020. 11.6% Efficient Pure Sulfide Cu(In,Ga)S2 Solar Cell through a Cu-Deficient and KCN-Free Process. ACS Applied Energy Materials, 3, 11974-11980.

Sun, H., Huang, J., O'Neill, A., Yun, J. S., Young, T. L., Yan, C., Sun, K., Li, J., Nielsen, M. P., Cui, X., Wang, A., Seidel, J., Stride, J. A., Green, M. A. & Hao, X. 2022a. Manipulating the Distributions of Na and Cd by Moisture-Assisted Postdeposition Annealing for Efficient Kesterite Cu2ZnSnS4 Solar Cells. Solar RRL, 6, 2200442.

Sun, H., Huang, J., Young, T. L., Cong, J., Li, J., Sun, K., Yan, C., Soufiani, A. M., Cui, X., Nielsen, M. P., Zhang, X., Stride, J. A., Green, M. A. & Hao, X. 2022b. Defect Engineering for Efficient Cu2ZnSnS4 Solar Cells via Moisture-Assisted Post-Deposition Annealing. Advanced Optical Materials, 10, 2200607.

Yuan, X., Li, J., Huang, J., Yan, C., Cui, X., Sun, K., Cong, J., He, M., Wang, A., He, G., Mahboubi Soufiani, A., Jiang, J., Zhou, S., Stride, J. A., Hoex, B., Green, M. & Hao, X. 10.3% Efficient Green Cd-Free Cu2ZnSnS4 Solar Cells Enabled by Liquid-Phase Promoted Grain Growth. Small, n/a, 2204392.

Publications

Ghorpade, U. V., Suryawanshi, M. P., Green, M. A., Wu, T., Hao, X. & Ryan, K. M. 2022. Emerging Chalcohalide Materials for Energy Applications. Chemical Reviews.

Guo, H., Meng, R., Wang, G., Wang, S., Wu, L., Li, J., Wang, Z., Dong, J., Hao, X. & Zhang, Y. 2022. Band-gap-graded Cu2ZnSn(S,Se)4 drives highly efficient solar cells. Energy & Environmental Science, 15, 693-704.

Li, J., Huang, J., Ma, F., Sun, H., Cong, J., Privat, K., Webster, R. F., Cheong, S., Yao, Y., Chin, R. L., Yuan, X., He, M., Sun, K., Li, H., Mai, Y., Hameiri, Z., Ekins_Daukes, N. J., Tilley, R. D., Unold, T., Green, M. A. & Hao, X. 2022b. Unveiling microscopic carrier loss mechanisms in 12% efficient Cu2ZnSnSe4 solar cells. Nature Energy, 7, 754-764.

Li, J., Huang, J., Cong, J., Mai, Y., Su, Z., Liang, G., Wang, A., He, M., Yuan, X., Sun, H., Yan, C., Sun, K., Ekins_Daukes, N. J., Green, M. A. & Hao, X. 2022a. Large-Grain Spanning Monolayer Cu2ZnSnSe4 Thin-

Film Solar Cells Grown from Metal Precursor. Small, 18, 2105044.
Qian, C., Li, J., Sun, K., Jiang, C., Huang, J., Tang, R., Green, M., Hoex, B., Chen, T. & Hao, X. 2022. 9.6%-Efficient all-inorganic Sb2(S,Se)3 solar cells with a MnS hole-transporting layer. Journal of Materials Chemistry A, 10, 2835-2841.

Sun K., Liu F. & Hao X. (2022) Kesterite $Cu_2ZnSnS_{4-x}Se_x$ Thin Film Solar Cells. In: Zaidi DB, Shekhar DC, editors. Thin Films Photovoltaics [Working Title] London: IntechOpen; 2021. https://www.intechopen.com/online-first/79871 doi: 10.5772/intechopen.101744.

Sun, H., Huang, J., O'Neill, A., Yun, J. S., Young, T. L., Yan, C., Sun, K., Li, J., Nielsen, M. P., Cui, X., Wang, A., Seidel, J., Stride, J. A., Green, M. A. & Hao, X. 2022a. Manipulating the Distributions of Na and Cd by Moisture-Assisted Postdeposition Annealing for Efficient Kesterite Cu2ZnSnS4 Solar Cells. Solar RRL, 6, 2200442.

Sun, H., Huang, J., Young, T. L., Cong, J., Li, J., Sun, K., Yan, C., Soufiani, A. M., Cui, X., Nielsen, M. P., Zhang, X., Stride, J. A., Green, M. A. & Hao, X. 2022b. Defect Engineering for Efficient Cu2ZnSnS4 Solar Cells via Moisture-Assisted Post-Deposition Annealing. Advanced Optical Materials, 10, 2200607.

Sun, K., Huang, J., Li, J., Yan, C. & Hao, X. 2022c. Recent progress in defect engineering for kesterite solar cells. Science China Physics, Mechanics & Astronomy, 66, 217302.

Sun, K., Wang, A., Su, Z., Liu, F. & Hao, X. (2021). Enhancing the performance of Cu2ZnSnS4 solar cell fabricated via successive ionic layer adsorption and reaction method by optimizing the annealing process. Solar Energy 220, 204-210.

Sun, Y., Qiu, P., Yu, W., Li, J., Guo, H., Wu, L., Luo, H., Meng, R., Zhang, Y. & Liu, S. F. (2021). N-Type Surface Design for p-Type CZTSSe Thin Film to Attain High Efficiency. Adv Mater, e2104330.

Teymur, B., Kim, Y., Huang, J., Sun, K., Hao, X. & Mitzi, D. B. 2022. Top Stack Optimization for Cu2BaSn(S, Se)4 Photovoltaic Cell Leads to Improved Device Power Conversion Efficiency beyond 6%. Advanced Energy Materials, 12, 2201602.

Wang, A., Chang, N. L., Sun, K., Xue, C., Egan, R. J., Li, J., Yan, C., Huang, J., Rong, H., Ramsden, C. & Hao, X. (2021). Analysis of manufacturing cost and market niches for Cu2ZnSnS4 (CZTS) solar cells. Sustainable Energy & Fuels 5, 1044-1058.

Wang, A., He, M., Green, M. A., Sun, K. & Hao, X. A Critical Review on the Progress of Kesterite Solar Cells: Current Strategies and Insights. Advanced Energy Materials, n/a, 2203046.

Yuan, X., Li, J., Huang, J., Yan, C., Cui, X., Sun, K., Cong, J., He, M., Wang, A., He, G., Mahboubi Soufiani, A., Jiang, J., Zhou, S., Stride, J. A., Hoex, B., Green, M. & Hao, X. 10.3% Efficient Green Cd-Free Cu2ZnSnS4 Solar Cells Enabled by Liquid-Phase Promoted Grain Growth. Small, n/a, 2204392.

Zeng, Y., Huang, J., Li, J., Sun, K., Shah, U. A., Deng, H., Zhang, X., Sha, C., Qian, C., Song, H. & Hao, X. 2022. Comparative Study of TiO2 and CdS as the Electron Transport Layer for Sb2S3 Solar Cells. Solar RRL, 6, 2200435.

Zhao, Y., Yu, Z., Hu, J., Zheng, Z., Ma, H., Sun, K., Hao, X., Liang, G., Fan, P., Zhang, X. & Su, Z. 2022. Over 12% efficient kesterite solar cell via back interface engineering. Journal of Energy Chemistry, 75, 321-329.

Zhou, S., Sun, K., Huang, J., Lu, X., Xie, B., Zhang, D., Hart, J. N., Toe, C. Y., Hao, X. & Amal, R. (2021). Accelerating Electron-Transfer and Tuning Product Selectivity Through Surficial Vacancy Engineering on CZTS/CdS for Photoelectrochemical CO2 Reduction. Small 17, 2100496.

Zhou, S., Sun, K., Toe, C. Y., Yin, J., Huang, J., Zeng, Y., Zhang, D., Chen, W., Mohammed, O. F., Hao, X. & Amal, R. 2022. Engineering a Kesterite-Based Photocathode for Photoelectrochemical Ammonia Synthesis from NOx Reduction. Advanced Materials, 34, 2201670.

PP2.5 PEROVSKITES

UNSW Team

Prof. Xiaojing Hao, A/Prof. Ziv Hameiri, Dr Jae S. Yun, Dr Xu Liu, Dr Meng Zhang, Dr Ziheng Liu, Dr Arman Mahboubi Soufiani, Dr Mingrui He, Prof. Martin Green

UoM Team

Dr David Jones, Dr Jegadesan Subbiah

Monash University Team

Prof. Udo Bach, Dr Sebastian Furer, Dr Wenxin Mao, Dr Boer Tan, Dr Tian Zhang, Dr David McMeekin, Dr Nadja Glueck, Dr Sudhaker Reddy, Dr Alexandr Simonov

ANU Team

Prof. Kylie Catchpole, Prof. Klaus Weber, Dr Thomas White, Dr Daniel Walter, Dr Hieu Nguyen, Dr The Duong, Dr Jun Peng, Dr Daniel Walter, Dr Md Arafat Mahmud, Dr Yiliang Wu, Dr Heping Shen, Dr Yiliang Wu

UQ Team

Prof. Paul Burn, Dr Paul Shaw, Dr Abdulaziz Bati

CSIRO Manufacturing Flagship Team

Dr Mei Gao, Ms Régine Chantler, Dr Doojin Vak, Dr Dechan Angmo, Dr Hasitha Weerasinghe, Dr Andrew Scully, Ms Fiona Glenn, Dr Anthony Chesman

Academic Partners

ARC Centre of Excellence in Exciton Science: Dr Christopher R. Hall, Dr Stefano Bernardi, Dr Asaph Widmer-Cooper, Prof. Trevor A. Smith
University of Queensland: Prof. Ian Gentle

Monash Centre for Electron Microscopy: Joanne Etheridge, Weilun Li, Zhou Xu, Xi-Ya Fang
Sun Yat-sen University: Dr Yuhao Ren

University of Oxford, UK: Henry J. Snaith, Dr David P. McMeekin, Philippe Holzhey
Ecole Centrale de Marseille, France KIT Germany: Dr Alexander Colsmann

Korea Research Institute of Chemical Technology (KRICT): Helen Hejin Park, Hyunmin Jung
Ulsan National Institute of Science and Technology (UNIST), Korea: Prof. Sang Il Seok

Wuhan Technology University, China: Jianfeng Lu, Wei Li

Central South University, China: Prof. Junliang Yang

Wuhan University: Prof. Qianqian Lin

University of Surrey

UNSW Students

Yihao Wang, Minwoo Lee, Jihoo Lim, Yuru He, Nursultan Mussakhanuly, Ziyue Feng

Monash Students

Jie Zhao, Qianying Guo, Qingdong Lin, Siqi Deng, Wenqi Yan

ANU Students
Mike Tebyetekerwa, Naeimeh Mozaffari, Grace Dansoa Tabi

CSIRO Students
Hengyue Li

UQ Students
Hui Li, Ronan Chu, Satakshi Gupta

Aims

The aim of this section is to establish an internationally leading activity in this exciting new materials group, being consistent with the original intent of ACAP. The teams will undertake highly innovative and competitive research with a strategic focus on perovskite materials, perovskite PV device technologies and long-term stability that targets breakthroughs in the cost of solar energy. With a focus on issues that need to be resolved to enable low-cost full-scale production, the work will enhance the commercial viability of perovskites.

This section is divided into the following main areas.

1. **Perovskite material fabrication and precursor engineering:** The use of additives and precursor engineering to improve the quality and uniformity of perovskite thin films.
2. **Materials and high efficiency perovskite solar cells:** The optimisation of numerous components of the perovskite solar cells, namely quasi-2D perovskite passivation layers, hole/electron transport layer (HTL/ETL) material optimisation, and novel cell designs, to improve device performance.**Lead-free perovskites** Investigation of prospects for Pb-free perovskite materials.
3. **Material and device durability:** The examination of material properties and encapsulation approaches to address issues regarding materials and device stability.
4. **Commercial prospects and upscaling:** The demonstration of scalable deposition methods, such as R2R processing and slot-die coating, to fabricate efficient large scale devices with a view to translate the technology to the marketplace.

Progress

1.Perovskite material fabrication and precursor engineering

Innovative perovskite fabrication methods have been developed by various nodes that use additive and wet-chemical precursor engineering. These results have allowed for the demonstration of improved processing and for devices with higher stability and efficiency, which will ultimately contribute to the development of a diverse range of upscaled manufacture methods.

The team led by Professor Udo Bach and Jie Zhao developed a lead acetate ($PbAc_2$)–based precursor route to form efficient and stable formamidinium-caesium (FACs) lead perovskite thin- film solar cells (Zhao et al. 2023). The team thoroughly studied the solution chemistry of lead acetate–based precursors for FACs perovskite. Through nuclear magnetic resonance (NMR) spectroscopy analysis, the chemical side reactions and the non-perovskite by-products formed were identified. Introducing NH_4+ as the volatile cation was shown to offer a simple and versatile approach to avoid detrimental side reactions, yielding pure FACs perovskite thin films (Figure PP2.5.1). Importantly, high -quality perovskite films are produced from this precursor solution using industrially scalable blade-coating techniques to give high efficiency perovskite single cells (21.0%, mask area 0.16 cm^2) and modules (18.8%, mask area 10 cm^2) as shown in Figure PP2.5.2. Moreover, the $PbAc_2$-based PSC devices displayed improved device performance and stability compared with devices prepared via the conventional PbI_2 route. The fast perovskite crystallisation process triggered by the facile removal of acetate during post-annealing demonstrated the control of the crystallisation process to obtain high quality materials for upscaling perovskite solar cell (PSC) technology.

In addition, the Monash team in collaboration with Oxford University investigated the control of intermediate precursor phases by introducing dimethylammonium chloride additives to the perovskite precursor solution, which achieved high crystal quality polycrystalline films and also obviated the need to use DMSO in the fabrication process (McMeekin et al. 2022). In this study, the teams at Monash University and Oxford University established the degradation of DMF to formic acid and dimethylamine, which is accelerated in the presence of hydrohalic acids. Interestingly, perovskite films prepared by a DMF/acid method show larger grain sizes, improved crystal quality and reduced compositional variation after ageing compared to films prepared from the commonly used DMF/DMSO method. It was observed that films prepared from precursor solutions aged with hydrohalic acids crystallised via distinct intermediate phases. Control over the crystallisation process originated from the unintentional presence of dimethylammonium (DMA^+) iodide. Deliberate addition of DMACl to the precursor solution, instead of ageing in the solution in presence of hydrohalic acids, leads to the same improved crystallisation process with the additional benefit of having precise control over the process and hence improved reproducibility. In the presence of DMACl hexagonal polytypes are formed as an intermediate phase that can template the perovskite orientation and control the speed at which the 2H-4H-6H-3C crystallisation sequence takes place. In PSCs these improved film properties result in higher stability. Accelerated ageing of a population of devices at 65 and 85°C showed a significantly improved device stability for PSCs prepared using the DMSO-free DMACl fabrication method. T80 lifetimes of about 1410 (1190) hours for the champion (median) DMF/DMACl device were achieved, which compare to 1040 (780) hours for the control DMF/DMSO devices (Figure PP2.5.3).

In regards to the study of metal halide additives, ANU PhD student Grace Tabi led an investigation into the role of lithium iodide (LiI) as an additive in perovskite solar cells. Whereas the larger alkali metal cations K^+, Rb^+ and Cs^+ have been studied extensively as beneficial additives, Li^+ has received much less attention, with reports of both positive and negative impacts on device performance (Tabi et al. 2022). In this work, LiI was added to the precursor solution of mixed-cation, mixed-halide perovskite films and solar cells and changes in device performance, film quality and optoelectronic properties were tracked as a function of LiI concentration.

Optimum device performance was found for a LiI concentration of 0.5%, resulting in a power conversion efficiency (PCE) of 21.5%, compared to 20.4% for undoped control cells (Figure PP2.5.4(a), (b)). The optimised cells also exhibited low current-voltage hysteresis across a wide range

of scan rates, whereas the control cells showed a significant scan-rate dependence (Figure PP2.5.4(c)).

Morphological and optoelectronic properties were investigated to identify the physical origin of the device performance trends. Comparison of doped and undoped films at low LiI concentrations revealed improved crystallinity with fewer lateral grain boundaries as seen in Figure PP2.5.5(a). These changes correlated with a reduction in non-radiative recombination and improved charge carrier mobility, consistent with the increase in open-circuit voltage and fill factor of the optimised devices. Optoelectronic simulations also showed that the low hysteresis observed in Figure PP2.5.4(c) for the 0.5% LiI-doped cells is consistent with low non-radiative recombination.

While the reduced hysteresis in the 0.5% LiI devices can be attributed to defect passivation, the transient response (Figure PP2.5.4(c)) at higher doping levels appears to be correlated to the changing ionic transport properties of the perovskite films. The team investigated this with chronopotentiometry (CP) measurements using the lateral contact structure where a step current was applied between the contacts while measuring the transient voltage. The resulting transient voltage curves are plotted, showing a qualitative change in behaviour with increasing LiI concentration, along with a dramatic reduction in the response rate. Comparing these results to numerical ionic drift-diffusion simulations, it was found that the observed trends are consistent with an initial reduction in mobile ion concentration up to 5% LiI concentration, followed by an increase in either the ion mobility or concentration between 5% and 10% LiI. This last change is correlated to a dramatic decrease in device performance for the 10% LiI devices.

In this work, LiI was found to improve the film quality and reduce bulk non-radiative recombination when introduced at very low concentrations. However, it is detrimental to device performance at higher concentrations. This may explain the conflicting reports of both positive and negative impacts of Li^+ doping in the literature. The transient measurements also revealed significant changes in the ionic properties of the doped films at higher LiI concentrations.

In other work, the effect of potassium iodide as an additive in inorganic perovskite $CsPbIBr_2$ and $CsPbBr_3$ was investigated by the team at Monash, led by Professor Udo Bach, Qianying Guo and Dr Tian Zhang. The major impacts from potassium incorporation into $CsPbIBr_2$ perovskite materials were thoroughly studied and a unique highly preferential oriented grain formation at high temperature was discovered, as shown in Figure PP2.5.6(a). Through X-ray diffraction analysis, scanning electron microscopy, grazing-incidence wide-angle X-ray scattering and transmission electron microscopy characterisation the major microstructure feature, including the grain size, orientation, and twinning domain structure, were observed and analysed. Importantly, uniaxially textured, smooth-surface polycrystalline thin films were achieved with a grain size of up to eight microns and alignment parallel to <101>. Possible underlying mechanisms are proposed to be related to potassium-induced low dimension phase materials. In addition, not only the microstructural changes are identified, but the solar cell performance of the $CsPbIBr_2$ perovskite was also investigated to show the improvements (Figure PP2.5.6(b)).

Organic additives were another class of material that have been widely recognised to be effective in perovskite precursor solutions. In their 2021 report, UQ introduced three fluorinated additives that all had a 2,3,4,5,6-pentafluorophenyl head and ammonium iodide tail that differed in the number of methylene units between the head and tail (Figure PP2.5.7). It was found that the length of the alkyl linker controlled the distribution of the fluorinated additive in the perovskite film and the overall device performance. Of the three additives, inverted devices containing 0.32 mol% of the 2,3,4,5,6-pentafluorophenyl ammonium additive with the methylene linking group (FMAI) achieved a maximum power conversion efficiency of 22.0% (Li et al. 2022). In 2022 UQ built on these results in two ways: first, exploring the effect of changing the counter anion from iodide to bromide (FMAI to FMABr), and second, using the fluorinated materials in combination with anode interlayer modifiers.

In their first study, UQ combined these two concepts by comparing methylammonium lead triiodide (MAPI)–based inverted planar perovskite solar cells with the basic architecture glass/ITO/PTAA/PFN-P2/perovskite/$PC_{61}BM$/BCP/Cu where PTAA = poly[bis(4-phenyl)(2,4,6-trimethylphenyl)amine, PFN-P2 = poly[(9,9-bis(3-(N,N-dimethylamino)propyl)-2,7-fluorene)-alt-2,7-(9,9-di-n-octylfluorene)], BCP = bathocuproine and $PC_{61}BM$ = [6,6]-phenyl-C_{61}-butyric acid methyl ester. The UQ team found that in line with their previous work on fluorinated additives that the devices containing 0.32 mol% of the FMABr had the best performance. The key results from the study were that when FPAI was added to the PTAA anode-modifying layer and FMABr was blended into the perovskite layer, hole extraction was improved and the perovskite film had reduced surface defects at the grain boundaries. The inverted devices containing an FPAI-treated anode-modifying layer and 0.32 mol% of FMABr in perovskite precursor solution led to inverted PCEs with a maximum power conversion of 22.3%, which was an absolute increase of 1.7% compared to the $MAPbI_3$ device (20.6%) of the same architecture but without the additives (Figure PP2.5.8). A critical feature of the devices is that the J-V scans showed minimal hysteresis between the forward and reverse scans.

Furthermore, the UQ team also investigated the use of a fluorinated additive to improve the performance of perovskite solar cells that used a p-type inorganic nickel oxide (NiO_x) interlayer. NiO_x has high transparency and tunable optoelectronic properties, but generally possesses surface defects that lead to high interface recombination and has an energy offset with the ionisation potential of perovskite films that reduces hole extraction. The UQ team found that FPAI could successfully be used to modify the electronic properties of the NiO_x anode interlayer. Critically, the FPAI treatment increased the work function of the NiO_x and improved charge extraction as well as providing a surface on which good perovskite crystal growth occurred, providing films with reduced surface defects. The better matching of the NiO_x work function and perovskite ionisation potential led to an increased V_{oc} compared with the control devices without FPAI modification –1.05 V versus 1.00 V, and a higher short-circuit current and larger fill factor. The devices had the architecture ITO/NiO_x/with or without FPAI/perovskite/LiF/C_{60}/BCP/Cu, where the perovskite layer had the structure $Cs_{0.05}[(FAPbI_3)_{0.85}(MAPbBr_3)_{0.15}]_{0.95}$ (CsFAMA). As a result, the best PSCs with the FPAI modified NiO_x had power conversion efficiencies of 19.3% (Figure PP2.5.9). It was noted that the concentration of FPAI used had a fine tolerance in improving the performance, with a concentration of 3 mg/mL leading to

poorer performance. Finally, a somewhat unexpected bonus was that the FPAI modified NiO_x interlayer–based devices were found to be more stable than the devices containing unmodified NiO_x. Under continuous illumination the PCEs of both device types were found to gradually increase over the first 30 minutes of illumination, which has previously been ascribed to the UV light releasing adhered perovskite precursor ions from the surface of the NiO_x films. However, the device containing the modified NiO_x retained 96% of its initial PCE at maximum power point after 80 minutes (duration of the experiment), while the device containing the unmodified NiO_x lost more than 10% of its efficiency.

Finally, the UNSW team also reported their discovery of using tetramethylene sulfoxide (TMSO) to improve their gas-quenching fabrication method. Gas quenching is a promising technique for the upscalable fabrication of PSC. However, it has been challenging to produce high quality gas-quenched perovskite film without the use of the methylammonium (MA) cation. By employing tetramethylene sulfoxide (TMSO) as a ligand in the precursor solution, high quality $FA_{0.9}Cs_{0.1}PbI_3$ perovskite films have been successfully obtained by gas-quenching. Study of the precursor solution and film-forming process revealed the effect of TMSO on the formation of large-grain films. The MA-free perovskite device exhibits superior stability over the PSCs produced with a MACl additive. The fabricated MA- and Br-free PSCs showed an efficiency of over 21% on small-area devices and 20% on 1 cm^2 devices without any passivation treatment. Moreover, this method enabled a wide gas pressure processing window and superior accessibility to low pressure processing, demonstrating its promising potential in upscaling the manufacturing of high efficiency MA-free PSCs.

2.Materials and high efficiency perovskite solar cells

Conventional three-dimensional (3D) perovskite films suffer from structural defects/trap states in their bulk and at interfaces with charge transport layers, which leads to non-radiative carrier recombination, and instability caused by strong interaction with moisture and oxygen from the ambient environment (Conings et al. 2015). To achieve high device performance and stability improvements, ACAP research nodes focused investigations on a number of perovskite passivation schemes, including quasi-2D perovskite passivation, hole/electron transport layer (HTL/ETL) material optimisation, and novel cell designs.

In terms of perovskite passivation utilising 2D Ruddlesden–Popper (RP) perovskite, the ANU team led by PhD student Naeimeh Mozaffari and Dr The Duong developed a novel passivation strategy for perovskite solar cells using a mixture of guanidinium (GA) and n-octylammonium (n-OA) cations, which were known to form one-dimensional (1D) perovskites and two-dimensional (2D) perovskites, respectively (Mozaffari et al. 2022). The team found that the bi-cation passivation layer formed a 1D/2D perovskite film on top of the 3D perovskite (Figure PP2.5.10), leading to a more hydrophobic and smoother surface than the uncoated film. A smooth surface can diminish non-radiative recombination and enhance charge extraction at the interface making better contact with the transport layer, resulting in improved short-circuit current. In addition, space charge–limited current measurements show a three times reduction in the trap-filled limit voltage in the mixed-cation passivated sample compared with unpassivated cells, indicating fewer trapped states.

The bi-cation passivated devices show greatly enhanced performance compared to mono-cation passivated and non-passivated devices (Figure PP2.5.11). The champion device showed a PCE of over 23%,V_{OC} of over 1.21 V, and negligible hysteresis.

Quasi-2D perovskites with RPPs offer enhanced stability and have been extensively explored to replace their 3D counterparts (Cao et al. 2015; Huang et al. 2020). The general formula of RPPs can be described as $R_2A_{n-1}Pb_nI3_{n+1}$, wherein A is the small-size ammonium cations (MA^+/FA^+), R is the spacer cations with long alkyl or aromatic chains (such as butylammonium or phenethylammonium, BA^+/PEA^+), and n represents the number of $[PbI_6]^{4-}$ octahedral layers composing the inorganic slab that is sandwiched by two layers of R+ cations (Stoumpos et al. 2016). The hydrophobicity and high dielectric constant of R+ are responsible for the robustness of quasi-2D perovskites against phase segregation and ion migration, making them highly attractive for constructing PSCs with long-term stability under ambient operating conditions.
The processing strategies for 2D perovskites for photovoltaics fall into two categories. One is overlaying a horizontally aligned 2D perovskite (parallel to the substrate) with a slab thickness of n = 1 or 2 on the surface of the 3D perovskite by either spin-coating or solid-transfer methods to form a 2D/3D stacking structure (Jang et al. 2021; Wang et al. 2017; Wu et al. 2022). This 2D protective capping layer can prevent oxygen and moisture from permeating into the 3D perovskite layer. However, this conventional method for depositing the ligands, which involves using a diluted ligand solution in isopropyl alcohol (IPA) and spin-casting at a very high speed, is not applicable for slower deposition processes, such as doctor blading or slot-die coating, due to damage to the perovskite film by IPA, and is thus not appropriate as a post-deposition strategy for large-scale fabrication.

The second processing strategy is constructing the active layer entirely from the quasi-2D perovskites with a designated slab thickness of <n> = 4 or 5 (Tsai et al. 2016; Yang et al. 2020; Zuo et al. 2019). These films are generally composed of 2D perovskite slabs with various slab thicknesses ranging from small-n (n = 3, 4, 5) to large-n (Quintero-Bermudez et al. 2018). Due to the insulating nature of the spacer layers, charge transportation is believed to be confined within the 2D plane and hindered along the face-to-face direction (Mauck & Tisdale 2019). CSIRO has maintained a steady effort in quasi-2D processing reporting on various fabrication strategies in previous years. However, upscaling trials of quasi-2D perovskite have delivered dismal efficiency despite lab record cells achieving 20% efficiency (Lai et al. 2022). This repeated outcome revealed the need to delve into the microstructure evolution of the quasi-2D films in good performing lab-scale devices, to establish a benchmark on microstructure, which will accelerate large-scale processing progress of quasi-2D films.

To further understand the 2D Ruddlesden–Popper (RP) phases, the CSIRO team thoroughly investigated the microstructure evolution of quasi-2D perovskite films using morphological and crystallographic characterisations. The morphology of the top/bottom surfaces and the interior of the quasi-2D film were studied by atomic force microscopy and scanning electron microscopy, before and after the films were partially peeled by tape or totally peeled from the substrate. Synchrotron-based grazing incidence wide-angle X-ray scattering (GIWAXS) measurements of the quasi-2D film were performed using both top-side and bottom-side (peeled) detection to compare the different crystal orientation profiles of RPs on the surfaces and in the film interior. Details on the

characterisation can be found in the associated publication (Zheng et al. 2022)

Their study unveiled a hierarchical microstructure formation: the quasi-2D film surface is capped by a thin assembly layer of horizontally stacked BAI sheets, appearing as a compact shell. Beneath this shell, small blocks composed of large-n RPs, and large blocks composed of small-n RPs, which are all vertically oriented, occupy the top and bottom part of the film, respectively (Figure PP2.5.12). The front surface of the film is more stable than the bottom surface revealed by peeling off the film from the substrate, implying 2D stability is due to the 2D capping layer. Based on these new findings, it can be proposed that the spacer ligand-based surface capping layer is responsible for the long-term stability of 2D PSCs, while the vertically oriented large-n/small-n RPs are responsible for the high PCEs found in these systems.

The UNSW team further designed a multifunctional passivation (MFP) strategy to decelerate the segregation of halide ions and minimise open-circuit voltage (V_{OC}) loss. Photoluminescence analysis revealed suppressed non-radiative recombination rates along with decelerated halide segregation (HS) dynamics upon MFP treatments. With the use of an optimal concentration of passivation agent (MFP 75) the PL intensity of samples nearly doubled, which could be due to the passivation of defective sites. To evaluate the stability of samples against HS, samples were measured under continuous illumination (CWPL 525 nm, LED) for 5 minutes. Under illumination with one-sun and five-sun equivalent photon flux, the control samples remained susceptible to HS despite the improved PL, which could be due to the trade-off between a slight enlargement of the bandgap and effective passivation of trap-related recombination rates. However, the optimal concentration of the modified solution (MFP 75) considerably decelerates HS. This could be due to the dual impact of passivation. Exceeding the optimal concentration (MFP 0) still suppressed the HS, however, the PL intensity is the second lowest with respect to the control sample (Figure PP2.5.13).

The improvements in film quality were also confirmed by time-resolved PL measurements. Charge carrier lifetime increased from ~760 ns to ~1250 ns with MFP 75, and to ~940 ns with MFP 0 (consistent with the enhanced steady-state PL results), while excess carrier density increased from 1.14×10^{15} cm^{-3} to 1.58×10^{15} cm^{-3} with MFP 75. Such improvement in charge carrier parameters is likely to be the result of suppressed non-radiative recombination losses.

To evaluate the impacts of the MFP method on the morphology of perovskite thin films, scanning electron microscopy (SEM) revealed nicely packed grains with an average size of ~320 nm for all samples (Figure PP2.5.14). However, control samples showed a considerable amount of undercoordinated PbI_2 particles that could potentially act as traps. After MFP 75 treatment, unreacted PbI_2 residue disappears, which could be due to a reaction between MFP and PbI_2. On the other hand, PbI_2 residue remained if it exceeded the optimal amount of MFP. Atomic force microscopy results revealed decreased surface roughness after MFP treatments. Mean surface roughness decreased from 19.1 nm to 17.9 nm with MFP 75 and further decreased to 14.7 nm with MFP 0. Improved surface roughness is likely to result in a better quality perovskite/HTL interface.

The impact of MFP treatment on photovoltaic performance was further summarised in Table PP2.5.1. It could be observed that the samples with a moderate ratio of MFP show improved performance with respect to control samples due to improvements in open-circuit voltage (V_{OC}) and fill factor (FF). The average V_{OC} increased by ≈20 mV while the average FF increased by 4% in MFP 75 samples compared with the control samples. This could be due to the passivation of defective sites both at the interface/bulk, improved chemical heterogeneity of the surface, and decelerated HS evident from PL and KPFM.

To further monitor the ambient stability, the unencapsulated devices were tested over 2800 hours in storage under 40% relative humidity at room temperature (Figure PP2.5.15). The results showed that MFP 75 samples retained 95% of their initial efficiency, while the control sample maintained 86% after 2800 hours. Interestingly, MFP 0 samples didn't show any considerable loss in efficiency (99%) for the same duration, despite significantly low average J-V characteristics.

With regards to the HTL and ETL materials and its passivation strategies, the teams of UNSW, University of Melbourne and ANU made impressive progresses.

To improve the power conversion efficiency (PCE) and stability of perovskite solar cells (PSCs), the fragile nature of the Li-dopant-based hole transport material, which is regarded as one of the main reasons for PSCs' degradation and the hysteresis issues, must be resolved. The UNSW team found the fragile nature of HTMs originates from the Li-dopant. The lithium compound reduces the HTMs' lifetime due to (i) its hygroscopic nature that leads to the films' instability in moisture, (ii) inducing films' crystallisation under heat/light, and (iii) mobile lithium ions that may diffuse into and impact other functional materials.

Therefore, the UNSW team developed a novel technology to manipulate the Li-dopant distribution in HTMs and thus simultaneously improved the devices' efficiency and stability under various stresses, including ambient air, wetting, thermal, and continuous illumination stimuli. Moreover, the team found that hysteresis highly depends on the crystalline dynamics of the perovskite material. We mitigated the hysteresis index [Hysteresis index = ($PCE_{reverse\text{-}scan}$ – $PCE_{forward\text{-}scan}$) / $PCE_{reverse\text{-}scan}$] from 40% to 15% (Figure PP2.5.16). Meanwhile, we found the importance of carrier transport material in mitigating hysteresis. We synthesised a new high quality electron transport layer which further reduces hysteresis index from 15% to 6%. The up-to-date cell (0.09 cm^2) demonstrated efficiency of up to 24.6% under reverse scanning condition and 23.1% under forward scanning condition. Also, we applied some technologies in centimetre-scale cells. The up-to-date large cell (1 cm^2) demonstrated an efficiency of up to 23.1% under reverse scanning condition and 21.4% under forward scanning condition. We observed the connection between hysteresis and standard power output for PSCs. Better power output (target benchmark 25%) can be expected in the near future after optimising our newly developed technologies.

A recent study by ANU scientists (Walter et al. 2022) demonstrated that the TCO layer is critically influential on performance within the perovskite solar cell. The equilibrium conditions of the perovskite transport layer (TL)-TCO interface can result in very different properties of the TCO-adjacent TL to those measured externally to the cell. In general, the consequence is reduced conductivity of the TL. The choice of TL material must therefore consider its interaction with the TCO.

This theory can explain historical trends in PSC fill factors (FFs). If a transport layer material has a relatively low free carrier density and/or majority carrier mobility, then when in situ with a TCO, its conductivity can fall significantly. This introduces series resistance that can cap FF at relatively low levels, even if the cell is otherwise ideal (Figure PP2.5.17). However, by selecting TCO-adjacent TL materials with sufficient doping and/or mobility, these FF losses can be reversed. Titanium dioxide (TiO_2), a relatively lowly doped ETL with low electron mobility, is predicted to be highly susceptible to this in situ resistance. This is consistent with a prolonged plateau in FF in TiO_2-based PSCs, which has only been resolved once n-i-p PSCs shifted to tin oxide (SnO_2) (Figure PP2.5.18). SnO_2 is a more highly doped ETL with significantly higher electron mobility. Indeed, the record FF achieved previously by ANU researchers can be understood through its amelioration of this in situ resistance using a novel titanium oxy-nitride film, which is heavily doped relative to TiO_2 (Peng et al. 2021).

Tin oxide (SnO_2) is widely used in perovskite solar cells as an electron transport layer (ETL) and it plays a critical role in extracting the photo-generated electrons from the perovskite layer into the electrode in addition to blocking the holes. However, its high surface trap density causes carrier losses in perovskite solar cells (PSCs) through carrier recombination at the surface, leading to poor performance.

The researchers from the UoM team discovered that DABCO can be adopted for surface passivation to eliminate the surface trap states between SnO_2 and perovskite that depress the electron transport barriers for efficient electron collection efficiency resulting in efficient PSCs.

To investigate the effect of DABCO passivation, PSCs were fabricated using an inverted geometry (Figure PP2.5.19(a)) via a one-step spin-coating method from precursors of $CsFaFAPbI_3$ with 10 mol% excess $PbCl_2$, followed by thermal annealing at 150°C. Figure PP2.5.19(c) shows the J-V curves of the perovskite solar cells with and without surface passivation using various concentrations of DABCO solution. The photovoltaic parameters for all devices with various concentrations of DABCO are shown in Table PP2.5.2. The control device without surface passivation demonstrates a PCE of 19.2%, whereas the device with the 5 mM exhibits the best performance of 21.2%.

As shown in the SEM images (Figure PP2.5.20), the perovskite film grown on the 5mM DABCO layer is highly crystalline with a large grain size compared to other ETL layers. To understand the enhanced performance of the PSC with the 5 mM DABCO layer, the electron transfer dynamics were studied by time-resolved photoluminescence (TRPL) spectroscopy using the time-correlated single photon counting (TCSPC) technique. Figure PP2.5.21 shows the TRPL spectra of a perovskite thin film coated on an SnO_2 layer with and without 5 mM DABCO. The average decay lifetime (τ_{ave}) values of 161.9 ns and 80.1 ns were observed with the perovskite coated on SnO_2 and SnO_2/DABCO layers, respectively, in Figure PP2.5.21(a). This indicates that the DABCO passivated layer extracts electrons effectively before they are recombined in the bulk of the perovskite layer. Charge carrier transport properties of PSCs with and without DABCO layers were studied using electrical impedance spectroscopy (EIS). Figure PP2.5.21(a) shows the EIS spectra of perovskite devices with a DABCO layer exhibiting a lower impedance of 4235 Ω comparing the device without a DABCO layer showing a higher impedance of 20,650 Ω, which means a more effective electron extraction and lower recombination loss at the interface of the DABCO layer and the perovskite layer than a device without a DABCO layer.

At last, with regard to novel cell design, the back contact perovskite cell theme developed by the Monash team achieved progress in higher efficiency and large-area devices. Being a novel division of PSCs, back contact perovskite solar cells (BC-PSC) also attracted great research interests due to the calculated maximum performance benefiting from reduced parasitic absorption and easier electrical connection between individual cells. However, the anomalous huge hysteresis and a poor stabilised power output has hugely hindered these devices from further development.

The team at Monash led by Dr Boer Tan focused on improving device performance, especially in the stabilised power output of the state-of-the-art quasi-interdigitated back contact perovskite solar cells with a finger electrode structure. Apart from improving the quality of the perovskite layer with alkali ion doping, a high quality SnO_2 film was also employed in the electrode structure for enhanced charge extraction. We found that the TRPL decay lifetime was enhanced to over 1 µs after doping, while the perovskite layer also demonstrated reduced lower defect density according to the space charge–limited measurement. We also found that the SnO_2 layer is more efficient in electron extraction and showed a more effective quenching in the steady-state measurement compared to the commonly used mesoporous TiO_2 that demonstrated the highest performance in a previous report (Figure PP2.5.22(a)). Through these approaches, we achieved a high performance of up to 11.7% (reverse scan) with a stabilised power output in the champion device (Figure PP2.5.22(b)). These devices also demonstrated a reduced hysteresis index of only 12.5% while devices with mesoporous TiO_2 demonstrated a stable power output (SPO) of 7.8% (11.9% in reverse scan) and a significant hysteresis of 45.3% that is comparable with previous works (Figure PP2.5.22(b)). We also found that the devices with SnO_2 and alkali doping in the perovskite layer had a reduced charge transport resistance and a higher charge collection efficiency via impedance spectroscopy and photocurrent mapping, which explains the higher efficiency. Overall, we found that the implementation of a high quality and less defective perovskite layer and a more efficient charge transfer at the interface can effectively improve the performance of BC-PSCs, reduce the hysteresis, and therefore guarantee an overall higher SPO.

In another study, led by Siqi Deng, a patterning process based on close packed microspheres was developed as a replacement to the conventional photolithography route (Deng et al., 2022). The reduction in electrode feature sizes and minimisation of fabrication defects enabled the stabilised PCE of honeycomb-shaped BC-PSC to increase from 4.4% to a record high of 8.6%. Microsphere lithography was used to fabricate the largest BC-PSC reported to date, having an active device area of 0.75 cm^2 and a stabilised PCE of 2.44% (Figure PP2.5.23). This work marks a milestone in progress towards high efficiency BC-PSCs by demonstrating that these devices can be fabricated using photolithography-free techniques at low cost and high scalability.

3.Material and device durability

Improving durability is a critical challenge for the commercialisation of perovskite solar cells. Durability is dependent on both intrinsic and extrinsic factors. Intrinsic factors comprise inherent material properties, such as phase stability, whereas extrinsic factors include stability of the materials and interfaces comprised in the solar cell against the interaction with environmental factors, such as moisture, oxygen, light and heat. Encapsulation is an effective way to alleviate the impact of external factors to extend the durability of the devices. However, what forms an effective encapsulation material is seldom delved in to detail. For one, the encapsulation materials and methods themselves can be a source of degradation factors within a device during the encapsulation process, such as encasing moisture and oxygen adhered to the surface of barrier films with the device during encapsulation.

Researchers at CSIRO delved in to their existing encapsulation material and methods and studied how the presence or absence of pre-conditioning the barrier films can impact perovskite solar cells in different architectures and with different absorber layers.

Five types of devices in both n-i-p and p-i-n configurations were studied as listed in Table PP2.5.3 with their general structure illustrated in Figure PP2.5.24(a). Details on materials and processing can be found in the published article (Sutherland et al. 2022). 3M Ultra Barrier Solar Film and AR Adhesives (ARcare 92734) were used as the barrier film and barrier adhesive, respectively.

The polymeric barrier materials were first prepared by roll-to-roll laminating the barrier adhesive onto the barrier film, creating a 225 µm thick barrier material stack. After cutting to size (25 mm × 16 mm), the barrier film and barrier adhesive stacks were pre-conditioned by storing at 50°C under constant vacuum pumping (<1 kPa) for various time intervals. This pre-conditioning procedure removes both moisture and oxygen from the barrier materials. It was assumed in this work that the proportion of oxygen removed by a given pre-conditioning treatment is the same as the proportion of moisture removed. The degree of retained moisture in the barrier materials is quantified in parts-per-million (ppm), using a moisture analyser (Computrac Vapor Pro, Arizona Instruments). The moisture desorption properties of the polymeric barrier materials used in this study are given in Figure PP2.5.24(b). As shown, the barrier materials are fully pre-conditioned after 10 hours of conditioning treatment (50°C, <1 kPa vacuum pumping). The barrier materials were prepared to exhibit four degrees of residual moisture content as follows: >2000 ppm (no pre-conditioning), 300–500 ppm (low pre-conditioning), 10–100 ppm (medium pre-conditioning), and <1 ppm (fully pre-conditioned).

The devices comprising a flexible PET substrate (nip-C and pin-A) were also tested for residual moisture content after the electrode evaporation and were found to be fully pre-conditioned, which precludes the potential for out-gassing from the substrate itself.

All devices were encapsulated inside a nitrogen-filled glovebox. The perovskite devices and flexible barrier materials were passed through a laminator to apply uniform pressure for adequate sealing of the device. An illustration of this procedure including the barrier architecture is shown in Figure2.5.24(c). The barrier layers were applied to the coated side of the devices only and were sized to fully cover the active device area while keeping the end of the evaporated electrodes exposed for electrical connection. No heat was applied during lamination.

Following encapsulation, the devices were stored in a nitrogen-filled glovebox for more than 1500 hours with intermittent J-V performance testing. Box plots of the PCE for each of the PSC devices over the 1500 hour storage period are shown in Figure PP2.5.25. With such a large data set (300 solar cells in total), the box plots allow for statistical analysis with the box range indicating 1 standard deviation (SD), the whiskers indicating 1.5 SD, and the yellow square marker indicating the mean value. As shown in 6 (right column), the perovskite devices encapsulated with fully pre-conditioned barrier materials experience minimal degradation over 1500 hours, demonstrating the intrinsic stability of the five perovskite device types when stored in an inert environment.

In contrast, severe degradation is observed in some of the perovskite structures encapsulated using barrier material without pre-conditioning (left column). Figure PP2.5.25 indicates that the sensitivity of these PSCs to unconditioned barrier material is not universal and can vary depending on the device composition and structure. This is particularly apparent in the pin-B perovskite devices which degraded by more than 50% of their initial PCE after 500 hours of storage with moisture-containing encapsulant materials. After 1500 hours, the PCE of the pin-B devices decayed by more than 75% compared to their initial performance. As a result, the pin-B devices were deemed to be the most sensitive structure in this work to the residual moisture and oxygen in the encapsulant materials. Degradation was also observed for the nip-A and pin-A devices which reduced by over 25% and 40% of the initial normalised PCE, respectively, over the 1500 h storage time.

As seen in Figure PP2.5.25 (left column), the nip-B and nip-C devices exhibited greater stability compared to the other three device types when encapsulated with barrier material without pre-conditioning. This is particularly evident for the nip-B devices which improve in performance over the first 200 hours of storage, irrespective of encapsulant pre-conditioning. The improvement suggests that ageing initially has a positive impact on the photoactive perovskite and/or interfacial charge transfer performance. This can be attributed to the oxidation of the Spiro-OMeTAD resulting in enhanced p-type conductivity and reduced series resistance of the HTL. Following 500 hours of storage, the fully pre-conditioned nip-B devices are seen to stabilise while those without pre-conditioning appear to degrade at a similar rate to the initial improvement before stabilising slightly above the original PCE. The greater stability of the nip-B devices compared to pin-A devices suggests that the conventional n-i-p perovskite architecture incorporating SnO_2 and Spiro-OMeTAD is more stable to out-gassing than the p-i-n structure with PEDOT:PSS, PCBM and PEIE, as both the nip-B and pin-A devices comprise identical perovskite compositions. It is thus likely that the degradation in performance is more likely associated with interfacial changes or degradation of the charge transfer materials, rather than degradation of the photoactive perovskite itself.

The IPCE, or external quantum efficiency (EQE), is defined as the number of charge carriers collected by the device, compared with the number of incident photons of a given wavelength (Figure PP2.5.26). IPCE measurements of the PSCs immediately after encapsulation (0

hours), and after 500 hours of storage revealed changes in the spectral response of the device types over the storage period. The EQE results of encapsulated PSCs with and without pre-conditioning are shown in Fig. PP2.5. 26. The solid lines represent the initial measurements taken after encapsulation (0 hours), while the dashed lines represent the measurements after 500 hours of storage.

All PSC device types encapsulated using fully pre-conditioned barrier material exhibited either equivalent or improved EQE performance after 500 hours of storage (Figure PP2.5.26, right column). In comparison, most PSC device types displayed degradation when encapsulated with barrier material without pre-conditioning (Figure PP2.5.26, left column). The nip-A cell exhibited the largest drop in EQE performance after 500 hours, with a decay of around 25% normalised EQE. This is consistent with J-V analysis where the decay in PCE for the nip-A structure was due to a decrease in J_{SC}, indicating reduced charge collection and generation of photocurrent. This suggests the decay in the nip-A PSCs is due predominantly to the out-gassing instability of the $Cs_{0.1}FA_{0.9}PbI_3$ perovskite crystal. In comparison, the nip-C cell only exhibited a slight reduction in EQE performance, while the nip-B cell demonstrates a very small improvement, particularly between 400 and 650 nm.

The CSIRO team have demonstrated the storage stability dependence of five different PSC device types with respect to the moisture content levels of the encapsulating flexible barrier materials. All the PSC device types studied in this work demonstrated negligible performance degradation on encapsulation with pre-conditioned barrier materials. However, the two inverted device types (pin-A and pin-B), and one of the conventionally structured device types (nip-A) were particularly susceptible to degradation when encapsulated with unconditioned barrier materials. This study not only demonstrates the importance of applying appropriate pre-conditioning protocols to encapsulation materials to mitigate out-gassing-induced degradation, but also shows that some PSC types can tolerate residual amounts of moisture and oxygen in the encapsulation materials. We showed that the sensitivity of PSCs to barrier material moisture content levels can significantly vary depending on the perovskite composition and device structure. Future work should delve into the impact of barrier pre-conditioning on accelerated operational lifetime, such as MPP tracking under one sun, which may reveal additional insights into the stability of the various device structures and perovskite materials vis-à-vis barrier pre-conditioning or lack thereof.

In addition to encapsulation, the metal electrode material is another crucial factor determining device durability, especially in heated environments. Copper (Cu) is now a widely utilised metal electrode for perovskites to replace expensive gold and silver. Cu is present not only in the electrode for inverted-structure perovskite solar cells, but also in transport layers such as copper iodide (CuI), copper thiocyanate (CuSCN), and copper phthalocyanine (CuPc), as alternatives to spiro-OMeTAD due to their improved thermal stability. While Cu or Cu-incorporated materials have been effectively utilised in halide perovskites, there is a lack of thorough investigation into the direct reaction between Cu and a perovskite under thermal stress. The UNSW team investigated the thermal reaction between Cu and a perovskite, as well as the degradation mechanism by X-ray diffraction (XRD), X-ray photoelectron spectroscopy (XPS), and Kelvin probe force microscopy (KPFM) (Lim et al. 2022).

It was found that the interaction between Cu and perovskite can result in degradation via XRD measurement. A very thin layer of Cu (1 nm and 3 nm) was deposited to investigate the thermal reaction under elevated temperatures. As can be seen, the intensity of the perovskite peak at 13.95° decreases as the Cu layer is deposited and further reduced after annealing. It is worth noting that deposition of Cu results in a reduction of the PbI_2 peak intensity, which indicates a potential reaction between Cu and PbI_2 at the grain boundaries of the perovskite layer. In addition, the perovskite peaks after Cu deposition and annealing have shifted to a higher angle of 13.96°, indicating a shrinkage of the perovskite lattice due to the incorporation of Cu into the perovskite lattice (Figure PP2.5.27).

To further investigate such a reaction, we explored the surface morphology of the perovskite film before and after Cu deposition and the subsequent annealing process (Figure PP2.5.28). Samples with the Cu layer initially show a morphology with no PbI_2 but uniformly deposited white bright particles were observed. However, after the annealing process, those white particles, which are thought to be most likely Cu or Cu-related particles, were gradually distributed throughout, with a higher density observed along the grain boundaries. This shows a preferential segregation of Cu particles reacted with PbI_2 into the grain boundaries.

To characterise those preferentially segregated particles, the team performed KPFM measurements on each sample as shown in Figure PP2.5.29. Comparing the topography images to SEM images, the results are in good agreement, as the distribution of Cu-related particles observed on the surface was significantly decreased after the annealing process. Moreover, those segregated Cu particles at the grain boundaries exhibit brighter contrast (higher CPD values) than grain interiors compared to other findings of the formation of new perovskite material, which is the Cu-rich and A-site poor at the grain boundaries.

4.Commercial prospects and upscaling

CSIRO has continued its work to improve the performance of printed perovskite solar cells and manufacturing process reliability for large-scale roll-to-roll manufacturing. The deposition of perovskite films through a single-step process is preferable, however, achieving defect-free perovskite layers from a single-step deposition process remains challenging. Consequently, a two-step sequential deposition method whereby a PbI_2 layer is first formed and then transformed into perovskite through a sequential deposition of cation solution was explored.

To study and optimise the influence of various processing parameters, first glass-based devices with slot-die coated layers were studied with a benchtop slot-die coater. Figure PP2.5.30 shows the fabrication schematic of PSCs using the two-step process with a device structure of ITO glass/SnO_2/Perovskite/Spiro-OMeTAD/Ag. Details on device fabrication materials and methods can be found in an associated publication (Li et al. 2022). Briefly, an SnO_2 nanoparticles solution diluted in de-ionised water was slot-die coated on glass, followed by the deposition of a PbI_2: CsI DMF/DMSO. The quality of the PbI_2 film was first checked by using a dipping process for the deposition of the cations (FAI: MABr: MACl). PSCs have been demonstrated to be more efficient and stable by combining MA, FA and Cs cations. Thereafter, this cation mixture was also slot-die coated followed by the hole transport layer Spiro-OMeTAD in chlorobenzene with the addition of

tBP Li-TFSI/ACN. Devices were completed by evaporating the counter electrode.

The gas-blowing and substrate-heating approaches are key processes that can be utilised in tandem with the slot-die coating of solutions to achieve the desired film quality. The SnO_2-coated substrates were heated at different bed temperatures, and the PbI_2 films were deposited on top of the heated substrates. The morphologies of the PbI_2 films were well controlled by precise adjustment of the bed temperature and monitored by SEM. As shown in Figure PP2.5.31(a)–(c), there are more pinholes present within the PbI_2 film when prepared at 60°C than there are at 70°C. When the bed temperature was further increased to 80°C, the PbI_2 films tend to become compact, which is attributed to the fact that the solvent evaporates faster at higher temperatures, causing PbI_2 crystals to precipitate quicker, forming a densely packed film. Figure PP2.5.31 contains the SEM images of perovskite films formed on the above-deposited PbI_2 films at room temperature via the slot-die coating of the FAI/MABr/MACl solution. The grain size increases initially along with the bed temperature increasing from 60°C to 70°C, and then decreases when the bed temperature is increased to 80°C. This trend can be attributed to the supersaturation of PbI_2 crystals at high bed temperature, leading to excessive incomplete conversion of PbI_2. The optimal number of pores will provide enough channels for FAI/MABr/MACl to diffuse into the PbI_2 films, enabling complete conversion to perovskite. In contrast, too densely packed PbI_2 films hinder solution diffusion into the PbI_2 bulk film, inhibiting efficient interaction between PbI_2 and FAI/MABr/MACl, causing incomplete conversion to perovskite. Therefore, the quality of PbI_2 films controlled by the bed temperature exhibits considerable effects on the fabrication of high quality perovskite films. Thus, the results suggest that an optimal porous morphology of the PbI_2 film is critical to form smooth, homogeneous, fully converted perovskite films with large grains, while a dense PbI_2 layer leads to the incomplete conversion into perovskite (Jacobsson et al. 2016).

To investigate the effect of bed temperature on photo-generated charge carriers of the perovskite film, the steady-state photoluminescence (PL) spectra were measured on perovskite films prepared on glass substrates using the same two-step process (Figure PP2.5.32(a)). The perovskite film fabricated at 70°C presents the highest PL intensity, implying that the non-radiative recombination of the perovskite film was significantly suppressed at this bed temperature. The PL peak of the perovskite film fabricated at 80°C has a small redshift, which indicates a higher trap density in a perovskite film (Tian et al. 2019). Therefore, the increased recombination loss and reduced charge collection of the perovskite film prepared at 80°C will have a negative influence on the solar cell performance.

The J-V curves and performance parameters of PSC devices fabricated from the above perovskite films prepared at different bed temperatures are shown and summarised in Figure PP2.5.33b and Table PP2.5 4, respectively. Slot-die coating was used for the deposition of SnO_2 and perovskite layers, except that the Spiro-OMeTAD hole transport layer was coated by drop casting. The short-circuit current (J_{sc}) increased when the bed temperature increased from 60°C to 70°C. In contrast, the J_{sc} slightly decreased with increasing the bed temperature to 80°C. The highest J_{sc} of 22.11 mA/cm^2 was achieved at the optimised bed temperature of 70°C. Meanwhile, the fill factor (FF) was also improved to 75.2%, resulting in the final PCE of 17.96%.

Translation to roll-to-roll (R2R) manufacturing

Slot-die coating was then translated to the R2R coating process (Figure PP2.5.33(a)). A flexible ITO/PET substrate is continuously moved from an unwind roller, passing the coating head and dryer, and finally to the rewind roller. When each coating run was completed, the substrate was collected on the rewind roller. To start, a thin SnO_2 film was first coated by micro-gravure printing, followed by slot-die coating of the PbI_2 layer which was dried by N_2 blowing, and finally converted to the perovskite film by slot-die coating of an FAI/MABr/MACl solution. As shown in Figure PP2.5.33, hot plate-1 is employed to heat the wet film during the coating process as a bed temperature, and the hot plate is used to anneal the deposited film. The best performing PSCs using the R2R coating process present a V_{OC} of 1.00 V, a J_{SC} of 21.45 mA cm^{-2}, an FF of 60.59% and a PCE of 13.00% in a reverse scan (Figure PP2.5.33(b) and Table PP2.5.5). Figure PP2.5.33(c) presents the statistical distribution of the PCEs based on 25 PSCs. The main difference between slot-die coated glass-based devices and R2R-coated flexible devices are the substrates and fabrication methods, resulting in different morphologies of SnO_2 layers.

In summary, high quality perovskite films were successfully prepared in ambient conditions via batch-to-batch slot-die coating on ITO/glass substrates and continuous R2R coating on flexible substrates. The influence of bed temperature on the morphology of PbI_2 during coating was fully investigated. Planar n-i-p PSCs with a PCE of 18.13% was achieved by fully slot-die coating on glass, with a PCE of 15.10% with an area of 1 cm^2. A 13% PCE was achieved on flexible substrates.

Highlights

Further exploration of additives and passivation strategies, including fluorinated organic cations, mixed large cation organic salts, LiI, KI and multifunctional passivation layers, were undertaken to understand the underlying perovskite passivation mechanisms.

Fundamental investigations into the microstructure formation of quasi-2D perovskite films were conducted to facilitate translation of the materials to large-scale processing.

Mitigated halide ion segregation and reduced open-circuit voltage loss by multifunctional passivation layer was demonstrated. Perovskite solar cells with an efficiency of up to 24.6% with significantly reduced hysteresis were fabricated.

In-depth analysis of the TCO and HTL/ETL interface provided insights into how to achieve high fill factors. New HTL/ETL interface processes were developed to improve device performance, including Li-salt destruction manipulation and DABCO interface treatment.

For the first time, high quality formamidinium-caesium (FACs) perovskite thin films were successfully synthesised from a lead acetate–based precursor solution. Utilising the advantages of lead acetate, efficient and stable perovskite solar cells (21.0%, mask area 0.16 cm^2) and modules (18.8%, mask area 10 cm^2) were produced using industrially scalable blade-coating techniques in an ambient air environment.

A high-temperature DMSO-free perovskite preparation method was developed using DMACl as a crystallisation agent. Improved operational stability, with a median T80 lifetime for the steady-state power conversion efficiency of 1190 hours, and a champion device showed a T80 of 1410 hours, under simulated sunlight at 65°C in air, under open-circuit conditions.

Efficient back contact perovskite solar cells were fabricated without the need for high-cost photolithography, removing a research hurdle for BC-PSC. Lower hysteresis and more efficient back contact perovskite solar cells can be achieved through fabricating perovskite layers with less defects and longer lifetime, as well as a more efficient charge extraction interface. A record efficiency of 10.9% was achieved.

Flexible encapsulation materials and methods were studied for their impact on the storage stability of various perovskite devices on both glass and PET. Fully slot-die coating fabrication of all layers was achieved with a PCE of 18.1% on an active area of 0.1 cm^2 on glass substrates and a PCE of 15.1% achieved on an active area of 1 cm^2. The R2R fabrication of a flexible perovskite solar cell with record efficiency of 13% was achieved.

Future Work

To achieve higher efficiencies and stabilities, researchers will further implement novel passivation strategies using bi-functional passivation materials for interface and bulk passivation. Further studies will reveal the fundamental mechanisms for superior interface/bulk passivation, material stability and enhanced carrier transport, allowing for the development of guidelines for new passivation material synthesis and process design.

In regard to precursor engineering, further investigation into the effects of different additives on the optoelectronic and device properties of perovskite materials are required. Future research efforts will not only determine the effect on device stability, but also the degree to which the additives improve perovskite formation on a module level. Lead acetate–based precursors were developed to achieve high efficiency blade-coated perovskite solar cells, with the printing parameters to be further optimised to achieve higher efficiencies in larger module sizes.

New lead-free perovskite materials are attracting more attention across the perovskite research community. An extensive study of a narrow bandgap lead-free perovskite and related structure modification, defect elimination and optoelectronic properties will overcome the major challenges associated with these materials.

Back contact perovskite solar cells continue to suffer from severe recombination losses, especially at the interfaces. Therefore, interface passivation techniques for less defective interfaces are under investigation to achieve a higher quality perovskite layer. Due to its unique lateral carrier transfer feature, in-depth charge carrier dynamics analysis is appealing to reveal charge extraction and interfacial properties.

In terms of scaling the deposition process to commercial scales, there will be further development of lab-to-fab translation through optimisation of R2R and slot-die fabrication processes. This will entail the R2R translation of quasi-2D films and studying the required conditions to optimise the required microstructure of these films. Operational stability investigations into the most promising formulations and device architecture emerged from the encapsulation study.

Publications

Deng, S., Tan, B., Chesman, A. S. R., Lu, J., McMeekin, D. P., Ou, Q., Scully, A. D., Raga, S. R., Rietwyk, K. J., Weissbach, A., Zhao, B., Voelcker, N. H., Cheng, Y.-B., Lin, X. & Bach, U. (2022). Back-contact perovskite solar cell fabrication via microsphere lithography. Nano Energy 102, 107695.

McMeekin, D. P., Holzhey, P., Fürer, S. O., Harvey, S. P., Schelhas, L. T., Ball, J. M., Mahesh, S., Seo, S., Hawkins, N. & Lu, J. (2023). Intermediate-phase engineering via dimethylammonium cation additive for stable perovskite solar cells. Nature Materials. 22, 73-83.

Zhao, J., Fürer, S. O., McMeekin, D. P., Lin, Q., Lv, P., Ma, J., Tan, W. L., Wang, C., Tan, B., Chesman, A. S. R., Yin, H., Scully, A. D., McNeill, C. R., Mao, W., Lu, J., Cheng, Y.-B. & Bach, U. (2023). Efficient and stable formamidinium–caesium perovskite solar cells and modules from lead acetate-based precursors. Energy & Environmental Science. (Accepted)

Guo, Q., Zhang, T., Etheridge, J. & Bach, U. (2023) Toward Uniaxially Textured CsPbIBr2 Perovskite Thin Films with Twin Domains by Potassium Incorporation. ACS Energy Letters (Accepted)

Lim, J., Choi, E., Kim, M., Lee, M., Chen, D., Green, M. A., Seidel, J., Kim, C., Park, J., Hao, X. & Yun, J. S. (2022). Revealing the Dynamics of the Thermal Reaction between Copper and Mixed Halide Perovskite Solar Cells. ACS Applied Materials & Interfaces 14, 20866-20874.

Hou, T., Zhang, M., Yu, W., Wang, X., Gu, Z., Chen, Q., Lan, L., Sun, X., Huang, Y., Zheng, B., Liu, X., Green, M. A. & Hao, X. (2022). Low-pressure accessible gas-quenching for absolute methylammonium-free perovskite solar cells. Journal of Materials Chemistry A 10, 2105-2112.

Zhang F., Sun X., Xie H., Cai X., Zheng B., Yu H., Liu E., Hao X.J. & Zhang M. (2022), Unravelling the mechanism of ion-migration suppression by interstitial doping for operationally stable CsPbI2Br perovskite solar cells. Chemistry of Materials, 34(3), 1010-1019.

Wang, Y., Duan, L., Zhang, M., Hameiri, Z., Liu, X., Bai, Y. & Hao, X. (2022), PTAA as Efficient Hole Transport Materials in Perovskite Solar Cells: A Review. Sol. RRL, 6: 2200234.

Liu, X., Zheng, B., Shi, L., Zhou, S., Xu, J., Liu, Z., Yun, J. S., Choi, E., Zhang, M. & Lv, Y. (2022). Perovskite solar cells based on spiro-OMeTAD stabilized with an alkylthiol additive. Nature Photonics.17,96-105.

Mozaffari, N., Duong, T., Shehata, M. M., Bui, A. D., Pham, H. T., Yin, Y., Mayon, Y. O., Zheng, J., Mahmud, M. A., Tabi, G. D., Andersson, G. G., Black, L. E., Peng, J., Shen, H., White, T. P., Weber, K. & Catchpole, K. R. (2022). Above 23% Efficiency by Binary Surface Passivation of Perovskite Solar Cells Using Guanidinium and Octylammonium Spacer Cations. Solar RRL 6, 2200355.

Tabi, G. D., Pham, H. T., Zhan, H., Walter, D., Mayon, A. O., Peng, J., Duong, T., Shehata, M. M., Shen, H., Duan, L., Mozaffari, N., Li, L., Mahmud, M. A., Nguyen, H. T., Weber, K., Catchpole, K. R. White, T. P. (2022). LiI doping of mixed-cation mixed-halide perovskite solar cells: Defect passivation, controlled crystallization and transient ionic response. Materials Today Physics 27, 100822.

Walter, D., Peng, J., Weber, K., Catchpole, K. R. & White, T. P. (2022). Performance limitations imposed by the TCO heterojunction in high efficiency perovskite solar cells. Energy & Environmental Science 15, 5202-5216.

Li, H., Bati, A. S. R., Chu, R., Zhang, G., Li, Y., Lin, Q., Burn, P. L., Shaw, P. E. & Gentle, I. R. (2022). Fluorinated Interlayer Modulation of NiO_x-Based Inverted Perovskite Solar Cells. ACS Applied Materials & Interfaces 14, 42071-42077.

Li, H., Chu, R., Zhang, G., Burn, P. L., Gentle, I. R. & Shaw, P. E. (2022). Influence of the Alkyl Chain Length of (Pentafluorophenylalkyl) Ammonium Salts on Inverted Perovskite Solar Cell Performance. ACS Applied Materials & Interfaces 14, 39939-39950.

Benitez-Rodriguez, J. F., Chen, D., Scully, A. D., Easton, C. D., Vak, D., Li, H., Shaw, P. E., Burn, P. L., Caruso, R. A. & Gao, M. (2022). Slot-die coating of a formamidinium-cesium mixed-cation perovskite for roll-to-roll fabrication of perovskite solar cells under ambient laboratory conditions. Solar Energy Materials and Solar Cells 246, 111884.

Li, H., Zuo, C., Angmo, D., Weerasinghe, H., Gao, M. & Yang, J. (2022). Fully Roll-to-Roll Processed Efficient Perovskite Solar Cells via Precise Control on the Morphology of PbI2:CsI Layer. Nano-Micro Letters 14, 79.

Sutherland, L. J., Benitez-Rodriguez, J. F., Angmo, D., Peiris, T. A. N., Simon, G. P., Gao, M. & Weerasinghe, H. (2022). Effect of out-gassing from polymeric encapsulant materials on the lifetime of perovskite solar cells. Solar Energy Materials and Solar Cells 246, 111887.

Zheng, F., Raeber, T., Rubanov, S., Lee, C., Seeber, A., Hall, C., Smith, T. A., Gao, M., Angmo, D. & Ghiggino, K. P. (2022). Spontaneous Formation of a Ligand-Based 2D Capping Layer on the Surface of Quasi-2D Perovskite Films. ACS Applied Materials & Interfaces 14, 51910-51920.

References

Cao, D. H., Stoumpos, C. C., Farha, O. K., Hupp, J. T. & Kanatzidis, M. G. (2015). 2D homologous perovskites as light-absorbing materials for solar cell applications. Journal of the American Chemical Society 137, 7843-7850.

Conings, B., Drijkoningen, J., Gauquelin, N., Babayigit, A., D'Haen, J., D'Olieslaeger, L., Ethirajan, A., Verbeeck, J., Manca, J., Mosconi, E., Angelis, F. D. & Boyen, H.-G. (2015). Intrinsic Thermal Instability of Methylammonium Lead Trihalide Perovskite. Advanced Energy Materials 5, 1500477.

Deng, S., Tan, B., Chesman, A. S. R., Lu, J., McMeekin, D. P., Ou, Q., Scully, A. D., Raga, S. R., Rietwyk, K. J., Weissbach, A., Zhao, B., Voelcker, N. H., Cheng, Y.-B., Lin, X. & Bach, U. (2022). Back-contact perovskite solar cell fabrication via microsphere lithography. Nano Energy 102, 107695.

Huang, W., Bu, T., Huang, F. & Cheng, Y.-B. (2020). Stabilizing high efficiency perovskite solar cells with 3D-2D heterostructures. Joule 4, 975-979.

Jacobsson, T. J., Correa-Baena, J.-P., Halvani Anaraki, E., Philippe, B., Stranks, S. D., Bouduban, M. E., Tress, W., Schenk, K., Teuscher, J. I. & Moser, J.-E. (2016). Unreacted PbI2 as a double-edged sword for enhancing the performance of perovskite solar cells. Journal of the American Chemical Society 138, 10331-10343.

Jang, Y.-W., Lee, S., Yeom, K. M., Jeong, K., Choi, K., Choi, M. & Noh, J. H. (2021). Intact 2D/3D halide junction perovskite solar cells via solid-phase in-plane growth. Nature Energy 6, 63-71.

Lai, X., Li, W., Gu, X., Chen, H., Zhang, Y., Li, G., Zhang, R., Fan, D., He, F. & Zheng, N. (2022). High-performance quasi-2D perovskite solar cells with power conversion efficiency over 20% fabricated in humidity-controlled ambient air. Chemical Engineering Journal 427, 130949.

Li, H., Chu, R., Zhang, G., Burn, P. L., Gentle, I. R. & Shaw, P. E. (2022). Influence of the Alkyl Chain Length of (Pentafluorophenylalkyl) Ammonium Salts on Inverted Perovskite Solar Cell Performance. ACS Applied Materials & Interfaces 14, 39939-39950.

Li, H., Zuo, C., Angmo, D., Weerasinghe, H., Gao, M. & Yang, J. (2022). Fully Roll-to-Roll Processed Efficient Perovskite Solar Cells via Precise Control on the Morphology of PbI2:CsI Layer. Nano-Micro Letters 14, 79.

Lim, J., Choi, E., Kim, M., Lee, M., Chen, D., Green, M. A., Seidel, J., Kim, C., Park, J., Hao, X. & Yun, J. S. (2022). Revealing the Dynamics of the Thermal Reaction between Copper and Mixed Halide Perovskite Solar Cells. ACS Applied Materials & Interfaces 14, 20866-20874.

Mauck, C. M. & Tisdale, W. A. (2019). Excitons in 2D organic–inorganic halide perovskites. Trends in Chemistry 1, 380-393.

McMeekin, D. P., Holzhey, P., Fürer, S. O., Harvey, S. P., Schelhas, L. T., Ball, J. M., Mahesh, S., Seo, S., Hawkins, N., Lu, J., Johnston, M. B., Berry, J. J., Bach, U. & Snaith, H. J. (2023). Intermediate-phase engineering via dimethylammonium cation additive for stable perovskite solar cells. Nature Materials. 22, 73–83

Mozaffari, N., Duong, T., Shehata, M. M., Bui, A. D., Pham, H. T., Yin, Y., Mayon, Y. O., Zheng, J., Mahmud, M. A., Tabi, G. D., Andersson, G. G., Black, L. E., Peng, J., Shen, H., White, T. P., Weber, K. & Catchpole, K. R. (2022). Above 23% Efficiency by Binary Surface Passivation of Perovskite Solar Cells Using Guanidinium and Octylammonium Spacer Cations. Solar RRL 6, 2200355.

Peng, J., Walter, D., Ren, Y., Tebyetekerwa, M., Wu, Y., Duong, T., Lin, Q., Li, J., Lu, T. & Mahmud, M. A. (2021). Nanoscale localized contacts for high fill factors in polymer-passivated perovskite solar cells. Science 371, 390-395.

Quintero-Bermudez, R., Gold-Parker, A., Proppe, A. H., Munir, R., Yang, Z., Kelley, S. O., Amassian, A., Toney, M. F. & Sargent, E. H. (2018). Compositional and orientational control in metal halide perovskites of reduced dimensionality. Nature Materials 17, 900-907.

Stoumpos, C. C., Cao, D. H., Clark, D. J., Young, J., Rondinelli, J. M., Jang, J. I., Hupp, J. T. & Kanatzidis, M. G. (2016). Ruddlesden–Popper hybrid lead iodide perovskite 2D homologous semiconductors. Chemistry of Materials 28, 2852-2867.

Sutherland, L. J., Benitez-Rodriguez, J. F., Angmo, D., Peiris, T. A. N., Simon, G. P., Gao, M. & Weerasinghe, H. (2022). Effect of out-gassing from polymeric encapsulant materials on the lifetime of perovskite solar cells. Solar Energy Materials and Solar Cells 246, 111887.

Tabi, G. D., Pham, H. T., Zhan, H., Walter, D., Mayon, A. O., Peng, J., Duong, T., Shehata, M. M., Shen, H., Duan, L., Mozaffari, N., Li, L., Mahmud, M. A., Nguyen, H. T., Weber, K., Catchpole, K. R. & White, T. P. (2022). LiI doping of mixed-cation mixed-halide perovskite solar cells: Defect passivation, controlled crystallization and transient ionic response. Materials Today Physics 27, 100822.

Tian, J., Xue, Q., Tang, X., Chen, Y., Li, N., Hu, Z., Shi, T., Wang, X., Huang, F. & Brabec, C. J. (2019). Dual interfacial design for efficient CsPbI2Br perovskite solar cells with improved photostability. Advanced Materials 31, 1901152.

Tsai, H., Nie, W., Blancon, J.-C., Stoumpos, C. C., Asadpour, R., Harutyunyan, B., Neukirch, A. J., Verduzco, R., Crochet, J. J. & Tretiak, S. (2016). High-efficiency two-dimensional Ruddlesden–Popper perovskite solar cells. Nature 536, 312-316.

Walter, D., Peng, J., Weber, K., Catchpole, K. R. & White, T. P. (2022). Performance limitations imposed by the TCO heterojunction in high efficiency perovskite solar cells. Energy & Environmental Science 15, 5202-5216.

Wang, Z., Lin, Q., Chmiel, F. P., Sakai, N., Herz, L. M. & Snaith, H. J. (2017). Efficient ambient-air-stable solar cells with 2D–3D heterostructured butylammonium-caesium-formamidinium lead halide perovskites. Nature Energy 2, 1-10.

Wu, G., Liang, R., Ge, M., Sun, G., Zhang, Y. & Xing, G. (2022). Surface passivation using 2D perovskites toward efficient and stable perovskite solar cells. Advanced Materials 34, 2105635.

Yang, Y., Liu, C., Mahata, A., Li, M., Roldan-Carmona, C., Ding, Y., Arain, Z., Xu, W., Yang, Y. & Schouwink, P. A. (2020). Universal approach toward high-efficiency two-dimensional perovskite solar cells via a vertical-rotation process. Energy & Environmental Science 13, 3093-3101.

Zhao, J., Fürer, S. O., McMeekin, D. P., Lin, Q., Lv, P., Ma, J., Tan, W. L., Wang, C., Tan, B., Chesman, A. S. R., Yin, H., Scully, A. D., McNeill, C. R., Mao, W., Lu, J., Cheng, Y.-B. & Bach, U. (2023). Efficient and stable formamidinium–caesium perovskite solar cells and modules from lead acetate-based precursors. Energy & Environmental Science.

Zheng, F., Raeber, T., Rubanov, S., Lee, C., Seeber, A., Hall, C., Smith, T. A., Gao, M., Angmo, D. & Ghiggino, K. P. (2022). Spontaneous Formation of a Ligand-Based 2D Capping Layer on the Surface of Quasi-2D Perovskite Films. ACS Applied Materials & Interfaces 14, 51910-51920.

Zuo, C., Scully, A. D., Vak, D., Tan, W., Jiao, X., McNeill, C. R., Angmo, D., Ding, L. & Gao, M. (2019). Self-assembled 2D perovskite layers for efficient printable solar cells. Advanced Energy Materials 9, 1803258.

PP3
OPTICS AND CHARACTERISATION

OVERVIEW

Program Package 3 (PP3), "Optics and Characterisation", aims to utilise, manipulate and characterise the fundamental interactions between light and matter to develop high efficiency, low-cost photovoltaic (PV) devices. This topic area includes, but is not limited to, thin-film organic and Earth-abundant solar cells. These devices seek to exploit special optical properties – imparted either by their constituent materials or by structural modifications – to enhance energy conversion efficiency well beyond what would be expected for a conventional PV device of comparable thickness. However, the characterisation of such devices can be much more challenging than for standard devices, requiring the development of a range of new characterisation techniques.

Previous reports for this Program Package have outlined ACAP achievements in these areas. In this report we present recent progress and suggest promising new directions for the work.

This Program Package is separated into three main sub-categories under which the individual projects are listed. Sub-category PP3.1 combines all projects that focus on the measurement of optical and electrical properties, which includes the following activities. ANU has developed two advanced cluster tools for optical and device characterisation and is developing imaging techniques for perovskites. CSIRO is developing an LED-based solar simulator with ultra-high spectral matching for characterising multi-junction devices. The University of Melbourne has established a comprehensive facility for ultrafast laser spectroscopic characterisation of photovoltaic materials spanning the femtosecond to the microsecond timescales.

No activities have occurred in the sub-category dedicated for Plasmonics and Nanoparticles, PP3.2.

In the sub-category to study degradation mechanisms, PP3.3, ANU is working on a stability testing system within the inert environment of a glovebox.

PP3.1 OPTICAL AND ELECTRICAL PROPERTIES

PP3.1A ADVANCED OPTICAL CHARACTERISATION CLUSTER

Lead Partner
ANU

ANU Team
Hieu Nguyen, Daniel Macdonald

Funding Support
ACAP, ANU

Aim

This project aims to establish an advanced optical characterisation cluster for photovoltaic (PV) research activities at the Australian National University (ANU) ACAP node. The cluster consists of a hyperspectral imaging tool and a time-resolved photoluminescence (TRPL) system. With a wide excitation (near-UV, visible, near-IR) and detection range (350–1700 nm), it is versatile for nearly all PV materials. This integrated suite of complementary techniques will

allow access to many structural, morphological and optical properties of solar cells across a large range of physical dimensions and carrier lifetimes.

Progress

The first tool in the cluster is a hyperspectral imaging system (Figure PP3.1.1). It was sourced from Photon Etc. and commissioned at the ANU in April 2021. Upon establishment, it can capture images of photoluminescence (PL)/ electroluminescence (EL)/ reflectance (R)/ transmission (T) with full spectral information for each pixel. When coupled through a microscope, images with spatial resolution of 1 micron are possible, allowing access to microstructures across cm-scale areas. We have tested the system on various perovskite and silicon samples. Some examples are given in Figures PP3.1.2 and PP3.1.3, respectively. Here, we can choose specific spectral ranges or wavelengths to display the images. Also, we can examine the full spectrum at each location of interest.

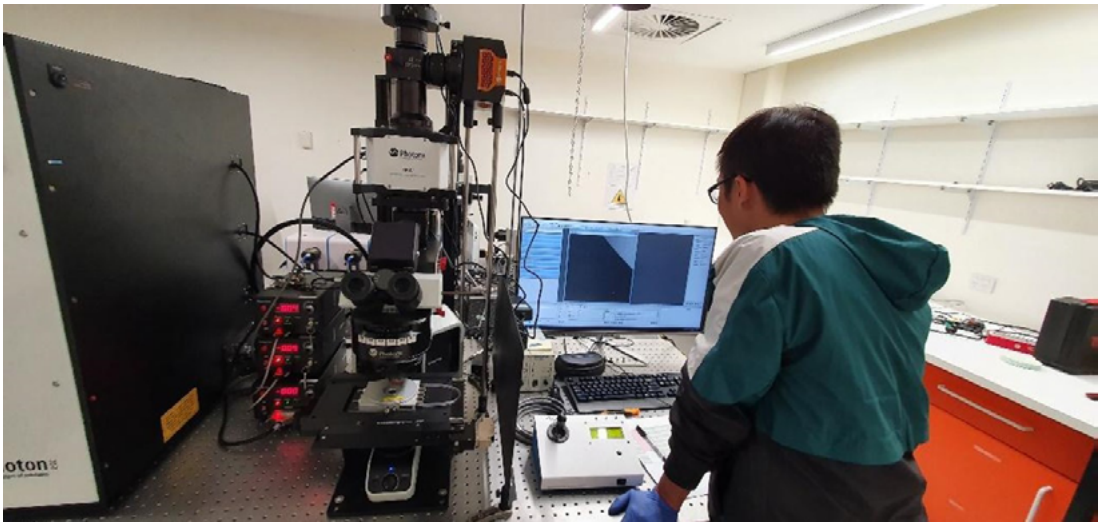

Figure PP3.1.1: Established hyperspectral imaging tool at the ANU node. Mr Anh Bui, PhD candidate, is shown making temperature-dependent measurements of photoluminescence from perovskite solar cells.

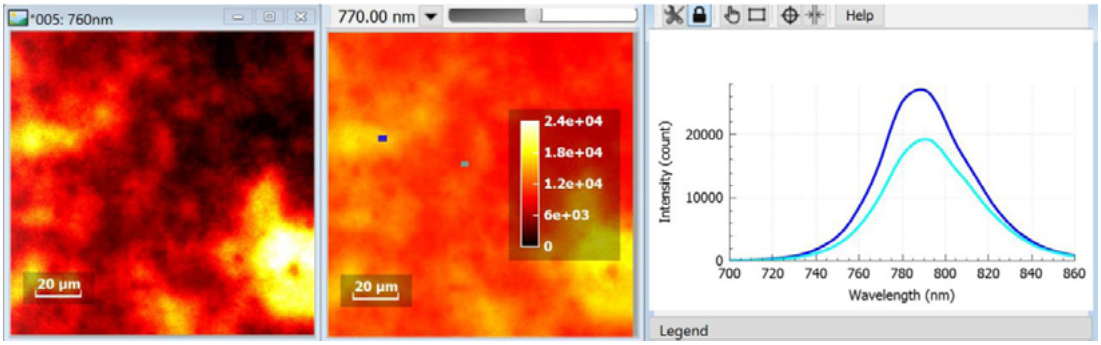

Figure PP3.1.2: PL intensity images of a complete perovskite solar cell at 760 nm (left) and 770 nm (middle). Representative PL spectra (right) at different locations marked in the intensity image. The excitation wavelength is 532 nm at room temperature.

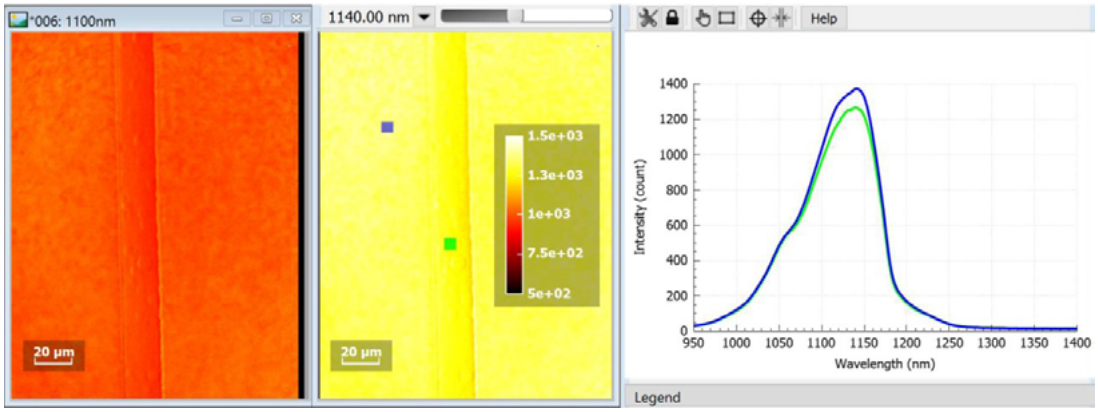

Figure PP3.1.3: PL intensity images of a silicon solar cell precursor at 1110 nm (left) and 1140 nm (middle). Representative PL spectra (right) at different locations marked in the intensity image. The excitation wavelength is 860 nm at room temperature.

The second tool in the cluster is a multi-excitation TRPL system (Figure PP3.1.4). It was sourced from Horiba Scientific and commissioned at the ANU in March 2021. It has a spectrometer to select emission wavelengths and lifetime analysis software. Upon establishment, it can capture a carrier lifetime range from sub-ns to ms. The excitation spot size can vary from 1 micron (in confocal mode) to tens of microns (in large-area illumination mode) via extra customised optics designed by Quark Photonics, an Australian distributor of Horiba products. The team selects ultra-sensitive high-end PPD900 and Hamamatsu H10330B-75 InGaAs PMT detectors for visible and near-IR wavelengths, respectively, as emissions from our many materials (silicon, oxygen and metal precipitates, SiN, polysilicon) are extremely weak. As illustrated, Figure PP3.1.5 shows typical TRPL curves of a perovskite solar cell (detection wavelength of 780 nm, excitation wavelength of 485 nm, and PPD900 detector) and a heavily doped silicon sample (P doping density of 2×10^{19} cm^{-3}, detection wavelength of 1160 nm, excitation wavelength of 785 nm, and InGaAs PMT detector). From these curves, the minority carrier lifetime can be extracted.

Both tools have three excitation wavelengths (near-UV, visible, near-IR) to excite nearly all materials of interest (silicon, perovskite, organics, thin films and 2D materials) and two detectors (silicon and InGaAs) covering 350–1700 nm to capture signals from all these materials.

The cluster is also very versatile and can be applied to various fabrication stages. Therefore, it readily and directly benefits a wide range of current activities across ACAP Programs (PP1: Silicon Solar Cells, PP2: Thin-Film, Third Generation and Hybrid Devices and PP3: Optics and Characterisation).Optics and Characterisation).

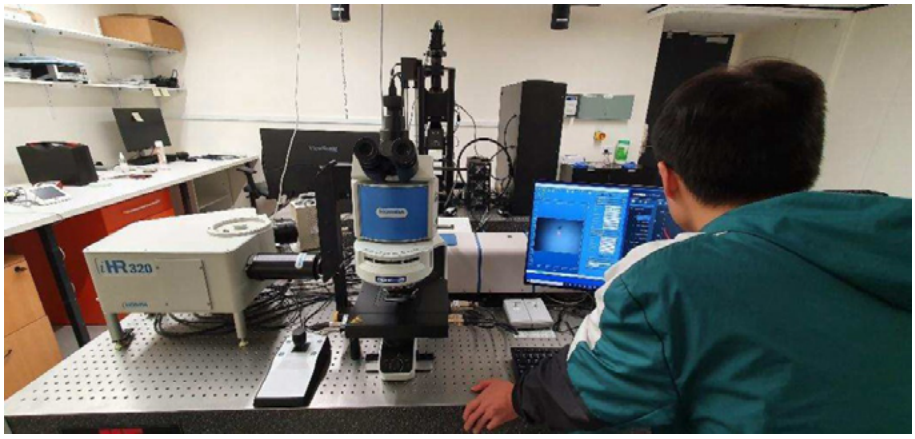

Figure PP3.1.4: Established TRPL tool at the ANU node. Mr Anh Bui, PhD candidate, is shown capturing decay lifetime curves from perovskite solar cells.

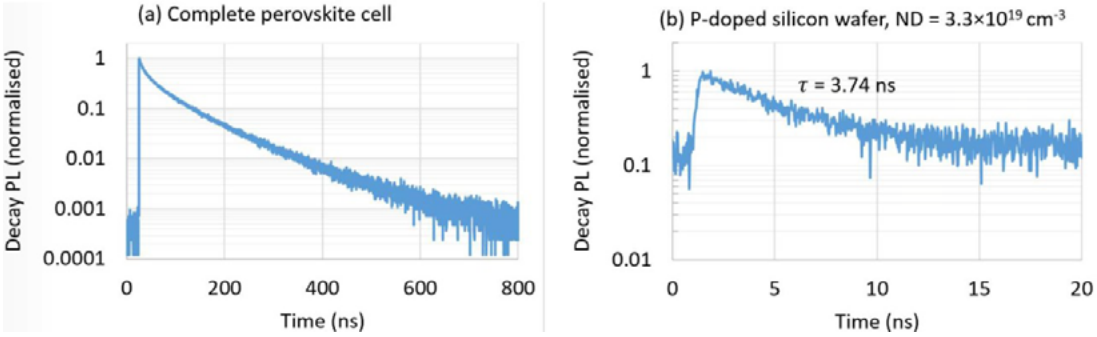

Figure PP3.1.5: Typical time-resolved PL decay curves from (a) a complete perovskite solar cell (excitation wavelength of 485 nm, detection wavelength of 780 nm, PPD900 detector) and (b) a heavy phosphorus-doped silicon wafer (uniformly doped across the wafer thickness, non-passivated, doping density of 3.3×10^{19} cm^{-3}, excitation wavelength of 785 nm, detection wavelength of 1160 nm, InGaAs PMT detector).

Highlights

- Commissioning and validation of the optical cluster consisting of the hyperspectral imaging and time-resolved photoluminescence tools.
- Establishment of Optical Spectroscopy & Imaging Laboratory hosting the optical cluster at the ANU.
- Approval of WHS documents, operating and training procedures.

Future Work

The ANU team will continue to validate, optimise and establish standard measurement parameters and procedures for the two tools with specific applications. Also, the team will promote the cluster to other research groups across ANU (physics, chemistry and engineering), ACAP nodes and beyond.

PP3.1B DEVELOPMENT OF AN ADVANCED DEVICE CHARACTERISATION CLUSTER

Lead Partner
ANU

Team
A/Prof. Tom White, Dr Marco Ernst, Dr Hieu Nguyen, Dr Kean Chern Fong, Dr Daniel Walter, Prof. Yuerui Lu, Prof. Daniel Macdonald

Students
Anh Bui

Funding Support
ACAP, ANU

Aim

This project aims to provide a suite of complementary multi-modal, multi-scale device characterisation tools to support next generation PV device development across the entire ACAP technology portfolio. The specifications of each tool have been selected to ensure maximum versatility for studying a range of single-junction and tandem/multi-junction devices, including perovskites and Earth-abundant materials, silicon and III-V materials.

The cluster consists of the following tools:

- Quantum efficiency measurement system
- Laser beam induced current (LBIC) system
- Lock-in-thermography system
- Photoluminescence quantum yield (PLQY) imaging module for an existing hyperspectral microscope
- Ultra-high power, multi-wavelength LED light source

Progress

The project faced significant delays during 2021 and 2022 due to COVID-related manufacturer, supply chain and shipping issues. Installation and commissioning of the final tool – the LBIC system – was completed in November 2022. The full capabilities of the cluster are now available to all ACAP researchers. Access to the tools can be via lab visits, sending samples to ANU for measurement, or through more structured research collaborations. The cost of operating and maintaining the equipment will be covered by the ANU for five years.

A short summary of each of the component tools, their specifications and research use is provided below.

Quantum efficiency (EQE/IQE) measurement system. The Enlitech QE-R3011EQE/IQE measurement system was delivered in December 2021 and installation and commissioning was completed in May 2022. The specifications of the system were carefully chosen to allow accurate quantum efficiency measurements of silicon, III-V, perovskite and multi-junction solar cells over small and large areas. It includes both DC and AC measurement modes, Si and Ge detectors spanning a wavelength range of 300–1800 nm, four LED bias lights (470/505/730/940 nm), and an automated mapping capability to image EQE/IQE across a cell. Quantum efficiency measurements are essential for accurate characterisation of solar cell performance and are particularly important for quantifying sub-cell performance in multi-junction devices. The system is currently being used to support multiple perovskite, silicon and tandem device projects at ANU.

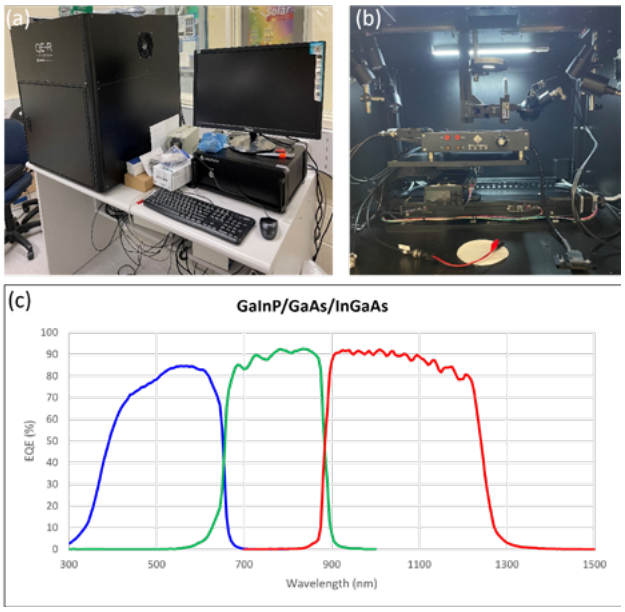

Figure PP3.1.6: (a), (b) Photos of the Enlitech quantum efficiency measurement tool installed at ANU. (c) External quantum efficiency measurement of a triple-junction GaInp/GaAs/InGaAs solar cell measured at ANU.

Laser beam induced current (LBIC) system. The ANU team has worked closely with German company Automatic Research to develop a customised LBIC system that will meet the immediate and future needs of ANU and ACAP PV research across a range of material systems and device configurations. The final specifications include two laser sources (445/915 nm), LED bias light, a 300 mm x 300 mm motorised scanning stage, and a magnification option to reduce the laser spot size when imaging small-area devices such as perovskite solar cells.

Lock-in-thermography (LIT) system. The customised LIT imaging tool was supplied by Scitech, and incorporates an Infratech mid-IR thermal imaging camera, microscope components, and IRBIS thermographic analysis software. The system was installed and commissioned in May 2022 at ANU. Under a reversed bias, shunted positions in solar cells are revealed by hot spots in thermal images captured by the LIT tool. The perovskite and silicon teams at ANU have used the tool to qualitatively monitor shunted locations across their devices. The next step will be to develop methodologies to extract quantitative data of shunt resistance and other important photovoltaic parameters from these thermal images.

Figure PP3.1.7: ANU PhD student Anh Bui with the lock-in-

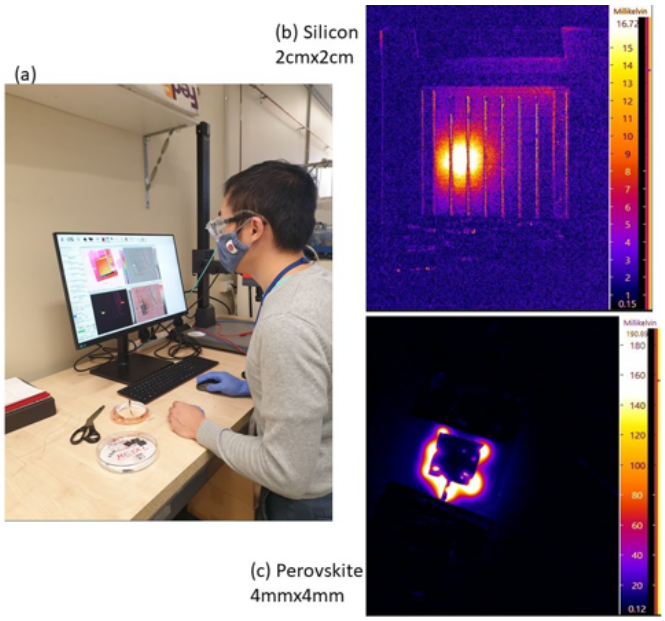

thermography (LIT) imaging tool. Examples of thermal images of (b) silicon and (c) perovskite solar cells captured by the LIT tool.

PLQY imaging module. The photometric calibration module was installed in the existing IMA hyperspectral imaging system (Photon inc) at ANU in December 2021. It has become an integral part of the hyperspectral system, allowing users to quickly capture images of photoluminescence quantum yield (PLQY) from their samples. Users can capture relative luminescence images as standard procedures, then apply calibration parameters from the photometric calibration module to convert the relative signal into an absolute number of photons emitted from a sample.

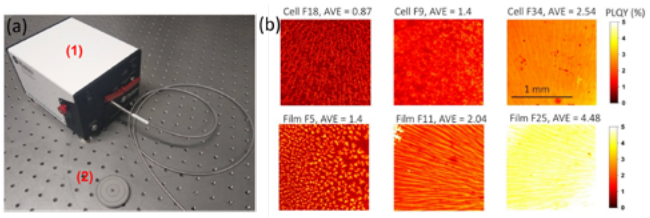

Figure PP3.1.8: (a) Photometric calibration module to convert relative PL intensity images into PLQY images. (b) PLQY images of various perovskite films and solar cells.

Multi-wavelength LED source. The high-powered, multi-wavelength LED (HPLED) light source (supplied by SDR Scientific) was delivered and commissioned in June 2022 at ANU. It is currently being integrated into an existing perovskite solar cell photoluminescence imaging system to provide a significant capability upgrade. The new source's power output is more stable with time; the light intensity is more uniform across the solar cell's area; and the advanced, computer-controlled electronics allows deeper integration with existing experimental systems. In addition, the multiple wavelength options will give more experimental flexibility and greater insight into perovskite physics.

The HPLED can produce stable, uniform, high intensity light at three wavelengths: near-UV (blue), green, and near-IR (red). These wavelengths produce markedly different conditions in perovskite films and solar cells. Under these conditions, different factors about the films and devices can become dominant. For example, under near-UV illumination, there is an increased influence of the interface and surface quality on cell performance and luminescence emission. By comparing the red- and blue-light response of perovskite solar cells at varying stages of completion, we can quantify and compare the quality of the transport layer interfaces. We intend for this type of characterisation protocol to become a core and routine step in perovskite solar cell development at ANU.

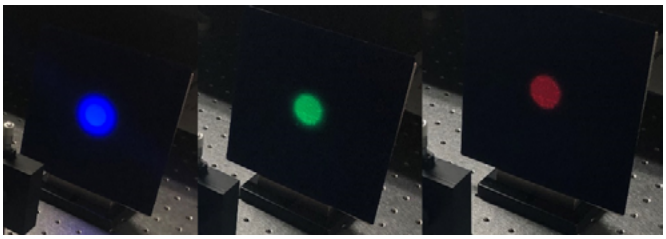

Figure PP3.1.9: Demonstration of each wavelength of emission over a 25 mm diameter illumination spot from the multi-wavelength high-power LED system.

Highlights

- New suite of multi-modal, multi-scale device characterisation tools to provide micron–cm scale characterisation of optoelectronic and device properties.
- Designed for maximum versatility for both single-junction and tandem/multi-junction devices, including perovskites, Earth-abundant, silicon and III-V materials.
- The cluster will be hosted by the ANU ACAP node, with free access provided to all ACAP researchers. The cost of operating and maintaining the equipment will be covered by ANU for five years.

Future Work

ANU staff and students will continue work to develop measurement protocols for combining and analysing the complementary data from multiple tools and will share these with other ACAP nodes. We anticipate the new capabilities provided by the cluster will lead to new cross-node collaborations that will further support ACAP research activities.

PP3.1C ADVANCED IMAGING TECHNIQUES FOR PEROVSKITES

Lead Partner
ANU

ANU Team
Dr Hieu Nguyen, Prof. Daniel Macdonald, A/Prof. Thomas White, Prof. Klaus Weber, Prof. Kylie Catchpole

ANU students
Anh Bui, Khoa Nguyen

Funding Support
ACAP, ARENA, ANU

Aim

Instability of perovskite solar cells is the main challenge for the commercialisation of this solar technology and for their integration in tandem configurations. The groups involved in this work aim to deepen the understanding of the complex degradation mechanisms observed in perovskite materials, with the objective of bringing this very promising technology to a high technology readiness level. Rapid, non-destructive, reliable methods for characterising these materials and devices will be critical for their commercial deployment.

Progess

The team at ANU, led by Dr Hieu Nguyen, has developed a contactless, imaging-based procedure to spatially resolve electronic properties of perovskite solar cells (PSCs) including implied open-circuit voltage (iV_{OC}) and its temperature coefficient, ideality factor (n_{id}), and activation energy of recombination (E_A) by employing illumination intensity and temperature-dependent photoluminescence. The illumination intensity dependence of iV_{OC} allows the extraction of n_{id} whereas its temperature dependence allows the extraction of the temperature coefficient and EA. This imaging approach is then applied to investigate changes of these electronic parameters on fully and partially fabricated devices.

Figure PP3.1.10(a) displays the average PL spectra across a working PSC at different illumination intensities. We observe that while the emission intensity decreases strongly with decreasing illumination intensity, the spectral shapes do not change, demonstrating that the illumination source does not cause any significant material phase segregation on the time scale of the measurements.

Figure PP3.1.10(b) shows the dependence of the global iV_{OC} on illumination intensity, yielding a global ideality factor of 1.55. In addition, the spatial variation (error bars in Figure PP3.1.10(b)) in the distribution of iV_{OC} at different illumination intensities demonstrates an advantage of the imaging technique over single-point or area-averaged measurements. Another advantage of the imaging-based technique is that it pinpoints the exact locations of problems across a device.

Figure PP3.1.10(c) and (d) show images of iV_{OC} under one-sun equivalent illumination intensity and n_{id} of the device, respectively. The average iV_{OC} value is 1.2 V, which is far below the Shockley–Queisser limit (V_{OC},SQ = 1.345 V, calculated directly from the material bandgap extracted from the peak of PL spectra) (Shockley & Queisser 1961; Rühle 2016). Furthermore, the variation in the n_{id} image (1.45 (green dotted line) to 1.63 (black dotted line) in Figure PP3.1.10(b), which are equivalent to 1 and 99 percentiles respectively in Figure PP3.1.10(d)) indicates different recombination mechanisms across the cell.

Furthermore, Figure PP3.1.11(a) displays PL spectra from another complete PSC at 258 K, 298 K and 318 K under one-sun illumination. Figure PP3.1.11(b) shows a representative temperature-dependent iV_{OC} curve of the PSC with an activation energy EA of 1.56 eV.

Figures PP3.1.11(c) and (d) display the images at 258 K and 298

K. At 298 K, the average iV_{OC} is 1.171 V, which is slightly higher than the final V_{OC} from the real current-voltage curve (1.167 V). Figures PP3.1.11(e) and (f) show the iV_{OC} temperature coefficient and EA images, respectively. The specific features marked in regions A and B (Figure PP3.1.11(d)) could be scratches that were introduced during the cell processing or handling. The same information can be obtained for n_{id} (not shown here). These imaging methods and their applications at various fabrication stages have been published in two journal papers (Bui, Mahmud et al. 2021; Bui et al. 2021).

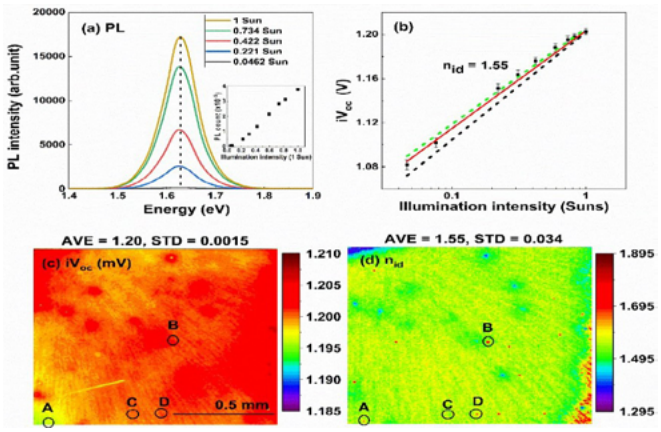

Figure PP3.1.10: (a) Average PL spectra of the PSC at different illumination intensities (inset: integrated PL intensity versus illumination intensity). (b) Extracted iV_{OC}-illumination intensity curve and average ideality factor. The red straight line is the fitting curve of iV_{OC} values averaged across the entire imaging area. The green dotted and black dotted lines represent the 1 and 99 percentiles, respectively. (c) iV_{OC} and (d) n_{id} images of the device.

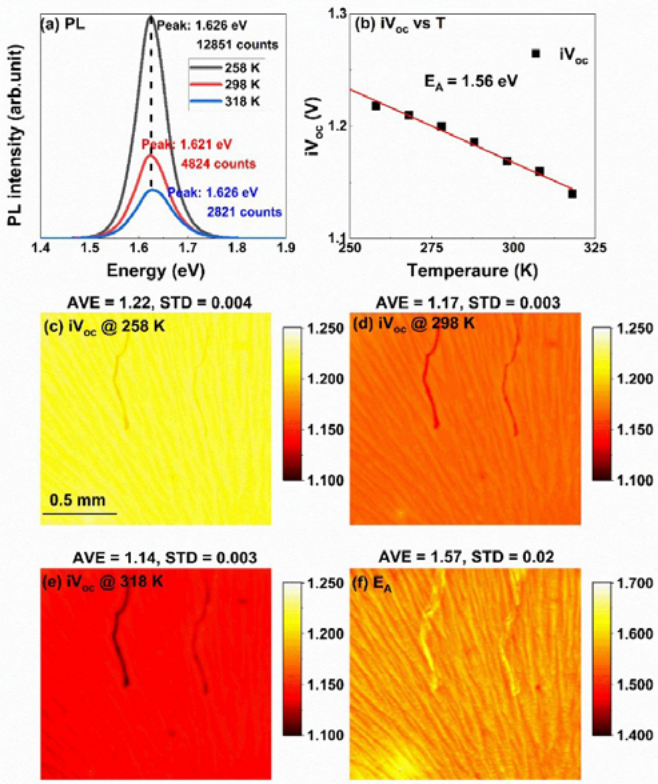

Figure PP3.1.11: (a) PL spectra of a working PSC at 258 K, 298 K and 318 K. (b) Temperature-dependent iV_{OC} curve extracted from temperature-dependent PL data. (c), (d) iV_{OC} images at 258 K and 298 K, respectively. (e), (f) images of the temperature coefficient and of the E_A, respectively.

Highlights

- Establishment of imaging-based procedures to spatially resolve electronic properties of perovskite solar cells including iV_{OC} and its temperature coefficient, n_{id}, and E_A.
- Demonstration of the methods on both finished and unfinished solar cells.

Future Work

The team will continue to refine their techniques to support the drive to near-term commercial viability of perovskite solar cells. Particularly, these techniques will be thoroughly quantified and their uses for characterisation of single-junction and tandem cells under various conditions will be explored.

References

Bui, Bui, A. D., Mahmud, M. A., Mozaffari, N., Basnet, R., Duong, T., Bartholazzi, G., Le, T. T., Truong, T. N., Tebyetekerwa, M., Wibowo, A., Weber, K. J., White, T. P., Catchpole, K. R., Macdonald, D. & Nguyen, H. T. (2021). Contactless and Spatially Resolved Determination of Current–Voltage Curves in Perovskite Solar Cells via Photoluminescence. Solar RRL 5, 2100348.

Bui, A. D., Mozaffari, N., Truong, T. N., Duong, T., Weber, K. J., White, T. P., Catchpole, K. R., Macdonald, D. & Nguyen, H. T. (2021). Electrical properties of perovskite solar cells by illumination intensity and temperature-dependent photoluminescence imaging. Progress in Photovoltaics: Research and Applications. https://doi.org/10.1002/pip.3498.

Rühle, S. (2016). Tabulated values of the Shockley–Queisser limit for single junction solar cells. Solar Energy 130, 139-147.

Shockley, W. & Queisser, H. J. (1961). Detailed balance limit of efficiency of p-n junction solar cells. Journal of Applied Physics 32, 510.

PP3.1D ADVANCED LED SOLAR SIMULATOR FOR ULTRA-HIGH SPECTRAL MATCH AND APPLICATION TO MULTI-JUNCTION DEVICES

Lead Partner
CSIRO

CSIRO Team
Dr Benjamin Duck, Dr Chris Fell, Dr Blago Mihaylov, Dr Tim Jones, Kenrick Anderson, Dr Noel Duffy, Dr Gregory J. Wilson

Industry Partner
Lastek

Funding Support
ARENA, CSIRO, Lastek

Aim

Ongoing improvements in the performance of solar photovoltaic (PV) technology have lately included the exploration of tandem (multi-junction) device architectures to circumvent the Shockley–Queisser performance limitation of single-junction devices. The inclusion of one or more perovskite junctions currently represents a promising avenue to develop low-cost tandem devices, however the metastable nature of the commonly used hybrid metal-halide perovskites leads to large measurement uncertainty when determining the device performance. In 2019 ARENA supported a partnership between CSIRO and Lastek for the design and development of a new LED-based solar simulator and protocols that are designed to mitigate this measurement problem.

The project takes advantage of the increasing availability and performance characteristics of commercial high power light emitting diode (LED) sources to develop a new light source for PV performance measurement. An increasingly better match of solar simulator spectral irradiance to the AM1.5G reference spectrum is obtained through careful selection of available LEDs. This match combined with the inherent flexibility of a multi-source system enables significant improvements in the measurement procedure and provides avenues to reduce the exposure of metastable devices to undesirable conditions.

Progress

LED development

In partnership with Lastek the CSIRO team has developed a prototype LED solar simulator (LEDSS) that uses 40 different colours that are independently controlled to achieve maximum system flexibility. When combined the system can achieve the closest match to the AM1.5G reported (Figure PP3.1.12). The system easily achieves a class A+ rating (as specified by IEC 60904-9) in spectral irradiance (Figure PP3.1.12) and temporal stability. Spatial homogeneity determined by the area of the device under test (DUT) is Class A at 80 x 80 mm (Figure PP3.1.13).

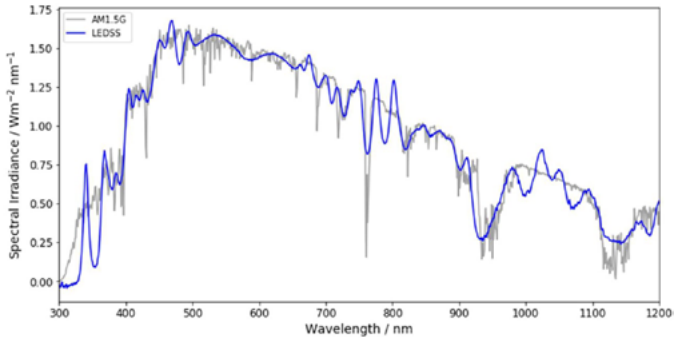

Figure PP3.1.12: LEDSS output vs AM1.5G reference.

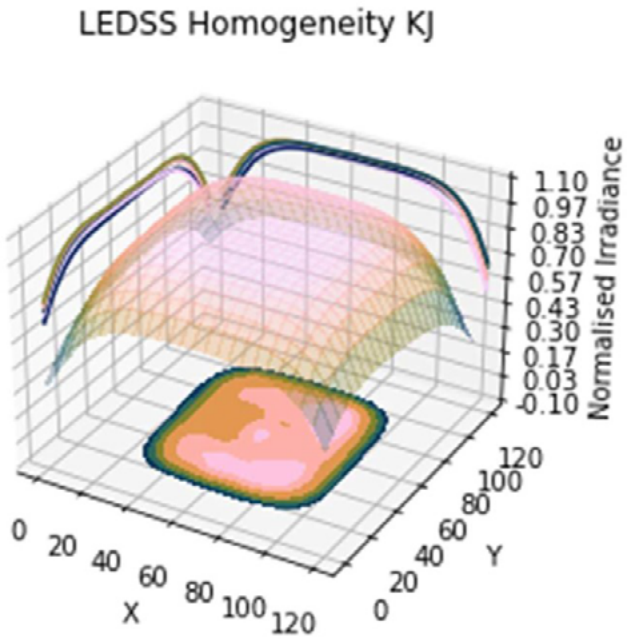

Figure PP3.1.13: Example LEDSS output spatial homogeneity.

Metastable tandem measurement protocol

A generalised protocol for metastable perovskite/silicon tandems has been developed and is currently undergoing further validation testing. The protocol uses a combination of adaptive and repeated pre-conditioning with interspersed performance measurement cycles.

The goal is to simultaneously measure the device architecture's best settled performance characteristic while minimising the impact of degradation mechanisms.

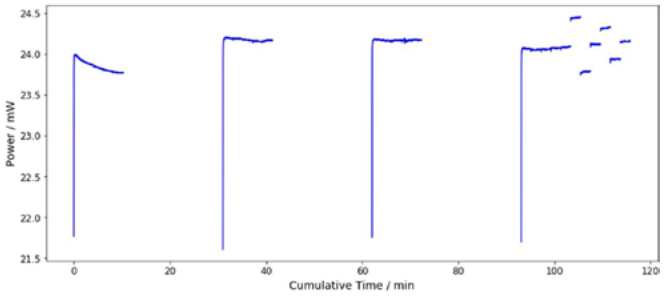

Figure PP3.1.14: Example testing protocol results. Initial pre-conditioning (before the first power measurement) is insufficient to maximise the device performance. Optimal performance is achieved on the second iteration of the protocol. Spectrometric testing indicates a well-matched top limiting device.

The power of the system for tandem performance measurements is shown in its ability for spectrometric testing. Here the output spectral irradiance of the simulator is carefully varied to achieve a desired change in the junction of interest. The overall device response will be impacted by the matching quality of the junctions and we can therefore determine the implications of a spectral mismatch on device performance. Figure PP3.1.15 shows an example of the testing conditions along with results from a well-matched and top limiting device.

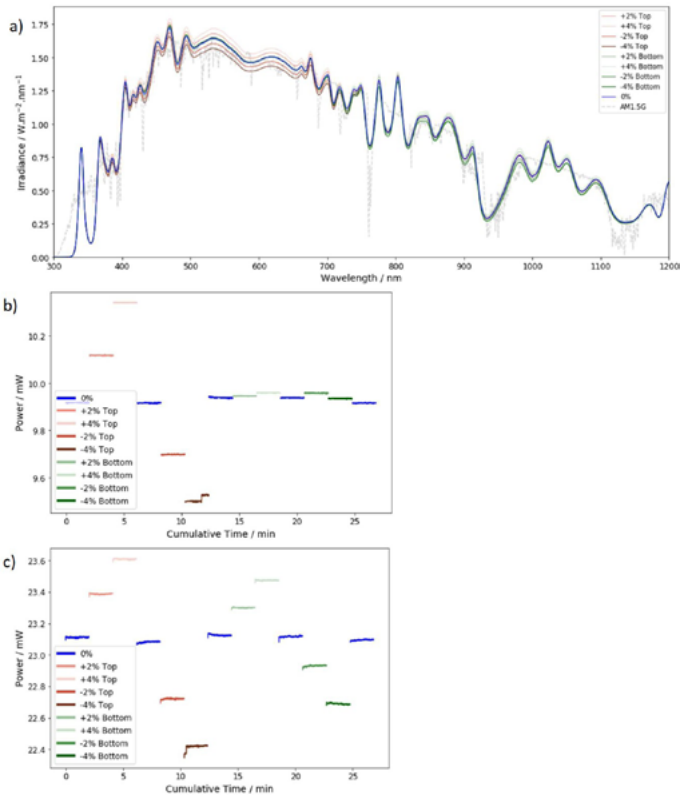

Figure PP3.1.15: (a) Spectrometric testing profile for perovskite/silicon tandem. Results for (b) a matched and (c) a top limiting tandem device.

Measurements without spectral response

A key improvement in tandem performance assessment is the ability to neglect the requirement for a spectral responsivity (SR) measurement in the characterisation process with only a modest impact on the final uncertainty. The low uncertainty is achievable through two mechanisms. Firstly, the excellent match to the AM1.5G reference means that not only are negligible mismatch factors trivial to achieve but any residual differences or errors in SR will not significantly impact the final result. Secondly, a careful choice of the spectral irradiance optimisation metric can minimise the potential impact of a large range of SR variations. This impact minimisation means only a rough estimate of the true SR is required (e.g. from previous measurements on similar architecture types) to maintain low measurement uncertainty. Figure PP3.1.16 shows the results of calculations performed on a pool of tandem, perovskite and silicon SR data with LEDSS spectral irradiance optimised by different methods. In the best case the additional uncertainty for a performance measurement without exact SR knowledge is only 0.32%.

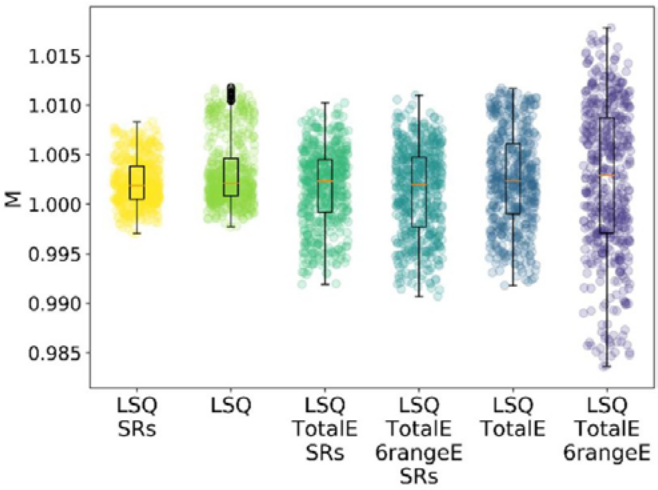

Figure PP3.1.16: Results of calculations performed on a pool of tandem, perovskite and silicon SR data with LEDSS spectral irradiance optimised by different methods.

Highlights

- Successful development of a new 40-channel LED simulator prototype.
- Closest reported match to AM1.5G spectrum.
- Performance measurements of metastable devices do not require spectral response to maintain low uncertainty.

Future Work

Further validation of the new tandem protocol is ongoing with ACAP partners. Potential commercialisation of the LEDSS IP is being pursued as well as the usage of a base module for complementary applications. The capabilities developed here will allow CSIRO's PVPL to pursue accreditation for tandem device measurements.
The capability will also directly support CSIRO's efforts for its (SIEF funded) demonstration and scale-up of its perovskite CVD process and adaptation to tandems based on textured silicon substrates. This work will be facilitated with the recent recruitment of two new early career researchers and collaboration with UNSW.

PP3.1E HIGH-THROUGHPUT SOLAR CELLS I-V AND LONG-TERM STABILITY CHARACTERISATION

Lead Partner
Monash University

Research Team
Dr Kevin Rietwyk, Dr Tian Zhang, Dr Adam Surmiak, Prof. Udo Bach

Funding Support
ACAP, Monash University, Exciton Science

Aim

There is a growing impetus in material science to discover, fabricate and characterise new materials, at rates previously unrealised. The development of new materials is often the cornerstone to new technologies and research breakthroughs. The core focus of this project is to accelerate the rate at which prototypical devices can be characterised and the feasibility of new devices and the constituent materials assessed. There are two key aspects, the high-throughput current-voltage (I-V) testing suitable for small-area laboratory thin-film solar cells and the environment chamber for long-term stability measurements at precisely controlled atmospheric conditions.

Progress

The high-throughput I-V solar cell testing system at Monash University that was the focus of a recent publication from Surmiak et al. has recently undergone two upgrades to include the capability of measuring perovskite back contact solar cells and to perform automated light intensity measurements. A custom jig was designed and implemented especially for the back contact devices studied at

Monash University via a single plug connection. This setup enjoys the same features of the original jig – simultaneous measurement of 16 solar cells with 4-wire sense. In addition, a series of large-area ND filters (10 cm × 10 cm) on motorised slide rails have been implemented between the AAA solar simulator and sample holder. Through software, the user is able to perform light-dependent I-V curve analysis using any combination of the ND filters to finely tune the light intensity. This will greatly expand the level of automated analysis possible and provide information on the ideality factor, series and shunt resistance, and transport efficiency. The cooling gas distribution system has also been redesigned with added thermocouples and humidity sensors to allow for direct measurement of the temperature and relative humidity of cells during testing.

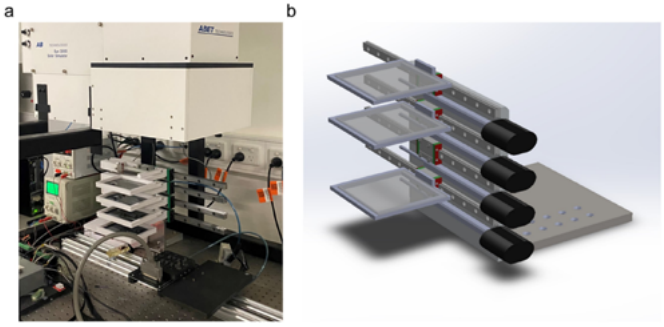

Figure PP3.1.17: (a) Photograph AAA solar simulator with the ND filter array and sample holder, and (b) schematic of ND filter array on linear drives with motors for automated control.

The electrical testing system in an ATLAS environment chamber has been completely revamped. A replacement for the very limited multiplexer, comprising a dozen dual-channel source measurement units for parallel real-time measurement, was built to accommodate high-throughput ageing and long-term stability testing. A custom-made graphical user interface allows for a range of measurement modes including current-voltage, constant voltage, constant current, maximum power point tracking and pre-biasing, that can be performed sequentially. The chamber provides control over the light intensity up to one-sun, temperature from -32 to 110°C and relative humidity from 0 to 100%, with day-night cycling options. All standard ISO accelerated ageing procedures are available. All sample mounting jigs and holders were designed and 3D printed in-house with capacity to expand to more cells..

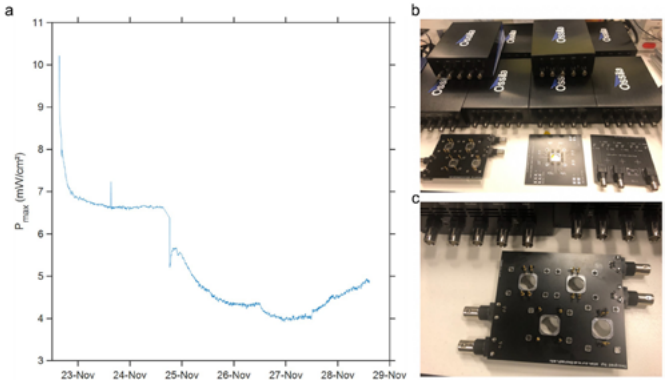

Figure PP3.1.18: (a) Example data, PMAX determined from J-V curves performed every 5 minutes across 6 days. (b), (c)Photographs of the source measurement units and sample holders used in the environmental chamber.

Highlights

- Development of a new jig suitable for back contact solar cell devices that can be switched in within minutes.
- Capacity to perform light intensity–dependent current-voltage analysis.
- Ability to characterise 24 solar cells independently for long-term stability or accelerated ageing studies.

Future Work

- Capability of running lock-In thermography and traditional thermography including mapping is currently under development.
- Further update for inert atmosphere measurement in the 16-channel solar simulator.

References

Surmiak, M. A., Zhang, T., Lu, J., Rietwyk, K. J., Raga, S. R., McMeekin, D. P. & Bach U. (2020) High-Throughput Characterization of Perovskite Solar Cells for Rapid Combinatorial Screening. *RRL Solar, 202000097*.

PP3.1F OPTICAL CHARACTERISATION TECHNIQUES AND RECOMBINATION ANALYSIS ROUTINES FOR UNDERSTANDING CARRIER DYNAMICS OF EMERGING PHOTOVOLTAIC MATERIALS AND DEVICES

Lead Partner

UNSW

UNSW Team

Dr Weijian Chen, Prof. Martin Green, A/Prof. Xiaojing Hao, Prof. Nicholas Ekins-Daukes

Academic Partner

King Abdullah University of Science and Technology (KAUST):
Prof. Omar F. Mohammed Swinburne University of Technology (SUT):
Prof. Baohua Jia,
Dr Xiaoming Wen

Funding Support

ACAP Fellowship

Aims

Photophysics in novel materials and devices are keys to photovoltaics research to improve efficiency, reduce cost and enhance stability. Perovskite and adamantine (such as kesterite, chalcopyrite) thin-film materials are the most promising materials. Interface and bulk defect engineering in perovskite and kesterite solar cells are the most viable approaches to improving their stability and efficiency. The microscopic physical mechanism of charge carriers in working condition solar cells is the key to guiding engineering strategies.

This project aims to develop 3D optical characterisation techniques and recombination analysis routines for emerging PV materials in operational single-junction and tandem solar cells. Photoluminescence (PL)-spectroscopy characterisation routine methods and numerical models are to be developed for perovskite, kesterite, and other adamantine thin-film solar cells with superior temporal, spatial and spectral resolutions, and methodological generalisation for

other adamantine thin films in operational single-junction solar cells and tandem silicon solar cells. With a thorough understanding of carrier dynamics, fundamental limitations to devices' performance (i.e. stability of perovskite and efficiency of kesterite/adamantine/ $Sb_2(S,Se)_3$) will be investigated to accelerate the development of high quality PV materials for silicon-based tandem cells.

This work directly contributes to the ACAP program PP2 Thin-Film, Third Generation and Hybrid Devices and PP3 Optics and Characterisation by developing advanced spectroscopy characterisation methods analysing and optimising emerging solar cells. With the characterisation methods aiming at analysing complicated structures in tandem solar cells, it also contributes to PP1 Silicon Solar Cells with a focus on PP1.3A(iv): III-V Materials and chalcogenides for silicon-based tandem cells.

Progress

A. Illumination-induced mobile ion dynamics in perovskite solar cells

Motivation

Dynamic processes of mobile ions and the interaction between charge carriers and mobile ions, are intimately correlated to the observed slow response in perovskites. PL and time-resolved PL (TRPL) imaging are unique tools to probe the dynamic processes of the slow response and the corresponding microscopic and temporal physical mechanisms. Therefore, investigation of mobile ions in perovskites using time-resolved micro-spectroscopy is essential not only for the perovskite community, but also for the broader semiconductor research community interested in ionic transports in polycrystalline materials.

Progress

The dynamic effect of mobile ions in halide perovskites is studied via time-resolved micro-spectroscopy (Chen et al. 2021a). PL quenching and fluorescence blinking are induced by mobile ion migration and accumulation in a single perovskite grain. The ion accumulation at the interface impacts the carrier extraction and the efficiency of perovskite solar cells. Using the PL-TRPL imaging technique, the light soaking effect has been dynamically monitored in a nanoscale, which exhibits a tight correlation to the performance of a perovskite solar cell. A comprehensive understanding of ionic dynamics is not only critically important for stable solar cells but also for new applications based on ionic properties. Micro-spectroscopic techniques combining confocal microscope and TRPL have been demonstrated as powerful tools to reveal the dynamic of mobile ions in both macroscopic and microscopic range.

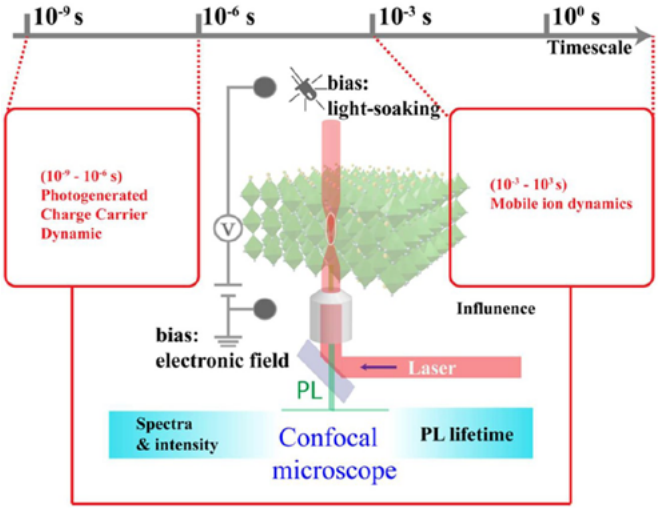

Figure PP3.1.19: Diagrams of the methodology of probing ion dynamics using time-resolved spectroscopic techniques.

B. Interface dynamics study on carrier extraction of perovskite solar cell

Motivation

For high photon conversion efficiency and long-term stability, the charge carrier transfer must be stable and efficient. Spiro-OMeTAD doped with Li-TFSI is the most widely used solid-state hole transport material in perovskite solar cells. However, the additive Li-TFSI is a highly hygroscopic material that affects long-term performance. High mobility of Li+ ions can also affect the stability of the PSCs, for example, I-V hysteresis. Therefore, alternative additives to Li-TFSI in Spiro-OMeTAD are essential (Chen et al. 2021b).

Progress

In this work, a Li-TFSI additive in the Spiro-OMeTAD is replaced by TFSI-salts (Mg-TFSI2, Ca-TFSI2), and the corresponding PSCs demonstrate higher efficiency with significantly boosted photostability. Spectroscopic investigations provide insights into efficient and stable hole transfer mechanisms by substituting Mg-TFSI2 and Ca-TFSI2 for Li-TFSI. The PSC's photoluminescence dynamics are monitored under continuous illumination, which reveals the behaviours of mobile ion accumulations at the perovskite/Spiro-OMeTAD interface (Chenet al. 2021).

The mobile ion accumulation is mitigated in the cases of Mg-TFSI2 and Ca-TFSI2, which ascribes to the improved hole mobilities of the Spiro-OMeTAD. Additives engineering in Spiro-OMeTAD provides a strategy to improve stability and photon conversion efficiency. The spectroscopic study in this work concludes that higher hole mobility in hole transport layers plays a vital role in suppressing mobile ion accumulation. With optimal engineering of conductive additives, a more efficient charge transfer can be attained, together with improved photostability.

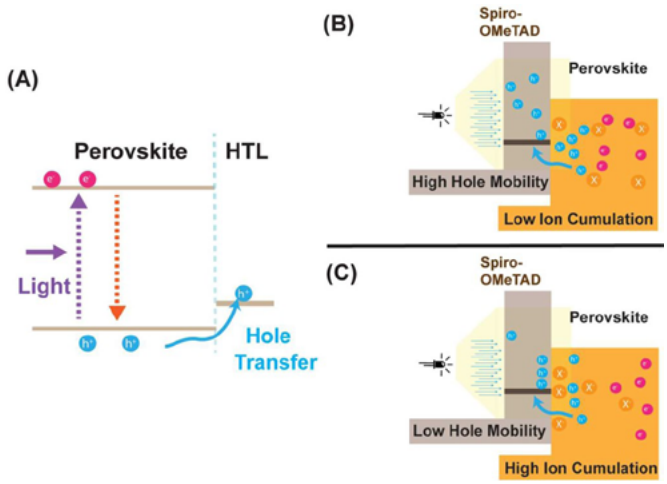

Figure PP3.1.20: Schematic of the (a) hole extraction dynamics for the interface of Spiro-OMeTAD and perovskite with (c) high hole mobility and (c) low hole mobility.

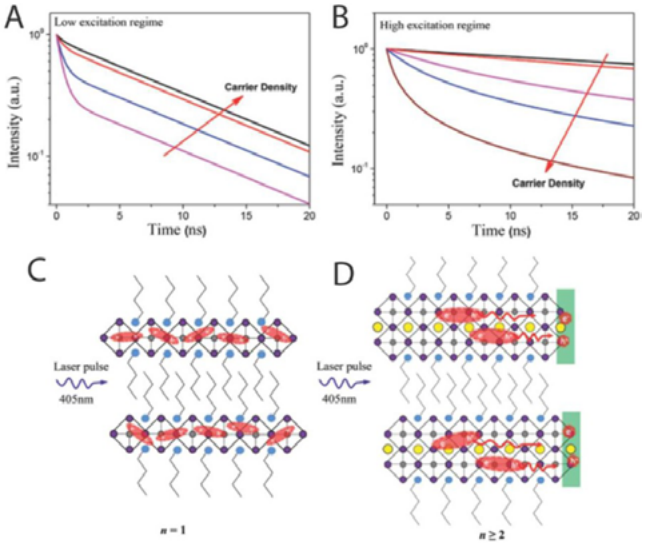

Figure PP3.1.21: Simulation for PL decay in the (a) low and (b) high excitation regime according to bi-exponential function; schematic of different carrier dynamics between n = 1 (c) and n ≥ 2 (d). The green area represents the edge state.

C. Photophysics of two-dimensional (2D) organic-inorganic hybrid lead halide perovskites

Motivation

Two-dimensional layered perovskites have recently attracted significant attention owing to their excellent environmental stability, a high degree of electronic tunability, and natural multi-quantum-well structures (Gan et al. 2021). This part of the project aims to study the special photophysics of 2D perovskites that are different from the conventional 3D congeners. Unlike the conventional inorganic quantum wells, the organic cationic ligands in the 2D perovskites can be flexibly modified. The design of organic sites has afforded a versatile platform for the modulation and functionalisation of the 2D perovskites.

Progress

Via Via characterising layer number–dependent exciton dissociation in 2D Ruddlesden–Popper (RP) halide perovskites, it is confirmed that 2D perovskites of $(BA)_2PbI_4$, with the number of $[PbX_6]_4$- layers n = 1, clearly exhibit exciton characteristic properties. Meanwhile, $(BA)_2(MA)Pb_2I_7$ and $(BA)_2(MA)_2Pb_3I_{10}$, n = 2 and 3, exhibit free carrier behaviour, which is inconsistent with their binding energies of more than 100 meV (Lu et al. 2021). Such anomalous exciton and free carrier behaviours are attributed to the effective exciton in-plane transport and dissociation by the edge state.The different carrier dynamics in 2D RP perovskites with n = 1, n = 2 and n = 3 are investigated using excitation intensity–dependent TRPL at room and low temperatures. The 2D RP perovskite with n = 1 exhibits exciton dominant carrier dynamics while the samples of n = 2 and n = 3 exhibit free carrier dominant behaviour. The thermal energy–driven exciton dissociation is excluded for the pathway of exciton dissociation. Instead, the edge state–induced exciton dissociation is attributed to be the mechanism. Although the binding energy is much larger than thermal energy at room temperature for small n (with n>2), they exhibit free carrier dominant behaviour similar to their 3D counterparts.

Highlights

- Promising Earth-abundant materials for high efficiency next generation PV technology.
- Advanced multi-dimensional imaging spectroscopy and microscopies for emerging materials both for single-junction solar cells and tandem solar cells.
- Collaboration with a variety of institutions in Australia and internationally.

Future Work

- Design and develop characterisation routine for active layers in a tandem cell structure.
- Generalisation of developed characterisation methods and models and application to tandem solar cells.
- Numerical modelling and complete design of multi-dimensional microscopies.

References

Chen, W., Gan, Z., Green, M. A., Jia, B. & Wen, X. (2021). Revealing Dynamic Effects of Mobile Ions in Halide Perovskite Solar Cells Using Time-Resolved Microspectroscopy. *Small Methods* 5, 2000731.

Chen, W., Pham, N. D., Wang, H., Jia, B. & Wen, X. (2021b). Spectroscopic Insight into Efficient and Stable Hole Transfer at the Perovskite/Spiro-OMeTAD Interface with Alternative Additives. *Acs Applied Materials & Interfaces* 13, 5752-5761.

Gan, Z., Chen, W., Liu, C., Zhang, J., Di, Y., Yu, L., Dong, L., Jia, B. & Wen, X. (2022). Energy Funneling in Quasi-2D Ruddlesden–Popper Perovskites: Charge Transfer versus Resonant Energy Transfer. *Advanced Photonics Research* 3, 2100283.

Lu, J., Chen, W., Zhou, C., Yang, S., Wang, C., Wang, R., Wang, X., Gan, Z., Jia, B. & Wen, X. (2021). Layer number dependent exciton dissociation and carrier recombination in 2D Ruddlesden–Popper halide perovskites. *Journal of Materials Chemistry* C 9, 8966-8974.

PP3.1J IDEALITY FACTOR MAPPING OF PEROVSKITE BACK CONTACT SOLAR CELLS

Lead Partner
Monash University

Research Team
Dr Kevin Rietwyk, Dr Xiongfeng Lin, Dr Boer Tan, Dr Tharindu Warnakula, Siqi Deng, Mr Boya Zhao, Adam Surmiak, Prof. Udo Bach

Funding Support
ACAP, Monash University, Exciton Science

Aim

The efficiency of back contact perovskite solar cells has steadily increased over the past few years and now exceeds 11%. In order to make further improvements in the efficiency of these devices it is necessary to understand the cause of the low fill factor, low open-circuit voltage (V_{OC}) and severe hysteresis. The ideality factor is a useful figure of merit to describe the recombination processes within photovoltaic devices. Here we perform a time and light intensity–dependent V_{OC} and micro-photoluminescence (PL) analysis to monitor the transient ideality factor spatially.

Progress

Based on the measurements of time and light intensity–dependent V_{OC} and micro-photoluminescence, we successfully developed a mapping technique that allows the visualisation of ideality factors and calculated analogues of PV devices to evaluate the temporal and evolution of recombination in microscopic scale.

At an electrode scale, we observe a spatial modulation in the various parameters related to the electrode pattern that permits direct comparison between the two sets of transport layers/electrodes. Upon carrying out statistical analysis across a batch of back contact PSCs with a mesoporous and/or a planar TiO_2 layer, we confirmed that implementing a mesoporous TiO_2 layer can drastically reduce recombination while achieving a 120 mV increment in mean V_{OC} and enhanced PL intensity. In the meantime, the electrode scale analysis reveals the mesoporous layer enhances the properties more strongly at the NiO_x interface with higher QLFS (5 meV) and $J_{SC,i}$ (0.99 mA/cm² at 1.22 suns) compared to the TiO_2 interface (Figure PP3.1.22).

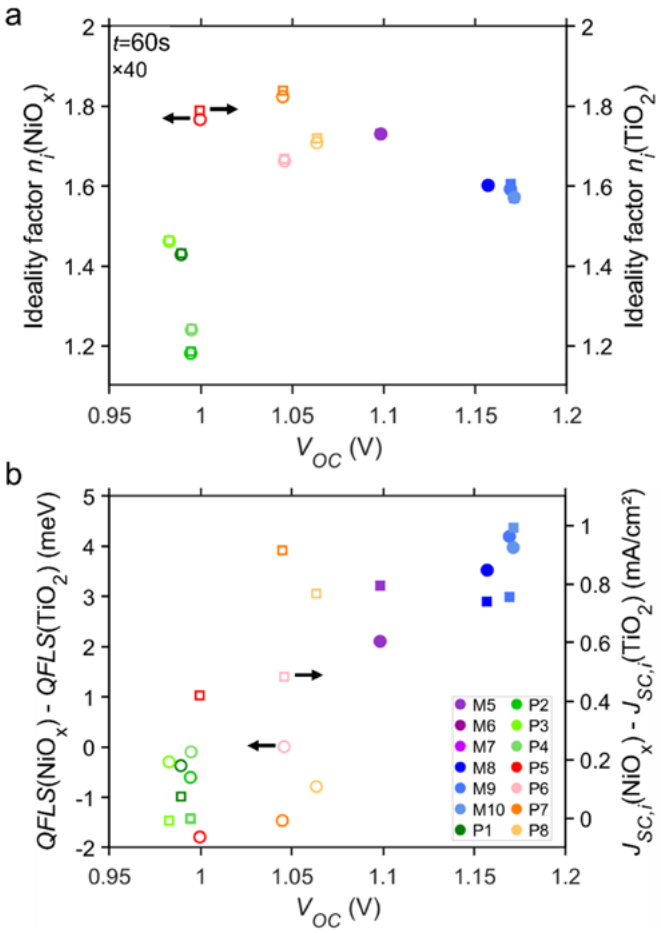

Figure PP3.1.22: (a). Plot of the mean ideality factors n_i for NiO_x and TiO_2 regions (measured at ×40) against the V_{OC} (measured at ×2). (b). Plot of the difference in the mean QFLS (left) and difference in the mean $J_{SC,i}$ (right) between NiO_x and TiO_2 regions, measured at ×40 against the V_{OC} (measured at ×2). The mean $J_{SC,i}$ is determined from the product of $J_{SC,i}/J_L$ with the J_L = 29.5 mA or 1.22 suns, for each cell. A scaled transmission map was used to discriminate between the electrode regions NiO_x (red) and TiO_2 (blue). Colours indicate the cell, circles and squares correspond to the left and right axes and solid and hollow symbols indicate whether the cells have mesoporous and planar TiO_2, respectively.

The experimental results are also corroborated with two-dimensional time-dependent drift-diffusion simulations that include ion migration with a single fixed anion and mobile cation representing halide vacancies. The results show that the change in the ion concentrations significantly impacted the electron and hole concentrations throughout the device and in turn the V_{OC}, PL intensity and ideality factors (Figure PP3.1.23).

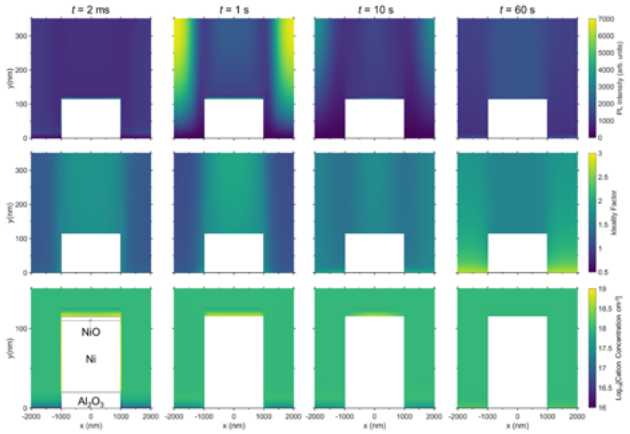

Figure PP3.1.23: Simulated cross-sectional maps of the photoluminescence, ideality factor and log_{10}[cation concentrations] (top to bottom) for the perovskite absorber layer at times t = 0.002, 1, 20 and 60 s under OC. The y-scale of the log_{10}[cation concentrations] plots have been truncated to emphasise the region near the transport layers. Line profiles of these plots are provided in SI. The black lines added to the t = 2 ms ion concentration map from top to bottom show the NiO, Ni and Al_2O_3 regions.

Highlights

- Developed a mapping technique that allows the visualisation of the ideality factor of a back contact perovskite solar cell.
- Analysis on overall rate of recombination to offer insights into the dominant recombination process.
- 2D drift-diffusion simulation found that the accumulation and depletion of ions at the transport layer interfaces.
- Publication in Advanced Energy Materials (Accepted).

Future Work

- Developing strategies to reduce ion migration is necessary for advancing back contact PSCs.
- Devising a metric to quantify the hysteresis of back contact PSCs at an electrodes scale.

References

Calado, P., Burkitt, D., Yao, J., Troughton, J., Watson, T. M., Carnie, M. J., Telford, A. M., O'Regan, B. C., Nelson J. & Barnes P. R. F. (2019). Identifying Dominant Recombination Mechanisms in Perovskite Solar Cells by Measuring the Transient Ideality Factor. *Phys. Rev. Applied* 11, 044005

PP3.1K ULTRAFAST LASER SPECTROSCOPIC CHARACTERISATION CAPABILITIES

Lead Partner

University of Melbourne (UoM)

Team

Prof. Trevor Smith, Prof. Ken Ghiggino, Dr Saghar Masoomi-Godarzi, Dr Chris Hall, Dr Rohan Hudson, Dr Jamie Laird

Funding Support

ACAP, UoM, ARC LIEF

Aim

To establish a comprehensive facility for ultrafast laser spectroscopic characterisation of photovoltaic materials, based on a high pulse repetition rate, high pulse energy ultrafast laser amplifier and dual optical parametric amplifiers with frequency doubling units. This will allow for techniques such as transient absorption, time-resolved photoluminescence and other methods to be performed with temporal resolution from tens of femtoseconds to microseconds, with high signal to noise.

Progress

The new ultrafast laser spectroscopy system, installed in 2021, has been fully commissioned along with a second, but related, laser amplifier system. Coupled together, this facility provides overall capabilities beyond those of either originally envisaged system.

The overall facility comprises two high pulse repetition rate (100 kHz), femtosecond laser amplifiers seeded from a common oscillator. The first amplifier (ACAP) pumps two independently tunable non-collinear optical parametric amplifiers (NOPAs) and provides a third beam for the generation of a white-light continuum probe. This is primarily used for transient absorption spectroscopy with excitation wavelengths available from the ultraviolet to near infrared. This source is coupled to a pair of high repetition rate spectrometers (visible and NIR) that can acquire spectra from every laser pulse up to 50 kHz.

The second system (LIEF) pumps a series of optical parametric amplifiers and different frequency generation devices, in addition to an independent white light probe beam. Wavelengths from the UV to mid infrared are available through independent outputs enabling broad spectral range excitation and probing. The IR pulses are of sufficient bandwidth to record information from the spectral fingerprint region by scanning out to ~11 µm. This system can be coupled to a high repetition rate infrared spectrometer to enable transient infrared spectra to be recorded to interrogate changes in IR frequencies in the excited state compared to ground-state frequencies, and the dynamics involved. This can be used to identify intermediate light-induced species, which are often difficult to separate through the broad, overlapping bands in the visible spectrum. The IR probe can also interrogate changes in bond stretch and bend frequencies that might result through excited-state energy relocation. This is a new capability for Australian PV researchers.

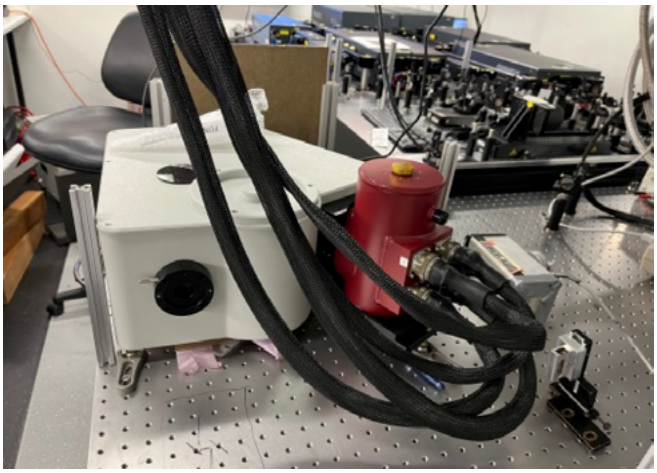

Figure PP3.1.24: Transient infrared absorption spectrometer.

Figure PP3.1.25: Complete dual amplifier ultrafast system.

A unique capability provided by combining these two systems is that by seeding both amplifiers from a common mode-locked oscillator all the light sources are perfectly synchronised, providing new capabilities that are of importance for characterising PV materials. Conventional pump-probe measurements on femtosecond to ~10 ns ranges are performed using optical delay stages, however, due to the synchronised amplifier arrangement, either amplifier/OPA source can be used as a pump, while the probe can be generated from the other amplifier, which can be triggered electronically in steps of ~12.5 ns relative to the excitation pulse. Combining the optical and electronic delay methods enables samples to be excited (from the UV-IR) and probed through the visible, NIR and IR from tens of femtoseconds to timescales limited by the repetition rate of the lasers – all with the same excitation pulse conditions. This is crucial to avoid multi-photon absorption (sometimes observed with nanosecond pulses) and multi-exitonic effects (when pulses of different energies are used). These factors need to be avoided in organic, perovskite and silicon photovoltaic materials.

By varying the laser repetition rate we have recently performed transient absorption measurements from tens of femtoseconds to about a millisecond from the same measurement.

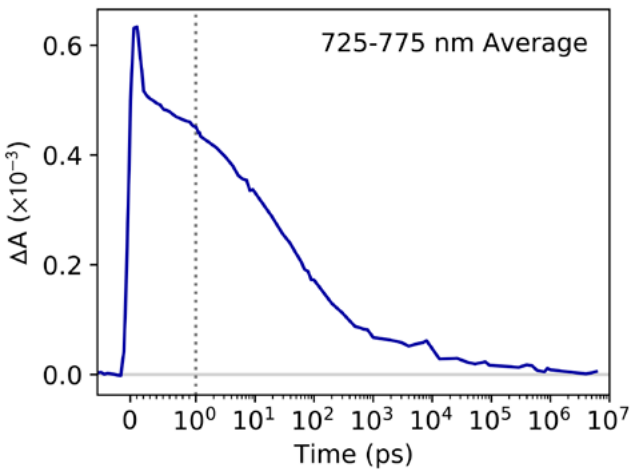

Figure PP3.1.26: Transient absorption of OPV material covering eight orders of magnitude in time.

These measurements can be conducted over temperature ranges from ~4 K to 310 K and simultaneously under the influence of a magnetic field up to 1 Tesla.

In addition to this new capability, other ultrafast laser spectroscopic characterisation capabilities include a transient absorption microscope with tunable excitation and white-light probe. This microscope can also be used to perform transmission spectral, photoconductivity and photoluminescence mapping capabilities.

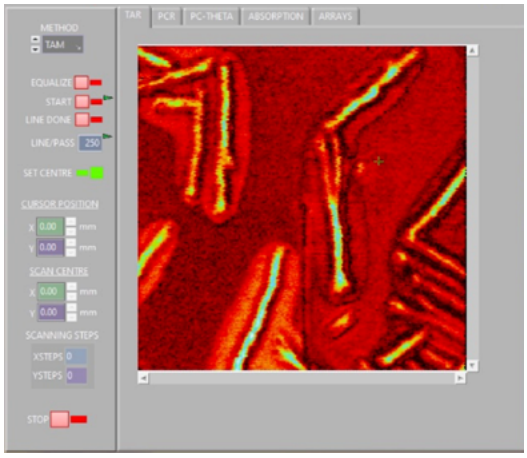

Figure PP3.1.27: Transient absorption microscopy of an OPV/PCBM blended film.

Highlights

- New femtosecond spectroscopic characterisation capabilities established.
- Time scales from femtoseconds to microseconds using the same excitation source.
- Transient infrared spectroscopy capabilities.
- Transient absorption and photocurrent mapping implemented

Future Work

The new ultrafast laser system is designed to be flexible enabling new techniques to be developed. The ability to perform multiple experimental techniques on a single laser system will enhance the characterisation of photovoltaic materials.

PP3.1L ADVANCING THE PDS TECHNIQUE FOR ALL PHOTOVOLTAIC THIN FILMS

Lead Partner
UNSW

Team
Dr Henner Kampwerth, Dr Michael Pollard, Prof. Gavin Conibeer, Prof. Xiaojing Hao

Academic Partners
Dr Meita Asami, Prof. Kentaroh Watanabe, Prof. Masakazu Sugiyama, Prof. Yoshitaka Okada, University of Tokyo
Dr Binesh Puthen Veettil, Macquarie University

Funding Support
ACAP, UNSW, Tokyo University, Open Instruments

Aim

The first photothermal deflection spectroscopy (PDS) setup was initially developed at UNSW through an ARENA Fellowship during 2013–2015 and further matured towards commercialisation in stages with industrial collaborator Open Instruments and support from ACAP (ACAP Collaboration Grant Round 3) and ARENA (ARENA Commercialisation of R&D). The relevant detail of this instrument is that it measures the heat generated by the photo-absorption of the sample. The heat signature represents the number of absorbed photons by assuming that all absorbed energy will recombine thermally. The resulting photo-absorption spectra are very similar to those from Reflectance-Transmission measurements (R&T). The primary difference is that the PDS technique has a significantly higher sensitivity, up to five orders of magnitude, whereas R&T barely exceeds two orders.

The aim of this project is to seed new collaboration activities between UNSW and Tokyo University. The groups under Prof. Sugiyama and Prof. Okada were chosen as they research superlattices of GaAs photo-active materials, for which it is challenging to measure any absorption features at sub-bandgap energies. We wanted to explore how well the PDS technique suits these materials as well. For this, the first commercial unit, which was developed with ARENA's support in collaboration with Open Instruments, is used.

Progress

Due to the impacts of COVID-19, the project was paused multiple times. Most research activity occurred during Dr Meita Asami's visit in 2022 (funded via a Collaboration Grant – please see Appendix 6.40). He focused his time on PDS measurements of specially prepared GaAs superlattice samples. Initial results are shown in Figure PP3.1.28, where clear differences can be seen between samples in the sub-bandgap region above 900 nm. Recent progress on advancing the performance of the PDS instrument is described in Appendix 6.12.

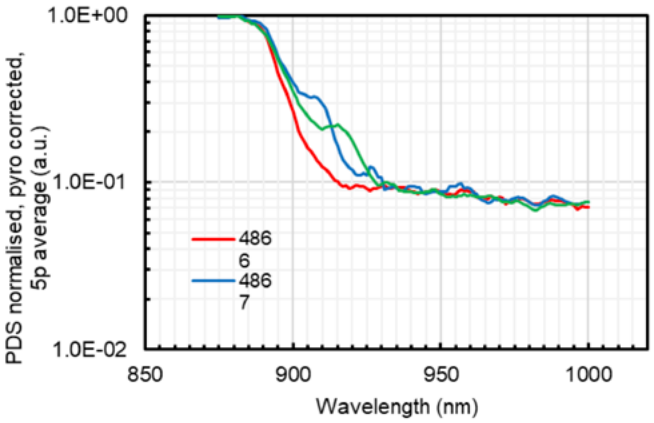

Figure PP3.1.28: Photo-absorption spectra of superlattice structures measured with the PDS technique show differences between samples in the sub-bandgap region above 900 nm.

Highlights

- First superlative GaAs samples from Tokyo University were measured at UNSW. A modified industrial prototype of the AURA PDS tool, from collaborator Open Instruments was used.
- Dr Asami visited UNSW for three weeks.
- Some of the team members met in person at the PVSEC-33 to discuss future steps in collaboration.

Future Work

We are preparing for an ongoing collaboration in the field of characterisation.

References

Kampwerth, H., Pollard, M., Conibeer, G., Hao, X., Asami, M., Watanabe, K. & Sugiyama, M. (2022). Spectral Filtering for High-Contrast Photoabsorption Measurements", ACAP Annual Report 2022

PP3.1M DETECTING LOW-LEVEL IMPURITY CONCENTRATIONS IN THIN FILMS FOR PHOTOVOLTAICS

Lead Partner
UNSW

Research Team
Dr Henner Kampwerth, Dr Michael Pollard

Funding Support
ACAP, Open Instruments

Aim

Identifying and eliminating material defects in the form of Urbach tails and low-level impurities is critical to maximising the performance of thin films for photovoltaics. Existing measurement techniques are either unable to detect non-radiative defects or come with specific sample requirements. Thin films present a particular sensitivity challenge to most measurement techniques, as the thin nature of the sample results in a very short interaction length with the probing light and therefore a weak absorption signal. Additionally, the supporting substrates also absorb light, with their signal often overwhelming that from the thin film of interest.

Photothermal deflection spectroscopy (PDS) is an ideal technique to study such samples, as it provides both unparalleled sensitivity on thin films along with reduced sensitivity to optical absorption by the substrate. It is an important characterisation tool for thin-film photovoltaics research that can make significant contributions to research in every laboratory.

The first fully integrated PDS instrument – the AURA from Open Instruments – debuted in 2022. The current functional prototype has already proven to be invaluable for many thin-film PV researchers, but unfortunately not all. As with all prototypes, areas of improvement have been identified that can enable even greater benefits for PV. Critical among these is an increase in the dynamic range of the tool, enabling researchers to accurately observe defects below to the band edge.

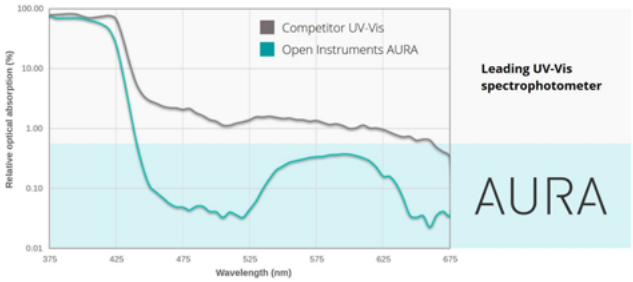

Figure PP3.1.29: A direct comparison of the relative optical absorption on both a leading UV-Vis spectrophotometer and the current prototype of the AURA PDS. The critical difference is that the large defect band between 525 nm and 650 nm remains undetectable by the conventional measurement tools.

Figure PP3.1.29 shows the photo-absorption spectrum of a single crystal 2D perovskite flake, kindly provided by our collaborators Dr. A. Mahboubi-Soufiani (UNSW) and Y. Zhang (UQ). The grey curve shows the absorption spectrum obtained from a conventional UV-Vis spectrophotometer. In green, we show the absorption spectrum from the AURA PDS. The significantly improved sensitivity of the AURA reveals a strong defect band between 525 nm and 650 nm, which cannot be detected by the UV-Vis measurement technique. However, the signal in the regions between 475 nm and 535 nm, and beyond 650 nm, is expected to be even less absorbing (<0.005%) than shown here. Preliminary experiments performed by Open Instruments demonstrated that the PDS measurement technique is able to measure well below this level, but that insufficient spectral filtering (stray light) of the broadband pump light source limits the sensitivity.

The aim of this project is to enhance an existing commercially available product, the AURA photothermal deflection spectrometer (PDS), to enable researchers to identify non-radiative defects close to the band edge, as well as the optical bandgaps of weakly absorbing films.

Progress

In collaboration with the ACAP grant "Advancing the PDS Technique for All Photovoltaic Thin-Films", it was found that the use of a single-monochromator limits the otherwise possible dynamic range of the technique. Since then, the AURA system has been redesigned around a double-monochromator. The proof-of-concept version is shown in Figure PP3.1.30.

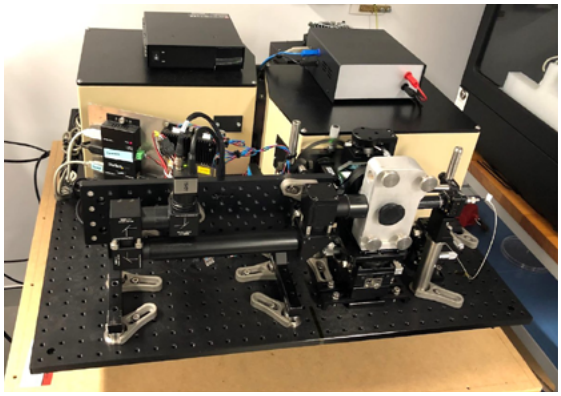

Figure PP3.1.30: Proof of concept setup of the PDS AURA system with a double monochromator.

Highlights

- Experiments have concluded that the previously used single-monochromator has insufficient filter characteristics, and a double-monochromator is required.
- The full optical train has been redesigned to optimise sensitivity and dynamic range.
- All needed parts have been ordered.

Future Work

The AURA PDS instrument is maturing increasingly and becoming a standard characterisation tool. The next step is to extend the measurement principle from relative spectra to absolute absorption spectra, enabling direct and automated measurement of absorption coefficients.

References

Kampwerth, H., Pollard, M., Conibeer, G., Hao,X., Asami, M., Watanabe, K. & Sugiyama, M. (2022). Spectral Filtering for High-Contrast Photoabsorption Measurements", ACAP Annual Report 2022.

PP3.3 DEGRADATION MECHANISMS

PP3.3A HIGH-THROUGHPUT GLOVEBOX-BASED STABILITY TESTING SYSTEM

Lead Partner
ANU

Team
A/Prof. Thomas White, Dr Hieu Nguyen, Dr Azul Osorio Mayon, Chris Jones, Prof. Klaus Weber, Prof. Kylie Catchpole

Students
Naeimeh Mozaffari

unding Support
ARENA, ACAP, ANU

Aim

Development of a high-throughput, glovebox-based solar cell stability testing system to investigate the intrinsic stability of perovskite and perovskite/silicon tandem solar cells under light and thermal stresses. With the ability to independently measure up to 32 cells at a time, and with three separate, temperature-controlled sample holders, the system is intended to provide statistically relevant cell stability data which is largely lacking in the perovskite solar cell research literature.

Progress

The system hardware was installed in early 2021 and work on integration of the system components and the control software progressed through the year. The first batches of cells were tested. A photo of the complete system is shown in Figure PP3.3.1. The main system components are an LED solar simulator, a Biologic BCS-805 battery cycling system with the capability to independently measure 32 solar cells at a time, and three temperature-controlled jigs (0–85°C), each with the capacity to hold 12 perovskite solar cells. The system is housed inside a purified nitrogen glovebox with very low humidity and oxygen levels. This allows the study of intrinsic durability of cells exposed to light and thermal stress, independent of the effects of oxygen and moisture. The solar simulator is sufficiently small that it also fits inside the glovebox.

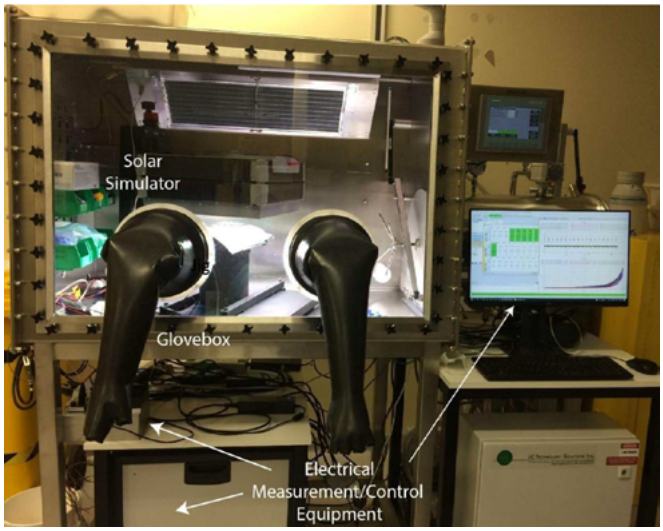

Figure PP3.3.1: Photograph of the high-throughput stability measurement system at ANU.

Test Type	Test ID	Elevated temperature	Electrical Bias	Light	ANU System Capability
Dark Storage	ISOS-D-1I	-	-	-	✓
	ISOS-D-2I	✓	-	-	✓
Bias Stability	ISOS-V-1I	-	✓	-	✓
	ISOS-V-2I	✓	✓	-	✓
Light Soaking	ISOS-L-1I	-	MPP or OC	✓	✓
	ISOS-L-2I	✓	MPP or OC	✓	✓
Thermal Cycling	ISOS-T-1I	Cycled	-	-	✓
	ISOS-T-2I	Cycled	-	-	✓
	ISOS-T-3I	Cycled	-	-	✓ *(lowest temp 0°C)
Light Cycling	ISOS-LC-1I	-	MPP or OC	Cycled	✓
	ISOS-LC-2I	✓	MPP or OC	Cycled	✓
	ISOS-LC-3I	✓	MPP or OC	Cycled	✓

Measurement protocols

The stability testing system described above is designed to perform a range of testing protocols defined in the recently published "Consensus Statement for Stability Assessment and Reporting for Perovskite Photovoltaics Based on ISOS Procedures" (Kheniken et al. 2020).

Table PP3.3.1 lists the suggested protocols from Kheniken et al. (2020) for stability testing in an inert atmosphere, and the ANU system capability, demonstrating almost complete coverage of all protocols, with the only limitation being the lower temperature limit of 0°C for thermal cycling tests (the suggested lower limit is -40°C for Test ISOS-T-3I). Ticks indicate the presence of the stress; dashes indicate absence, or, in the case of temperature, room temperature. MPP = maximum power point; OC = open-circuit.

Measurement protocol demonstration

Here we provide an example of the application of light soaking protocol ISOS-L-I1 to a batch of perovskite solar cells. This batch consisted of six cells: one control cell and five cells with different passivation layer conditions labelled from A to E. The duration of the light soaking test was 60 hours during which I-V curves were measured every 60 minutes; between the I-V scans, the cells were held at a constant maximum power point voltage (V_{mmp}) and the resulting current was measured. The temperature of the cells was held constant at 25°C.

The open-circuit voltage (V_{OC}), short-circuit current (J_{SC}), fill factor (FF) and power conversion efficiency (PCE) for each cell calculated from the I-:V curves are shown in Figure PP3.3.2. From this figure, we can visualise the spread and centres of the data such as the interquartile range, median, average, minimum, maximum and outlier values.

The behaviour of the cells and their statistical distribution can be correlated to the cell fabrication process and materials. When combined with other characterisation methods such as the advanced photoluminescence techniques developed at ANU, more in-depth and complete analysis of the cells can be performed.

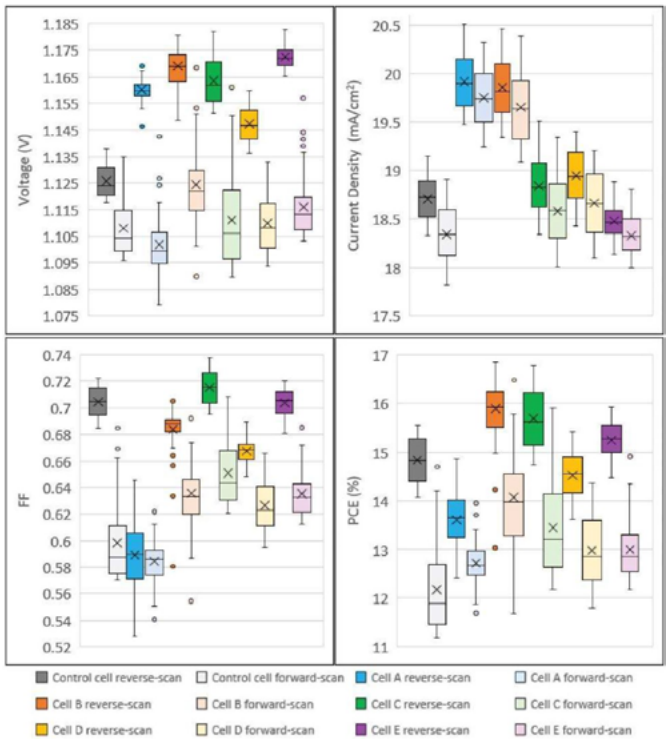

Figure PP3.3.2: Cell parameters V_{OC}, J_{SC}, FF and PCE calculated from the I-V curves measured every hour in reverse and forward scan. Each individual box consists of 61 data points for each cell parameter whether in reverse or forward scan.

Highlights

- High-throughput, 32-cell stability testing system.
- Glovebox-based to allow unencapsulated cells to be tested under inert atmosphere conditions (focus is on intrinsic stability, rather than extrinsic)
- Automated J-V scanning; can be individually controlled for each cell.
- Cell temperature range 0–85°C (three jigs, each can be set to a different temperature).

Future Work

The testing system will be used to support multiple projects related to perovskite and perovskite/silicon tandem cells, with the aim of collecting sufficiently large data sets to allow statistical analysis.

Correlations between stability, cell architecture and processing conditions will be investigated with the aim of improving perovskite cell stability towards commercial viability. The system capabilities will also continue to be developed to allow programmed light cycling, and independent MPP tracking of each cell.

References

Khenkin, M. V., Katz, E. A., Abate, A., Bardizza, G., Berry, J. J., Brabec, C., Brunetti, F., Bulović, V., Burlingame, Q., Di Carlo, A., Cheacharoen, R., Cheng, Y.-B., Colsmann, A., Cros, S., Domanski, K., Dusza, M., Fell, C. J., Forrest, S. R., Galagan, Y., Di Girolamo, D., Grätzel, M., Hagfeldt, A., von Hauff, E., Hoppe, H., Kettle, J., Köbler, H., Leite, M. S., Liu, S., Loo, Y.-L., Luther, J. M., Ma, C.-Q., Madsen, M., Manceau, M., Matheron, M., McGehee, M., Meitzner, R., Nazeeruddin, M. K., Nogueira, A. F., Odabaşı, Ç., Osherov, A., Park, N.-G., Reese, M. O., De Rossi, F., Saliba, M., Schubert, U. S., Snaith, H. J., Stranks, S. D., Tress, W., Troshin, P. A., Turkovic, V., Veenstra, S., Visoly-Fisher, I., Walsh, A., Watson, T., Xie, H., Yıldırım, R., Zakeeruddin, S. M., Zhu, K. & Lira-Cantu, M. (2020). Consensus statement for stability assessment and reporting for perovskite photovoltaics based on ISOS procedures. Nature Energy 5, 35-49.

PP4
MANUFACTURING ISSUES

OVERVIEW

PP4, entitled "Manufacturing Issues" concentrates on costs, both financial (PP4.1) and environmental (PP4.2). The methods in each have a great deal of similarity since both rely heavily on inventories of estimates and measurements of inputs and outputs of manufacturing processes.

In PP4.1, there has been analysis of (i) manufacturing of PV modules in Australia, (ii) assessment of module and mounting technologies for improved future LCOE, (iii) an assessment of the net cost of CdTe module recycling, and (iv) assessment of LCOE under 100% renewable scenarios in Bolivia and Japan.

In PP4.2, (i) Life cycle analysis methods were used to evaluate the impacts of both module production and deployment, (ii) a recycling reverse logistics trial has been started, (iii) future projections of PV waste in Australia have been estimated, (iv) analysis of modules for material quantities and quality for recycling, and (v) a new method of recovering silver has been tested and evaluated from an LCA perspective.

PP4.1 FINANCIAL COST

Lead Partners
UNSW, ANU

UNSW Team
Dr Nathan Chang, Dr Rong Deng, Dr Phillip Hamer, Dr Anna Kuczyńska-Łażewska, Prof. Renate Egan, Prof. Martin Green

ANU Team
Prof. Andrew Blakers, Ass./Prof. Matthew Stocks, Dr Bin Lu

Partners
SolarCycle: Pablo Dias
Sun Cable: Luke Marshall

UNSW Students
Mohammad Dehghanimadvar, Natalia Pereira Gutierrez

ANU Students
Cheng Cheng

Aims

ACAP's Program Package 4 (PP4) aims to assess the financial cost related to the manufacturing, use and end-of-life management of different photovoltaic technologies. The financial analysis may involve the proposal of models, the actual modelling of cost, competitiveness assessment, financial decision-making tools, etc. This assists in guiding the direction of future research and industry developments, as well as quantifies the financial advantages a given process (or technology) has over another. Additionally, it aims to highlight the main processes that should be addressed to reduce cost, as well as to point out the specific actions that can be taken to enable the implementation of a new development.

Progress

A. Module assembly manufacturing in Australia (UNSW)

With increasing interest in diversifying the supply chain for PV module manufacturing, this study (Dehghanimadvar 2022) considered the economic competitiveness of producing solar modules in Australia from imported materials (solar cells, glass, frame, etc.), compared to importing modules (Figure PP4.1.1). Because of higher cost structures in Australia (e.g. labour rates), local manufacturing would result in higher module prices.

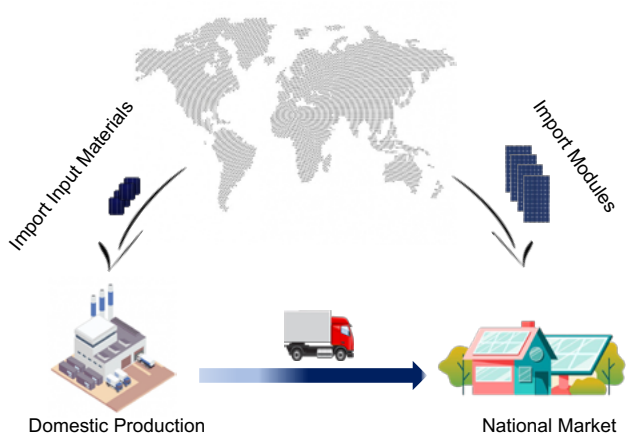

Figure PP4.1.1: Schematic for Australian Module Manufacturing Analysis.

Various alternatives to help Australian manufacturing to become competitive were considered, including increasing the scale of the Australian factories, import tariffs (which would increase the cost of modules to Australian consumers), and supportive incentives such as a "Buy Australian" rebate. The impact of these were assessed, as shown for example in Figure PP4.1.2.

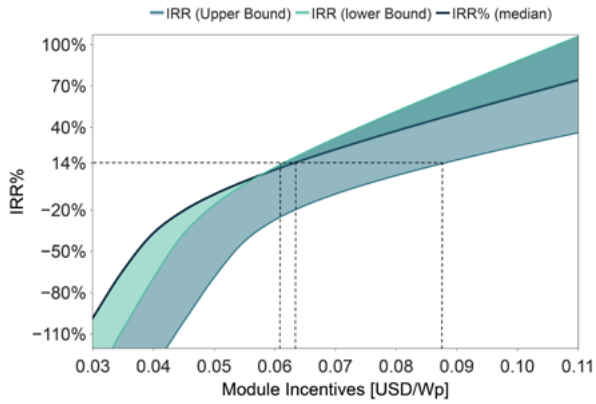

Figure PP4.1.2: Impact of Government incentives on local module assembly profitability.

B. LCOE for large-scale solar (UNSW, Sun Cable))

In this collaboration with Sun Cable, a cost model for levelised cost of Electricity (LCOE) and profitability was built to help Sun Cable evaluate alternative module and mounting structure options for their Australia-Asia Power Link (AAPL) project. A key feature of the model was the ability to consider uncertainties in cost and yield parameters, particularly looking into the future, since AAPL is expected to be delivered over a number of years.

The results of the modelling are confidential to the project, but representative outputs are shown in Figure PP4.1.3 – showing that different module types and mounting structures can have different LCOE values, but importantly the actual value is not exactly known because of uncertainties.

Within these uncertainties, it is possible to identify key parameters that dominate a comparison between two alternatives. An example of this is shown in Figure PP4.1.4.

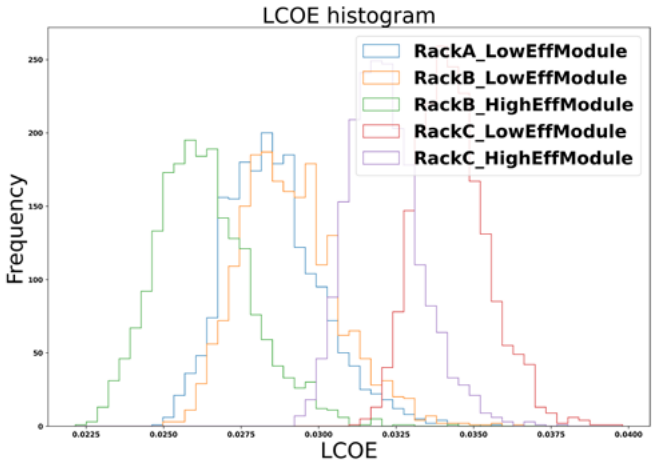

Figure PP4.1.3: Distributions of LCOE for alternative module and mounting structure options..

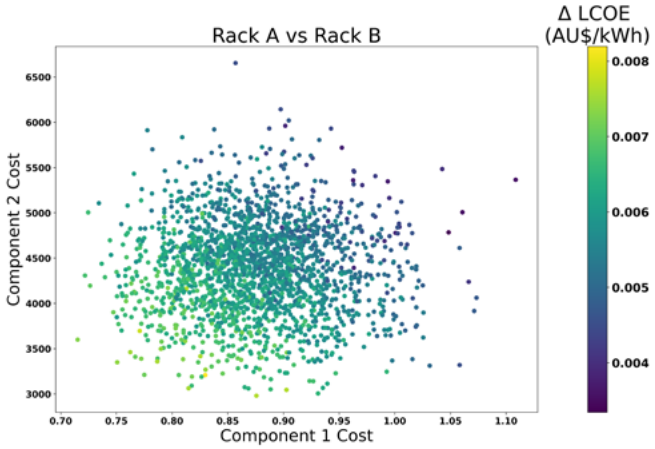

Figure PP4.1.4: Impact of two important variables on the relative LCOE between two options.

C. CdTe module recycling – economic assessment (UNSW and Solar Cycle)

ACAP has worked with a new recycling startup in the USA – SolarCycle, who wanted some analysis of CdTe module recycling costs and revenues. The exact results are confidential to SolarCycle, but representative (normalised cost) contribution bar charts (Figure PP4.1.5) are shown, with the impact of key input factors on net cost shown in Figure PP4.1.6.

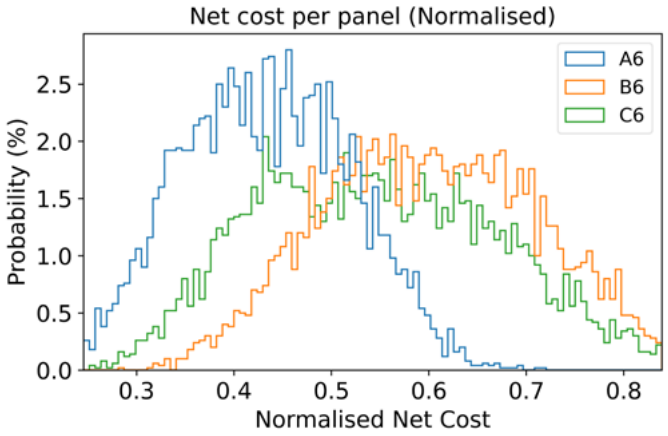

Figure PP4.1.5: Distributions of (normalised) net cost for alternative recycling processes for CdTe modules.

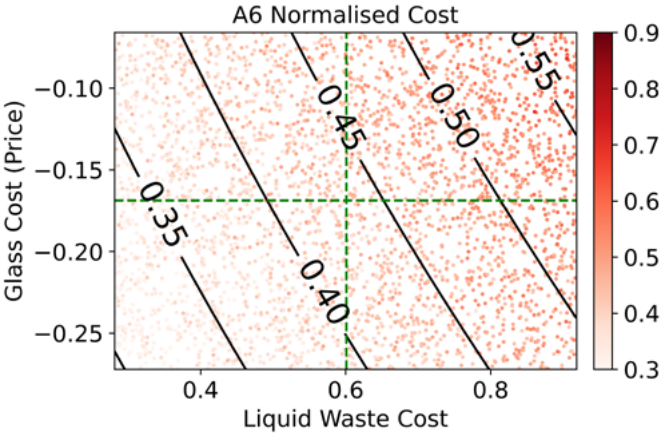

Figure PP4.1.6: The impact of key uncertainty variables on the normalised net cost of one recycling process.

D. CdTe module recycling – economic assessment (UNSW and Solar Cycle)

Following on from the work in the previous year, ACAP has analysed two further scenarios for 100% renewable electricity.

The first (Cheng 2022a) is Bolivia in South America. This country relies heavily on fossil fuels, and its energy demand is expected to increase 10-fold. Looking at the potentially available wind, solar and hydro generation and pumped hydro storage and HV transmission, there is enough available renewable resources to meet the expected 10x increase in demand, at an average LCOE of 44–53 $/MWH (Figure PP4.1.7), which would be lower than the cost of making new hydro or gas plants. This important result shows that even for a less economically developed country, renewables would be both lower cost and more sustainable than continuing to rely on fossil fuels.

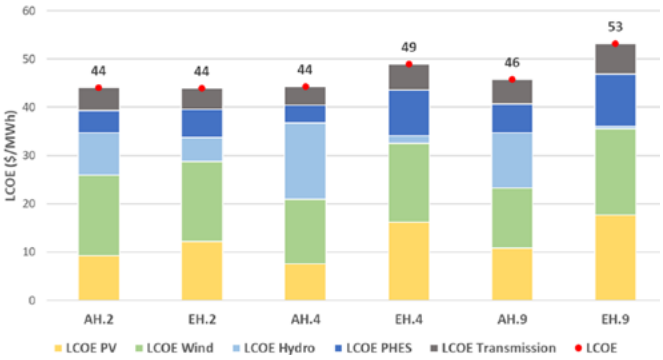

Figure PP4.1.7: Estimated average LCOE contributions for 100% renewables scenarios in Bolivia.

The second study (Cheng 2022b) focuses on Japan, which has commitments to zero greenhouse emissions by 2050. Electricity is one-third of emissions currently. This study looks at solar and offshore wind's place in this transition.

Even if transport, heat and industry are all electrified, there is enough solar and offshore wind potential to supply five to seven times Japan's energy needs. A vast amount of off-river pumped hydro energy storage potential is available to balance variable renewables at low cost. The estimated average LCOE was between 86 and 110 $/MWh. This is only slightly higher than current average prices and lower cost than electricity from imported hydrogen (Figure PP4.1.8).

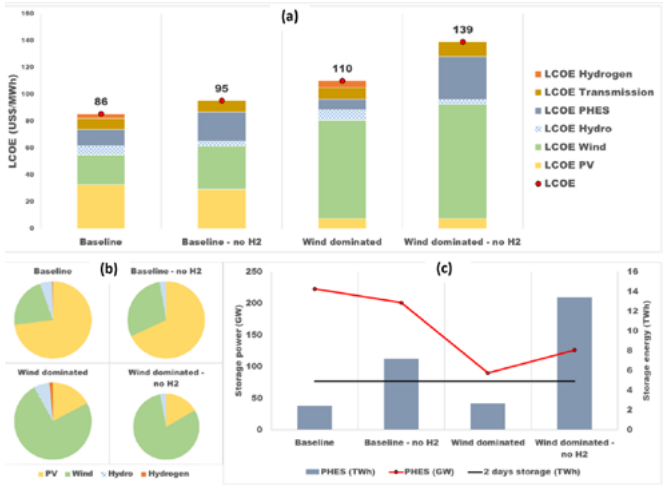

Figure PP4.1.8: Breakdown of LCOE for (a) generation mix, (b) storage requirements, and (c) for four scenarios.

Summary

Cost analysis continues to be an important task within ACAP, and the scope has expanded in recent years beyond individual cell and module technologies, to consider the economics of Australian manufacturing, large-scale solar deployment, recycling and 100% renewable scenarios.

Highlights

- New focus on Australian manufacturing of PV.
- Collaboration with Sun Cable on future LCOE incorporating uncertainties.
- Collaboration with SolarCycle on recycling of CdTe modules.
- Cost estimates of 100% renewable electricity (with storage) in Bolivia and Japan.

Future Work

- Examination of Australian PV manufacturing along the entire value chain.
- Continuing collaborations with industry examining deployment cost.
- Commercial assessment of cell and module technologies under development within ACAP.
- Ongoing analysis of 100% renewable energy scenarios worldwide.

References

Cheng, C., Blakers, A., Stocks, M. & Lu, B. (2022). 100% renewable energy in Japan. Energy Conversion and Management 255, 115299.

Cheng, C., Gutierrez, N. P., Blakers, A. & Stocks, M. (2022). GIS-based solar and wind resource assessment and least-cost 100 % renewable electricity modelling for Bolivia. Energy for Sustainable Development 69, 134-149.

Dehghanimadvar, M., Egan, R. & Chang, N. L. (2022). Economic assessment of local solar module assembly in a global market. Cell Reports Physical Science 3, 100747.

PP4.2 ENVIRONMENTAL COST

Lead Partner
UNSW

UNSW Team
Dr Rong Deng, Dr Nathan Chang, Dr Moonyong Kim, Dr Pablo R. Dias, Dr Marina Monteiro Lunardi, Dr Richard Corkish, A/Prof. Brett Hallam, Prof. Renate Egan, Prof. Martin Green

Academic Partners
Gdańsk University of Technology, Gdańsk: Dr Anna Kuczyńska-Łażewska

Students
Storm Drury, David Leyton, Verity Tan, Olivia Brown

Aims

The PP4.2 program aims to address environmental manufacturing costs and end-of-life issues. It mainly uses life cycle assessment (LCA) but is also concerned with end-of-life management analysis, development of recycling processes and creation of decision-making tools concerning environmental impacts. This allows the photovoltaic technology to grow with minimum environmental impact, which assists in achieving its goal of being a reliable and renewable source of energy that is eco-friendly and less harmful to the environment than competing technologies.

Progress

The PP4.2 outputs should provide guidance around the environmental impact of PV technologies. An important outcome is arriving at conclusions in respect to competing manufacturing and end-of-life processes so as to inform the ideal option in terms of environmental impact. In addition, PP4.2 is dedicated to improving the understanding of PV end-of-life issues in Australia, including a recycling reverse logistics trial, projection of future PV waste volume in Australia, and assessing material recyclability in the Australian second-hand market.

A.Pathways to reduce emission intensity of PV deployment (UNSW)

This study (Drury 2022) used life cycle analysis to identify methods to reduce carbon emission intensity of PV production and deployment using a case study of a 30 MW solar farm located in Queensland. As shown in Figure PP4.2.1, silicon, aluminium and concrete are the main contributors to global warming potential because Si production and purification require high amounts of electricity, and Al and concrete production processes are carbon intensive. A roadmap proposed that emissions can be reduced by 60%, from currently ~21 to 8 g $CO_{2\text{-eq}}$/kWh when considering a 30% efficient module.

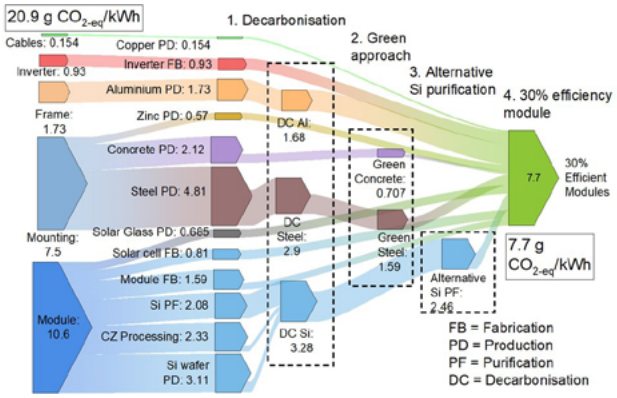

Figure PP4.2.1: A roadmap to reduce global warming potential (kg $CO_{2\text{-eq}}$) and emission demands during PV production and deployment, case study of a 30 MW PV plant.

B. Solar Reverse Logistics Model (UNSW)

Solar Reverse Logistics Model (SRLM) is a method proposed by student David Leyton that makes use of efficient and tracked logistics modelled on systems currently in existence in the solar and electrical industry in Australia, where electricians would return end-of-life solar modules to a solar wholesaler, who would, in turn, return them to a city-wide central logistics centre for processing.

A trial of reverse logistics for collecting modules more efficiently and with more care (to improve the chances of repair and reuse) has begun, with data collected to evaluate its effectiveness. Figure PP4.2.2 shows the setup at a PV module wholesaler site.

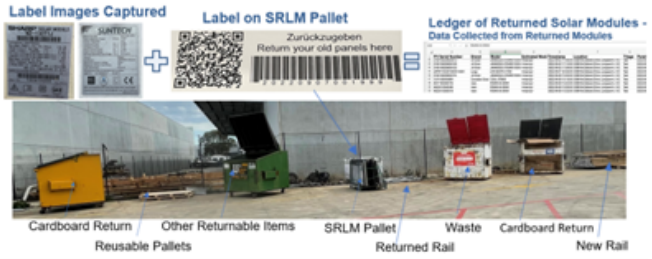

Figure PP4.2.2: Solar Reverse Logistics Model in action at a PV module wholesaler site (the SRLM pallet).

C. Improved waste module projections in Australia (UNSW)

Using more realistic estimates for the actual lifetime before end of first life and considering the change of material usage in PV modules over time, estimates were made of annual waste of PV modules in Australia to 2050 (Figure PP4.2.3). The results estimate 1,000,000 tonnes of cumulative PV waste in Australia between 2033 and 2042 dependent upon the lifetime and rate of forecast installations, mainly from distributed small-scale PV systems (<100 kW). In 2050, cumulative PV waste is estimated to reach 2,000,000–3,000,000 tonnes. With expected waste and installation volumes, EoL modules have the potential to supply significant amounts of Al and Ag for new module fabrication.

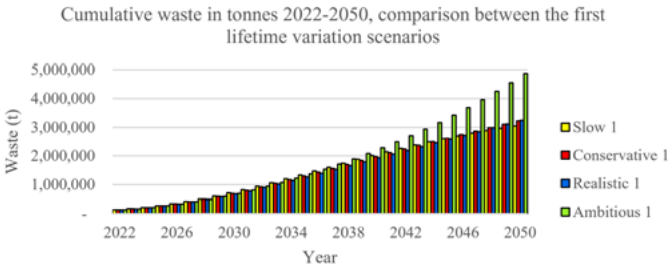

Figure PP4.2.3: Cumulative solar panel waste in tonnes 2022–2050 considering different rates of forecast installation: slow, conservative, realistic and ambitious (Tan 2023).

D.Characterising the composition of PV panels for recycling in Australia (UNSW)

Understanding the variation in material composition of EoL modules is important to be able to estimate material availability for reuse and recycling. This study examined the amounts, composition and quality of glass, aluminium and solar cells from a variety of module manufacturers and different manufacturing years. For example, Figure PP2.2.4 shows the glass composition. Experimental results and statistical analysis showed the level of variability among panels is not extreme enough to reduce recyclability, with all main components able to be recycled.

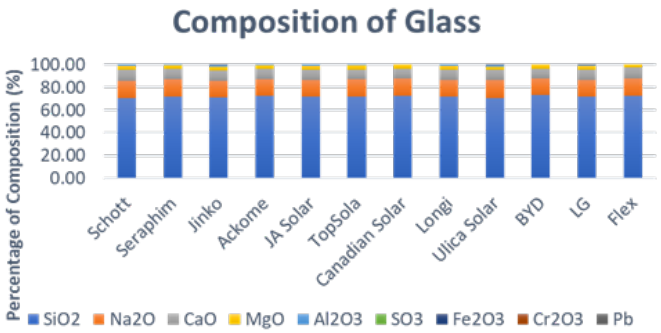

Figure PP4.2.4: XRD analysis of solar panel glass from 12 end-of-life panels sourced from different manufacturers and manufacturing years.

E.Novel silicon/silver recycling method with low environmental impacts (UNSW)

This work (Deng 2021) developed a circular chemistry process, reverse electroplating, to recycle silver from solar cells, which achieved 95% recycling yield. This process minimises (almost eliminates) chemical consumption and disposal. Life cycle assessment results showed this method has lower environmental impacts compared to other alternative silver recycling methods.

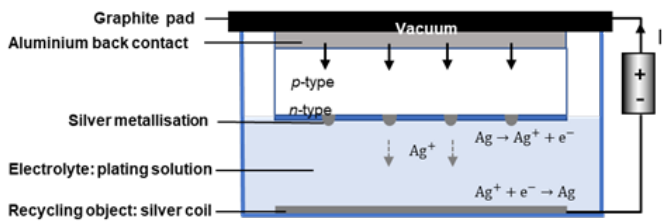

Figure PP4.2.5: Schematics of the prototype full-area contact reverse electroplating for recycling high-purity silver (Deng 2021).

Summary

The PP4.2 program has continued to deliver significant work concerning the environmental costs of PV manufacturing, use and end-of-life issues.

These have shown how the already low environmental impacts of PV for electricity generation can be further reduced by a greener electricity mix, greener approach to make concrete and steel for ground mounting, and by innovation in recycling methods.

The PV end-of-life problem will emerge in Australia in the next decade. Collecting and sustainably recycling these modules from distributed systems posts a significant challenge.

Highlights

- New focus on Australian PV end-of-life issues, including updated waste volume projection to 2050 and material recyclability characterisation.
- Trial of solar reverse logistics.
- LCA of PV module production and utility-scale deployment.
- Recycling method for silver recovery with LCA analysis.

Future Work

- Development of additional recycling processes.
- Assessments of PV module EoL logistics.
- Environmental assessment of new technologies being developed in the PV industry.
- Environmental impact of local manufacturing
- Social acceptance / altitudes towards PV reuse and recycling.

References

Deng, R., Dias, P. R., Lunardi, M. M. & Ji, J. (2021). A sustainable chemical process to recycle end-of-life silicon solar cells. Green Chemistry. 23(24), 10157-10167.

Tan, V., Dias, P. R., Chang, N. & Deng, R. (2022). Estimating the Lifetime of Solar Photovoltaic Modules in Australia. Sustainability. 14(9), 5336.

PP5
EDUCATION, TRAINING AND OUTREACH

Nodes Involved

All

Industry Partners

Australian Photovoltaic Institute (APVI)

Funding Support

All nodes, ACAP

Overview

Within the PP5 Education, Training and Outreach package, ACAP has specific targets for high quality publications and for the number of researchers in different categories who benefit from the infrastructural support it provides, as well as for the number and length of researcher exchanges. A significant number of outreach events are also targeted for each year. As well as major events such as those reported in the PP5 section of this annual report, other outreach activities in 2022 included public lectures on material relevant to ACAP's activities, newspaper and magazine articles, visits, information papers and presentations for policy developers and their advisors.

The ACAP nodes continue to educate future investors, industry partners, practitioners, researchers and educators to support the necessary rapid expansion of the national and global photovoltaics (PV) industry and to develop more effective educational tools.

In 2022, COVID-19-related restrictions limited the activities included in this package. Mask requirements, indoor gathering size limits, and institutional duty of care policies at ACAP nodes and interacting research institutions, universities, companies and schools resulted in many activities being postponed indefinitely or moved online. As 2022 progressed, many of these restrictions were gradually eased, allowing face-to-face activities to resume.

Aim

TThe work described here is about promoting knowledge of the opportunities and successes of Australian photovoltaics research, adding to the global body of knowledge, engaging the next generation of researchers, and sharing knowledge with the broader community including industry, government and the general public.

Progress

ACAP holds an annual research conference near the end of each year to keep ARENA and its National Steering Committee informed, to exchange research results, enhance collaboration and reinforce face-to-face contacts between students and staff from the different nodes.

On 1 December 2022, ACAP held its first conference day as a stream of the Asia-Pacific Solar Research Conference (APSRC) and on 2 December ACAP hosted its closed session, consisting of the director's welcome, presented by Professor Martin Green, followed by the presentation of ACAP PP1–PP5 summaries.

The APSRC, organised by the Australian PV Institute (APVI) (29 November – 1 December 2022), was held in Newcastle. Staff and students from ACAP's various nodes participated in the APSRC in person, allowing them to present their research and engage in meaningful discussions with other members in attendance.

The APVI's APSRC aims to provide a forum for the development and discussion of content specific to Australia and its region, allow an opportunity to foster collaboration between institutes and promote engagement between industry and academics. ACAP partners with the APVI to support the development of the conference program through financial sponsorship, participation in its organisation and through scheduling ACAP presentations as a stream of the conference.

Representatives from UNSW and ACAP nodes helped with the organisation of the conference and staff and students from all the nodes participated in academic review committees and contributed papers and posters to the conference.

ACAP Conference

Attending a conference provides a student or researcher an opportunity to present their work to a wider audience and receive valuable feedback on their findings. It also provides networking opportunities, enabling researchers to connect with their peers, form collaborations, stay up to date on the latest developments and develop new research ideas.

The ACAP Conference was a specific stream within the APVI's APSRC and was coordinated by Dr Richard Corkish. It consisted of the following presentations from ACAP nodes:

- Jessica Yajie Jiang (UNSW), "Super-efficient coloured photovoltaics: enabling sustainable building and vehicle applications";
- Jiali Wang (ANU), "Inkjet printing for polycrystalline silicon passivating contacts";
- Adam Surmiak (Monash), "The end of traditional manual research, a new era of robotics for rapid energy materials discovery";
- Hui Li (UQ), "Fluorinated additives for perovskite solar cells";
- Saghar Masoomi-Godarzi (Uni Melb), "Breaking the efficiency limit of perovskite solar cells using singlet fission material";
- Jueng-Eun Kim (CSIRO), "Flexible, Light Weight and Highly Efficient Perovskite Solar Modules Manufacturing via High Throughput Roll-to-Roll Process for Space Photovoltaics";
- The Duong (ANU), "Bulk Incorporation with 4-methylphenethylammonium chloride for Efficient and Stable Perovskite Cells";
- Calvin Lee (Uni Melb), "Biradical character modification through steric perturbations: a twisted route towards silicon-match";
- Wenxin Mao (Monash), "Light Induced reversal of ion segregation in mixed-halide perovskite";
- Neil Mallo (UQ), "Tuning the high frequency dielectric constant of organic semiconductors for organic photovoltaics";
- Jianjun Li (UNSW), "Microscopic carrier loss mechanisms in 12% efficient CZTSe thin-film solar cells"; and
- Doojin Vak (CSIRO), "Reliable fabrication and testing of roll-to-roll printed PV for digital revolution in PV research".

Over the three days of the APSRC, ACAP members presented or attended presentations in the streams:

1. Photovoltaic Devices;
2. Renewable Electricity Deployment & Integration;
3. Solar Buildings and Solar Heating & Cooling;
4. Concentrating Solar Thermal; and
5. Process Heat & Chemistry.

These streams were broken into specific sub-streams.

PV Perovskite; REDI Optimisation; CST Simulation/Modelling; PV Characterisation; Special session: REDI – PV end-of-life and sustainability; PV end-of-life and sustainability; CST – Particles; SBSHC – Hot water (PV & thermal) and solar resources; PV Silicon – Passivating Contacts; REDI Community batteries, Ground Albedo & EVs; CST Novel Concepts; SBSHC – Solar buildings; PV Mix of Goods; REDI – End of life and manufacturing; PHC – Chemistry & Process Heat; and, REDI A mixed bag.

The plenary presentations of the APVI's APSRC were given by the notable speakers:

- Scientia Prof. Martin Green, UNSW & ACAP Director – Opening Address – "Recent Developments in Photovoltaics";
- Dan Sturrock, Director Business Development & Transactions, ARENA – "ARENA's Ultra Low-Cost Solar mission";
- Dr Nicole Kuepper-Russell, Deputy CEO, 5B – "The solar revolution – rapid solar at scale";
- Dominic Zaal, ASTRI Director, CSIRO Energy – "The role of Concentrated Solar Thermal (CST) within integrated energy systems";
- Wes Stein, Chief Technologist, CSIRO Energy – "Emerging Trends in CSP Technology";
- Prof. Stefaan De Wolf, Material Science & Engineering, Interim Associate Director, KAUST Solar Center, Saudi Arabia – "Pathways to Efficient and stable perovskite/silicon tandem solar cells";
- Hank Price, Managing Director, Solar Dynamics, LLC Colorado, USA – "Concentrating Solar Power Best Practices – Findings and Updates";
- Joshua S. Stein, Sandia National Laboratory, USA – "Technical Barriers to the Commercialization of Perovskite Photovoltaics: How do we overcome them?";
- Prof. Paul Dastoor, Director, Centre for Organic Electronics, University of Newcastle – "Printed Solar: Green Energy for Industrial, Warehouse and Commercial (IWC) Buildings";
- Dr Christoph Brunner, CEO of AEE INTEC, Austria – "The role of solar energy for a sustainable hydrogen production";

- Christine Lins, Executive Director, GWNET – Global Women's Network for the Energy Transition – "Energising women to advance the energy transition";
- Prof. Graham "Gus" Nathan, Research Director, HILTCRC – "Opportunities for a growing role of solar energy in the decarbonisation of high temperature industrial processes";
- Prof. Alison Lennon, Chief Scientist, SunDrive Solar Pty Ltd – "The Ascent of Silicon Heterojunction Technology, but can it be Sustainably Manufactured at TW Annual Production Levels?";
- Christoph Falter, Head of Strategy, Synhelion SA, Switzerland – "Flying with Sunlight"; and
- Michelle Blakeley, Founder "My Home". Perth WA – "An Initiative to deliver high performance housing for people who are homeless or at risk of becoming homeless".

The proceedings of the APSRC are available at the following url:

https://apvi.org.au/solar-research-conference/proceedings-apsrc-2022/

Professional bodies

In addition to involvement in the APSRC, ACAP has continuing strong engagement with the APVI, one of the more effective vehicles for Australian policy development through its focus on data, analysis and collaborative research. ACAP was a founding "Large Organisation" member of the APVI and ACAP partners were active members of APVI throughout 2022. Additionally, ACAP collaborators contributed to and participated in Australian representation on the Executive Committee for the International Energy Agency: Photovoltaic Power Systems.

Researcher Exchanges

- Anna Kuczyńska-Łażewska Gdańsk University of Technology, Poland Lecturer, located at UNSW
- Khoa Nguyen and Anh Bui, Fraunhofer ISE (Germany), PhD students, located at ANU
- Edris Khorani and Nick Grant, University of Warwick, (UK), located at UNSW
- Thomas Feeney, Karlsruhe Institute of Technology (Germany), located at ANU
- Heping Shen, ANU, located at École Polytechnique Fédérale de Lausanne (Switzerland).

New ACAP PhD, Masters and Honours Students

In 2022, we have welcomed:

- 49 Honours Students;
- 16 Masters Students; and
- 22 PhD students.

Education and training

ACAP is a strong driver in education. Overall, to date, ACAP has supported at least in each category 182 early career researchers, 349 Honours, 172 Masters students, and 390 PhD students. More than 256 PhD graduates have come out of the ACAP program. See Chapter 8 for additional theses added in 2022.

News and Magazines

ACAP's research is driving the development of next generation solar cell technologies and is helping pave the way for a more sustainable and low-carbon future. As a result, ACAP attracts international attention and during 2022 there were over 200 news articles, tv and radio interviews and speaking engagements.

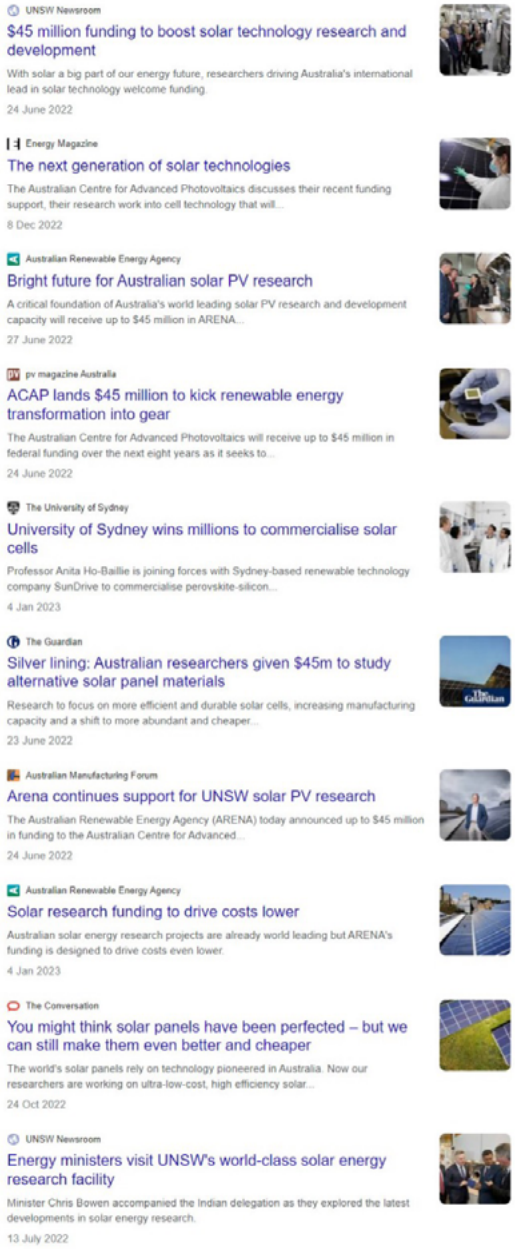

Figure PP5.1: A small snippet from Google News indicating ACAP's prominence in the news.

Selected News and Media

ACAP has made significant impact in the media and the three items selected are indicators of the value ACAP brings to the public conversation. There is a compiled table for 2022 listing many of the media items with their corresponding web links at the end of this section PP5.

Professor Renate Egan (ACAP, UNSW) published in The Conversation – a unique collaboration between academics and journalists that is the world's leading publisher of research-based news and analysis. The monthly audience to The Conversation Australia is 4.7 million unique users onsite, and 14.1 million through republication.

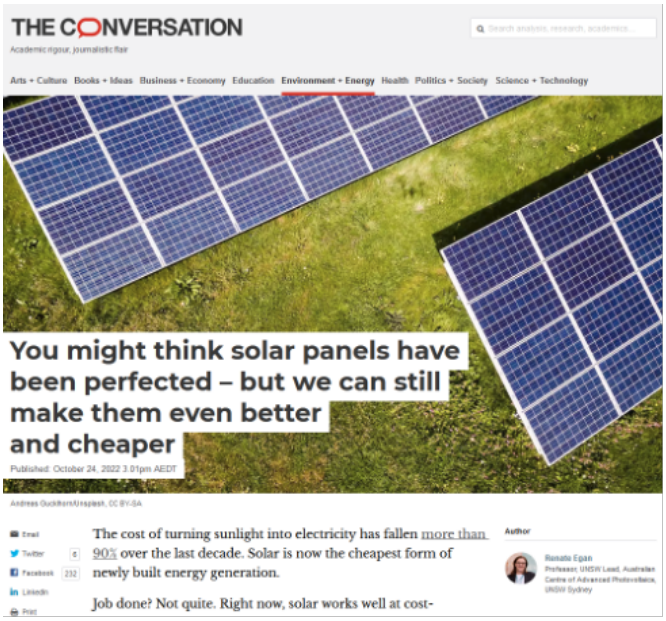

Figure PP5.2: Professor Renate Egan's argument was published in The Conversation

A summary of the article:

Australia is poised to play a pivotal role in the global advancement of solar technology. For several decades, we have been at the forefront of both the development and implementation of solar technology. Notably, we have held the performance record for silicon solar cells for 30 of the past 40 years. Currently, we have the highest per capita deployment of solar technology among OECD countries, which meets almost 15% of our electricity requirements. Moreover, over 80% of new solar panels worldwide rely on the PERC cell technology, which was developed in Australia.

Moving forward, the focus of hundreds of Australian researchers is to achieve two objectives. Firstly, to further decrease the costs associated with solar technology. Secondly, to maximise the electricity output from incoming sunlight.

The article can be found at the following url:

https://theconversation.com/you-might-think-solar-panels-have-been-perfected-but-we-can-still-make-them-even-better-and-cheaper-191755

Luke Sutherland (ACAP, Monash) has had his group's research published in PV Magazine

PV Magazine averages 1.3 million total visits per month.

Figure PP5.3: Luke Sutherland and team's accomplishment with printed flexible perovskites were publicised in PV Magazine.

A summary of the article:

Australian scientists have demonstrated a flexible perovskite solar cell using roll-to-roll compatible "printing" type processes, which could potentially be applied in large-scale manufacturing. Of note is the development of a viable roll-to-roll process to deposit the electrode layer, which has thus far been a major challenge. Cells fabricated by the group achieved a maximum efficiency of 16.7%

The article can be found at the following url:

https://www.pv-magazine.com/2022/09/12/flexible-roll-to-roll-printed-perovskite-solar-cell-hits-16-7-efficiency/

Luke Sutherland is first author on the publication Vacuum-Free and Solvent-Free Deposition of Electrodes for Roll-to-Roll Fabricated Perovskite Solar Cells published in Advanced Energy Materials.

Luke Sutherland's academic research paper Vacuum-Free and Solvent-Free Deposition of Electrodes for Roll-to-Roll Fabricated Perovskite Solar Cells is available at this url:

https://onlinelibrary.wiley.com/doi/full/10.1002/aenm.202202142

Authors: Luke J. Sutherland, Doojin Vak, Mei Gao, Thelge Anton Nirmal Peiris, Jacek Jasieniak, George P. Simon, Hasitha Weerasinghe

WION Climate Tracker: Australian study proposes new cost-effective way to recycle solar modules

WION's YouTube channel has 7.3 million subscribers and PV Magazine averages 1.3 million total visits per month.

Figure PP5.4: ACAP's research into module recycling on WION.

A summary of the news video:

Solar power is a clean and renewable energy source, but the limited lifespan of solar panels raises concerns about the volume of waste generated by their disposal. Australian researchers from the University of New South Wales have developed a process to recycle solar panels more efficiently and cost-effectively.

The process involves collecting and inspecting solar panels to extract valuable materials such as silver and copper. The procedure is environmentally friendly and does not require any hazardous chemicals.

With solar panel waste projected to reach 145,000 tons per year by 2030, smaller scale recycling facilities located closer to the source of waste are necessary to reduce transportation emissions.

https://youtu.be/27DYgsCSY1I

The research paper High yield, low cost, environmentally friendly process to recycle silicon solar panels: Technical, economic and environmental feasibility assessment is available at this url:

https://www.sciencedirect.com/science/article/abs/pii/S1364032122007821

Authors: Pablo R. Dias, Lucas Schmidt, Nathan L. Chang, Marina Monteiro Lunardi, Rong Deng, Blair Trigger, Lucas Bonan Gomes, Renate Egan, Hugo Veit

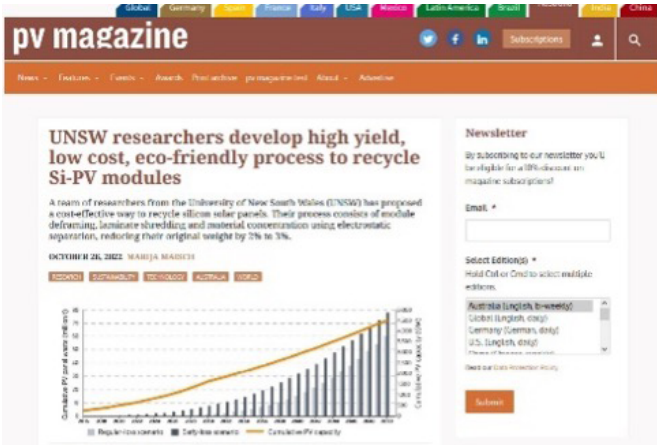

Figure PP5.5: ACAP's research into module recycling on WION.

PV Magazine also published an article on the research paper.

Outreach and external engagement

Figure PP5.6: CSIRO CEO Larry Marshall at ABC program Q&A.

CSIRO CEO Larry Marshall took part in ABC program Q&A on 4 August 2022 talking about CSIRO's latest Megatrends report. He took the opportunity to showcase flexible solar cells as an Australian technology that could be deployed worldwide. Other panellists include Jenny McAllister (Assistant Minister for Climate Change and Energy), Sarah Hanson-Young (South Australian Greens Senator), Warren Mundine (Director, Indigenous Forum, Centre for Independent Studies) and Hannah Diviney (writer and disability advocate).

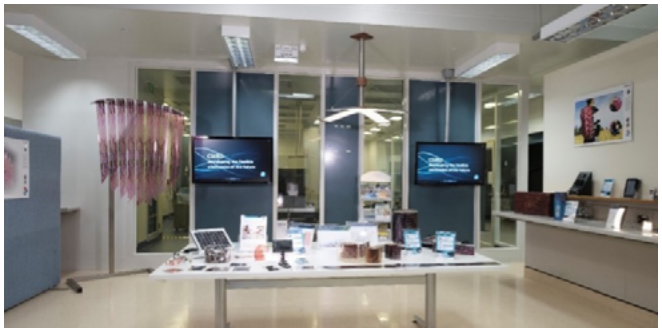

Figure PP5.7: CSIRO Flexible Electronics Laboratories.

As COVID-19 restrictions continue to ease, the Flexible Electronics Laboratories at CSIRO have begun welcoming visitors once again. While most of the visits have occurred within the last few months, it is anticipated to have a significant increase in the number of visitors in the near future.

Figure PP5.8: Top: Dr Alan Finkel (L) and ARENA CEO Darren Miller (R); Bottom: 250 Solar Name Tags made by CSIRO.

The Sydney Energy Forum, organised by the Department of Prime Minister and Cabinet and ARENA in July 2022, presented a unique opportunity to upcycle solar cell rolls. Experimental printing trials conducted by CSIRO resulted in a significant quantity of solar film, which was utilised to produce more than 250 name tags for the event. In Figure PP5.8, Dr Alan Finkel, Special Adviser to the Australian Government on Low Emissions Technology and ARENA CEO Darren Miller, are seen wearing these name tags.

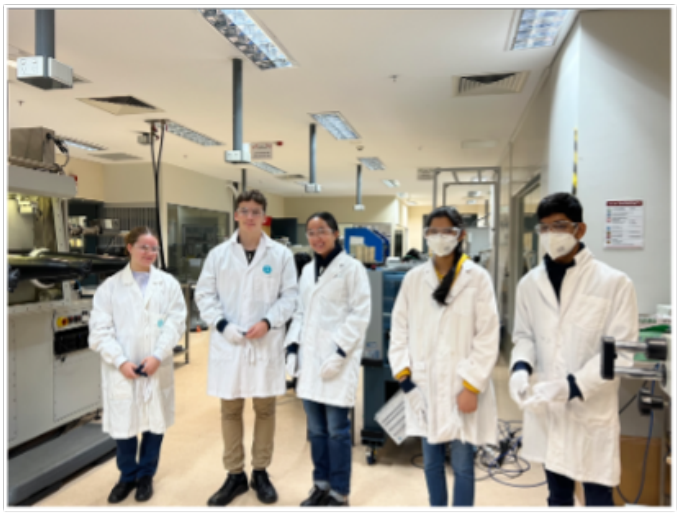

Figure PP5.9: Work experience students return to the thin-film lab.

After two years of absence due to COVID restrictions, work experience students have returned to CSIRO in person. This group of five students was introduced to thin-film solar cell research and had a go at testing some cells in the glovebox.

New Online Courses

ACAP has supported the development of two publicly available, internationally accessible, online PV short courses: Solar Cells (convened by Dr Fiacre Rougieux) and Photovoltaic Technology and Manufacturing (convened by Professor Bram Hoex) with both having started enrolments in 2022. Information about both courses is available at the following url:

https://www.unsw.edu.au/engineering/our-schools/photovoltaic-and-renewable-energy-engineering/study-with-us/short-courses

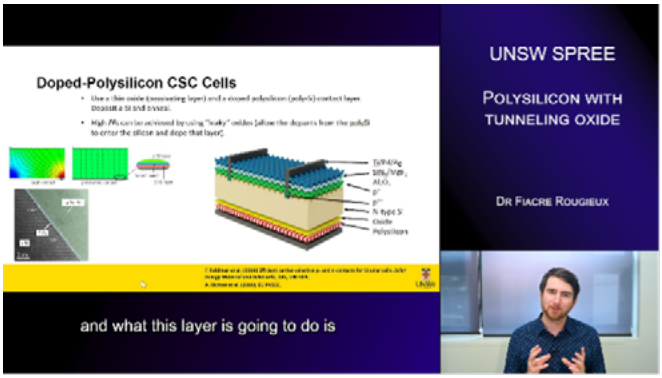

Figure PP5.10: Dr Fiacre Rougieux (ACAP/UNSW) shown from his six-week professional development course "Solar Cells".

Solar Cells (six weeks) provides an extensive introduction to the operational principles of solar cells, as well as an exploration of the latest advancements in solar cell technology. It is tailored to professionals already working or seeking to work in the photovoltaics or renewable energy sectors. The course examines crucial topics such as the fundamental workings of solar cells, the factors that hinder their efficiency, and the most recent trends in photovoltaic cell technology.

Figure PP5.11: Professor Bram Hoex (ACAP/UNSW) developed the six-week professional development course 'Photovoltaic Technology and Manufacturing'.

Photovoltaic Technology and Manufacturing (six weeks) is an introduction to solar cell production and the latest trends in the industry. It is designed for professionals who work or want to work in renewable energy or photovoltaic fields. The course covers the manufacturing process for solar cells and modules, from raw materials like sand to finished PV modules, as well as the latest advancements in photovoltaic technology.

UNSW SPREE's Public Research Seminars

Featuring SPREE academics, ACAP members and internationally renowned visiting researchers, the SPREE weekly seminar series has over 200 video seminars available to researchers around the world via YouTube url: https://www.youtube.com/unswspree.

Additionally, webpages located at the short url: **unsw.to/pvseminars** show the seminar videos and also allow researchers to download the speaker's presentation in PDF format.

The two most popular seminars are Professor Martin Green's The Emergence of Perovskite Solar Cells with 22,500 views (https://youtu.be/ALHea8qW1jc) and Pablo Dias's seminar PV Recycling: What SPREE Needs to Know with 12,500 views (https://youtu.be/hsXtMMwmfyc).

Figure PP5.12: A/Professor Brett Hallam's SPREE Public Research Seminar as seen on the short url: unsw.to/pvseminars. The web page shows the video, slides, abstract and biography.

During 2022 there were 15 seminars delivered. With COVID-19 restrictions it was required that some of the seminars be delivered via Zoom or MS Teams.

- 9 December 2022 – Janne Halme – Aalto University, Finland
  When I see a solar cell, it works – Colouring photovoltaics across science, technology, design and art
- 8 December 2022 – Nicholas Grant – University of Warwick, UK
  Mitigation of bulk and surface recombination for high efficiency silicon solar cells
- 29 November 2022 – Marina Freitag – Newcastle University, UK
  Diffuse Light Harvesting to Structured Information with Hybrid Photovoltaics
- 1 November 2022 – Anatoly Rozenfeld – University of Wollongong
  Recent development of solid state mini- and micro-dosimetry radiation detectors and its applications in particle therapy and space
- 27 October 2022 – Milad Mohsenzadeh – UNSW SPREE
  Self-cleaning Solar Desalination System for Low-cost Water Generation in Remote Areas
- 16 August 2022 – Tommy Wiedmann – UNSW
  Scientists' Warning on Affluence – Implications for Renewable Energy
- 4 August 2022 – Munkhbayar Batmunkh – Griffith University
  Exploring 2D materials in emerging solar cells
- 14 July 2022 – David Moser – EURAC Research
  Solar PV performance and reliability: the role of digitalization
- 22 May 2022 – Sudhanshu Shukla – IMEC Belgium
  What limits the performance of wide bandgap Cu(In,Ga)S2 solar cells?

- 11 May 2022 – Omer Sarood – Independent Consultant
  Solar PV Power Plants From The Eyes of End-User
- 21 April 2022 – Martin Green – UNSW Sydney (SPREE) –
  Australian Centre for Advanced Photovoltaics (ACAP)
  Photovoltaics – State of the Art and Perspectives
- 20 April 2022 – Yang Guo – Arctech Solar
  Increase PV Energy Yield with Superior Stow Parameters Enabled by Rigid Trackers
- 5 April 2022 – Martin Green – UNSW Sydney (SPREE) –
  Australian Centre for Advanced Photovoltaics (ACAP)
  Si heterojunctions: How close can HJTs get to 29% cell efficiency?
- 23 March 2022 – Brett Hallam – UNSW SPREE
  Key Material Limitations and Challenges Towards Sustainable Silicon PV Manufacturing at the Terawatt Scale
- 13 February 2020 (permission to publish granted November 2022) – Gianluca Coletti – TNO Energy Transition
  Four-terminal bifacial perovskite on silicon tandem devices: Concept, devices, energy yield and outdoor results

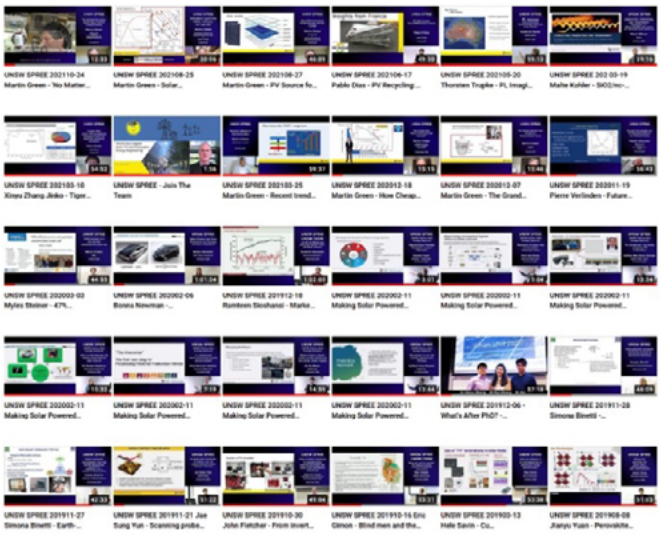

Figure PP5.13: SPREE's Public Research Seminars as seen on YouTube.

The YouTube seminar link is: https://www.youtube.com/unswspree

School Tours – Loreto Kirribilli

Figure PP5.14: One group of Loreto Kirribilli Year 10 students in front of the MAiA during their visit to the Solar Industrial Research Facility (SIRF).

During the 2022 school year, there was a period when a COVID-safe school tour could occur and in early June, Loreto Kirribilli became the only school in 2022 to tour the Solar Industrial Research Facility (SIRF). Forty-eight Year 10 students were split into morning and afternoon groups of 24 and these were divided into groups of 12. The students toured the fabrication facility and also saw presentations about the technology in the SIRF, the importance of Australia's role in photovoltaic R&D and the value of photovoltaic and renewable energy in supplying the clean energy needs of the world.

Visits to Schools

Figure PP5.15: High school students built and raced solar cars using kits.

Due to COVID safety regulations, it was challenging for high schools to visit the Solar Industrial Research Facility. However, SPREE's academics and undergraduate student ambassadors were able to visit schools instead.

To overcome the difficulties of bringing high school groups onto campus, funding was provided for solar car kits to be used during visits to schools. High school students listened to presentations, made solar cars and competed against each other in solar car races.

Between February and December 2022, SPREE conducted 11 visits to high schools, reaching a total of 748 high school students.

ENGG1000 Introduction to Engineering Design and Innovation

Figure PP5.16: ENGG1000 – Top: Term 1 with solar cars; Bottom: Term 3 with Solar Cable Cars.

ENGG1000 is a first-year undergraduate engineering course requiring teams of six students to design, build, test and (in the PV strand) compete against other teams. Most of the students who choose the PV strand of ENGG1000 are from other engineering disciplines so this course may be their only chance to learn about PV during their time at university. These students develop project management skills and an understanding of PV and PV systems that they wouldn't get in their field of study.

The students experience first-hand one of the major things that engineers do: designing and building creative solutions to problems. They learn to think the way that engineers think, coming up with good solutions to problems despite being limited by budget, time and resources. There are also requirements to meet environmental and social objectives.

Term 1 with the solar racing cars with 112 students had their final event on 21 April 2022 where they spent a signifcant amount of time under umbrellas.

There is a video called UNSW SPREE DESN1000 2022 Solar Raceway located at the following url:

https://youtu.be/kK2G5Ti0Bzw.

Term 3 with the solar cable car with 80 students had their final event in full sunshine.

Engineers Australia Immersion

Figure PP5.17: Engineers Australia had immersive experience days for high school students at SPREE – Top: 20 April; Bottom: 4 July 2022.

Engineers Australia collaborated with UNSW SPREE to organise two events for their high school outreach program on 20 April and 4 July 2022. Each day had 50 high school students, split into two groups of 25. The students received a brief presentation followed by a construction project.

Engineers Australia places great importance on solar and renewable energy and looks to create an immersive experience that enables students to explore solar and renewable energy engineering. This also helps to promote UNSW as a leading provider of courses in this subject area.

The construction project was comprised of a solar cell, a motor, a propeller and a laser-cut frame. Although students were not allowed to solder, they could take their materials to the soldering station and observe the process. After completing the project, there was an opportunity for discussions, and the students were provided with the finished product to take home.

Renewable Energy Society (RESOC)

Figure PP5.18: Dr Fiacre Rougieux (ACAP/UNSW) shown from his six-week professional development course "Solar Cells".

UNSW's Renewable Energy Society (RESOC) provides support to undergraduate and postgraduate students in the School of Photovoltaic and Renewable Energy Engineering (SPREE) and is a society run by students, which strives to create a strong sense of community and expose students to a wide range of networking opportunities.

In 2022, with the assistance of ACAP, the society successfully organised the following events as students returned to campus following quarantine:

An Industry Night, which was attended by over 80 students and 40 members of the industry;

- Educational seminars and panel talks;
- A peer mentoring program to support new first-year students; and
- Barbecues, sports days and other social activities.

In 2023, RESOC intends to continue organising similar events, facilitating interactions between industry and students, and maintaining the thriving community with the help of ACAP.

SunSprint Solar Challenge

ACAP supports the UNSW SunSprint Solar Challenge for students from kindergarten to Year 12. The challenge is a series of solar-powered races that are both fun and suitable for each age group.

In 2022, the UNSW SunSprint event featured five different races, with 23 schools and over 270 students participating. The event was held on the UNSW campus.

Figure PP5.19: The UNSW SunSprint Solar Challenge occurs each year in October with schools from NSW and the ACT.

The aim of the challenge is to encourage students to use their imagination, develop their learning, enhance their academic skills and embrace challenges through age-appropriate, science and engineering-based events that involve planning, construction, experimentation and competition.

One of the main races is the SunSprint, which takes place on a 100-metre figure-eight track. Teams of up to four students (from Year 6 to Year 12) usually build the cars, which can take up to six months to design and construct.

Another race is the MiniSprint, which takes place on a 20-metre straight track. These cars are built from a kit made up of a solar module, motor, gears, wheels and corflute chassis.

There is also a Solar Boats race, which takes place in a 10-metre pool using fishing line for guidance and the Solar Pursuit race involving MiniSprint-style cars chasing each other around a single-lane oval track until one car catches up and touches the other.

UNSW Sunswift

The Sunswift Racing team, made up of students from UNSW Sydney, set a Guinness World Record for the "Fastest EV over 1000km on a single charge" with its solar-powered electric car, the Sunswift 7.

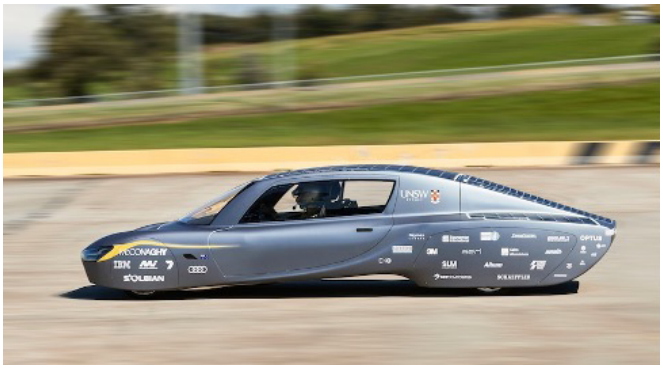

Figure PP5.20: UNSW Sunswift 7 on the Guinness World Record attempt (photo by Sunswift).

The world record was the result of hands-on learning, teamwork, collective problem-solving and academic oversite. Moreover, the Guinness World Record challenge provided students with a sense of purpose and an opportunity to see the results of their hard work. Participating in a world record attempt can help to inspire students to work harder, think more critically and strive for excellence.

Sunswift is the solar racing team of UNSW and is part of the worldwide Vertically Integrated Projects Consortium, spanning 45 universities across 12 countries. Sunswift combines innovative research with hands-on skills to create clean energy transport solutions. The team designs and builds solar-powered cars to race in the biennial Bridgestone World Solar Challenge (WSC). With COVID having cancelled the last WSC, the team is preparing for the next event scheduled for 22–29 October 2023.

The world record is recorded at the following url:

https://www.guinnessworldrecords.com/world-records/713449-fastest-1000-km-achieved-by-an-electric-car-on-a-single-charge-prototype.

The UNSW Newsroom article "EV record breakers! Sunswift 7 goes 1000km on a single charge in world's best time" can be seen at the following url:

https://newsroom.unsw.edu.au/news/science-tech/ev-record-breakers-sunswift-7-goes-1000km-single-charge-world%E2%80%99s-best-time.

MEDIA AND PROMINENT EVENTS

Throughout 2022, ACAP, its researchers and its research attracted media attention. Some of the articles, podcasts, reports, and events are listed below:

7NEWS: Solar funding to be supercharged with $45m

ABC Australia: The solar energy future is already here - Fiacre Rougieux | This Talk | YouTube

ABC News: Australian researchers show solar power can be generated at night

ABC News: Brian Burke, Kerry Stokes, Kevin Reynolds among major players in race to unlock Western Australia's green power future

ABC News: Renewable energy records tumble around the country as rooftop solar power soars

ABC News: What is renewable energy curtailment and how does it affect rooftop solar?

ABC News: World's first 'sand battery' can store heat at 500C for months at a time. Could it work in Australia?

ABC News: Worldwide demand for solar panels presents 'global warming risk' through aluminium production

Academic Gates: UNSW solar innovator and world-leading oceanographer awarded Prime Minister's Prizes for Science

AltEnergyMag: SOLARCYCLE Announces Company Launch to Accelerate a Circular Economy for the Solar Industry

ANU Events: ANU Solar Oration 2022 - Drew Clarke AO

ANU News: $45m injection to electrify innovation in Aussie solar tech

ANU News: Extra 1,500 pumped hydro sites offer potential to bolster Australia's clean energy grids

APVI: Improvements in PV recycling are necessary to meet strong future demand

ARENAWIRE: 5B Maverick robots set to transform solar

ARENAWIRE: ANU breakthrough smashes solar record

ARENAWIRE: Bright future for Australian solar PV research

ARENAWIRE: Watch this space: Ultra Low Cost Solar

ARS Technica: Emissions from aluminum production are bad news for solar energy

ASC Publications: Solar Panels Face Recycling Challenge

ATSE : Australian Academy of Technology and Engineering - Making the Cut – Emerging Technologies Required (Renta Egan)

AuManufacturing: Arena continues support for UNSW solar PV research

AuManufacturing: GREEN HYDROGEN IS ELECTRIFICATION

AuManufacturing: TINDO SOLAR TO COMMERCIALISE AGRIPV SOLAR PANELS

Australian Financial Review: Malcolm Turnbull joins Cannon-Brookes with stake in solar disrupter

Australian Financial Review: Rising solar prices won't stop the revolution, says renewables guru

Boerse-Express: DGAP-News - Aurora Solar Technologies erwirbt BT Imaging zur Wachstumsbeschleunigung (deutsch)

Campus Morning Mail: Prime Minister's Prize for Science announced

Campus Review: Top university experts sweep PM's science awards

Canberra Times: Ask Fuzzy - Solar panels reflect light and heat. Do they increase global warming and contribute to increased local temperatures?

Chemical & Enginering News: Solar panels face recycling challenge

China.org.cn: Australia provides new funding to boost solar panel research

CleanTechnica: Just The Facts: The Cost Of Solar Has Fallen More Quickly Than Experts Predicted

CNN: This giant 'water battery' under the Alps could be a game-changer for renewable energy in Europe

COSMOS: Generating heat and light

COSMOS: The risks and rewards of aluminium in solar panels

Courier Mail: 'Not a prank' - 2022 Prime Minister's Prizes for Science revealed

EAST ASIA FORUM: Getting real about the hydrogen economy

Eco Generation: Feds pursue "ultra low cost" solar with R&D funding

Eco Generation: PV recycling - Has anyone worked out how to do it yet?

Eco Generation: Solar Pioneers Night celebrates past 25 years of PV industry in Australia

EcoWatch: Meeting Net-Zero Solar Needs Would Require Nearly Half of World's Aluminum Production

EENEWS: Record efficiency of 26.81% for large silicon solar cells

Energy Central: Mass storage is a solved problem

Energy Central: 100% renewable energy in Japan

Energy Central: 15 GW of pumped hydro announced in Australia

Energy Central: Dramatic changes in Australia illustrate the future of the American electricity system

Energy Central: Fully Electrified Land Transport is Straightforward

Energy Central: Mass storage is a solved problem

Energy Central: Renewables in 2021

Energy Central: Texas - the (potential) renewable energy superstate

Energy Central: Texas can become the largest exporter of solar and wind power to other states if it strongly interconnects. How can connection-phobia be overcome?

Energy Live News: Australia announces $40m to drive ultra low cost solar energy

Energy Live News: Bright future for Australian solar research with $45m funding boost

Energy Magazine: $40 million boost for ultra low cost solar

Energy Magazine: $45 million for solar PV research

Energy Matters: Australia's Road To Ultra Low-Cost Solar

Energy Matters: Can Solar Power be Generated at Night? Australian Researchers Say Yes

Energy Source: Government pledges $45m towards "ultra low cost" solar

Europapress: Solar Cell Pioneer Wins the €1 Million Millennium Technology Prize

EXBULLETIN: UNSW Sydney Solar Pioneer Wins Europe's Biggest Innovation Award

Financial Post: Green Tech Boom Threatened as Solar Prices Surge to Decade High

Foresight: The forgotten power of water

Futura Science: Pourquoi la croissance du marché de panneaux solaires photovoltaïques pourrait devenir une menace pour le climat?

GIZMODO: More Efficient Solar Panels Could Be Coming With a $45 Million Grant to Researchers

Google Podcast: Thrive | Fiacre Rougieux | The solar energy future is already here...

Heinrich-Böll-Stiftung: Solar, wind and clean hydrogen: Asia's energy transition without the hype

Heinrich-Böll-Stiftung: Solar, wind and clean hydrogen: Asia's energy transition without the hype

Hydro Review: Researchers identify 1,500 'bluefield' pumped hydro sites in Australia

India EducationDiary: Two UNSW Academics Recognised As Fellows By The Australian Academy Of Technological Sciences And Engineering

India EducationDiary: University Of New South Wales - UNSW Sydney - Solar Pioneer Wins Europe's Biggest Technology Innovation Prize

India EducationDiary: University Of New South Wales: $45 million funding to boost solar technology research and development

India EducationDiary: University Of New South Wales: Early Career Researchers At UNSW Awarded $7.6m In Funding

India EducationDiary: University Of New South Wales: Energy Ministers Visit UNSW's World-Class Solar Energy Research Facility

India EducationDiary: University Of New South Wales: UNSW Sydney Awarded More Than $2.1m For ARC Linkage Projects

India EducationDiary: UNSW Researchers Awarded More Than $7.9m For Infrastructure And Linkage Projects

Indian EducationDiary: University Of New South Wales: UNSW Takes Top Spot For Number Of New Start-Ups And Spinouts

Industry Gov Au: 2022 Prize for New Innovators

Industry Update: Copper on solar cells, fly-ash in paint - UNSW start-ups on show at Expo

Industry Update: Solar pioneer wins biggest European innovation prize

InnovationAus: Double honours for innovation at PM Science Awards

InnovationAus: Manufacturing is key in SunDrive's $21m capital raise

InnovationAus: Solar energy - A tale of research commercialisation

LabOnLine: Safer Labs for SPREE

Leader: $45m funding to supercharge low-cost solar

Legislative Assembly for the ACT: Inquiry into renewable energy innovation in the ACT (heavily quoted)

MarkeyScreener: Vaisala Oyj - Solar cell pioneer wins the EUR 1 million Millennium Technology Prize

Medium: Powering the Future - Photovoltaics

Medium: Solar Energy's Biggest Problem Has Just Been Solved

Mercom: New Laser Technique to Reduce Amount of Silver in Solar Modules

Minister Industry Gov Au: Press conference with Assistant Minister Matt Thistlethwaite and Professor Renate Egan

Mirage News: $45m injection to electrify innovation in Aussie solar tech

Mirage News: UNSW researchers awarded more than $7.9m for infrastructure and linkage projects

Mirage News: UNSW solar innovator and world-leading oceanographer awarded Prime Minister's Prizes for Science - Associate Professor Brett Hallam Prize for New Innovators

Mirage News: UNSW Sydney awarded more than $2.1m for ARC Linkage Projects

Mirage News: UNSW Sydney solar pioneer wins Europe's biggest technology innovation prize

Mirage News: Up to $45 million to extend operations of Australian Centre for Advanced Photovoltaics

Nature: Solar power's need for a carbon-intensive metal is set to soar

New Atlas: Bizarre night-time solar cell generates power in a backwards process

Newcastle Herald: $45m funding to supercharge low-cost solar

News Com Au: 'Not a prank' - 2022 Prime Minister's Prizes for Science revealed

NEWSBREAK: The aluminium demand risk of terawatt photovoltaics for net zero emissions by 2050

Newsfile: Aurora Solar Technologies to Acquire BT Imaging to Accelerate Growth

North West Star: ACAP lands $45 million to kick renewable energy transformation into gear

One Step Off The Grid: Four critical lessons from Australia's world-leading solar industry pioneers

One Step Off The Grid: Great Solar Business Podcast: Are grants worth the effort?

OpenGov: Australia Prioritising Ultra-Low-Cost Solar Tech

PARLIAMENT OF VICTORIA: Inquiry into renewable energy in Victoria (extensive quoting)

PRESSPORTAL: Jolywood gewinnt pv magazine Annual Award 2021

PV Magazine Australia: 'Ultra low-cost solar' gets AUD 40 million R&D boost from ARENA

PV Magazine Australia: Aussie analysis of the fine art of gettering

PV Magazine Australia: Behind-the-scenes look at solar panel production shines light on Australian manufacturing

PV Magazine Australia: Flexible, roll-to-roll printed perovskite solar cell hits 16.7% efficiency

PV Magazine Australia: Green rates feat after Longi achieves record 26.81% with silicon cell

PV Magazine Australia: Martin Green's solar cell efficiencies at a glance updated

PV Magazine Australia: Solar is the cheapest power, and a literal light-bulb moment showed us we can cut costs and emissions even further

PV Magazine Australia: SunDrive lands $21 million to scale copper-based solar tech

PV Magazine Australia: SunDrive sets 26.07% efficiency record for HJT cell in mass production setting

PV Magazine Australia: UNSW researchers crack 'night-time' solar

PV Magazine Australia: UNSW researchers patent low-cost additive to solve perovskite's stability problem after achieving world-class results

PV Magazine Australia: UNSW's Martin Green picks up $1.5 million Millennium Technology Prize

PV Magazine Australia: Weekend read: A sustainability swan song

PV Magazine Australia: Weekend read: Automate, foldout for a ultra-low-cost solar future

PV Magazine Austrlia: UNSW researchers develop high yield, low cost, eco-friendly process to recycle Si-PV modules

PV Magazine Germany: Forscher des ISFH entdecken Ursache für Degradation von Gallium-dotierten Solarzellen

PV Magazine: 'Ultra low-cost solar' gets AUD 40 million R&D boost from ARENA

PV Magazine: ACAP lands $45 million to kick renewable energy transformation into gear

PV Magazine: Aussie analysis of the fine art of gettering

PV Magazine: Australian researchers claim solar cell efficiency record

PV Magazine: Cubical luminescent solar concentrator devices in urban environments

PV Magazine: Demanda estable y tendencia de precios sostenible, la otra cara del aumento de los precios de los módulos

PV Magazine: Determining solar cells' optical properties with conventional flatbed office scanners

PV Magazine: Gallium doping and solar cell degradation

PV Magazine: Higher PV module prices may point to stable demand and more sustainable pricing trends

PV Magazine: IEA PVSP predicts high-cost, low-revenue scenario for solar recycling

PV Magazine: IEA report confirms Australia remains a solar PV stronghold

PV Magazine: New process to recycle Si-PV modules

PV Magazine: Perovskite solar cell with record-breaking fill factor of 86.6%

PV Magazine: pv magazine Roundtables: Videos on EU manufacturing, solar sustainability, decarbonizing homes, and PV on wheels sessions

PV Magazine: Reverse bias - a hidden challenge for perovskite solar cell stability

PV Magazine: Semi-transparent agrisolar module tuned for Aussie crops being developed by UNSW, Tindo

PV Magazine: Solar cell efficiencies at a glance – updated

PV Magazine: SunDrive sets 26.07% efficiency record for heterojunction PV cell in mass production

PV Magazine: Sunman opens 1GW lightweight PV module factory

PV Magazine: Sunrun signs on to recycle solar panels with Solarcycle

PV Magazine: The PV industry needs 12 times more polysilicon production capacity by 2050

PV Magazine: The solar tech check - Key takeaways from SiliconPV 2022

PV Magazine: The Solar Tech Check -Toward 50-year modules, and how the numbers add up for HJT

PV Magazine: UNSW Exclusive - unlocking the potential of singlet fission for future PV devices

PV Magazine: UNSW researchers develop high yield, low cost, eco-friendly process to recycle Si-PV modules

PV Magazine: Water 'secret ingredient' in new processing mechanism for perovskite nanocrystals

PV Magazine: WCPEC-8 makes research findings available worldwide

PV Tech: ARENA to provide US$30m for R&D into 'ultra-low cost solar', aims to drive down cost of green hydrogen

PV Tech: Australian PV research centre secures AU$45m in government funding

PV Tech: Future industrial solar PV technologies: Record cell efficiency announcements versus industrial reality

PV Tech: Technology requirements for Ni/Cu plating metallization in commercial PV

PV Tech: Technology, manufacturing & profitability in the PV industry

RedGreenAndBlue: Solar is the cheapest power, and a literal light-bulb moment showed us we can cut costs and emissions even further

Renew Economy Solar Insiders Podcast: "Turn it off, turn it on"

Renew Economy: Solar Insiders Podcast - What we can learn from solar pioneers

Renew Economy: "Forget nuclear and simplify electrification." - The message from energy experts

Renew Economy: "Huge moment" Australia's Sundrive claims new solar cell efficiency milestone

Renew Economy: "Sun King" launches gigafactory for lightweight, flexible solar panels

Renew Economy: Australia plans to be a big green hydrogen exporter to Asian markets – but they don't need it

Renew Economy: Australia plots leap from world-leading solar R&D to global solar manufacturer

Renew Economy: Australia's only solar manufacturer names new CEO as it branches into agrivoltaics

Renew Economy: Australian researchers beat their own record for next-gen solar cell efficiency

Renew Economy: Australian researchers harvest "night-time solar" to provide power in the dark

Renew Economy: Batteries of gravity and water: We found 1,500 new pumped hydro sites next to existing reservoirs

Renew Economy: Big battery plans for Pilbara ignore massive pumped-hydro potential

Renew Economy: CEFC joins Cannon-Brookes in funding round for Aussie solar innovator

Renew Economy: CSIRO says Australia can - and must - build its own silicon and solar cell supply chain

Renew Economy: CSIRO, NREL boost collaboration as net zero becomes "centrepiece" of Aus-US alliance

Renew Economy: Have solar panels been perfected, or can we make them even better and cheaper?

Renew Economy: How solving solar's aluminium problem is key to keeping its climate credentials

Renew Economy: Labor tips $45m into Australian pursuit of "ultra low cost" solar

Renew Economy: NSW grants $3 million to Cannon-Brookes backed solar cell innovator

Renew Economy: Renewables snapshot - Are we on track to decarbonise the globe?

Renew Economy: Renewables snapshot: Are we on track to decarbonise the globe?

Renew Economy: RenewEconomy's Giles Parkinson inducted into Solar Hall of Fame

Renew Economy: Rush to rooftop solar doubles sales for Australia's only PV manufacturer

Renew Economy: Sydney solar pioneer Martin Green wins prestigious Millennium Technology prize

Renew Economy: There's a huge surge in solar production under way - and Australia could show the world how to use it

Renew Economy: To triple transmission capacity, landowners and neighbours need to be paid more

Renew Economy: Ultra-low cost solar "stretch goal" gets federal funding boost

Renew Economy: UNSW Sydney solar pioneer wins Europe's biggest technology innovation prize

Renewable Energy Magazine: ARENA Announces $40 Million Funding Round to Drive Ultra Low Cost Solar

Renewables Now: Australia to support PV research centre with USD 31m till 2030

Saur Energy International: Australian RE Agency Grants $40 M to Drive Ultra Low Cost Solar

SCHEERPOST: We Can Still Make Solar Panels Even Better and Cheaper

Science Alert: New Kind of 'Solar' Cell Shows We Can Generate Electricity Even at Night

Science Alert: The World's Massive Need For More Solar Panels Has One Shiny Catch

ScienceDaily: Major infrared breakthrough could lead to solar power at night

Scimex: Bringing attention to critical silicon sustainability in solar cell production

Shepparton News: $45m funding to supercharge low-cost solar

Solar Builder: LONGi breaks world record for silicon solar cell efficiency

Solar Builder: Sunrun signs on with new PV recycling venture SOLARCYCLE

Solar Industry Mag: SOLARCYLE Chooses Sunrun as First Partner for Sustainable PV Recycling

Solar Power World: Solaria company founder launches solar panel recycling company Solarcycle

Solar Quotes: Sunman Energy Cranks Up Lightweight Solar Production Capacity

SOLARQUOTES: Pioneers Of Australian Solar Energy Revealed

Stockhead: ASX Renewable Energy Stocks - ARENA drops $45m in funding towards solar PV research

StreetInsider: Aurora Solar Technologies to Acquire BT Imaging to Accelerate Growth

Sydney Morning Herald: NSW professor wins world's best technology prize

Sydney Morning Herald: Seizure forecasts, longer-lasting solar panels take top science prizes

Sydney Morning Herald: Solar panels on public housing could save tenants $750 a year

Sydney Morning Herald: Tech billionaires and former PM back 'game-changer' solar startup

Sydney Morning Herald: Ultra low-cost solar power a priority for Australia

Tech Smart Voonze: They develop a system to capture "solar energy" at night

Tech X plorer: 'Night-time solar' technology can now deliver power in the dark

TECHJUICE: Australian Researchers Find Cost-Effective Way To Recycle Solar Panels

TECHXPLORER: Calculating the coming aluminum demand for solar panels and how to mitigate its greenhouse impact

The Australian: Australia has broad and deep expertise in renewable energy

The Conversation (USA): Batteries get hyped, but pumped hydro provides the vast majority of long-term energy storage essential for renewable power – here's how it works

The Conversation: Australia plans to be a big green hydrogen exporter to Asian markets - but they don't need it

The Conversation: Batteries of gravity and water: we found 1,500 new pumped hydro sites next to existing reservoirs

The Conversation: Duet energi surya dan 'baterai' berbasis air bisa jadi opsi terandal transisi energi Indonesia

The Conversation: Groundbreaking studies of Earth's churning oceans recognised at Australia's most prestigious science prizes this year

The Conversation: Sunshine by day, water by night - Indonesia could pair its vast solar and hydro storage to decarbonise the country

The Conversation: There's a huge surge in solar production under way - and Australia could show the world how to use it

THE FIFTH ESTATE: Snowdon Developments, Powerhouse Ultimo, Renewable Energy Agency, Countrywide Renewable Hydrogen, Flinders University, and more...

THE FITH ESTATE: Driving powerful innovation: your next car might come with solar panels and smart chargers that give back to the grid

The Guardian: Australian research finds cost-effective way to recycle solar panels

The Guardian: Beam me down - can solar power from space help solve our energy needs?

The Guardian: Silver lining - Australian researchers given $45m to study alternative solar panel materials

The Guardian: Trevor McDougall wins $250,000 science prize for researching 'thermal flywheel' of climate system

The Thinking Ape Podcast: Solar and Renewable Energy with Dr Richard Corkish

TweekTown: 'Night-time solar' breakthrough makes power in the dark from infrared

UNSW News: Rise of renewables - How Ukraine war has changed global energy policies

UNSW News: $45 million funding to boost solar technology research and development

UNSW News: Caroline Kennedy praises solar initiatives during visit to UNSW

UNSW News: Two UNSW academics recognised as Fellows by the Australian Academy of Technological Sciences and Engineering

UNSW News: University Of New South Wales - Energy Ministers Visit UNSW's World-Class Solar Energy Research Facility

UNSW News: UNSW research projects shortlisted for Trailblazer program

UNSW News: UNSW researchers awarded more than $7.9m for infrastructure and linkage projects

UNSW: Meet Angela Begg, a photovoltaics engineer working to make the world a greener place!

UPLB Energy Forum 2022: Andrew Blakers delivers an invited talk to the Philippines

WhoWhatWhy: Our Solar Powered Future Is Already China's Reality

WION: WION Climate Tracker - Australian study proposes new cost-effective way to recycle solar panels

WOMADelaide 2022: Electric Future Now. The Planet Talks - Podcast

Women Love Tech: Sustainable Futures Consultant Angela Begg Talks About Her Inspiring Career in STEM

World Bio Market Insights: Australia Invests £21m to Drive Ultra Low-Cost Solar Energy

Yahoo Finance: Aurora Solar Technologies Completes BT Imaging Acquisition and Concurrent Non-Brokered Private Placement

Yahoo Finance: Aurora Solar Technologies Corporate Update

Yahoo Finance: Solar Cell Pioneer Wins the €1 Million Millennium Technology Prize

COLLABORATIVE ACTIVITIES

The Australian Centre for Advanced Photovoltaics' international collaborations are directed at the highest level through an International Advisory Committee, with representatives from the key partners in Australia and from the world's most active PV R&D nations, with engagement fostered through the development of collaborative research programs, the annual ACAP conference and the major global research conferences.

Specific project activities that leverage the benefits of the international relationships include the following key projects.

The collaboration described in Section 6.4 is a long-standing one that records the status of a whole range of photovoltaic technologies in the maintenance and publication of Solar Cell Efficiency Tables.

- Section 6.8 is about progress on a UNSW collaboration with SunDrive Solar to analyse optical and electrical loss mechanisms for experimental mini-modules comprising two Cu-plated bifacial M6 half cells encapsulated in glass-back sheet configuration. The study has shown that the main losses were front cover reflection, encapsulant absorption, interconnection shading and tabbing ribbon cabling.
- Section 6.10 describes an ANU–SunDrive Solar partnership about performance evaluation of bifacial modules on Australian roofs. It explores this market opportunity by estimating the share of light-coloured roofs and computing the yield potential of bifacial versus monofacial silicon heterojunction modules mounted on light-coloured roofs.
- Section 6.9 concerns a study to inform approaches for modelling the impact of shading on PV arrays to maximise accuracy with minimal (system and site) information.
- In Section 6.11 a partnership of UNSW and Geni.Energy, using data from Solar Analytics, is developing an open-source model for community batteries in the grid.
- UNSW and Open instruments are working together in a project on the photothermal deflection spectroscopy (PDS) characterisation technique for characterisation of thin-film PV materials and progress is described in Section 6.12.

In addition to the specific activities captured in this section, many of the reports already presented as detailed research reports also involve collaborations with international partners. Since late 2015 the organisation has had six rounds of small collaboration grants to researchers based at ACAP nodes. Many of the hot topics of the advancing silicon cell technology are being addressed by the collaboration grants. The progress reports for those still active in 2022 are presented online at https://www.acap.org.au/post/acap-s-annual-reports-2013-present and their titles and participants are listed there.

Many of the 55 ACAP Fellowships awarded in three rounds also involved collaborations and there is a report for each one that had 2022 activity included in https://www.acap.org.au/post/acap-s-annual-reports-2013-present and their titles and participants are listed here.

Additionally, this year, we are able to report on progress on 19 Infrastructure Grants (8 in Round 1 and 11 in Round 2) that are supporting the renewal of the nation's PV research tools and equipment.

Finally, the education, training and outreach activities reported in PP5 include a wide range of international interactions, the ACAP Conference, regular and special public lectures, and partnership arrangements in teaching and on-line learning, such as the development and delivery of courses between institutes in Australia and around the world.

6.4 SOLAR CELL PERFORMANCE DOCUMENTATION

Lead Partner
UNSW

UNSW Team
Prof. Martin Green, Prof. Xiaojing Hao

NREL Team
Dr Nikos Kopidakis

Academic Partners
CSIRO, Newcastle
NPVM, China
Fraunhofer Institute for Solar Energy Systems, Germany
ISFH, Germany
JRC, Ispra, Italy
AIST, Japan
JET, Japan

Funding Support
ACAP, UNSW, NREL

Aim

To improve accuracy and quality of photovoltaic device measurement and reporting.

Progress

A long-standing research collaboration between UNSW and NREL, now being conducted as an ACAP international collaborative project, involves the reliable documentation of the status of the whole range of photovoltaic technologies worldwide. This is by the biannual publication of the "Solar Cell Efficiency Tables" in the Wiley journal, Progress in Photovoltaics. More information about the scope and history of these Tables is given elsewhere (Green 2020).

By enforcing guidelines for the inclusion of solar cell efficiency results into these Tables, they not only provide an authoritative summary of the current state of the art but also ensure measurements are reported on a consistent basis. One criterion that has been important to enforce has been that results be independently certified at one of a limited but increasing number of "designated test centres", generally of a national facility status, with a certified measurement capability and additionally involved in international "round robin" testing. CSIRO (Newcastle) is the first test centre in the southern hemisphere accepted as a designated test centre.

This rigour has been important particularly as new device technologies come to the fore and groups relatively inexperienced with cell testing suddenly are thrust into the limelight. The other important role has been in developing measurement standards when international standards are not available. Figure 6.4.1 shows standards in this category developed for defining the area used for efficiency determination for experimental laboratory cells.

Several results from the ACAP program have set new world standards and are featured in these Tables. In 2022, these included the retention of two UNSW record efficiencies for CZTS cell performance, with 10.0% confirmed for a 1 cm² device and 11.0% for a smaller device, an ANU 22.6% record for a perovskite solar cell, a 20.1% record for a GaAsP/Si monolithic tandem solar cell (UNSW with Ohio State University and SolAero), a 32.9% efficiency for a GaInP/GaAs multi-junction solar cell involving multiple quantum wells (UNSW with NREL), a 34.5% UNSW record for a GaInP/GaInAs/Ge plus Si spectral split mini-module, a UNSW 40.6% result for a concentrator submodule using a similar cell combination and 21.7% for a large-area UNSW Si concentrator cell.

The Tables are widely used and referenced by the photovoltaic research community. According to the ISI Web of Knowledge, the sixteen versions prepared since 2013 under the ACAP banner have all been among the most cited papers published since then in the engineering discipline worldwide.

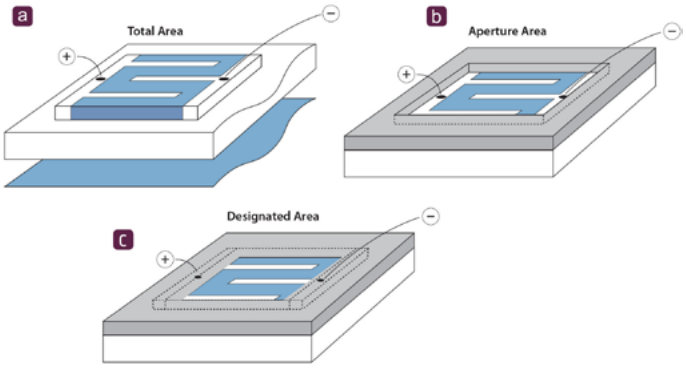

Figure 6.4.1: Cell area definitions: (a) total area; (b) aperture area; and (c) designated illumination area.

Highlight

- Value and widespread use of Tables validated by exceptionally high citation rates.

Future Work

- Publish two updated versions of the Tables during 2023.

Reference

Green, M.A. (2020). Tracking solar cell conversion efficiency. *Nature Reviews Physics 2*, 172-173.

6.8 COPPER-PLATED SILICON HETEROJUNCTION MODULES WITH EFFICIENCIES EXCEEDING 23%

Lead Partner
UNSW

UNSW Team
Dr Pei-Chieh Hsiao

UNSW Students
Wenxin Shi

SunDrive Solar
Chris Huang
Dr Daniel Chen
Prof. Alison Lennon

Funding Support
ACAP, UNSW

Aim

The highest single-junction cell efficiency of crystalline cells has been obtained using silicon heterojunction (SHJ) technology. To convert the high cell efficiency into module efficiency, optical and electrical losses are the two main factors to be considered in module design. Optical losses arise from reflection at the material interfaces and absorption by the materials are evaluated, whereas electrical losses are incurred from the power resistive loss occurring in the interconnect ribbons/wires and tabbing ribbons. This project aims to analyse these for mini-modules comprising two Cu-plated bifacial M6 half cells encapsulated in glass-backsheet configuration. Module efficiencies were independently measured at SERIS's ISO/IEC 17025 accredited laboratory, and the cell-to-module (CTM) losses of the modules were analysed.

Progress

Glass is typically used as the front cover to provide the primary mechanical support for the modules. The reflectance of three glass candidate materials is compared in Figure 6.8.1(a). Planar glass without an anti-reflection coating (ARC) and a thickness of 2 mm showed higher reflectance in the mid wavelength range. The average 0.2% reflectance decrease in the 300–1000 nm region of 2 mm textured glass with no ARC was possibly due to different manufacturers and the scattering effect from the rear textured surface. Textured glass with an ARC showed broadband reduction in measured reflectance, with an average of 8.2% in the 300–1000 nm region. However, improvement in reflection with ARC appeared significantly lower than the expected 3–4% which is reported in the literature (Helsch & Deubener 2012; Priyadarshini & Sharma 2016). As the absorption in glass is minimal, the 3 mm thick ARC coated textured glass was selected as the front cover for the mini-modules.

Ethylene-vinyl acetate (EVA) is the most widely used encapsulant in PV modules with over 80% world market share in 2021 according to the ITRPV 2022 report. The acetic acid generated from EVA decomposition can potentially lead to Cu corrosion which has been attributed to power degradation in modules subjected to damp heat test (Gawlinska-Necek et al. 2021). Polyolefin elastomers (POE) are an alternative encapsulant commonly used for SHJ modules, bifacial applications and when Cu metallisation is employed. Based on the compatibility with Cu cell metallisation, along with the advantage of increased transmittance in the UV wavelengths and lower water vapour transmission rates over EVA (Oreski et al. 2020), POE was used for these experimental modules.

Interconnect ribbons affect module performance both optically and electrically. Optical shading and resistive loss resulting from the ribbons should be minimised simultaneously. Figure 6.8.1(b) plots the reflectance measured on cells interconnected by three types of ribbons with similar cross-sectional areas (i.e. electrical loss was controlled). Structured ribbons presented ~1.6% higher reflectance owing to their larger 1 mm ribbon width. Theoretically triangular ribbons can achieve higher optical gain than circular wires by redirecting the incident light to the cell surface, however this advantage is compromised by the round apex and curved solder coating in the actual ribbons. Consequently, reflectance of triangular ribbons and circular wires were optically comparable, except for wavelengths >1000 nm where the triangular ribbons reflected less light. Ribbon geometry is also related to cell spacing in the modules. Ribbons with low aspect are typically used for high packing density modules which implement zero cell gap or tiled configuration. For these modules they can reduce both the encapsulant thickness and the thermomechanical stress which is induced during lamination. Sectional ribbons using different geometries (e.g. triangular/circular at the front and flat at the rear) can provide the benefits of increased front surface optical performance and reduced encapsulant cost and induced Si stress. The process temperature for stringing/interconnection is determined by the solder composition. As SHJ cells are sensitive to thermal processes >200°C, low melting temperature solders are more ideal to prevent potential damage to the a-Si:H passivation layers. As such circular wires coated with SnBiAg solder were used for interconnection with a 1 mm cell gap.

Selection of back cover material is mainly determined by the electrical insulation and moisture protection. The mainstream white backsheet was used as it provides higher optical coupling than a black backsheet.

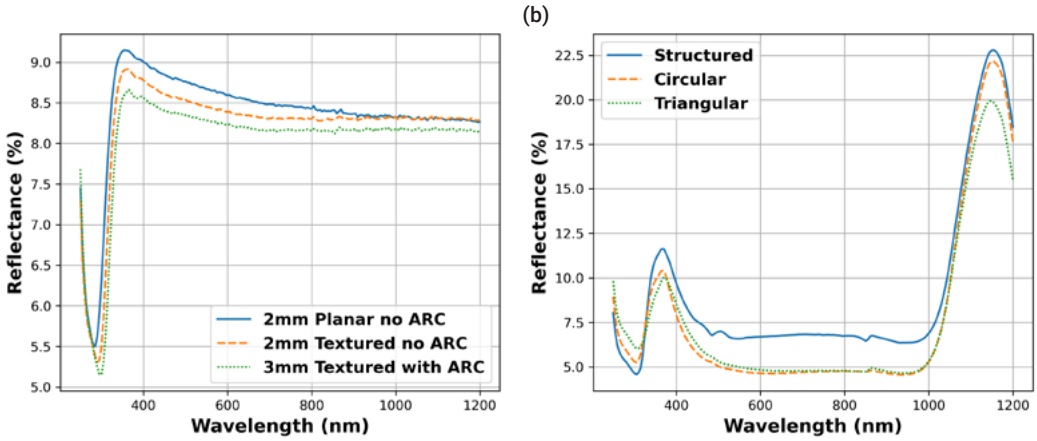

Figure 6.8.1: (a) Measured reflectance of glass; and (b) measured reflectance of SHJ cells interconnected by different ribbons and laminated in AR coated textured glass-glass modules.

Five mini-modules were fabricated by interconnecting two Cu-plated bifacial M6 half cells. Module IV was characterised using a Class A+A+A+ 100 ms h.a.l.m. cetisPV-XF2-M pulsed solar simulator. The measurement uncertainty for maximum output power (P_{MAX}) was ±1.4%. Due to the total internal reflection in the mini-modules (200 ´ 200 mm in dimension), masking was applied to avoid light being reflected by the white backsheet into the cells. A module area of 277.22 cm^2 was used to calculate the module efficiencies. The measured IV performance is summarised in Table 6.8.1. The average P_{MAX} was 6.327±0.085 W and calculated efficiency was 22.820.31%. The best module achieved an efficiency of 23.17% with the certified IV curve shown in Figure 6.8.2.

	V_{OC} (V)	I_{OC} (A)	FF (%)	P_{MAX} (W)	h (%)
Average	1.487± 0.002	5.257± 0.026	80.96± 0.81	6.327± 0.085	22.82± 0.31
Best	1.489	5.292	81.52	6.423	23.17

Table 6.8.1: Module IV performance of five mini-modules (with an active area of 277.22 cm^2).

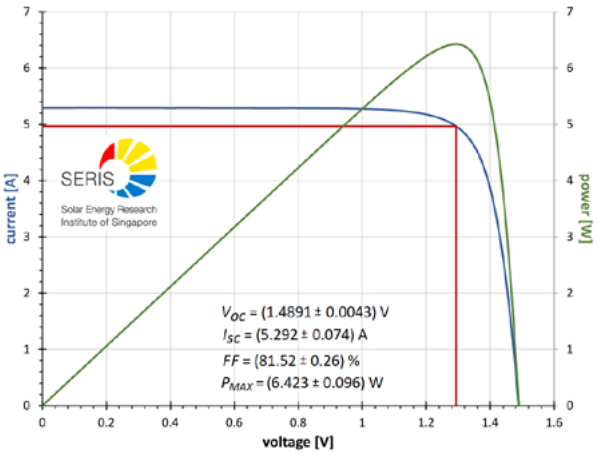

Figure 6.8.2: Certified IV curve from SERIS ISO/IEC 17025 accredited laboratory.

To investigate the optical and electrical losses of fabricated modules and provide guidance for future improvement, a CTM analysis using SmartCalc.CTM version 1.3 (Haedrich et al. 2014; Mittag & Ebert 2017) was conducted. The resulting waterfall diagram is shown in Figure 6.8.3. The analysis started with a half-cell efficiency of 25%, assuming an absolute 0.3% loss from the cell cutting process. Figure 6.8.3 clearly shows that the greatest loss (1.04%) resulted from front cover reflection (k3), probably because the ARC was not optimally deposited on small-sized glass. This cover reflection loss is expected to be reduced to 0.43% if the average glass reflectance can be reduced by 3%. The second largest loss was encapsulant absorption (k6). Reduction of light absorption by POE is possible if circular wires with decreased diameter are used, which may require adjustment of the busbar numbers. The next largest optical loss arose from the interconnection shading, despite using circular wires. This highlights that interconnect ribbons are one of the most crucial components of a module's design as they contribute to non-negligible electrical loss (k12) in the modules. The largest electrical loss of 0.34% resulted from

junction box and cabling (k15), in which the resistive loss in the tabbing ribbons was considered (assumed a ribbon length of 150 mm from the connector of the solar simulator to the centre busbar). This loss can be reduced by using thicker tabbing ribbons or matching the glass size to the cells. The estimated module efficiency was 23.31%, 0.14% greater than the highest mini-module efficiency. The difference may at least be partly due to the electrical mismatch between the two half cells that was not evaluated in the analysis.

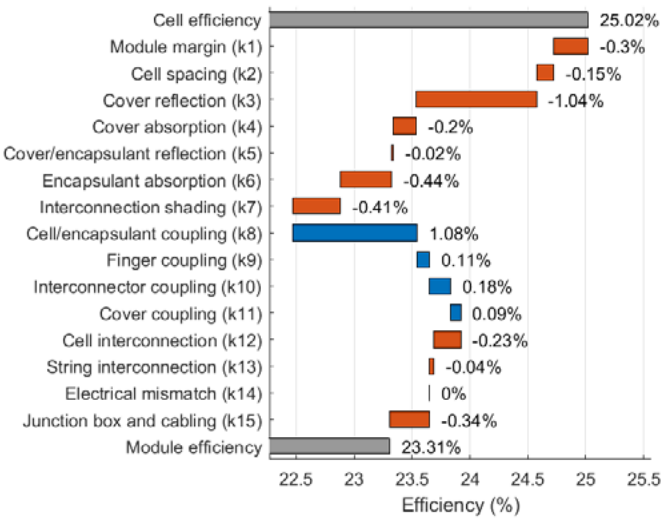

Figure 6.8.3: Waterfall diagram of CTM analysis of glass-backsheet modules with two Cu-plated M6 half SHJ cells.

Highlights

- Mini-modules with two Cu-plated bifacial M6 half cells were fabricated using AR coated textured glass, POE, white backsheet and circular wires for cell interconnection with 1 mm gap.
- The average and highest module efficiency, measured at SERIS's ISO/IEC 17025 accredited laboratory, were 22.82±0.31% and 23.17%, respectively.
- A CTM analysis revealed that the main losses were front cover reflection, encapsulant absorption, interconnection shading and tabbing ribbon cabling.

Future Work

- Reduce optical reflectance with appropriate AR coated textured glass.
- Upscale to full-sized module.

References

Gawlinska-Necek, K., Socha, R. P., Balawender, P., Stodolny, M. K., Van Aken, B. B., Starowicz, Z. & Panek, P. (2021). Silicon solar cells and modules with front contact paste containing copper-based component. Progress in Photovoltaics: Research Applications 29, 1008-1019.

Haedrich, I., Eitner, U., Wiese, M. & Wirth, H. (2014). Unified methodology for determining CTM ratios: Systematic prediction of module power. Solar Energy Materials Solar Cells 131, 14-23.

Helsch, G. & Deubener, J. (2012). Compatibility of antireflective coatings on glass for solar applications with photocatalytic properties. Solar energy 86, 831-836.

Mittag, M. & Ebert, M. (2017). Systematic PV-module optimization with the cell-to-module (CTM) analysis software. Photovoltaics International, 36th edition, 97-105.

Oreski, G., Omazic, A., Eder, G. C., Voronko, Y., Neumaier, L., Mühleisen, W., Hirschl, C., Ujvari, G., Ebner, R. & Edler, M. (2020). Properties and degradation behaviour of polyolefin encapsulants for photovoltaic modules. Progress in Photovoltaics: Research Applications 28, 1277-1288.

Priyadarshini, B. G. & Sharma, A. K. (2016). Design of multi-layer anti-reflection coating for terrestrial solar panel glass. Bulletin of Materials Science 39, 683-689.

6.9 PRAGMATIC MODELLING OF PV SHADING IMPACT

Lead Partner
UNSW

UNSW Team
Mike Roberts
Laura Johnson
Simon Heslop
Anna Bruce
Rob Passey
Navid Haghdadi

Funding Support
ACAP

Aims

Inform approaches for modelling the impact of shading on PV arrays to maximise accuracy with minimal (system and site) information.

With support from the Commonwealth Government Department of Industry, Science, Energy and Resources, SunSPoT is undergoing a development project including development of an alternative version for regions where suitable LiDAR data is unavailable. The LiDAR-free version of SunSPoT will require users to input the slope of their roof and some information to describe the shading.

Evaluating the impact of near shading on PV systems is a complex and critical step in the PV design process, dependent on a range of factors including the sun's path in the sky, the nature of the shading object and PV system topology. Despite record levels of uptake, consumers

have traditionally been discouraged from installing solar systems with unavoidable near shading due to potentially disproportionate power losses (MCS Solar Photovoltaic Working Group 2012). However as the cost of solar comes down, non-optimal roof areas become more financially viable sites for solar, and modelling tools to allow users to assess the impacts of partial shading can inform their PV investment decisions.

Approaches to model partial shading generally either use simplified empirical correlations such as a "shading factor", or require detailed simulation of the current-voltage (IV) curve to determine PV cell characteristics. Despite the emergence of some hybrid models, a review of the literature reveals that there is generally a compromise between model simplicity and model accuracy (Saint-Drenan & Barbier 2019). Furthermore, consumers often lack detailed system information –and access to sophisticated tools to accurately describe shading obstructions, particularly at the early design stage. There remains limited understanding of the impact of error in input information on simulated PV output. This gap in the literature highlights a need for further research into modelling approaches and assumptions which can best mitigate the output error in the absence of detailed system information.

This two-stage study presents a detailed investigation into the sensitivity of simulated PV output to accuracy of inputs for small-scale residential PV systems modelled in NREL's System Advisor Model (SAM). The first stage of the study investigates the impact of error in measurement of system orientation and tilt angles on simulated output for unshaded systems. The second stage conducts error testing in shading object description of selected systems using SAM's inbuilt 3D shade calculator.

The findings of this research will inform design and delivery of the improved shading input implemented in SunSPoT v3.1. Note that there is existing literature relating to modelling the impacts of shading and fault diagnosis. However, the contribution of this study is the focus on maximising accuracy of modelling given minimal system and site data, as would be the case for the average residential household using SunSPoT.

Progress

Methodology

Study 1: Sensitivity to system description

To test sensitivity to error in system tilt and orientation, a 6.4 kWDC unshaded residential PV system was modelled using PVWatts default assumptions and residential load profile. Systems were modelled at seven baseline orientations and four baseline roof tilts based on common construction types found in the housing stock[1]. Each of the orientation and tilt combinations was simulated in 16 locations across Australia using ERMY weather files (Exemplary Energy Partners 2022), generating 448 scenarios in total. Error in orientation from $\pm 7.5^0$ to $\pm 22.5^0$ and error in tilt in $\pm 4^0$ increments up to $\pm 12^0$ were introduced, to represent potential estimation error.

A default residential load profile and time of use (ToU) tariff structure were then applied within SAM to determine the impacts of input error on the annual yield and payback period for each scenario. Table 6.9.1 below provides a sample summary of results for Sydney, demonstrating the percentage absolute error in annual yield for errors of $\pm 22^0$ in orientation and ±12% in slope for each baseline scenario.

Table 6.9.1: Maximum absolute error in annual yield for Sydney

		Baseline roof tilt and error tested			
		Near flat	**Skillion**	**Traditional**	**Steep**
Baseline orientation and error tested		$5^0 \pm 12^0$	$15^0 \pm 12^0$	$25^0 \pm 12^0$	$35^0 \pm 12^0$
N	$0^0 \pm 22.5^0$	6.59%	6.76%	5.33%	8.97%
NE	$45^0 \pm 22.5^0$	5.55%	7.70%	11.67%	15.14%
E	$90^0 \pm 22.5^0$	9.80%	14.49%	18.76%	22.54%
SE	$135^0 \pm 22.5^0$	13.69%	18.85%	23.89%	28.22%
SW	$225^0 \pm 22.5^0$	12.25%	18.81%	24.78%	29.60%
W	$270^0 \pm 22.5^0$	5.10%	10.88%	15.43%	19.11%
NW	$315^0 \pm 22.5^0$	6.75%	6.46%	7.41%	10.84%

[1]. There are no fixed standards for roof slope in Australia beyond minimum slopes to ensure drainage. South facing systems were not modelled. Note also that the PV modules were assumed to lie flush with the roof, so the module tilt equals the roof slope and there is no self-shading.

It can be seen that south-east and south-west facing systems demonstrate heightened error relative to north-oriented systems. This error is greatest for a steep roof, with maximum error of almost 30% of system output, almost double that for a near flat roof at the same orientation. These errors were further amplified in evaluation of the payback period, resulting in maximum error of up to 70% for steep, south facing systems. West facing systems are found to be marginally more resilient to input error compared to east facing systems, and have a higher overall annual yield, on average, by 9%. The lowest errors on average are achieved by north-facing systems, which tend to have a higher resilience to design flaws including system tilt[2].

These patterns of relative error were found to be consistent across all modelled locations across Australia despite large variations in solar insolation. The percentage error in system output was found to be consistent across all climate zones, while error in payback period is approximately 10% higher for cool temperate zones (i.e. Hobart) compared to tropical zones (i.e. Darwin).

Study 2: Sensitivity to shading object description

Sensitivity to error in shading object description was modelled with SAM's detailed residential PV model and inbuilt 3D shading tool which uses a "look-up" style shading matrix of pre-computed shading factors to estimate the loss in annual yield (MacAlpine, et al. 2017). A 6.2 kWDC, north facing PV system at 25^0 tilt was chosen for modelling in two string configurations (see Figure 6.9.1), both with a central inverter.

- Configuration A: Five horizontal strings of eight modules (unshaded annual yield 9772 kWh)
- Configuration B: Four horizontal strings of ten modules (unshaded annual yield 9776 kWh)

Four shading objects were designed in SAM's CAD-based shading tool to represent common shading obstructions, each modelled at nine equidistant locations from the base of the array in the north of the sky. Figure 6.9.1 demonstrates the equidistant locations for the "block" object (see Table 6.9.2 for block specifications):

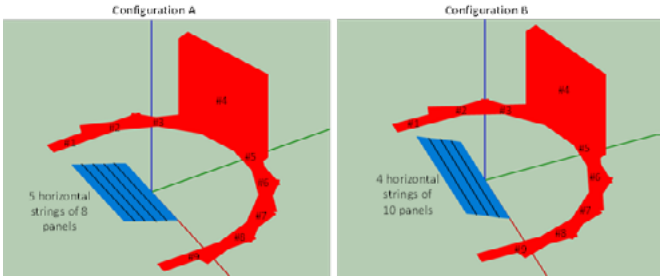

Figure 6.9.1: Equidistant testing locations for the "block" object (both configurations).

Table 6.9.2 below depicts object specifications and average simulated annual yield reduction across each of the nine object locations for both configurations. Note that the heights are measured relative to the base of the active surface, which is assumed to be mounted on a roof.

Table 6.9.2: Baseline shading object specifications and average reduction in annual yield.

	Block (building)	Cylinder (pole)	Large tree	Small tree
Configuration A	**11.08%**	**2.45%**	**23.08%**	**3.83%**
Configuration B	**12.44%**	**2.49%**	**24.76%**	**5.11%**
Diagram	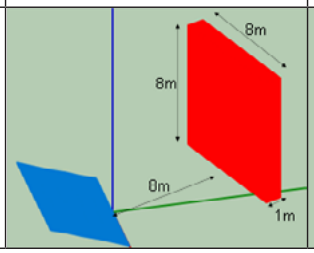	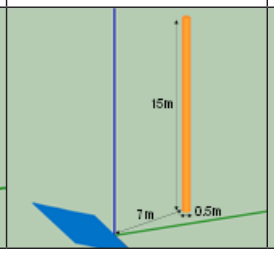	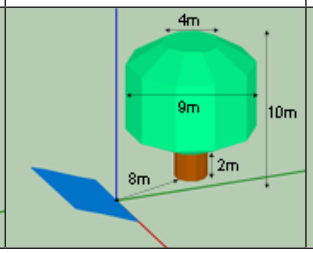	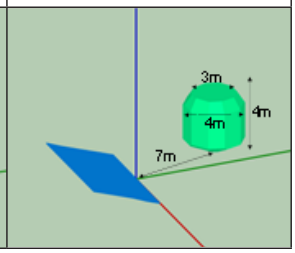

Reduction in annual yield in configuration B is 1% higher on average than configuration A. This result is consistent with several studies which investigate the impact of string configuration on PV performance under partial shading conditions (Pachauri, et al. 2020). As expected, the large tree results in the greatest reduction in annual yield on average, while the cylinder results in the lowest. Note that SAM's methodology does not account for production losses across blocks of cells or modules in the event of partial shading. While SAM models reduced yield as roughly proportional to the shaded area, in reality, the cylinder is likely to result in disproportionately large shade losses as more blocks will be impacted at any time (Deline 2009).

For each object orientation and configuration, ±20% error was introduced to the object height and distance from the base of the array[3]. Results are shown in Figures 6.9.2 and 6.9.3, respectively, with each of the nine object orientations shown from the point of reference of the active surface on the horizontal axis (north = 0 degrees). The results below are presented as an average of string configurations A and B, as the difference between each was found to be marginal.

[2] The output of a 'flat' system is effectively independent of its orientation.
[3] Error in cylinder radius, system tilt and orientation were also modelled under partial shading conditions, however the resulting error was found to be insignificant compared to the same input error in height and distance shown here.

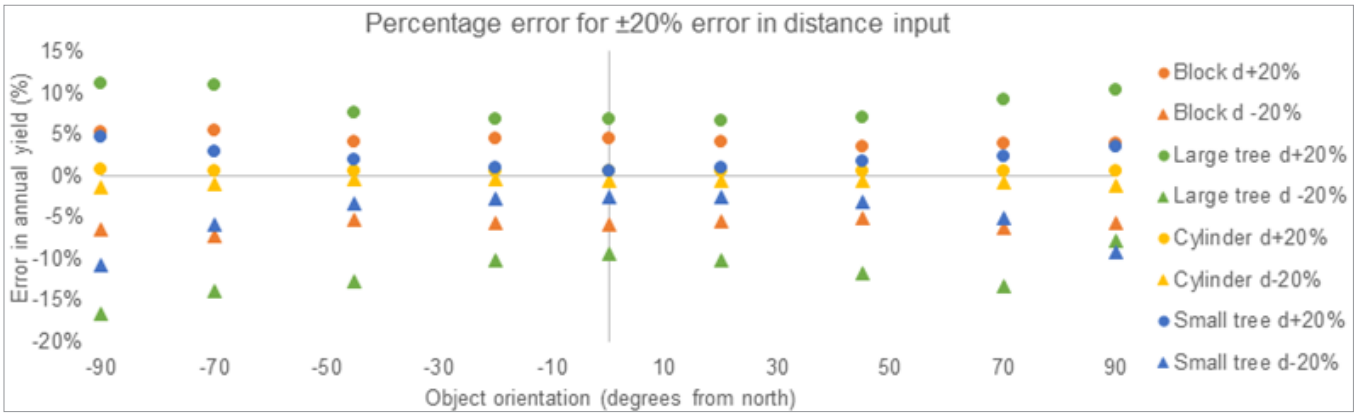

Figure 6.9.2: Error in annual yield for ±20% error in object distance from base of array.

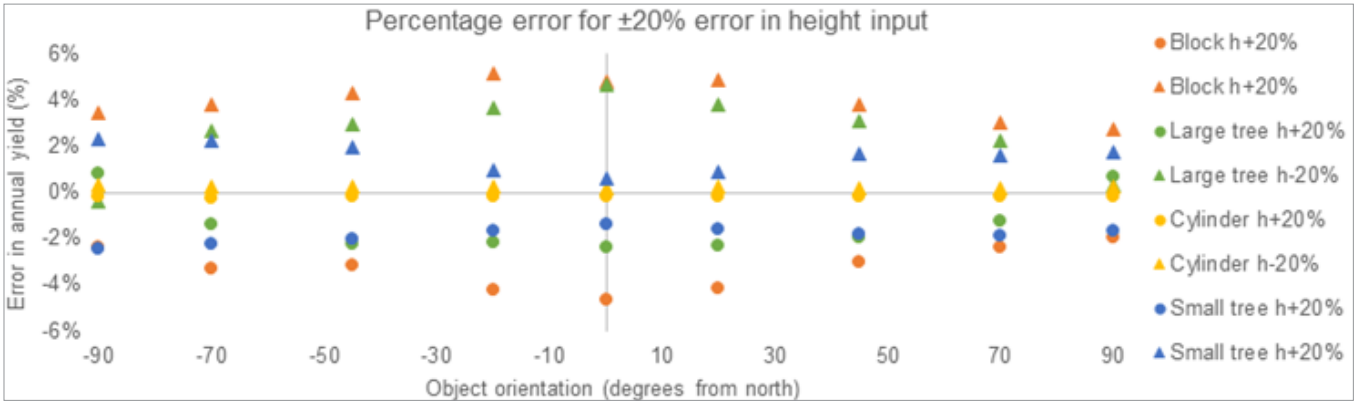

Figure 6.9.3: Error in annual yield for ±20% error in object height above base of array.

In general, the impact of input error is highest for objects with the greatest shading impact (Table 6.9.2). The large tree is the most sensitive to error in distance input, while the block is the most sensitive to error in height input. This may be because the large tree contains a trunk which also changes height proportionally by ±20%, controlling the amount of light to filter beneath the crown and partially offsetting error in annual yield. This observation highlights the crude simplification of trees as shading objects which are diverse and complex by nature yet are reduced in this study to the sum of several opaque polygons (MacAlpine, et al. 2017).

For error in distance, results are most sensitive when the shading object is located in the east or west of the sky (object orientation ±90^0). This is because the sun's angle in the sky is generally lower during morning and evening, when a small error in distance from the base of the array can result in disproportionate shadows and consequent reduction in output. The opposite appears to be true for error in height, where large objects in the north of the sky (large tree and block) are most sensitive to error since relatively small changes in height can block a larger amount of radiation. However, smaller objects (small tree and cylinder) exhibit the inverse pattern, indicating that there is a lower threshold for object size where the sun's angle in the north of the sky becomes sufficiently high to avoid major changes to annual yield when height error is introduced.

On average, the absolute error in simulated annual yield resulting from ±20% error in measured distance from the base of the array is 4.91%, which is significantly higher than that caused by similar error in height (1.93%). This is particularly true when the distance is underestimated, resulting in an average error of -5.89% compared to 3.92% increase when overestimated by the same amount for all shading objects.

Highlights

- The combined results demonstrate that simulated PV output is appreciably sensitive to the accuracy of inputs, though the degree to which error is amplified depends on key system characteristics. Systems most vulnerable to heightened error in simulated annual yield include south facing systems with steep tilt and significant near shading, with the most dramatic errors emerging from inaccurate description of the shading object.
- In all cases, the error was inflated to almost double in the calculation of payback period. Insights on system profitability would be strengthened by further investigation into the impact of seasonal and regional variations, combined with diverse load profiles against a range of tariff structures.
- This study confirms PV system modelling software should be designed to encourage maximum possible input accuracy to ensure the integrity of simulated output. This is particularly

pertinent for partially shaded systems which are inherently challenging to describe without sophisticated tools. •

- These results were presented at the Asia Pacific Solar Research Conference in December 2022.

Future Work

- A key limitation of this study is SAM's shading method which stores the shade loss factor for each string at each time step over the year in a "look-up" style shading matrix to achieve fast computation times. Furthermore, the CAD-based shading tool is limited in its ability to define complex shading scenes, compared to some emerging methods which instead use graphical processing units. Indeed, further work is required to validate the conclusions in this study by performing similar tests in other PV simulation software and by comparing results to experimental data.
- Further work understanding the impact of inverter type and string layout and the best modelling approach in the absence of string layout data is required, in particular, understanding how these impacts may vary across small and large systems in the field.
- This work is planned for submission to a journal for peer review.

References

Deline, C. (2009). Partially shaded operation of a grid-tied PV system. 2009 34th IEEE Photovoltaic Specialists Conference (PVSC), 001268-001273.

Exemplary Energy Partners. (2022). Australian Long Term Solar and Weather and Climate Data (1990 - 2017). [Online]
Available at: http://www.exemplary.com.au/solar_climate_data/solar-weather-climate-data-1990_2017.php.

MacAlpine, S., Deline, C. & Dobos, A. (2017). Measured and estimated performance of a fleet of shaded photovoltaic systems with string and module-level inverters. Progress in Photovoltaics: Resesarch and Applications 25(12), 714-726.

MCS Solar Photovoltaic Working Group. (2012). Guide to the Installation of Photovoltaic Systems, London: Electrical Contractors Association.

Pachauri, R. K., Mahela, O. P., Sharma, A., Bai, J., Chauhan, Y. K., Khan, B. & Alhelou, H. H. (2020). Impact of Partial Shading on Various PV Array Configurations and Different Modeling Approaches: A Comprehensive Review. IEEE Access 8.

Saint-Drenan, Y. M. & Barbier, T. (2019). Data-analysis and modelling of the effect of inter-row shading on the power production of photovoltaic plants. Solar Energy 184, 127-147.

6.10 ANU-SUNDRIVE COLLABORATION: PERFORMANCE EVALUATION OF BIFACIAL MODULES ON AUSTRALIAN ROOFTOPS

Lead Partner
ANU

ANU Team
Marco Ernst, Xuesi Liu

Industry Partners
SunDrive Solar Pty Ltd: Alison Lennon, Daniel Chen, Chris Huang, Vincent Allen

Funding Support
SunDrive Solar Pty Ltd, ACAP (ANU Node), ANU

Aims

The energy yield potential of bifacial solar modules for roof applications has not yet been investigated in detail. This project explores this market opportunity by analysing the share of light-coloured roofs in a selected area (Canberra) and computing the yield potential of bifacial versus monofacial silicon heterojunction modules provided on a light-coloured roof.

Project outcomes

A. Proof-of-concept rooftop analysis

This analysis aimed to automate detection of rooftops, their type and colour based on aerial imagery to estimate the distribution of rooftop reflectivity. Aerial imagery over satellite imagery was required due to their higher resolution and obtained through Nearmap. The analysis is demonstrated for a selected region (Canberra). To accommodate complex imagery characteristics, a machine learning (ML) approach was applied to build a framework with Mask Recurrent Convolutional Neural Network (Mask R-CNN) being the central component of the auto-detection process. For each image fed, the model extracts graphic features contained within, then detects and indicates potential roof area pixels from the image based on such features. Subsequently, the model performs classification based on the characteristics of pixel-selected regions and assigns each region a label from pre-defined rooftop types.

Figure 6.10.1: (left) Two examples of ML-detected rooftops. (right) Rooftop Lightness results from this study.

Compared to previous research, the proposed model was trained on a small data set (4781 images with roof shape information in total) across three ACT suburbs. With limited pre-processing of data, the model achieved an 80.2% precision and 95.9% recall rate on test sets. A visual inspection of nearly 400 images in one suburb yielded a detection region accuracy (i.e. if the detected area is part of a rooftop) of approximately 85%, some examples are shown in Figure 6.10.1. Based on these detection results, an analysis was performed to extract the average colour characteristics and categorising roofs by their lightness value. Figure 6.10.2 shows our overall analysis results of images for approximately 250,000 detected roof surfaces (note that this number includes residential, commercial and industrial roof surfaces) with about 45% of rooftops categorised as light-coloured.

While the workflow has been able to produce required data in general, there have been some limitations that need to be addressed. The first limitation was the availability of training data in this project, which was mainly limited by access to only a subset of roof shape information for about 4800 roofs. This limitation also has the potential to introduce a bias towards certain roof types. Secondly, with a demand to obtain finer details for subsequent detection of solar panels, the model runs on a higher zoom level which caused the rooftop shapes to be more fragile hence harder to detect. In terms of colour analysis, the limitations are mainly on whether the approach taken to convert colours into reflectance values is reliable and verified. The mapping between colour and rooftop reflectance can, for example, be impacted by weather conditions and lighting conditions at the time of the aerial survey. Although further work is needed to fill these gaps and provide a more robust model and analysis, the current project results demonstrate the potential of the developed model for rooftop identification and classification.

B. Estimate bifacial gain

The second aim of this project was to estimate the energy yield potential of bifacial modules in rooftop applications. For a selected light-coloured roof, we compared the estimated yield of bifacial and monofacial silicon heterojunction (SHJ) modules. Monte Carlo ray tracing (MCRT) was utilised to accurately compute bifacial illumination allowing to estimate the energy yield of each scenario.

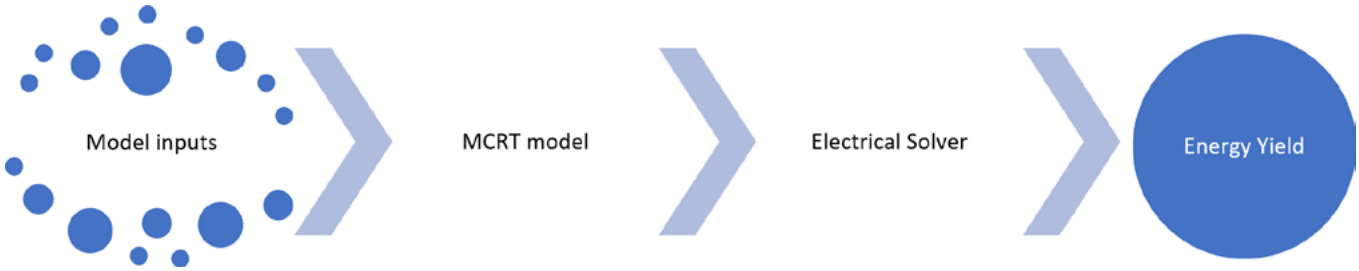

Figure 6.10.2: Simplified schematic of the modelling workflow.

Figure 6.10.2 shows a summary of the modelling workflow. Modelling inputs to the MCRT model were the geometric and optical properties of the components (rooftop, modules ...) as well as the information on solar radiation (sun position, direct and diffuse irradiance). The MCRT model computes the absorption of each individual cell in a module at both the front side and the rear side. This information, together with additional electrical cell parameters, is used by the electrical solver to compute the output power of the module. By integrating electrical power for a typical year, we obtain the annual (DC) energy yield of the system.

Simulations were performed on an exemplary rooftop system, illustrated in Figure 6.10.3, with solar irradiance and weather data for Canberra. The house is located in a 615 m^2 rectangular block typical of current and recent housing developments in the region, with a 12.4 m x 23.0 m roof sloped at 7.2° and facing north. We applied period boundary conditions to the block to account for the effects of neighbouring houses. The photovoltaic system consisted of two rows of eight solar panels connected as separate strings, on a light roof. The modules used 144 half-cut high efficiency SHJ solar cells. The modelled STC power in monofacial and bifacial configurations are listed in Table 6.10.1. The monofacial front illumination performance is approximately 3% higher than the front performance of the bifacial panel due to the greater light capture from reflection from the backsheet into the module in the monofacial module.

Table 6.10.1: STC performance of SHJ modules.

Parameter	Monofacial	FF (%)
P_{mpp} [W] front	482.8	470.3
P_{mpp} [W] rear	-	430.0

Figure 6.10.3 shows the annual energy yield of the monofacial and bifacial system in Canberra relative to the annual yield of the monofacial system with optimum 35° tilt. We optimised the tilt angle for both the monofacial and bifacial solar panels. We observed that the monofacial panels are less sensitive to tilt compared to the bifacial panels, with an optimum tilt of 35°. For the light roof, the bifacial panels achieve their maximum output at a slightly higher tilt of 40°, indicating the large contribution of rear irradiance to the output power. Overall, the bifacial yield gain exceeds 20% in this scenario.

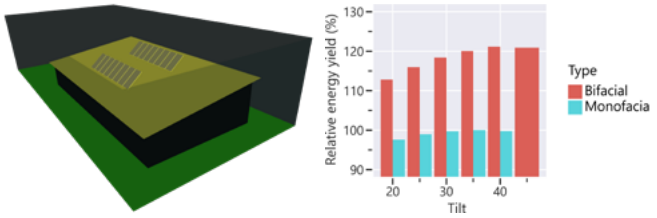

Figure 6.10.3: (left) Illustration of the rooftop scene with the installed PV system comprising two rows of either monofacial or bifacial modules. (right) Relative annual energy yield of the monofacial and bifacial rooftop system in Canberra.

Highlights

- This project demonstrated the feasibility of rooftop detection and classification of roof colour from aerial imagery.
- Accurate energy yield modelling based on MCRT analysis for monofacial and bifacial rooftop systems in Canberra showed that rooftop systems comprising bifacial modules could result in up to a 20% gain in annual electricity yield over monofacial modules for light-coloured roofs.
- The analysis also highlighted that bifacial rooftop PV systems are more sensitive to tilt angle than equivalent monofacial systems; however, estimating the optimum tilt angle for a bifacial system is more complex due to the need to accurately model the reflection from the roof and hence the rear irradiance on the bifacial modules.

Acknowledgements

This research was supported by use of the Nectar Research Cloud, a collaborative Australian research platform supported by the NCRIS-funded Australian Research Data Commons (ARDC), and the National Computational Infrastructure, which is supported by the Australian Government.

6.11 COMMUNITY BATTERY MODELLING PROJECT

Lead Partner
UNSW

UNSW Team
Phoebe Dennis, Rob Passey, Baran Yildiz, Siddharth Nair

Funding Support

ACAP

Aims & Objectives

The project had the following aims and objectives:

- Develop an energy model for the operations of a community battery within Narrabri, NSW region.
- Model the interactions of the battery with the community, spot market, FCAS market and behind-the-meter solar systems.
- Run sensitivity analysis on various battery characteristics.
- Estimate revenue for different stakeholders under different financial revenue models and tariffs.
- Build an open-source tool.

Progress

Enova Community Energy went under administration due to unprecedented spot market events in 2022 and therefore the project continued to work with the other industry partner Geni.Energy. We obtained and studied a data set provided by Solar Analytics which included 420 households with rooftop solar systems. The household load and solar power data consisted of five-minute-interval measurements over one calendar year in 2021. Historical spot and frequency control ancillary service (FCAS) market prices were obtained from AEMO's website to match the dates of the original data set.

Literature & market review

Community-scale battery systems have a power capacity of up to 5 MW and are generally connected to the distribution network. In recent years the uptake of distributed energy resources has increased significantly, posing new challenges such as power quality management, increasing PV exports, decreased minimum demand and increased ramp rates to meet peak demand. Community-scale battery systems can help to reduce these impacts while providing economic and environmental benefits to the local communities. The review undertaken in this report focuses on community-scale battery deployments within Australia.

Classification of Community-Scale Battery Systems

This section of the report classifies the various types of community-scale batteries in operation in Australia. This excludes virtual power plants (VPPs) and stand alone power systems (SAPS) as they are outside this project's scope. The community-scale batteries can be broadly classified based on their ownership and if the battery is located in front of or behind the meter.

A.DNSP-owned, in front of the meter

Distribution network service provider–owned in-front-of-the-meter community-scale battery energy storage systems (BESS) have had wide implementation in Western Australia. In the National Electricity Market (NEM), Ausgrid has started trials at three different locations in New South Wales (Cameron Park, Beacon Hill and Bankstown) (Ausgrid 2022a). DNSP-owned, in front-of-the-meter BESS offer participants financial value while also providing value to the DNSP in terms of avoiding costly network upgrades.

Western Power - PowerBank Trials

Western Power has 12 community batteries with capacities ranging from 105 kW/420 kWh to 116 kW/464 kWh (Western Power 2022). The financial value for the trial participants comes in the form of virtual storage. All customers in the PowerBank trial are "non-contestable" (i.e. have Synergy as their retailer) and must have a PV system at their premises. The way virtual storage works is that any excess solar exported to the grid by the participants is "virtually" stored in the BESS and can be used by them 1 to 1 at peak times according to their time-of-use tariff. The participants are encouraged to use stored electricity during peak periods to maximise the value of their stored energy. The PowerBank participants have two storage options: 6 kWh at $1.2/day or 8 kWh at $1.4/day which can be stored between 7 am and 3 pm (Synergy 2022). Any export above the storage limit earns the standard feed-in tariff and any quantity of unused storage at the end of a billing period has a buy-back rate of 7.135 cents/kWh.

Table 6.11.1: Synergy PowerBank Saver Plan Details.

PowerBank Saver Plan Price	Price (inc. GST)		When charged
Daily supply charge	$1.0514 per day		This charge is for supplying electricity to your premises for each day of the billing cycle irrespective of the amount of electricity you consume
Daily subscription fee	6 kWh storage option	$1.2/day	A daily subscription fee payable for the product
	8 kWh storage option	$1.4/day	
Everyday Off-Peak Period electricity charge	15.3645 cents per unit		9pm – 7am all days
Weekday Shoulder Period electricity charge	29.2100cents per unit		7am – 3pm weekdays
Weekend Shoulder Period electricity charge	29.2100cents per unit		7am – 9pm weekends
Peak Period electricity charge	55.7734 cents per unit		3pm – 9pm weekdays

Alkimos Beach Community Energy Storage Device

The Alkimos Beach Community Battery is located in a 6 Star Green Star residential community in Perth. There is 100% solar penetration in this community. The trial project commenced in April 2016 and was completed in May 2021. The BESS has a capacity of 250 kW/1100 kWh and a total project cost of $5.65 million ($5140/kWh). This is significantly higher than other cost estimates for community-scale batteries and could be for several reasons, including the reduction in cost of Li-Ion batteries since the commissioning of the project. This trial offered participants unlimited virtual storage with a subscription fee of $11/month. Unused solar credits at the end of every billing period were credited to participants at the now expired REBS (Renewable Energy Buyback Scheme – which at the time of the trial was 7.13 cents/kWh). The tariff structure for the participants was:

Table 6.11.2: Alkimos Beach Community BESS Trial Tariff.

Time Bands	Rates
Off-peak day (midnight – 4pm)	26.8145 c/kWh
Off-peak evening (8pm – midnight)	26.8145 c/kWh
Peak daily (4pm – -8pm)	51.1995 c/kWh

Ausgrid Community Battery Trials

Ausgrid has community battery trial projects at three locations (Ausgrid 2022b) with capacities ranging from 150 kW/267 kWh in Beacon Hill (RenewEconomy 2021a) to 130 kW/232 kWh+320 kW/550 kWh (two systems) in Bankstown (RenewEconomy 2021b). The NEM has full retail competition and so there is no vertical integration between the DNSP and the retailer (unlike the PowerBank trials in WA). To circumvent this challenge, Ausgrid installed a separate smart meter at every participant's premises next to the solar inverter. The participants may have any retailer or retail plan. The exported solar can be stored up to a daily limit of 10 kWh at 10 cents/kWh. The power drawn from the grid by the participant is metered from the smart meter installed by Ausgrid up until the virtually stored electricity is used up, after that point their usage is metered by their main electricity meter. Like the PowerBank trials these participants will be encouraged to use the stored electricity during peak times according to their time-of-use tariff to maximise value. Unused electricity is stored as credit which is credited to the participants at their respective feed-in tariff based on their retail plan. This requires an extra level of accounting which the PowerBanks in WA do not require. The capital costs for these trials are estimated to be between $1200/kWh and $1498/kWh (KPMG 2020; RenewEconomy 2021a).

B.DNSP-owned, behind the meter

Western Power has installed a behind-the-meter BESS with a capacity of 464 kWh at Margaret River Recreation Centre. The BESS is installed to manage the centre's solar generation before it is exported into the grid. The Margaret River Recreation Centre community battery is reported to offer virtual storage to local residents like the other Western Power PowerBanks (Matich 2020).

C.Third-party-owned, in front of the meter

Several third-party-owned, in-front-of-the-meter BESS are being developed as hybrid systems where they are co-located with mid-size PV systems. Goulburn Community Energy Cooperative is developing a 1.4 MW solar farm and 1200 kW/2300 kWh BESS (Goulburn Community Energy Cooperative n.d. a) with a total project cost reported at $4.8 million (Goulburn Community Energy Cooperative n.d. b). Energy Democracy Central West NSW Co-operative (EDCWNC) is developing a 5 MW solar farm and 5 MWh BESS (Central West NSW Co-operative 2022). Revenue for these projects will be from the sale of Power Purchase Agreements (PPAs) and Large-Scale Generation Certificates (LGCs) and possible spot arbitrage and FCAS. Yarra Energy Foundation has installed a 110 kW/284 kWh BESS in Fitzroy North which is discussed in further detail in this report (Yarra Energy Foundation 2022).

D.Third-party-owned, in front of the meter

Third-party-owned, behind the meter is the most commonly used configuration of community-scale BESS for large industrial or commercial loads and embedded networks. In addition to the value from trading in the electricity markets, the BESS can provide value by offsetting the peak demand charge and reducing demand during peak tariff periods. Narara Ecovillage Co-operative Ltd (NEV) is planning a 525 kW solar farm with a 464 kWh BESS for stage 1 of the development of their Ecovillage in Narara Valley (NEV). This will be a behind-the-meter system incorporated into their smart grid which is an embedded network owned and controlled by NEV (Narara Ecovillage 2022). The University of Queensland has installed a 1.11 MW/2.15 MWh within the university's St Lucia campus in Brisbane which is discussed in further detail in this report (Wilson et al. 2020).

E.Operational third-party-owned community-scale BESS

Yarra Energy Foundation (YEF) YESS FN1 Community Battery

The Yarra Energy Storage System (YESS) Fitzroy North 1 (FN1) was commissioned in June 2022 and is located in Melbourne (Yarra Energy Foundation 2022). It is owned by the not-for-profit organisation YEF and was installed in front of the meter by Ventia. The FN1 battery is located close to a power pole on land that is leased from CitiPower, the distribution network operator in the region. It is connected to a low voltage (LV) distribution network.

Table 6.11.3: Technical specifications of the YEF YESS FN1 BESS.

TECHNICAL SPECIFICATIONS	
Make & Model	Pixii PowerShaper
Capacity	110 kW/284 kWh
Footprint (Area)	5.5 m^2 approx

Project Costs : YEF has reported that the FN1 project cost including just the hardware and installation costs was below $1000/kWh. After network connection and artwork, the total installation cost was estimated to be $1100/kWh. The final cost of the project is reported as $ 1.5 million ($5280/kWh). The funding for the project was $950,000 ($3345/kWh) and the remainder is an estimation of the value of the work done and the other contributions made by the project partners. The overall capital cost per kWh reported by YEF for the FN1 project is much higher than the University of Queensland (UQ) BESS (detailed in the next section). Software development for the BESS control is estimated as half of the funded work, unlike UQ BESS, which does not explicitly include their in-house software development costs in the capital costs. The FN1 BESS was a pilot project, and YEF has reported the software and other soft costs can be used for the expansion of this project or the development of other projects.

Business Model

The FN1 battery participates in the FCAS and wholesale spot market through the aggregator Acacia Energy. The FN1 BESS also has a trial network tariff from CitiPower which incentivises charging during midday and discharging during peak demand.

Table 6.11.4: CitiPower tariff applied to the YEF FN1 BESS.

Time Band	Import Rate (c/kWh)	Export Rate (c/kWh)
10am – -3pm	-1.5	0
4pm – 9pm	25	-1
All other times	0	0
Fixed 45c/Day		

YEF has reported that this tariff is essential to the FN1 business model. FN1 BESS has a one cycle per day of charging (between 10 am and 3 pm) and discharging (between 4 pm and 9 pm) to maximise solar self-consumption and arbitrage. This also allows them to maximise value from their trial network tariff. FN1 has reported an operating cost of $17,000/year ($60/kWh/year). YEF has not provided a specific breakdown of these operating costs but has reported that this will not increase linearly with the addition of more systems. These operating costs are much higher than reported by the UQ BESS.

Unlike UQ, which has not included ongoing software development and IT infrastructure in its operating costs, FN1 may have included commissions to Acacia Energy and have additional costs around IT system management and the control system. No financial performance is reported for FN1 to date. For the project to pay itself back in 10 years (considering a discount rate of 5%) it will have to have a net revenue of over $40,000 per year.

University of Queensland's Tesla Battery

The University of Queensland's (UQ's) Tesla Battery was commissioned in November 2019 and is located within the university's St Lucia campus in Brisbane. It is a privately owned and behind-the-meter BESS. The autonomous control system for performing arbitrage in the NEM was developed in-house by UQ and is called the Demand Response Engine (DRE) (Wilson et al. 2020). Technical specifications of the BESS:

Table 6.11.5: Technical specifications of the UQ BESS.

TECHNICAL SPECIFICATIONS	
Make & Model	Tesla Powerpack 2.5
Capacity	1.11 MW/2.15 MWh
Footprint (Area)	44 m^2
Weight	25.7 tonnes

The reports published by UQ about the business case and performance of their batteries are the most comprehensive freely available source for community-scale battery projects in the NEM.

Project Costs

The total capital cost for the project was reported as $ 2.05 million ($954/kWh). The cost of developing their control system was not explicitly included in the breakdown of the capital costs detailed in the project report. The capital costs also exclude all in-house project management costs.

Table 6.11.6: Breakdown of capital costs for the UQ BESS.

Project Costs	Ex -GST	$/kWh
Battery supply cost	$ 1,700,000	$ 791
Battery BOS and Commissioning	$ 182,000	$ 84
Site Prep & Construction	$ 135,000	$ 63
Soft Costs	$ 35,000	$ 16
Total Cost	$ 2,052,000	$ 954

Business Model

The UQ BESS has three streams of revenue: spot arbitrage, FCAS and a virtual cap (Wilson et al. 2021). The reports published by UQ do not include any operating costs outside the costs incurred in participating in the NEM. UQ does not have an electricity retailer and is exposed to wholesale prices and their battery operation is autonomous, which may justify the lack of inclusion of other operating costs. They do not include costs for maintenance or cloud services (Amazon Web Services in this case) where their DRE is running.

UQ's DRE system trades automatically in the NEM. At the time their reports were published the NEM followed the 30-minute settlement. The UQ BESS creates a schedule for charging and discharging 40 hours into the future and revises this schedule every 5 minutes as AEMO's 5-minute and 30-minute forecasts are updated. Their decision model takes into account the battery degradation and the maximum price spread to optimise its charging and discharging cycles. In addition to the model-based control, the UQ BESS uses what they call "trickle" charging where the BESS commences charging at a certain rate when the prices are at a "seasonal" low and ramps up charging as the prices go lower. This is to take advantage of sudden price spikes. However, this rule-based control may prevent the BESS taking advantage from the lower or negative pricing if the BESS charges prematurely. For the future, UQ is looking into creating its own forecasts for the spot market to reduce its reliability on AEMO's forecasts.

The variable operating costs for the UQ BESS include direct losses due to round-trip efficiency (average round-trip efficiency was 85.2% over 2020) and additional ancillary charges which the UQ BESS is exposed to due to the round-trip efficiency. The ancillary charges include AEMO market fees, transmission-use-of-service (TUOS) charges, large-scale generation certificates (LGC) costs and small-scale technology (STC) costs.

The UQ BESS is partnered with Enel X for their FCAS trading. UQ always reserves 185 kWh of capacity (10 minutes of maximum power) to bid into the three types of raise FCAS markets depending on which has the highest price unless it's already discharging. In the future, the UQ BESS aims to have co-optimisation between arbitrage and the FCAS markets, which will allow it to have a variable capacity for FCAS and so maximise value between both these markets.
The virtual cap contract is a novel concept used by UQ BESS. It operates by discharging the battery to decrease demand when spot prices are high, thereby reducing purchase costs. UQ estimated the premium payable by them for a financial cap contract in 2020 to be $40,476. The payout from this contract would be $13,583 which brings the overall cost of having such a contract in 2020 to $26,893. UQ decided to opt out of purchasing this financial cap and instead discharge their battery during periods of high spot prices. The cost of the volume (MWh) which is not covered due to the capacity of the battery to discharge during these periods is subtracted from the avoided cost of the financial cap to estimate the net value of the "virtual cap" which was worth $21,905 in 2020.

UQ BESS 2020 Performance:

Table 6.11.7: Revenue generated by the UQ BESS in one year of operation.

Arbitrage revenue	$44,712
FCAS revenue	$ 91,000
Value from virtual cap (vs. financial cap)	$21,905
Total	$157,617
Simple Payback (Years) based on 2020 performance	13.01

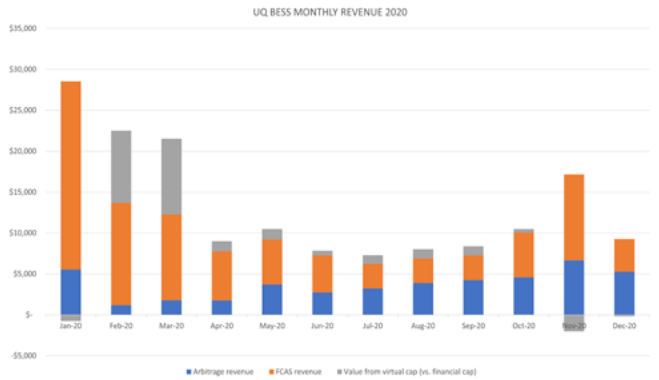

Figure 6.11.1: Monthly revenue generated by the UQ BESS over 2020.

Community battery model development

To assess the operation of a community-scale battery in Narrabri and allow for comparison of various operating models and battery configurations, an optimisation model was developed. It was formulated as a mixed integer linear programming problem and written in python using the Pyomo package (Hart et al. 2021). The model is iteratively fed half-hourly customer net load, large-scale solar generation, and historical spot and FCAS price data and, within the assigned parameters, solves for the maximum battery revenue one day at a time. The battery has a choice of bidding into the spot market, buying/selling from/to local households/businesses (through a retailer, and hereafter referred to as participants) and bidding into the six contingency FCAS markets. Additional revenue can be generated by discharging during pre-set peak demand events as a form of network support. It can also value-stack by participating in multiple revenue streams at the same time.

The results were simulated using historical solar, load and price traces for 2021. The participant solar and load traces were provided by Solar Analytics (2022), while the large-scale solar was sourced from AEMO's 2019 ISP database (AEMO 2022). The network and retail tariffs were based on tariffs proposed by the relevant DNSP, Essential Energy, and are detailed further in the next section. For the scenario analysis, the model had perfect foresight of demand, generation and pricing within each iteration and therefore, the results presented in this paper can be treated as the upper end of potential revenue.

When modelling FCAS participation, it was determined that contingency events are rare and require small amounts of electricity compared to the capacity of the battery. Therefore, it was assumed that, although the battery was enabled for FCAS (and so still receiving FCAS revenue for being available), no electricity was used by the battery to deliver FCAS services (Bayborodina et al. 2021). A cycling penalty in $/kWh throughput was used to minimise the degradation of the battery. This approach is over-simplified and does not take into account the varying degradation rates at different depth of discharge but is sufficient for reducing the reactivity to small price fluctuations and hence reducing the number of cycles completed by the battery within each day.

The default parameters used for this case study are shown in Table 6.11.8.

Table 6.11.8: Summary of the default parameters used when modelling a community-scale BESS.

Parameter	Value
Battery Capacity (MW)	5
Storage duration (hrs)	2
Minimum SoC	10%
Round trip efficiency	90%
Cycling penalty ($/MWh)	40
Forecast type	Perfect foresight

Figure 6.11.2 below shows a schematic for the developed community battery energy model.

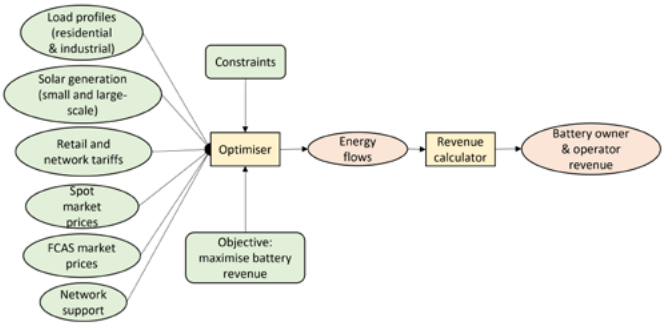

Figure 6.11.2: Flow diagram detailing the inputs and outputs of the optimisation model.

Tariffs

Retail tariffs

The retail tariffs used in the model were based on Essential Energy's 2022/23 pricing proposal, with a few changes to make it more suitable for a BESS. Most notably, the middle of the day from 9am to 5pm is switched to off-peak to encourage use of local solar exports. A peak feed-in-tariff (FiT) was also added to incentivise the battery to discharge during this time and reduce peak demand.

Table 6.11.9: Tariff applied for BESS consumption from and exports to the participants.

	Costs	Rebates
Daily charge (c/day)	105.7	
Peak (c/kWh)[1]	45.73	16
Shoulder (c/kWh)	16.63	6
Off-peak (c/kWh)	11.49	6

Table 6.11.10: Tariff applied when BESS is located behind the meter with an industrial load.

	Costs	Rebates
Daily charge (c/day)	216.61	
Peak (c/kWh)	33.25	6.12
Shoulder (c/kWh)	27.21	6.12
Off-peak (c/kWh)	17.25	6.12

Network tariff

Essential Energy have proposed a trial bi-directional distribution support tariff to be used by batteries installed in their network. The tariff is quite complex, including a separate demand charge and consumption cost for each time-of-use period as well as a variable FiT and an export charge for any exports during the middle of the day. The structure is shown in Figure 6.11.3.

[1]The peak period is 5–8pm weekdays, the shoulder is 7–9am and 8–10pm weekdays, with the off-peak period being all other times.

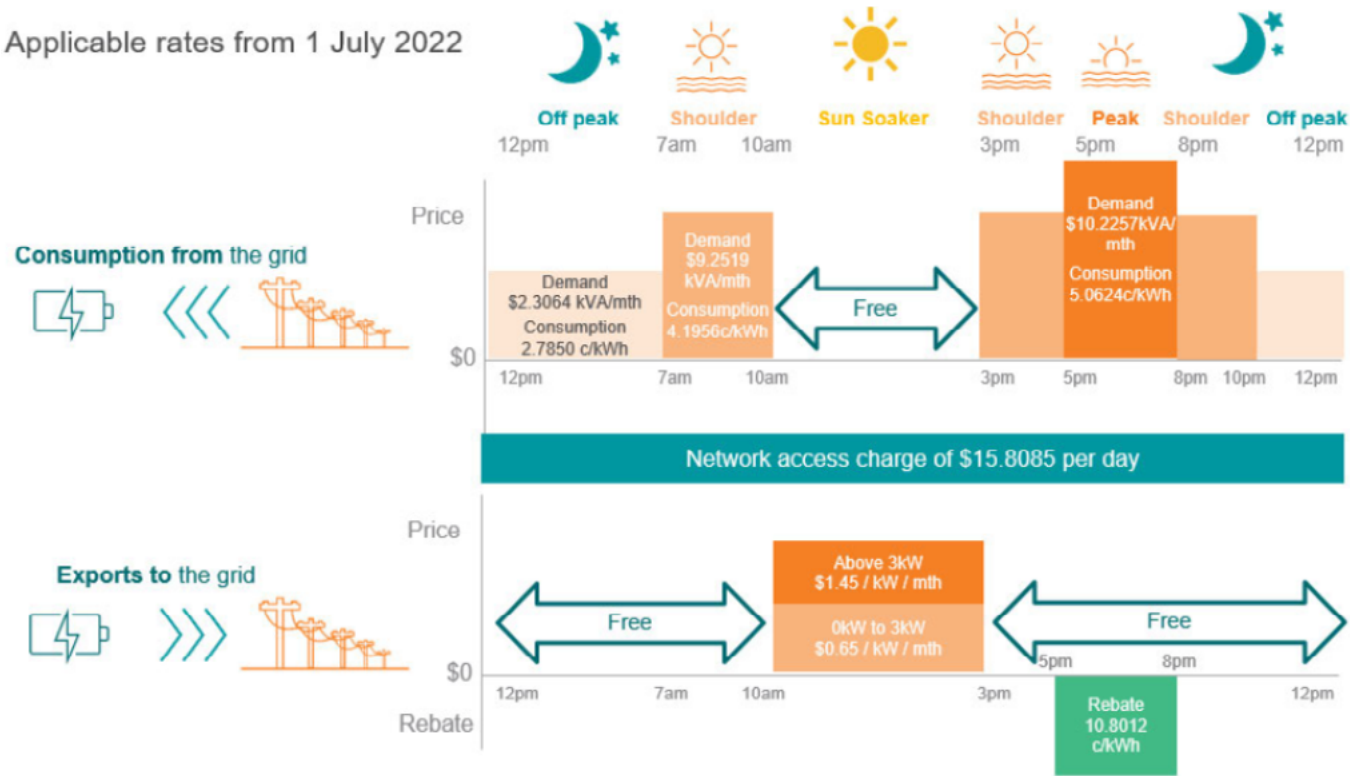

Figure 6.11.3: Structure of Essential Energy's proposed bi-directional distribution support tariff.

Modelling scenarios

As part of our collaboration with Geni.Energy, the optimisation model was used to assess the financial outcomes for four key battery configurations. These case studies evolved over time as different business cases and tariff structures were identified. The scenarios presented in this report are as follows: a small-scale battery that does not interact directly with community members and participates in the spot and FCAS markets through an aggregator, a large-scale battery that does facilitate local energy trading as well as market participation, a large-scale battery co-located with a behind-the-meter solar farm, and a smaller battery installed behind the meter with an industrial load and rooftop solar system.

Small-scale community-scale battery
Key features:

- 250 kW/ 500 kWh (2 hours storage).
- No participants.
- Participates in spot and FCAS markets.

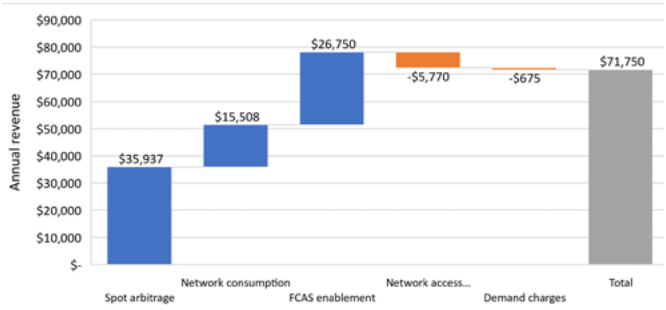

Figure 6.11.4: Modelled revenue stacking for a small-scale community-scale battery for 2021.

The small-scale battery was able to make $71,750/year. Fifty per cent of the annual revenue came from spot arbitrage, 13% from the network tariff and 37% from FCAS enablement.

The battery charges during the day, making the most of the $0/kWh network tariff and cheaper spot prices. It typically discharges most of its capacity during the evening peak and receives the 10.8 cents/kWh rebate on top of the spot price. The battery reserves at least 4 kWh at the top and bottom of its cycle to participate in FCAS. For a 250 kW battery, 4 kWh represents one minute of storage at full capacity which can be used to bid into the 6-second raise and lower FCAS markets.

At $1000/kWh, the battery has a capital cost of $500,000 and a simple payback time of seven years. However, as seen in the literature review there tend to be other upfront costs which are particularly significant

at small sizes. This also does not account for operating costs, which at $60/kWh/year would increase the simple payback time (SPT) beyond the expected 10-year life of these batteries.

Large-scale community-scale battery
Key features:

- 3 MW/ 6 MWh battery (2 hours storage).
- Participates in local energy trading, spot and FCAS markets.
- 420 residential participants.

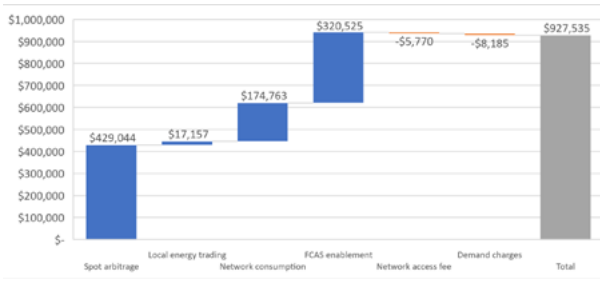

Figure 6.11.5: Modelled revenue stacking for a large-scale community-scale battery for 2021.

The large-scale battery made $927,535/year, close to a 12 times increase compared to the small-scale battery. A small amount of additional revenue was generated through facilitating virtual trading with the participants.

The battery tends to purchase energy from the spot market rather than the participants, unless the spot price is higher than the retailer local energy trading (LET) purchase price of 11c/kWh ($110/MWh). Similarly, in the evening peak the battery will sell to the participants when the spot price is lower than the LET sale price of 6c/kWh.

At $1000/kWh, the battery has a capital cost of $6M and a simple payback time of 6.5 years.

Community-scale battery with behind-the-meter solar

Key features:

- 3 MW/ 6 MWh battery (2 hours storage).
- Co-located with a 0–2 MW behind-the-meter PV system.
- Participates in local energy trading, spot and FCAS markets, and can sell excess PV generation to the spot market or the participants.
- Was modelled with the Essential Energy network tariff for simplicity, though this tariff is not applicable when the battery is co-located with other generation or loads.
- 420 residential participants.

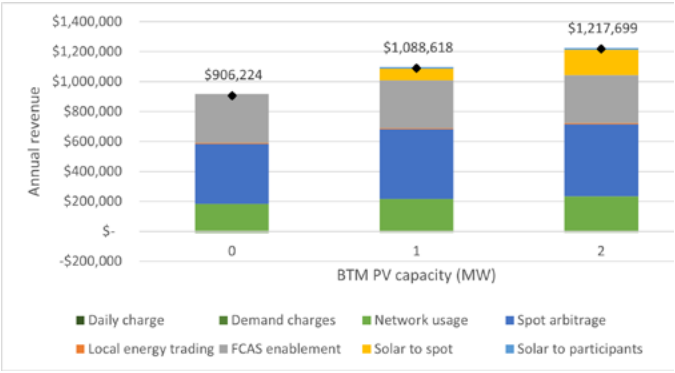

Figure 6.11.6: Comparison of annual revenue for a battery with and without a behind-the-meter PV system.

The base-case BESS makes $906,224/year. A 1 MW behind-the-meter PV system increases the annual revenue by $182,393/year while a 2 MW PV system increases it by $311,475/year. With a PPA of $50/MWh, the PV system alone would make $142,369/MW/year so the BESS is able to increase the value of the PV generation by shifting it to periods of high prices.

When looking at revenues alone, the PV system increases the SPT of the combined BESS-PV system, however the operating costs of the BESS are much higher than that of a large-scale PV array and the PV also has a longer expected lifetime.

Community-scale battery co-located with behind-the-meter solar and industrial load

Key features:

- 200 kW / 600 kWh battery (3 hours storage).
- Co-located with 175 kW be¬¬hind-the-meter PV system and 75 kWh/day industrial load.
- Participates in local energy trading, spot market, FCAS markets, and has a PPA with the industrial load. Can also sell excess PV generation to the spot market.
- Subject to a commercial retail tariff for all energy passing through the meter.
- 420 residential participants.

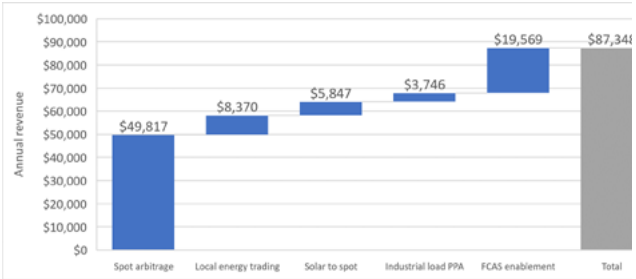

Figure 6.11.7: Modelled revenue stacking for a behind-the-meter community-scale battery co-located with solar and load

Sensitivity Analysis

The following sensitivity analysis was undertaken:

- Looking at the impact of combining various sizes of behind-the-meter solar with the community-scale battery.
- Assessing the impact of forcing a community-scale battery to use local solar or just encouraging this use of a spot price threshold.
- Quantifying the degree of overlap between operating a community-scale battery to provide benefits to the local community versus simply maximising revenue by participating in the spot and FCAS markets.

The results of this analysis are not included in this report as they will be published in an upcoming journal paper. These results will be submitted in the final ACAP report later this year.

Highlights

Here we describe our key take-aways from the project as below:

- The ability to participate in the spot and FCAS markets significantly increases revenue for the battery owner.
- The largest revenue stream for the community-scale batteries modelled for 2021 was spot arbitrage followed by FCAS participation.
- Larger community-scale batteries tend to have shorter paybacks, primarily due to lower capital costs per MWh.
- In contrast to the common beliefs, community-scale batteries aiming to maximise revenue have limited charging from community solar and resulted in mostly buying/selling from/to the

Future Work

The next steps for this project include:

- Revenue calculation for individual households.
- Modelling uncertainty by incorporating forecast price data.
- Incorporating solar forecasts/load forecasts.
- Repeating the analysis for other years with different spot and FCAS prices as these can have a large impact on the modelled revenue.
- Expanding the analysis to other regions including looking at community-scale battery tariffs proposed by other DNSPs

References

AEMO (2022). https://aemo.com.au/en/energy-systems/major-publications/integrated-system-plan-isp/2020-integrated-system-plan-isp/2019-isp-database.

Ausgrid. (2022a). Community Battery FAQs. https://www.ausgrid.com.au/In-your-community/Community-Batteries/Community-battery-FAQ (accessed 16 December 2022).

Ausgrid. (2022b). Trial location maps – Ausgrid. https://www.ausgrid.com.au/In-your-community/Community-Batteries/Trial-locations (accessed 16 December 2022).

Bayborodina, E., Negnevitsky, M., Franklin, E. & Washusen, A. (2021). Grid-scale battery energy storage operation in Australian electricity spot and contingency reserve markets. Energies (Basel), 14 23. doi: 10.3390/en14238069.

Central West NSW Co-operative. (2022). Energy Democracy. https://energydemocracy.net/central/ (accessed 16 December 2022).

Goulburn Community Energy Cooperative. (n.d. a). Technicals – Goulburn Community Energy Cooperative. https://goulburnsolarfarm.com.au/technicals/ (accessed 16 December 2022).

Goulburn Community Energy Cooperative. (n.d. b). Financials – Goulburn Community Energy Cooperative. https://goulburnsolarfarm.com.au/financials/ (accessed 16 December 2022).

Hart, W. E., Laird, C., Watson, J.-P. & Woodruff, D. L. (2012). Pyomo – Optimization Modeling in Python. Advances in Modeling Agricultural Systems, 67.

KPMG. (2020). Ausgrid Community Battery Feasibility Study Report A report for Ausgrid Operator Partnership. February 2020. https://www.ausgrid.com.au/-/media/Documents/Reports-and-Research/Battery/Ausgrid-Community-Battery-Feasibility-Study-Report-2020.pdf (accessed 16 December 2022).

Matich, B. (2020). WA community battery rollout continues: Tesla battery launched in Margaret River – pv magazine Australia. https://www.pv-magazine-australia.com/2020/07/14/wa-community-battery-rollout-continues-tesla-battery-launched-in-margaret-river/ (accessed 16 December 2022).

Narara Ecovillage. (2022). NEV Power. https://nararaecovillage.com/nev-power/ (accessed 16 December 2022).

Prakash, A. (2022). NEMSEER, Dec. 2022, doi: 10.5281/ZENODO.7397527.

RenewEconomy. (2021a). Ausgrid installs "first of many" community batteries on Sydney network https://reneweconomy.com.au/ausgrid-installs-first-of-many-community-battery-installations-in-Sydney-network/ (accessed 16 December 2022).

RenewEconomy. (2021b). Ausgrid unveils new community battery project in Sydney's Bankstown. https://reneweconomy.com.au/ausgrid-unveils-new-community-battery-project-in-sydneys-bankstown/ (accessed 16 December 2022).

Solar Analytics (2022). https://www.solaranalytics.com.au/.

Synergy. (2022). PowerBank Saver Plan Terms & Conditions. https://www.synergy.net.au/UtilityLinks/Terms-and-conditions/PowerBank-Saver-Plan-8kwh (accessed 16 December 2022).

Western Power. (2022). Where are the community batteries located? https://www.westernpower.com.au/faqs/community-batteries/community-batteries/where-are-the-community-batteries-located/ (accessed 16 December 2022).

Wilson, A., Esterhuysen, D. & Hains, D. (2020). The business case for behind-the-meter energy storage. https://sustainability.uq.edu.au/files/11868/EPBQtyRptq12020.pdf (accessed 16 December 2022).

Wilson, A., Esterhuysen, D. & Hains, D. (2021). 2020 Performance Review UQ's 1.1 MW Battery Project. https://sustainability.uq.edu.au/files/16942/2020%20Performance%20Review%20FINAL%20REPORT.pdf.

Yarra Energy Foundation. (2022). Neighbourhood Battery Initiative Final Report: Yarra Community Battery Project.

6.12 ADVANCING THE PDS TECHNIQUE FOR ALL PHOTOVOLTAIC THIN-FILMS

Lead Partner
UNSW

UNSW Team
Dr Henner Kampwerth

Industry Partners
Open Instruments

Funding Support
Open Instruments, ACAP (UNSW Node)

Summary

High-contrast photo-absorption spectra are required for reliably characterising Urbach tails and sub-bandgap impurities in various thin films involved in photovoltaic devices. A tool recently commercialised by Open Instruments can meet this requirement by the addition of a light source with enhanced filtering. This ACAP collaboration will enable this enhancement and permit researchers to identify efficiency-limiting defects.

Aim

Identifying and eliminating material defects in the form of Urbach tails and low-level impurities is critical to maximising the performance of thin films for photovoltaics. Existing measurement techniques are either unable to detect non-radiative defects or come with specific sample requirements. Thin films present a particular sensitivity challenge to most measurement techniques, as the thin nature of the sample results in a very short interaction length with the probing light and therefore a weak absorption signal. Additionally, the supporting substrates also absorb light, with their signal often overwhelming that from the thin film of interest.

Photothermal deflection spectroscopy (PDS) is an ideal technique to study such samples, as it provides both unparalleled sensitivity on thin films along with reduced sensitivity to optical absorption by the substrate. It is an important characterisation tool for thin-film photovoltaics research that can make significant contributions to research in every laboratory.

The first fully integrated PDS instrument – the AURA from Open Instruments – will debut in 2022. The current functional prototype has already proven to be invaluable for many thin-film PV researchers, but unfortunately not all. As with all prototypes, areas of improvement have been identified that can enable even greater benefits for PV. Critical among these is an increase in the dynamic range of the tool, enabling researchers to accurately observe defects below to the band edge.

Figure 6.12.1 shows the photo-absorption spectrum of a single crystal 2D perovskite flake, kindly provided by our collaborators Dr A. Mahboubi Soufiani (UNSW) and Y. Zhang (UQ). The grey curve shows the absorption spectrum obtained from a conventional UV-Vis spectrophotometer. In green, we show the absorption spectrum from the AURA PDS. The significantly improved sensitivity of the AURA reveals a strong defect band between 525 nm and 650 nm, which cannot be detected by the UV-VIS measurement technique. However, the signal in the regions between 475 nm and 535 nm, and beyond 650 nm, is expected to be even less absorbing (<0.005%) than shown here. Preliminary experiments performed by Open Instruments demonstrated that the PDS measurement technique is able to measure well below this level, but that insufficient spectral filtering (stray light) of the broadband pump light source limits the sensitivity.

The aim of this project is to enhance an existing commercially available product, the AURA photothermal deflection spectrometer (PDS), to enable researchers to identify non-radiative defects close to the band edge, as well as the optical bandgaps of weakly absorbing films.

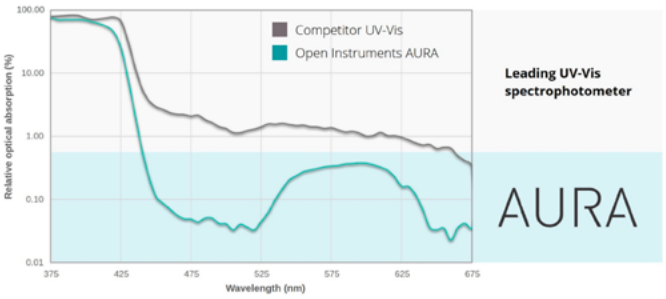

Figure 6.12.1: A direct comparison of the relative optical absorption on both a leading UV-Vis spectrophotometer and the current prototype of the AURA PDS. The critical difference is that the large defect band between 525 nm and 650 nm remains undetectable by the conventional measurement tools.

Progress

In collaboration with the ACAP grant "Advancing the PDS Technique for All Photovoltaic Thin-Films", it was found that the use of a single-monochromator limits the otherwise possible dynamic range of the technique. Since then, the AURA system, see Figure 6.12.2 (top) has been re-designed around a double-monochromator. The proof of concept version is shown in Figure 6.12.2 (bottom).

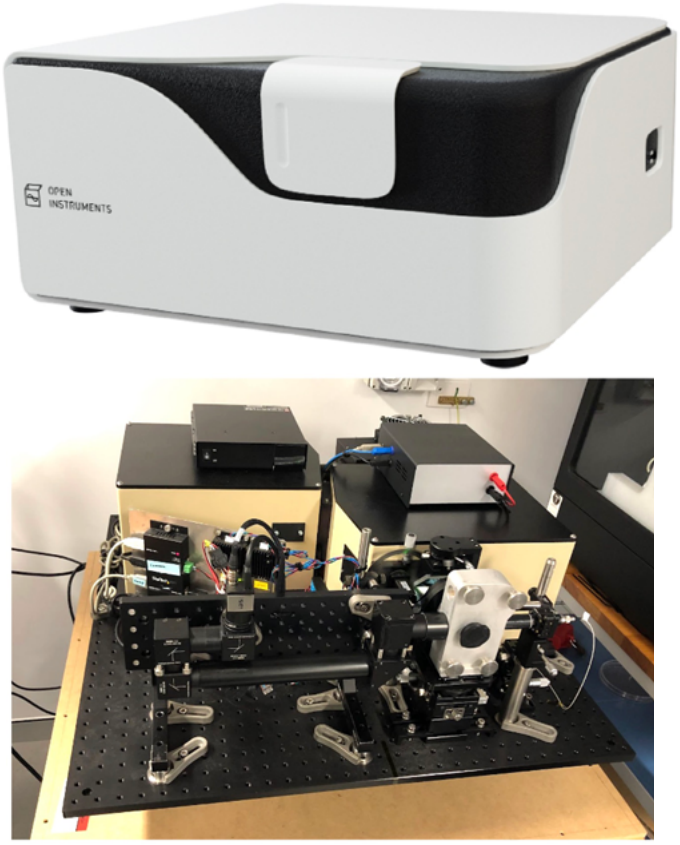

Figure 6.12.2: Top: The commercial AURA system before rework. Bottom: Proof of concept setup of the PDS AURA system with a double monochromator.

Highlights

The highlights so can be summarized to

- Experiments have concluded that the previously used single-monochromator has insufficient filter characteristics, and a double-monochromator is required.
- The full optical train has been redesigned to optimise sensitivity and dynamic range.
- All needed parts have been ordered.

Deliverables and outcomes

Demonstrated a contrast ratio of at least four orders of magnitude between the strongly and weakly absorbing regions of the same photo-absorption spectra.

Milestones

10 August 2022 - Grant awarded and fund released
December 2022 - Request for extension to 31 March 2023 approved
16 December 2022 - Annual Report

COLLABORATION GRANTS

ACAP's competitively selected Collaboration Grants, whose titles are shown below, are reported online at acap.org.au/post/acap-s-annual-reports-2013-present.

6.40 ADVANCING THE PDS (PHOTOTHERMAL DEFLECTION SPECTROSCOPY) TECHNIQUE FOR ALL PHOTOVOLTAIC THIN FILMS

Lead Partner

UNSW

UNSW Team

Prof. Xiaojing Hao, Dr Henner Kampwerth, Prof. Gavin Conibeer, Dr Michael Pollard

Academic Partners

Tokyo University: Prof. Masakazu Sugiyama, Prof. Yoshitaka Okada

Macquarie University: Dr Binesh Puthen Veettil

Industry Partner

Open Instruments:

Funding Support

Open Instruments, ACAP (UNSW Node)

6.52 MICROSTRUCTURAL CHARACTERISATION OF THERMALLY EVAPORATED PEROVSKITE SOLAR CELLS FOR THE APPLICATION OF MONOLITHIC PEROVSKITE-SILICON TANDEM SOLAR CELLS

Lead Partner

Monash University

Monash Team

Prof. Udo Bach

Academic Partner

Wuhan University of Technology (WHUT), China: Dr Wei Li, Prof. Yi-Bing Cheng

Funding Support

ARENA, Monash, WHUT

6.64 DEVELOPMENT OF UPSCALING TECHNOLOGY FOR MONOLITHIC SI/ PEROVSKITE TANDEM PHOTOVOLTAICS

Lead Partner

ANU

ANU Team

Dr Heping Shen (lead), Dr Yiliang Wu, Dr Leiping Duan, Prof. Kylie Catchpole

Academic Partner

IMEC, Belgium: Dr Tom Aernouts, Dr Yinghuan Kuang, Dr Bart Vermang

Funding Support

ARENA, ACAP, ANU, IMEC

6.69 SCALABLE LAMINATION TECHNIQUES FOR LOW-COST PEROVSKITE SOLAR CELLS

Lead Partner

Monash University

Monash Team

Prof. Udo Bach, Dr Alexandr N. Simonov, Dr Gaveshana Sepalage

Industry Partners

CSIRO, Clayton: Dr Anthony Chesman. Dr Hasitha Weerasinghe

RLA POLYMERS-NAN PAO, Mr Frank Lord, Mr Sin Chang, Terry Tsai

Funding Support

ACAP

6.70 SURFACE, CONTACT AND AUGER RECOMBINATION AT ELEVATED TEMPERATURES

Lead Partner

UNSW

UNSW Team

A/Prof. Ziv Hameiri, Dr Nino Borojevic, Anh Le

Academic Partner

University of Oxford (UK): A/Prof. Ruy Sebastian Bonilla

Funding Support

ACAP Collaboration Grant, UNSW, University of Oxford

6.71 SUPER-EFFICIENT COLOURED PV FOR VEHICLES

Lead Partner

UNSW

UNSW Team

Dr Jessica Yajie Jiang, Dr Nathan Chang, Dr Mark Keevers, A/Prof. N.J. Ekins-Daukes, Scientia Prof. Martin Green

Industry Partners

AZUR SPACE Solar Power, ACE Electric Vehicle Group

Funding Support

ACAP

6.72 DEVELOPMENT OF III-V CELLS ON GAAS AND INP FOR A 50% EFFICIENT SPECTRUM SPLITTING CPV RECEIVER

Lead Partner

UNSW

UNSW Team

Dr Mark Keevers, Dr Yajie Jiang, Dr Anastasia Soeriyadi, A/Prof. Ned Ekins-Daukes, Prof. Martin Green

Industry Partners

RayGen Resources Pty Ltd (Australia): Dr John Lasich

IQE plc (UK): Dr Andrew Johnson

SolAero Technologies Corp. (USA): Dr Daniel Derkacs

ANU, Department of Electronic Materials Engineering (Australia): Prof. Hoe Tan

Funding Support

ACAP, UNSW

6.73 SURVEY OF SOLAR MODULE QUALITY ON AUSTRALIAN SOLAR FARMS USING OUTDOOR PHOTOLUMINESCENCE IMAGING AND FOURIER TRANSFORM INFRARED SPECTROSCOPY

Lead Partner

UNSW

UNSW Team

Dr Oliver Kunz

Academic Partner

Australian National University: Dr Marco Ernst

Industry Partners

ScanPro:, Luke Magon

5B Solar:, Dr Rhett Evans

Impact Investment Group:, Stephen Callis

SolarShare:, Nicolas Fejer

Funding Support

ACAP

6.74 GALLIUM-DOPED CZOCHRALSKI SILICON FOR MASS PRODUCTION OF HIGH EFFICIENCY AND STABLE P-TYPE SILICON SOLAR CELLS

Lead Partner

ANU

ANU Team

Dr Sieu Pheng Phang, Dr Hang Cheong Sio, Dr Rabin Basnet, Dr Anyao Liu, Prof. Daniel Macdonald

Industry Partner

Jinko Solar: Dr Xinyu Zhang, Dr Menglei Xu

Funding Support

ACAP, Jinko Solar

6.76 PRINTABLE GRAPHENE INKS FOR LOW-COST AND HIGH PERFORMANCE ORGANIC PV

Lead Partner

CSIRO

CSIRO Team

Dr Doojin Vak

Academic Partner

Nanyang Technological University (NTU, Singapore):
Dr Leonard WT Ng, Prof. Lam Yeng Ming

Industry Partner

Qualinks Co. Pte Ltd (Singapore)

Funding Support

ACAP and CSIRO

FELLOWSHIPS

ACAP's competitively selected Fellowships, whose titles are shown below, are reported online at acap.org.au/post/acap-s-annual-reports-2013-present

F7 PRACTICAL 50% EFFICIENT SPECTRUM SPLITTING CPV RECEIVERS USING INTERMEDIATE BRAGG REFLECTORS

Lead Partner

UNSW

UNSW Team

Dr Yajie Jiang, Dr Mark Keevers, Scientia Prof. Martin Green, Dr Anastasia Soeriyadi, A/Prof. N.J. Ekins-Daukes

Industry Partners

AZUR SPACE Solar Power

RayGen Resources Pty Ltd

Funding Support

ACAP

F11 NEW IMPURITY REMOVAL TECHNOLOGIES FOR LOW-COST, HIGH EFFICIENCY SILICON SOLAR CELLS

Lead Partner

ANU

ANU Team Fellow

Dr AnYao Liu, Prof. Daniel Macdonald

Academic Partners

Fraunhofer Institute for Solar Energy Systems (Fraunhofer-ISE), Germany: Dr Frank Feldmann

Leibniz University Hannover, Germany: Dr Jan Krügener

University of New South Wales: Dr Ran Chen

University of Western Australia: Matvei Aleshin SIMS laboratory, Centre for Microscopy, Characterisation and Analysis

Funding Support

ACAP

F15 DEVICE ARCHITECTURE DESIGN FOR COMMERCIAL KESTERITE SINGLE-JUNCTION AND MULTI-JUNCTION SOLAR CELLS

Lead Partner

UNSW

UNSW Team

Dr Kaiwen Sun, Prof. Xiaojing Hao, Prof. Martin Green, Dr Jialiang Huang, Dr Chang Yan, Dr Jianjun Li, Dr Xin Cui, Dr Heng Sun, Ao Wang, Guojun He

Academic Partners

Nanyang Technological University (NTU): A/Prof. Lydia Helena Wong

Duke University: Prof David B. Mitzi, Dr Betul Teymur

Funding Support

ACAP

F21 THE ROLE OF SOLAR PHOTOVOLTAICS IN A 100% RENEWABLE ENERGY FUTURE

Lead Partner

ANU

Supervisor

Dr Bin Lu, Prof. Andrew Blakers, Prof. Kylie Catchpole, A/Prof. Matthew Stocks, Anna Nadolny, Cheng Cheng, David Silalahi

Funding Support

ACAP Fellowship

F24 NOVEL APPROACH FOR THE INTEGRATION OF CARRIER-SELECTIVE PASSIVATING CONTACTS ON THE FRONT OF INDUSTRIAL SILICON SOLAR CELLS

ACAP Fellow

Josua Stuckelberger

Supervisor

Prof. Daniel Macdonald

Funding Support

ACAP

F26 TOWARDS SINGLE-CRYSTALLINE PEROVSKITE SOLAR CELLS

Lead Partner

Monash

Monash Team

Dr Wenxin Mao, Prof. Udo Bach

Monash Student

Mr Jie Zhao

Academic Partners

CSIRO, Wuhan University of Technology

Funding Support

ARENA, ACAP Fellowship

F27 A LOW-COST STRATEGY FOR P-DOPED AND STABLE HOLE-TRANSPORT-MATERIAL LAYER FOR HIGH PERFORMANCE STABLE SINGLE-JUNCTION PEROVSKITE AND/OR SI-PEROVSKITE TANDEM SOLAR CELLS

Lead Partner

UNSW

UNSW Team

A/Prof. Xiaojing Hao

Funding Support

ACAP Fellowship

F29 HYDROGEN PASSIVATION OF $SI_{1-X}GE_X$ FOR $SI_{1-X}GE_X$/SI TANDEM SOLAR CELLS

Lead Partner

UNSW

UNSW Team

Dr Li Wang, Zhenyu Sun, Hao Luo, A/Prof. Brett Hallam

Funding Support

ACAP Fellowship

F31 INTERFACE ENGINEERING BY ATOMIC LAYER DEPOSITION FOR HIGH PERFORMANCE EARTH-ABUNDANT SOLAR CELLS

Lead Partner

UNSW

UNSW Team

Dr Xin Cui, Prof. Xiaojing Hao, Prof. Bram Hoex, Dr Kaiwen Sun, Dr Chang Yan, Dr Jialiang Huang, Ao Wang, Xiaojie Yuan, Guojun He

Funding Support

ACAP Fellowship

F33 RECYCLING END-OF-LIFE SILICON PHOTOVOLTAIC MODULES USING LOW-COST AND LOW-EMISSION PROCESSES

Lead Partner

UNSW

UNSW Team

Dr Pablo Ribeiro Dias, Dr Rong Deng, Dr Marina Monteiro Lunardi, Dr Nathan L. Chang, Dr Moonyong Kim, Prof. Renate Egan, Dr Richard Corkish, A/Prof. Brett Hallam

Funding Support

Fellowship

Academic Partners

Federal University of Rio Grande do Sul (UFRGS), Brazil

F34 PRINTED SELECTIVE CONTACTS FOR HIGH EFFICIENCY SILICON SOLAR CELLS

Lead Partner

University of Melbourne

UoM Team

Dr James Bullock, Jesús Ibarra, Dr Di Yan

Funding Support

ACAP Fellowship

Academic Partners

RMIT University (Della Gaspera group), ANU (Macdonald and Chern Fong groups), École Polytechnique Fédérale de Lausanne (EPFL, Ballif group)

F35 THE DEVELOPMENT OF HIGH EFFICIENCY QUANTUM DOT-ORGANIC TANDEM SOLAR CELLS FOR NEW GENERATION WEARABLE AND LIGHTWEIGHT PHOTOVOLTAICS

Lead Partner

UQ

UQ Team

Dr Peng Chen, Prof. Lianzhou Wang, Prof. Paul Burn

Funding Support

ACAP Fellowship

F36 POLY-SILICON PASSIVATING CONTACTS: STRUCTURES, OPTOELECTRONIC PROPERTIES, AND DEFECT ENGINEERING

Lead Partner

ANU

ANU Team

Dr Peng Chen, Prof. Lianzhou Wang, Prof. Paul Burn

Academic Partners

National Renewable Energy Laboratory (NREL), Fraunhofer-ISE

Funding Support

ACAP

F38 TOWARDS 30% EFFICIENCY FOR FOUR-TERMINAL PEROVSKITESILICON TANDEM SOLAR CELLS

Lead Partner

ANU

ANU Team

Dr The Duong

Academic Partners

Karlsruhe Institute of Technology: Prof. Bryce Richards, Dr Ulrich Paetzold

UNSW: A/Prof Anita Wing Yi Ho-Baillie

Funding Support

ACAP

F39 PATHWAYS TO ACHIEVE A SOLAR CELL EFFICIENCY ABOVE 26%

Lead Partner

ANU

UNSW Team

Dr Teng Choon Kho, Prof. Andrew Blakers

Funding Support

ACAP Fellowship

F40 HIGH PERFORMING LEAD-FREE EARTH-ABUNDANT SOLAR CELLS

Lead Partner

Monash University

UNSW Team

Dr Narendra Pai, Dr Alexandr Simonov, Prof. Udo Bach

Academic Partners

CSIRO Manufacturing,

Melbourne Centre for Nanofabrication

Institut Català de Nanociència i Nanotecnologia, Universitat Autònoma de Barcelona

Jiangsu Key Laboratory for Carbon-Based Functional Materials & Devices Institute of Functional Nano & Soft Materials (FUNSOM), Soochow University, China

Simon Fraser University, Surrey, Canada

Wuhan University of Technology, P.R. China

Funding Support

ACAP

F41 APPLICATION OF STABLE LEAD-FREE ABSORBER LAYERS IN PHOTOVOLTAICS

Lead Partner

Monash University

Monash University Team

Dr Nadja Glueck (Giesbrecht), Prof. Udo Bach

Funding Support

ACAP Fellowship

F42 DEVELOPMENT OF EFFICIENT INTERFACIAL MATERIALS FOR STABLE, HIGH PERFORMANCE LARGE-SCALE PEROVSKITE SOLAR CELLS

Lead Partner

Monash University

Fellowship Holder

Dr Sudhaker Reddy Saripally

Supervisor

Prof. Udo Bach

Funding Support

ACAP Fellowship

F44 DEVELOPMENT OF ACCELERATED LID TESTING METHODS WITH IN SITU PL CHARACTERISATION AND NUMERICAL MODEL TO IMPROVE THE UNDERSTANDING OF DEGRADATION MECHANISMS IN SILICON SOLAR CELLS

Lead Partner

UNSW

UNSW Team

Moonyong Kim

Funding Support

ACAP Fellowship

F45 PHOTOLUMINESCENCE IMAGING WITH SPATIALLY NON-UNIFORM ILLUMINATION FOR THE CHARACTERISATION OF SILICON WAFERS AND SOLAR CELLS

Lead Partner

UNSW

UNSW Team

Yan Zhu, Shuai Nie, Oliver Kunz, Arman Soufiani, Thorsten Trupke, Ziv Hameiri

Funding Support

ACAP Fellowship

F46 CHARACTERISING THE PERFORMANCE, CONTRIBUTION, AND IMPACT OF DISTRIBUTED PV SYSTEMS IN AUSTRALIA'S ELECTRICITY GRIDS

Lead Partner

UNSW

UNSW Team

Dr Navid Haghdadi, Assoc. Prof. Anna Bruce, Prof. Iain MacGill

Funding Support

ACAP Fellowship

F47 LOW TEMPERATURE GRAPHENE OXIDE FILM PROPERTIES AND APPLICATIONS FOR ADVANCED AND HIGH PERFORMANCE PHOTOVOLTAICS

Lead Partner

UNSW

UNSW Team

Dr Michelle Vaqueiro Contreras

Funding Support

ACAP Fellowship

F49 IN SITU BACK SURFACE FIELD-ENHANCED HIGH EFFICIENCY $CU_2ZNSN(S,SE)_4$ SOLAR CELLS WITH SURFACE DEFECT PASSIVATION

Lead Partner

UNSW

UNSW Team

Dr Jianjun Li, A/Prof. Xiaojing Hao, Prof. Martin A. Green, Dr Jialiang Huang, Dr Kaiwen Sun, Dr Chang Yan, Mingrui He, Xiaojie Yuan, Heng Sun, Jialin Cong, Ao Wang

Funding Support

ACAP Fellowship

F50 TWO EXCITONS FOR THE PRICE OF ONE PHOTON: TOWARDS BETTER UNDERSTANDING OF SINGLET FISSIONN

Lead Partner

University of Melbourne

UNSW Team

Dr Saghar Masoomi-Godarzi, Prof. Trevor Smith

Funding Support

ACAP Fellowship

F51 BEYOND THE THEORETICAL LIMIT: SILICON PHOTOVOLTAIC EFFICIENCIES THROUGH SINGLET FISSION AUGMENTATION

Lead Partner

University of Melbourne

UNSW Team

Dr Calvin Lee

Funding Support

ACAP Fellowship

F52 NON-FULLERENE ACCEPTOR-BASED TANDEM PEROVSKITE:OPV DEVICES

Lead Partner

University of Queensland (UQ)

UQ Team

Dr Hui Jin, Shaun McAnally

Funding Support

ACAP, UQ

F53 NOVEL QUANTUM DOT SOLAR CELL TOWARDS HIGH POWER CONVERSION EFFICIENCY AND SCALABLE PRODUCTION (FINAL REPORT)

Lead Partner

University of Queensland (UQ)

ACAP Fellow

Dr Mengmeng Hao

Supervisor

Prof. Lianzhou Wang

Funding Support
ACAP Postdoctoral Fellowship

F54 STABLE DOPANT-FREE CARRIER-SELECTIVE CONTACTS FOR SILICON SOLAR CELLS

Lead Partner

ANU

ANU Team

Dr Jingnan (Taffy) Tong, Prof. Andrew Blakers

Academic Partner

Prof. Bram Hoex, UNSW

Funding Support

ACAP

F55 DEVELOPMENT OF PHOTOLUMINESCENCE IMAGING-BASED METHODS FOR ELECTRICAL CHARACTERISATION OF SUB-CELLS IN MONOLITHIC TANDEM SOLAR CELL TOWARDS INDUSTRIAL APPLICATION

Lead Partner

UNSW
UNSW Team

Dr Arman Mahboubi Soufiani, Dr Robert Lee-Chin, Prof. Thorsten Trupke, A/Prof. Ziv Hameiri

Funding Support

ACAP Fellowship

Funding Support

BT Industries, Oxford PV

INFRASTUCTURE GRANTS

ACAP's competitively selected Infrastructure Grants, whose titles are shown below, are reported online at acap.org.au/post/acap-s-annual-reports-2013-present

AIF102 CLIMATE CHAMBER WITH INTEGRATED SOLAR SIMULATOR AND IN SITU CURRENT-VOLTAGE MEASUREMENTS

Lead Partner

UNSW

UNSW Team

Bram Hoex, Nino Borojevic

Industry Partners
Eternalsun Spire

Funding Support

ACAP

AIF104 COMBINATORIAL SPUTTERING FACILITY

Lead Partner

Monash

Monash University Team

Jacek Jasieniak, Udo Bach

Funding Support

ACAP

AIF105 ADVANCED PEROVSKITE PROCESSING CAPABILITY

Lead Partner

Monash

Monash University Team

Jacek Jasieniak, Udo Bach

Funding Support

ACAP

AIF107 NEXT GENERATION SI AND TANDEM HETERO-CONTACT LABORATORY

Lead Partner

ANU

ANU Team

Dr Kean Chern Fong, Prof. Andrew Blakers, Prof. Daniel Macdonald, A/Prof. Klaus Weber, A/Prof. Thomas White, Prof. Kylie Catchpole, Dr Matthew Stocks, Dr Lachlan Black, Dr Di Yan, Dr Pheng Phang, Dr Wensheng Liang, Dr Osorio Mayon

Funding Support

ACAP

AIF108 TANDEM CLUSTER

UNSW Team

ANU

Funding Support

ACAP

AIF 201 LOW-DAMAGE PHYSICAL VAPOUR DEPOSITION (PVD) FACILITY FOR SOFT CONTACTS

Lead Partner

UoM

UoM Team

James Bullock, Amanda Ellis, David Jones, Di Yan

Funding Support

ACAP

AIF202 TUNABLE FEMTOSECOND LASER SYSTEM FOR LOW-DAMAGE ABLATION FOR ADVANCED SOLAR CELLS

Lead Partner

ANU

ANU Team

Marco Ernst, Andrew Blakers

Funding Support

ACAP

AIF203 ADVANCED DEVICE CHARACTERISATION CLUSTER

Lead Partner

ANU

ANU Team

A/Prof. Tom White, Dr Marco Ernst, Dr Hieu Nguyen, Dr Kean Chern Fong, Dr Daniel Walter, Prof. Yuerui Lu, Prof. Daniel Macdonald

Funding Support

ACAP, ANU

AIF204 UHV KELVIN PROBE WITH AMBIENT-PRESSURE PHOTOEMISSION SPECTROSCOPY

Lead Partner

ANU

ANU Team

Dr Lachlan Black, Prof. Daniel Macdonald, Dr Heping Shen, Prof. Kylie Catchpole

Funding Support

ACAP

AIF205 ENERGY DATA PLATFORM (EDP)

Lead Partner

UNSW

UNSW Team

A/Prof. Anna Bruce (Principal), Dr Navid Haghdadi (ACAP Fellow), Dr Mike Roberts, Dr Nargess Nourbakhsh, Dr Baran Yildiz,

Dr Rob Passey, Dr Merlinde Kay, Dr Jose Bilbao, Dr Alison Ciesla, Dr Catherine Chan, Prof. Renate Egan, Prof. Bram Hoex, Prof. Alistair Sproul

Industry Partners

Solar Analytics, Wattwatchers, APVI

Funding Support

ACAP

AIF206 ROLL-TO-ROLL PV FILM PRINTING/LAMINATING FACILITY

Lead Partner

Commonwealth Scientific and Industrial Research Organisation (CSIRO)

UNSW Team

Dr Mei Gao, Dr Andrew Scully, Dr Christopher Dunn, Karl Weber

Industry Partners

Solar Analytics, Wattwatchers, APVI

Funding Support

ACAP, CSIRO

AIF207 LOANA - SOLAR CELL ANALYSIS SYSTEM

Lead Partner

UNSW

UNSW Team

Bram Hoex, Nino Borojevic, Malcolm Abbott

Funding Support

ACAP

AIF208 INFRARED-VARIABLE ANGLE SPECTROSCOPIC ELLIPSOMETER

Lead Partner

UNSW

UNSW Team

Dr Jessica Yajie Jiang, A/Prof. Nicholas J. Ekins-Daukes, Prof. Martin Green

Funding Support

ACAP

AIF209 SINGLE SIDE ETCHER

Lead Partner

UNSW

UNSW Team

Bram Hoex, Fred Qi

Funding Support

ACAP

AIF210 LARGE-AREA MULTI-ZONE SOLAR SIMULATOR

Lead Partner

UNSW

UNSW Team

Prof. Nicholas Ekins-Daukes, Dr Mark Keevers, Prof. Xiaojing Hao, Prof. Stephen Bremner, Prof. Gavin Conibeer

Industry Partners

TS-Space Systems, AZUR SPACE Solar Power GmbH

Funding Support

ACAP

AIF211 ATMOSPHERICALLY CONTROLLED PV PROCESSING AND ACCELERATED TESTING FACILITY

Lead Partner

UNSW, Monash University

UNSW Team

Prof. Xiaojing Hao, Prof. Bram Hoex, A/Prof. Nicholas J. Ekins-Daukes, A/Prof. Ziv Hameiri

Monash University Team

Prof. Jacek Jasieniak, Prof. Udo Bach

Funding Support

ACAP

FINANCIAL SUMMARY

In December 2012, a grant of $33.2 million from the Australian Government through ARENA was announced to support an initial eight-year program of the Australian Centre for Advanced

Photovoltaics (ACAP). This support leveraged an additional $55.4 million cash and in-kind commitment from ACAP participants taking the total value of the project to $88.6 million.

ACAP commenced on 1 February 2013 after the signing of the Head Agreement between ARENA and UNSW, and with the receipt of letters of confirmation of participation under the terms of the Head Agreement by the other project participants. Collaboration Agreements with the Australian participants in the Australian Centre for Advanced Photovoltaics (ACAP) were completed on 1 July 2013.

An extension to the program, to undertake an Australian Solar PV Cell and Module Research Infrastructure Plan and Feasibility Study was signed in October 2014, generating an additional milestone, 4A. This project was completed and Milestone 4A was paid in October 2015. A further extension was formalised through Variation #4, executed in February 2016. It extended perovskites research in ACAP and generated two new Milestones for each year 2016 - 2019. Disbursements were made to each node following confirmation of institutional cash contributions for each completed year.

Variation #5 in June 2016 added a new partner, Dyesol Pty Ltd (subsequently known as Greatcell Solar Pty Ltd) and pooled the cash and in-kind contributions of most of the collaborating international research institutions and of the collaborating industry participants.

RayGen Resources Pty Ltd joined as a new collaborating industry participant during 2017 and Tindo Operations Co. Pty Ltd joined in 2019. Greatcell Solar Pty Ltd, ceased to trade during Q4 of 2018 and is no longer a collaborating industry participant in ACAP. 5B Australia Pty Ltd, Evolving Energy, Microsolar Pty. Ltd., Sun Cable Pty Ltd, SunDrive Solar Pty Ltd and the University of Sydney joined in 2021 and Australian Photovoltaics Institute, CubicPV Inc. (USA), Green Energy Institute (Korea), Neoen Australia Pty Ltd, One Stop Warehouse Pty. Ltd. and Scipher Technologies Pty Ltd all became collaborating industry participants in 2022.

Variation #6 in October 2017 and #6A in December 2017 implemented many of the changes proposed by the Mid-Term Review Panel in 2016, including the provision of additional funding for Capacity Building (Fellowships) and Small Grants, and made several minor updates and corrections. These variations brought the total funds granted to $46.0 million. A robust and transparent process to distribute Small (Collaboration) Grants was developed in 2015 and implemented in a small first funding round in that year. Since 2015, five rounds of small project / collaboration grant funding have been started, releasing amounts of $20,000 to $66,000 over a total of 63 small projects and $3,108,105 to 2020. A further eight grants, valued at $422,655, were offered through Round 6 in Q4 of 2020.

Twenty ACAP Fellowships were all taken up during 2018. One Fellow has since resigned to take up a leadership position in an overseas cell and module manufacturer and unspent funds are available for a planned offering of additional Fellowships in 2019. The fourth round of Small Grants were selected in Q2 of 2018, offering a total of 17 projects sharing $821,800. A further, fifth, round was offered late in 2018 (for projects to start in 2019). Again, 17 projects were successful and shared $856,305.

Variation #7 was executed on 4 April 2019. This provided additional funding of $19.0 million in the overall budget to extend the life of ACAP for an extra two years (its ninth and tenth) until the end of 2022, an additional two rounds each of 15 Fellowships – Round 2 in 2019 and Round 3 in 2020, and an additional round of Small Grants in 2020.

Partnerships with Sandia National Laboratories and the University of California, Santa Barbara were formally ended through Variation #7.

Variation #7 also included an agreement for support for infrastructure funding up to $19 million, which has led to two funding rounds. This brought the total cash support from ARENA to $84.0 million.

The Collaboration Agreement, between UNSW and the five Collaborating Australian Research Institutions was renegotiated during 2019 and was executed in Q4 of 2020.

All technical milestones for 2022 were achieved, apart from two where the intended outcomes were not fully achieved.

The breakdown by institution of the $14,6 million total cash and in-kind budget (including Infrastructure) for 2022 is shown in Figure 7.1(a). The actual total 2022 cash and in-kind expenditure for all categories was $28 million and its breakdown is shown in Figure 7.1(b). This variance is due to ARENA funding towards Infrastructure being fully received in 2020.

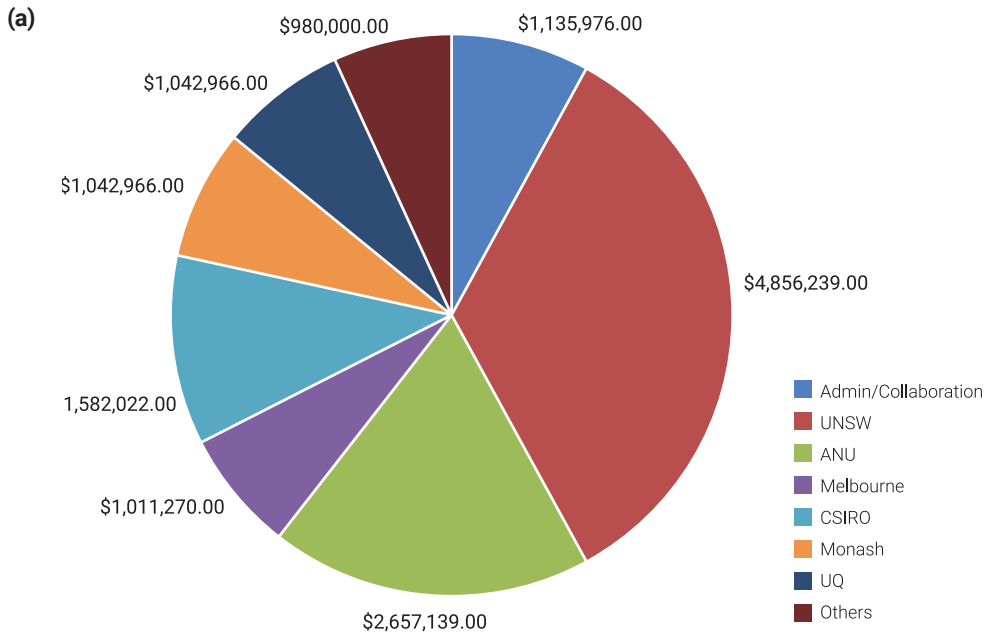

Figure 7.1(a): Total ACAP cash and in-kind expenditure budget ($m) for 2022 broken down by institution.

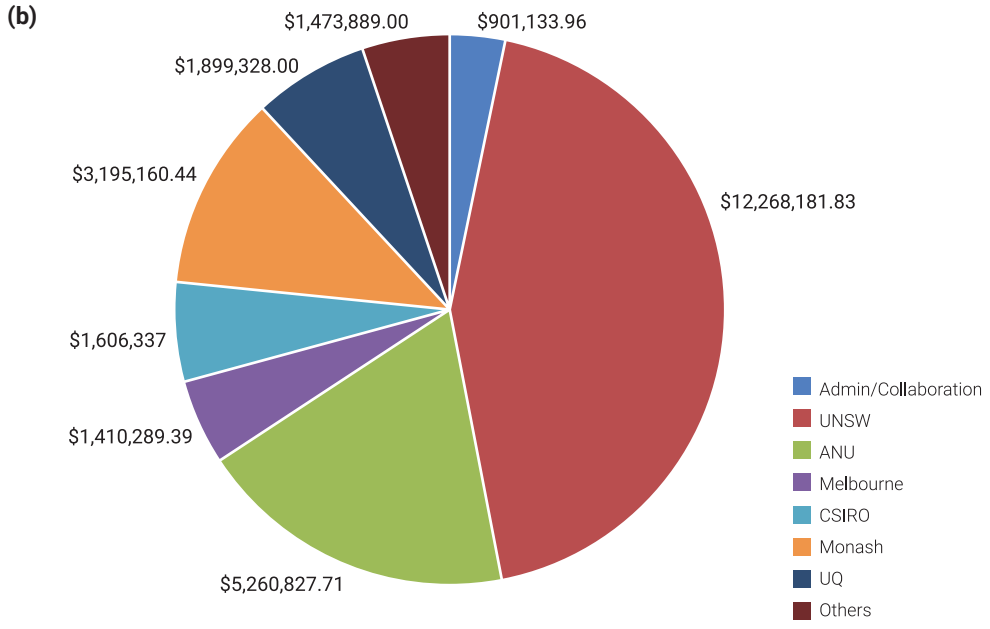

Figure 7.1(b): Actual cash and in-kind expenditure ($m) breakdown by institution for 2022.

PUBLICATIONS

8.2. BOOK CHAPTERS

Cleveland, E. R., Kotulak, N., Tomasulo, S., Jenkins, P. P., Mellor, A., Pearce, P., Ekins-Daukes, N. J. & Yakes, M. K. (2022). Interstitial Light Trapping and Optical Confinement in Multijunction Solar Cells. Light-Matter Interactions Towards the Nanoscale, 311-313.

Dipta, S. S. & Uddin, A. (2022). Solar Perovskite Technologies. Reference Module in Earth Systems and Environmental Sciences.

Munro, P., Jacome, V. & Samarakoon, S. (2022). Off-Grid Enterprise: A Critical History of Small-Scale Off-Grid Solar in Sub-Saharan Africa. Off-Grid Solar Electrification in Africa, 25-64.

Rondiya, S. R., Roy, A., Roy, A., Rahane, G. K., Jadhavar, A., Jadhavar, A., Kamble, M. M., Puneeth, K. P., Hareesh, K., Suryawanshi, M. P., Dzade, N. Y. & Jadkar, S. R. (2022). Physical Methods for Synthesis and Thin-Film Deposition. Applications of Nanomaterials for Energy Storage Devices, 77-96.

Rougieux, F., Coletti, G., Gaal, S., Guo, B., Fu, N., Veirman, J., Liu, A. & Øvrelid, E. J. (2022). n-type silicon material. n-Type Crystalline Silicon Photovoltaics: Technology, applications and economics, 27-68.

Samarakoon, S. & Zalengera, C. (2022). Framing Energy Justice: Perspectives from Malawi's Off-Grid Solar Market. Off-Grid Solar Electrification in Africa, 167-196.

Schmidt, T. W., Tayebjee, M. J. Y. & Alves, J. (2022). Upconversion. Comprehensive Renewable Energy, 499-517.

Song, N. & Deng, S. (2022). Thin Film Deposition Technologies and Application in Photovoltaics. Thin Film Deposition - Fundamentals, Processes, and Applications [Working Title].

Tayebjee, M. J. Y., Alves, J., Schmidt, T. W. & Conibeer, G. (2022). Downconversion. Comprehensive Renewable Energy, 518-533.

Uddin, A. (2022). Organic solar cells. Comprehensive Guide on Organic and Inorganic Solar Cells, 25-55.

8.3. PATENTS AND PATENT APPLICATIONS

Green, M., Hao, X., Liu, X. & Liu, Z. (2022). Perovskite solar cell and method of making the same. National Phase, United States.

Green, M., He, M., Hao, X., Liu, X. & Liu, Z. (2022). An apparatus for perovskite fabrication. Provisional, Australia

Huang, J., Sun, K. & Green, M. (2022). A copper-based chalcogenide photovoltaic device and a method of forming the same. National Phase, United States. Granted.

Lennon, A., Roemer, C. Song, N., Hsiao, P.-C., & Li, Y. (2022). Solar cell structure. PCT.

Li, C., Green, M., Zhang, P., Hao, X. & Liu, Z. (2022). A method to fabricate conductive polymer. Provisional, Australia.

Li, C., Mehrvarz, H., Green, M., Hao, X., Zhang, Y. & Liu, Z. (2022). Method of producing monograin membranes. Provisional, Australia.

Rey, G., Juhl, M., Kunz, O. &Trupke, T. (2022). Outdoor photoluminescence imaging of photovoltaic arrays via optical string modulation. PCT

Shen, H. P., Catchpole, K. & Duan, L.P. (2022). Tandem Photovoltaic cell. PCT, international.

Slade, A. & Edwards, M. (2022). Bifacial PERC solar cells and methods for the production thereof. Provisional, Australia.

Sun, H., Huang, J., Li, J., Green, M. Young, T. & Hao, X. (2022). Chalcogenide semiconductors. Provisional, Australia.

Wright, B., Hallam, B., Chan, C. Chen, D. & Zhang, Y. (2022). Metallization for silicon solar cells. PCT.

8.4 PAPERS IN REFEREED SCIENTIFIC AND TECHNICAL JOURNALS

Ahmed, M. I., Arachchige, L. J., Su, Z., Hibbert, D. B., Sun, C. & Zhao, C. (2022). Nitrogenase-Inspired Atomically Dispersed Fe–S–C Linkages for Improved Electrochemical Reduction of Dinitrogen to Ammonia. ACS Catalysis 12, 1443-1451.

Alim, M. A., Tao, Z., Saeed, N., Hao, X., Abden, M. J. & Rahman, A. (2022). Effect of reflective coating on thermal and electrical performances of solar roof tiles. Energy Conversion and Management 270.

Almora, O., Baran, D., Bazan, G. C., Cabrera, C. I., Erten-Ela, S., Forberich, K., Guo, F., Hauch, J., Ho-Baillie, A. W. Y., Jacobsson, T. J., Janssen, R. A. J., Kirchartz, T., Kopidakis, N., Loi, M. A., Lunt, R. R., Mathew, X., McGehee, M. D., Min, J., Mitzi, D. B., Nazeeruddin, M. K., Nelson, J., Nogueira, A. F., Paetzold, U. W., Rand, B. P., Rau, U., Snaith, H. J., Unger, E., Vaillant-Roca, L., Yang, C., Yip, H. L. & Brabec, C. J. (2022). Device Performance of Emerging Photovoltaic Materials (Version 3). Advanced Energy Materials 13.

Baldacchino, A. J., Collins, M. I., Nielsen, M. P., Schmidt, T. W., McCamey, D. R. & Tayebjee, M. J. Y. (2022). Singlet fission photovoltaics: Progress and promising pathways. Chemical Physics Reviews 3.

Ballif, C., Haug, F.-J., Boccard, M., Verlinden, P. J. & Hahn, G. (2022). Status and perspectives of crystalline silicon photovoltaics in research and industry. Nature Reviews Materials 7, 597-616; Ballif, C., Haug, F.-J., Boccard, M., Verlinden, P. J. & Hahn, G. (2022). Author Correction: Status and perspectives of crystalline silicon photovoltaics in research and industry. Nature Reviews Materials 7, 926-926.

Bao, W., Wang, R., Qian, C., Li, M., Sun, K., Yu, F., Liu, H., Guo, C. & Li, J. (2022). Photoassisted High-Performance Lithium Anode Enabled by Oriented Crystal Planes. Acs Nano 16, 17454-17465.

Bao, W., Wang, R., Sun, K., Qian, C., Zhang, Y. & Li, J. (2022). Interface Crystallographic Optimization of Crystal Plane for Stable Metallic Lithium Anode. ACS Appl Mater Interfaces 14, 38696-38705.

Basnet, R., Sio, H. C., Sun, C., Nguyen, H. T. & Macdonald, D. (2022). Passivation of Ring Defects in Czochralski-Grown Silicon Using Magnesium Fluoride Films. ACS Applied Energy Materials 5, 9877–9884.

Bell, N. O., Bilbao, J. I., Kay, M. & Sproul, A. B. (2022). Future climate scenarios and their impact on heating, ventilation and air-conditioning system design and performance for commercial buildings for 2050. Renewable and Sustainable Energy Reviews 162.

Benitez-Rodriguez, J.F., Chen, D., Scully, A.D., Easton, C.D., Vak, D., Li, H., Shaw, P.E., Burn, P.L., Caruso, R.A. & Gao, M. (2022). Slot-die coating of a formamidinium-cesium mixed-cation perovskite for roll-to-roll fabrication of perovskite solar cells under ambient laboratory conditions. Solar Energy Materials and Solar Cells 246, 111884.

Bing, J., Caro, L. G., Talathi, H. P., Chang, N. L., McKenzie, D. R. & Ho-Baillie, A. W. Y. (2022). Perovskite solar cells for building integrated photovoltaics—glazing applications. Joule 6, 1446-1474.

Black, L. E. & Macdonald D. H. (2022). Improved Auger recombination models: Consequences for c-Si solar cells. Solar Energy Materials and Solar Cells 246, 111914.

Black, L. E. & Macdonald D. H. (2022). On the quantification of Auger recombination in crystalline silicon. Solar Energy Materials and Solar Cells 234, 111428.

Bruce, J., Mazuquin, B., Mistry, P., Rees, S., Canaway, A., Hossain, A., Williamson, E., Padfield, E. J., Lall, R., Richmond, H., Chowdhury, L., Lait, C., Petrou, S., Booth, K., Lamb, S. E., Vidya, R. & Thompson, A. M. (2022). Exercise to prevent shoulder problems after breast cancer surgery: the PROSPER RCT. Health Technol Assess 26, 1-124.

Bui, A. D., Mozaffari, N., Truong, T. N., Duong, T., Weber, K. J., White, T. P., Catchpole, K. R., Macdonald, D. & Nguyen, H. T. (2021). Electrical properties of perovskite solar cells by illumination intensity and temperature-dependent photoluminescence imaging. Progress in Photovoltaics: Research and Applications 1–7.

Buratti, Y., Dick, J., Le Gia, Q. & Hameiri, Z. (2022). Deep Learning Extraction of the Temperature-Dependent Parameters of Bulk Defects. ACS Appl Mater Interfaces 14, 48647-48657.

Buratti, Y., Sowmya, A., Dumbrell, R., Dwivedi, P., Trupke, T. & Hameiri, Z. (2022). Automated efficiency loss analysis by luminescence image reconstruction using generative adversarial networks. Joule 6, 1320-1332.

Chang, N. L., Dehghanimadvar, M. & Egan, R. (2022). The cost of risk mitigation—Diversifying the global solar PV supply chain. Joule 6, 2686-2688.

Chang, N. L., Newman, B. K. & Egan, R. J. (2022). Future cost projections for photovoltaic module manufacturing using a bottom-up cost and uncertainty model. Solar Energy Materials and Solar Cells 237.

Chang, N. L., Poduval, G. K., Sang, B., Khoo, K., Woodhouse, M., Qi, F., Dehghanimadvar, M., Li, W. M., Egan, R. J. & Hoex, B. (2022). Techno-economic analysis of the use of atomic layer deposited transition metal oxides in silicon heterojunction solar cells. Progress in Photovoltaics: Research and Applications 31, 414-428.

Chang, Y.-C., Wang, S., Deng, R., Li, S., Ji, J. & Chong, C. (2022). Investigation of laser doping and plating process for cost-effective PV metallization. Solar Energy Materials and Solar Cells 235.

Chaudhari, A., Cui, X., Hoex, B., Hyde, L., Ironside, C. N., Jadwisienczak, W. M., Kordesch, M. E., Rahman, F. & Vispute, R. D. (2022). Zinc oxide family semiconductors for ultraviolet radiation emission – A cathodoluminescence study. Materials Research Bulletin 153.

Chen, H., Zheng, J., Ballestas-Barrientos, A., Bing, J., Liao, C., Yuen, A. K. L., Fois, C. A. M., Valtchev, P., Proschogo, N., Bremner, S. P., Atwater, H. A., Boyer, C., Maschmeyer, T. & Ho-Baillie, A. W. Y. (2022). Solar-Driven Co-Production of Hydrogen and Value-Add Conductive Polyaniline Polymer. Advanced Functional Materials 32.

Chen, X., Fan, W., Dai, X., Yun, J. S., Huang, Y., Wang, X., Zhang, Z. & Kim, D. J. (2022). Spatially confined atomic dispersion of metals in thermally reduced graphene oxide films. Carbon 188, 367-375.

Chen, Y., Chen, D., Altermatt, P. P., Zhang, S., Wang, L., Zhang, X., Xu, J., Feng, Z., Shen, H. & Verlinden, P. J. (2022). Technology evolution of the photovoltaic industry: Learning from history and recent progress. Progress in Photovoltaics: Research and Applications.

Chin, R. L., Pollard, M., Nielsen, M. P. & Hameiri, Z. (2022). Bulk Lifetime and Doping in Crystalline Silicon via Two-Photon Absorption Time-Resolved Photoluminescence Decay. IEEE Journal of Photovoltaics 12, 778-786.

Choi, E., Zhang, Y., Soufiani, A. M., Lee, M., Webster, R. F., Pollard, M. E., Reece, P. J., Lee, W., Seidel, J., Lim, J., Yun, J.-H. & Yun, J. S. (2022). Exploration of sub-bandgap states in 2D halide perovskite single-crystal photodetector. npj 2D Materials and Applications 6.

Choi, K., Jeong, M. J., Lee, S., Alosaimi, G., Seidel, J., Yun, J. S. & Noh, J. H. (2022). Suppressing Halide Segregation in Wide-Band-Gap Mixed-Halide Perovskite Layers through Post-Hot Pressing. ACS Appl Mater Interfaces 14, 24341-24350.

Chowdhury, H., Chowdhury, T., Sharifi, A., Corkish, R. & Sait, S. M. (2022). Role of Biogas in Achieving Sustainable Development Goals in Rohingya Refugee Camps in Bangladesh. Sustainability 14.

Chowdhury, T., Chowdhury, H., Islam, K. S., Sharifi, A., Corkish, R. & Sait, S. M. (2023). Resilience analysis of a PV/battery system of health care centres in Rohingya refugee camp. Energy 263, 125634.

Dehghanimadvar, M., Egan, R. & Chang, N. L. (2022). Economic assessment of local solar module assembly in a global market. Cell Reports Physical Science 3.

Dehghanimadvar, M., Shirmohammadi, R., Ahmadi, F., Aslani, A. & Khalilpour, K. R. (2022). Mapping the development of various solar thermal technologies with hype cycle analysis. Sustainable Energy Technologies and Assessments 53.

Deng, R., Zhuo, Y. & Shen, Y. (2022). Recent progress in silicon photovoltaic module recycling processes. Resources, Conservation and Recycling 187, 106612.

Deng, S., Tan, B., Chesman, A.S.R., Lu, J., McMeekin, D.P., Ou, Q., Scully, A.D., Raga, S.R., Rietwyk, K.J., Weissbach, A., Zhao, B., Voelcker, N.H., Cheng, Y-B., Lin, X. & Bach U. (2022). Back-contact perovskite solar cell fabrication via microsphere lithography. Nano Energy 102, 107695.

Dias, P. R., Schmidt, L., Chang, N. L., Monteiro Lunardi, M., Deng, R., Trigger, B., Bonan Gomes, L., Egan, R. & Veit, H. (2022). High yield, low cost, environmentally friendly process to recycle silicon solar panels: Technical, economic and environmental feasibility assessment. Renewable and Sustainable Energy Reviews 169.

Ding, S., Hao, M., Fu, C., Lin, T., Baktash, A., Chen, P., He, D., Zhang, C., Chen, W., Whittaker, A. K., Bai, Y. & Wang, L. (2022). In Situ Bonding Regulation of Surface Ligands for Efficient and Stable FAPbI(3) Quantum Dot Solar Cells. Advanced science (Weinheim, Baden-Wurttemberg, Germany) 9, e2204476.

Dipta, S. S., Uddin, A. & Conibeer, G. (2022). Enhanced light management and optimization of perovskite solar cells incorporating wavelength dependent reflectance modeling. Heliyon 8, e11380.

Duong, T., John, A. T., Chen, H., Pham, H., Murugappan, K., Tran-Phu, T., Tricoli, A. & Catchpole, K. (2022). Mixed-dimensional organic–inorganic metal halide perovskite (OIMHP) based gas sensors with superior stability for NO2 detection. Materials Advances 3, 1263-1271.

Ehrler, B., W. Y. Ho-Baillie, A., Hutter, E. M., Milić, J. V., Tayebjee, M. J. Y. & Wilson, M. W. B. (2022). Scalable ways to break the efficiency limit of single-junction solar cells. Applied Physics Letters 120.

Ernst, M., Conechado, G. E. J., Asselineau, C.-A. (2021). Accelerating the Simulation of Annual Bifacial Illumination of Real Photovoltaic Systems with Ray Tracing. iScience, p. 103698. DOI: 10.1016/j.isci.2021.103698.

Farshchimonfared, M., Bilbao, J. I. & Sproul, A. B. (2022). Corrigendum to "Channel depth, air mass flow rate and air distribution duct diameter optimization of photovoltaic thermal (PV/T) air collectors linked to residential buildings" [Renew. Energy. 76 (2015) 27–35]. Renewable Energy 188.

Gandhi, H. H., Hoex, B. & Hallam, B. J. (2022). Strategic investment risks threatening India's renewable energy ambition. Energy Strategy Reviews 43.

Gao, Y., Xu, W., Zhang, S. W., Fan, T., Zhang, M., Ran, A., Zhang, X., Kang, F. & Wei, G. (2022). Double Cascading Charge Transfer at Integrated Perovskite/Organic Bulk Heterojunctions for Extended Near-Infrared Photoresponse and Enhanced Photocurrent. Small 18, e2106083.

Garcia-Marcos, L., Asher, M. I., Pearce, N., Ellwood, E., Bissell, K., Chiang, C. Y., El Sony, A., Ellwood, P., Marks, G. B., Mortimer, K., Martinez-Torres, A. E., Morales, E., Perez-Fernandez, V., Robertson, S., Rutter, C. E., Silverwood, R. J., Strachan, D. P. & Global Asthma Network Phase, I. S. G. (2022). The burden of asthma, hay fever and eczema in children in 25 countries: GAN Phase I study. Eur Respir J 60.

Ghasemi, M., Zhang, Y., Zhou, C., Tan, C., Choi, E., Yun, J. S., Du, A., Yun, J. H., Jia, B. & Wen, X. (2022). Controllable Acceleration and Deceleration of Charge Carrier Transport in Metal-Halide Perovskite Single-Crystal by Cs-Cation Induced Bandgap Engineering. Small 18, e2107680.

Ghorpade, U. V., Suryawanshi, M. P., Green, M. A., Wu, T., Hao, X. & Ryan, K. M. (2023). Emerging Chalcohalide Materials for Energy Applications. Chem Rev 123, 327-378.

Gilmore, N., Koskinen, I., van Gennip, D., Paget, G., Burr, P. A., Obbard, E. G., Daiyan, R., Sproul, A., Kay, M., Lennon, A., Konstantinou, G., Hemer, M., Gui, E. M. & Gurieff, N. (2022). Clean energy futures: An Australian based foresight study. Energy 260.

Gorman, N., Bruce, A. & MacGill, I. (2022). Nempy: A Python package for modelling the Australian National Electricity Market dispatch procedure. Journal of Open Source Software 7.

Gour, K. S., Karade, V. C., Lee, M., Jang, J. S., Jo, E., Babar, P., Shim, H., Yun, J. S., Park, J. & Kim, J. H. (2022). Engineering of Interface and Bulk Properties in Cu2ZnSn(S,Se)4 Thin-Film Solar Cells with Ultrathin CuAlO2 Intermediate Layer and Ge Doping. ACS Applied Energy Materials 5, 2024-2035.

Green, M. A. (2022). Corrigendum to "Improved Silicon Optical Parameters at 25°C, 295K and 300K including Temperature Coefficients" [Prog. Photovolt: Res. Appl. 2022; 30: 164–179]. Progress in Photovoltaics: Research and Applications 30, 1144-1145.

Green, M. A., Dunlop, E. D., Hohl-Ebinger, J., Yoshita, M., Kopidakis, N., Bothe, K., Hinken, D., Rauer, M. & Hao, X. (2022). Solar cell efficiency tables (Version 60). Progress in Photovoltaics: Research and Applications 30, 687-701.

Greulich, J. M., Wirtz, W., Höffler, H., Wöhrle, N., Juhl, M. K., Kunz, O., Rein, S. & Bett, A. W. (2022). Contactless measurement of current-voltage characteristics for silicon solar cells. Solar Energy Materials and Solar Cells 248.

Guan, P., Zhu, R., Hu, G., Patterson, R., Chen, F., Liu, C., Zhang, S., Feng, Z., Jiang, Y., Wan, T., Hu, L., Li, M., Xu, Z., Xu, H., Han, Z. & Chu, D. (2022). Recent Development of Moisture-Enabled-Electric Nanogenerators. Small 18, e2204603.

Gunawan, D., Toe, C. Y., Sun, K., Scott, J. & Amal, R. (2022). Improved carrier dynamics in nickel/urea-functionalized carbon nitride for ethanol photoreforming. Photochem Photobiol Sci 21, 2115-2126.

Guo, J., Bilbao, J. I. & Sproul, A. B. (2022). Parametric number of transfer unit analysis of a photovoltaic thermal coupled desiccant dehumidifier. Energy Conversion and Management 255.

Guo, Q., Zhang, T., Etheridge, J., Bach, U. (2023) Toward Uniaxially Textured CsPbIBr2 Perovskite Thin Films with Twin Domains by Potassium Incorporation. ACS Energy Letters (Accepted)

Hadia, N. M. A., Abdelazeez, A. A. A., Alzaid, M., Shaban, M., Mohamed, S. H., Hoex, B., Hajjiah, A. & Rabia, M. (2022). Converting Sewage Water into H(2) Fuel Gas Using Cu/CuO Nanoporous Photocatalytic Electrodes. Materials (Basel) 15.

Hallam, B., Kim, M., Underwood, R., Drury, S., Wang, L. & Dias, P. (2022). A Polysilicon Learning Curve and the Material Requirements for Broad Electrification with Photovoltaics by 2050. Solar Rrl 6.

Hallam, B., Kim, M., Zhang, Y., Wang, L., Lennon, A., Verlinden, P., Altermatt, P. P. & Dias, P. R. (2022). The silver learning curve for photovoltaics and projected silver demand for net-zero emissions by 2050. Progress in Photovoltaics: Research and Applications.

Hameiri, Z. & Moser, D. (2022). Introduction: focus on characterisation and reliability of photovoltaic modules in utility-scale plants. Progress in Energy 4.

Hameiri, Z. (2022). Photovoltaics literature survey (no. 172). Progress in Photovoltaics: Research and Applications 30, 204-208.

Hameiri, Z. (2022). Photovoltaics literature survey (No. 173). Progress in Photovoltaics: Research and Applications 30, 318-321.

Hameiri, Z. (2022). Photovoltaics literature survey (No. 174). Progress in Photovoltaics: Research and Applications 30, 447-451.

Hameiri, Z. (2022). Photovoltaics literature survey (No. 175). Progress in Photovoltaics: Research and Applications 30, 679-683.

Hameiri, Z. (2022). Photovoltaics literature survey (No. 176). Progress in Photovoltaics: Research and Applications 30, 1054-1058.

Hameiri, Z. (2022). Photovoltaics literature survey (No. 177). Progress in Photovoltaics: Research and Applications 30, 1247-1251.

Hameiri, Z. (2022). Photovoltaics literature survey (no. 178). Progress in Photovoltaics: Research and Applications 30, 1447-1452.

Heslop, S., Yildiz, B., Roberts, M., Chen, D., Lau, T., Naderi, S., Bruce, A., MacGill, I. & Egan, R. (2022). A Novel Temperature-Independent Model for Estimating the Cooling Energy in Residential Homes for Pre-Cooling and Solar Pre-Cooling. Energies 15.

Hou, H., Hu, T., Zhang, F., Liu, R., He, J., Liu, C., Yu, Y., Chen, D., Wu, Q., Zhang, M. & Yu, H. (2022). Small molecule interfacial cross-linker for highly efficient two-dimensional perovskite solar cells. Journal of Energy Chemistry 68, 35-41.

Hu, L., Guan, X., Wan, T., Lin, C.-H., Liu, S., Zhu, R., Chen, W., Yao, Y., Huang, C.-Y., Yuan, L., Shahrokhi, S., Chu, D., Cazorla, C., Chen, J., Yang, J., Yi, J., Huang, S. & Wu, T. (2022). Valence-Regulated Metal Doping of Mixed-Halide Perovskites to Modulate Phase Segregation and Solar Cell Performance. Acs Energy Letters 7, 4150-4160.

Jafari, S., Abbott, M., Zhang, D., Wu, J., Jiang, F. & Hameiri, Z. (2022). Bulk defect characterization in metalized solar cells using temperature-dependent Suns-Voc measurements. Solar Energy Materials and Solar Cells 236.

Jiang, W., Jin, H., Babazadeh, M., Loch, A.S., Raynor, A., Mallo, N., Huang, D.M., Jiao, X., Tan, W.L., McNeill, C.R., Burn, P.L. & Shaw, P.E. (2022). Dielectric Constant Engineering of Organic Semiconductors: Effect of Planarity and Conjugation Length. Advanced Functional Materials. Wiley, 32, 2104259.

Jin, H., Wang, X., Chu, R., Subbiah, J., Jones, D. J., Nelson, A. R. J., Gentle, I. R., Burn, P. L. & Shaw, P. E. (2022). Power losses in conventional and inverted non-polymeric donor:fullerene bulk heterojunction solar cells - The role of vertical phase separation in BQR:PC71BM blends. Organic Electronics. Elsevier BV, 108, 106594.

Juhl, M. K., Veettil, B. P., Scardera, G. & Payne, D. N. R. (2022). Determining the optical properties of solar cells using low cost scanners. Sci Rep 12, 17697.

Kang, D, Sio, H. C., Stuckelberger, J., Yan, Di., Phang, S. P., Liu, R., Truong, T. N., Le, T., Nguyen, H. T., Zhang, X. & Macdonald, D. (2022). Comparison of firing stability between p- and n-type polysilicon passivating contacts. Progress in Photovoltaics: Research and Applications 30, 970–980.

Kang, D, Sio, H. C., Stuckelberger, J., Yan, Di., Phang, S. P., Liu, R., Truong, T. N., Le, T., Nguyen, H. T., Zhang, X. & Macdonald, D. (2022). Comparison of firing stability between p- and n-type polysilicon passivating contacts. Progress in Photovoltaics: Research and Applications 30, 970–980.

Karade, V. C., Lim, J., Gour, K. S., Jang, J. S., Shin, S. J., Kim, J. H., Yang, B. S., Choi, H., Enkhbat, T., Kim, J., Yun, J. S., Jang, H. N., Yun, J. H., Park, J. & Kim, J. H. (2022). Overcoming the limitations of low-bandgap Cu2ZnSn(S,Se)4 devices under indoor light conditions: from design to prototype IoT application. Journal of Materials Chemistry A 10, 23831-23842.

Karade, V. C., Suryawanshi, M. P., Jang, J. S., Gour, K. S., Jang, S., Park, J., Kim, J. H. & Shin, S. W. (2022). Understanding defects and band tailing characteristics and their impact on the device performance of Cu2ZnSn(S,Se)4 solar cells. Journal of Materials Chemistry A 10, 8466-8478.

Karas, J., Phua, B., Mo, A., Iqbal, N., Davis, K., Bowden, S., Lennon, A. & Augusto, A. (2022). Copper Outdiffusion from Copper-Plated Solar Cell Contacts during Damp Heat Exposure. ACS Appl Mater Interfaces 14, 12149-12155.

Kenny, R., Manshanden, P., Coletti, G., Rosca, V., Jansen, M. J., de Groot, K., de Graaff, G. J., Creatore, M., Simurka, L., Najafi, M., Zardetto, V., Dogan, I., Fledderus, H., Veenstra, S. C. & Serra, J. M. (2022). Quantifying the performance gain of 100 cm2 bifacial four terminal perovskite-Si tandem modules. EPJ Photovoltaics 13.

Khan, T. A., Burr, P. A., Payne, D., Juhl, M., Das, U., Hallam, B., Bagnall, D. & Puthen Veettil, B. (2022). Molecular dynamic simulation on temperature evolution of SiC under directional microwave radiation. J Phys Condens Matter 34.

Kim, D., Lim, J., Lee, S., Soufiani, A. M., Choi, E., Ievlev, A. V., Borodinov, N., Liu, Y., Ovchinnikova, O. S., Ahmadi, M., Lim, S., Sharma, P., Seidel, J., Noh, J. H. & Yun, J. S. (2022). Correction to Microstructural Evaluation of Phase Instability in Large Bandgap Metal Halide Perovskites. Acs Nano 16, 6939.

Kunz, O., Schlipf, J., Fladung, A., Khoo, Y. S., Bedrich, K., Trupke, T. & Hameiri, Z. (2022). Outdoor luminescence imaging of field-deployed PV modules. Progress in Energy 4.

Lan, D. & Green, M. A. (2022). Combatting temperature and reverse-bias challenges facing perovskite solar cells. Joule 6, 1782-1797.

Lennon, A., Lunardi, M., Hallam, B. & Dias, P. R. (2022). The aluminium demand risk of terawatt photovoltaics for net zero emissions by 2050. Nature Sustainability 5, 357-363.

Li, C., Gu, X., Chen, Z., Han, X., Yu, N., Wei, Y., Gao, J., Chen, H., Zhang, M., Wang, A., Zhang, J., Wei, Z., Peng, Q., Tang, Z., Hao, X., Zhang, X. & Huang, H. (2022). Achieving Record-Efficiency Organic Solar Cells upon Tuning the Conformation of Solid Additives. J Am Chem Soc 144, 14731-14739.

Li, C., Ma, Y., Zhang, X., Chen, X., Xi, F., Li, S., Ma, W. & Chang, Y. (2022). Enhanced Efficiency of Graphene-Silicon Schottky Junction Solar Cell through Pyramid Arrays Texturation. Silicon 14, 8765-8775.

Li, C., Ma, Y., Zhang, X., Chen, X., Xi, F., Li, S., Ma, W. & Chang, Y. (2022). Performance Improvement of Graphene/Silicon Solar Cells via Inverted Pyramid Texturation Array. Silicon 14, 10485-10493.

Li, H., Bati, A. S. R., Chu, R., Zhang, G., Li, Y., Lin, Q., Burn, P. L., Shaw, P. E. & Gentle, I. R. (2022). Fluorinated Interlayer Modulation of NiOx-Based Inverted Perovskite Solar Cells. ACS Applied Materials & Interfaces. American Chemical Society (ACS), 14, 42071–42077.

Li, H., Chu, R., Zhang, G., Burn, P. L., Gentle, I. R. & Shaw, P. E. (2022). Influence of the Alkyl Chain Length of (Pentafluorophenylalkyl) Ammonium Salts on Inverted Perovskite Solar Cell Performance. ACS Applied Materials & Interfaces. American Chemical Society (ACS), 14, 39939–39950.

Li, H., Zuo, C., Angmo, D., Weerasinghe, H., Gao, M. & Yang J. (2022). Fully roll to roll processed efficient perovskite solar cells via precise control on the morphology of PbI2:CSI layer. Nano-Micro Lett. 14, 79.

Li, J., Huang, J., Ma, F., Sun, H., Cong, J., Privat, K., Webster, R. F., Cheong, S., Yao, Y., Chin, R. L., Yuan, X., He, M., Sun, K., Li, H., Mai, Y., Hameiri, Z., Ekins-Daukes, N. J., Tilley, R. D., Unold, T., Green, M. A. & Hao, X. (2022). Unveiling microscopic carrier loss mechanisms in 12% efficient Cu2ZnSnSe4 solar cells. Nature Energy 7, 754-764.

Li, J., Liu, H., Sun, K., Wang, R., Qian, C., Yu, F., Zhang, L. & Bao, W. (2022). Dual-functional iodine photoelectrode enabling high performance photo-assisted rechargeable lithium iodine batteries. Journal of Materials Chemistry A 10, 7326-7332.

Lian, Y., Lan, D., Xing, S., Guo, B., Ren, Z., Lai, R., Zou, C., Zhao, B., Friend, R. H. & Di, D. (2022). Ultralow-voltage operation of light-emitting diodes. Nat Commun 13, 3845.

Liang, W., Narangari, P., Tong, J., Michel, J.I., Murdoch, B.J., Sio, H.C., Kho, T., Kremer, F., Armand, S., McIntosh, K., Bullock, J. & Fong, K.C. (2023). Effect of Al Electrodes on Surface Passivation of TiOx Selective Heterocontacts for Si Solar Cells. Phys. Status Solidi RRL, 2200304.

Liao, B., Wu, W., Yeo, R. J., Wu, X., Ma, S., Wang, Q., Wan, Y., Su, X., Shen, W., Li, X., Li, W., Xing, G. & Hoex, B. (2022). Atomic scale controlled tunnel oxide enabled by a novel industrial tube-based PEALD technology with demonstrated commercial TOPCon cell efficiencies > 24%. Progress in Photovoltaics: Research and Applications 31, 220-229.

Liao, B., Wu, X., Wu, W., Liu, C., Ma, S., Wang, S., Xie, T., Wang, Q., Du, Z., Shen, W., Li, X., Li, W. & Hoex, B. (2022). Tube-type plasma-enhanced atomic layer deposition of aluminum oxide: Enabling record lab performance for the industry with demonstrated cell efficiencies >24%. Progress in Photovoltaics: Research and Applications 31, 52-61.

Liao, C. H., Chen, C. H., Bing, J., Bailey, C., Lin, Y. T., Pandit, T. M., Granados, L., Zheng, J., Tang, S., Lin, B. H., Yen, H. W., McCamey, D. R., Kennedy, B. J., Chueh, C. C. & Ho-Baillie, A. W. Y. (2022). Inorganic-Cation Pseudohalide 2D Cs2 Pb(SCN)2Br2 Perovskite Single Crystal (Adv. Mater. 7/2022). Advanced Materials 34.

Lim, J., Choi, E., Kim, M., Lee, M., Chen, D., Green, M. A., Seidel, J., Kim, C., Park, J., Hao, X. & Yun, J. S. (2022). Revealing the Dynamics of the Thermal Reaction between Copper and Mixed Halide Perovskite Solar Cells. ACS Appl Mater Interfaces 14, 20866-20874.

Lin, Q., Bernardi, S., Shabbir, B., Ou, Q., Wang, M., Yin, W., Liu, S., Chesman, A.S., Fürer, S.O., Si, G. and Medhekar, N., 2022. Phase-Control of Single-Crystalline Inorganic Halide Perovskites via Molecular Coordination Engineering. Advanced Functional Materials, 32(16), p.2109442.

Liu, B., Li, J., Wang, G., Ye, F., Yan, H., Zhang, M., Dong, S. C., Lu, L., Huang, P., He, T., Xu, P., Kwok, H. S. & Li, G. (2022). Lattice strain modulation toward efficient blue perovskite light-emitting diodes. Sci Adv 8, eabq0138.

Liu, D., Wright, M., Goodarzi, M., Wilshaw, P. R., Hamer, P. & Bonilla, R. S. (2022). Observations of contact resistance in TOPCon and PERC solar cells. Solar Energy Materials and Solar Cells 246.

Liu, J., Wang, M., Lin, J., Chen, G., Liu, B., Huang, J., Zhang, M., Liang, G., Lu, L., Xu, P., Tian, B., Kwok, H.-S. & Li, G. (2022). Mitigating deep-level defects through a self-healing process for highly efficient wide-bandgap inorganic CsPbI3−xBrx perovskite photovoltaics. Journal of Materials Chemistry A 10, 17237-17245.

Liu, M., Römer, U., Ekins-Daukes, N. J. & Lennon, A. (2022). Optical analysis of light management for finger designs in CPV systems. Progress in Photovoltaics: Research and Applications 30, 1219-1227.

Liu, Q., Ma, Z., Li, Y., Yan, G., Huang, D., Hou, S., Zhou, W., Wang, X., Ren, J., Xiang, Y., Ding, R., Yue, X., Du, Z., Zhang, M., Zhang, W., Duan, L., Huang, Y. & Mai, Y. (2022). Heterogeneous lead iodide obtains perovskite solar cells with efficiency of 24.27%. Chemical Engineering Journal 448.

Liu, X., Zheng, B., Shi, L., Zhou, S., Xu, J., Liu, Z., Yun, J. S., Choi, E., Zhang, M., Lv, Y., Zhang, W.-H., Huang, J., Li, C., Sun, K., Seidel, J., He, M., Peng, J., Hao, X. & Green, M. (2022). Perovskite solar cells based on spiro-OMeTAD stabilized with an alkylthiol additive. Nature Photonics 17, 96-105.

Lu, J., Zhou, C., Chen, W., Wang, X., Jia, B. & Wen, X. (2022). Origin and physical effects of edge states in two-dimensional Ruddlesden-Popper perovskites. iScience 25, 104420.

Ma, D., Lan, G., Hu, C., Hassan, M., Hu, W., Mushfika, U., Uddin, A. & Youssef, M. (2022). Recognizing Hand Gestures using Solar Cells. IEEE Transactions on Mobile Computing, 1-1.

Ma, Z., Huang, D., Liu, Q., Yan, G., Xiao, Z., Chen, D., Zhao, J., Xiang, Y., Peng, C., Li, H., Zhang, M., Zhang, W., Duan, L. & Huang, Y. (2022). Excess PbI2 evolution for triple-cation based perovskite solar cells with 21.9% efficiency. Journal of Energy Chemistry 66, 152-160.

Mahmud, M. A., Zheng, J., Tang, S., Liao, C., Wang, G., Bing, J., Leung, T. L., Bui, A. D., Chen, H., Yi, J., Bremner, S. P., Nguyen, H. T. & Ho-Baillie, A. W. Y. (2022). Water-Free, Conductive Hole Transport Layer for Reproducible Perovskite–Perovskite Tandems with Record Fill Factor. Acs Energy Letters 8, 21-30.

Mahmud, M. A., Zheng, J., Tang, S., Wang, G., Bing, J., Bui, A. D., Qu, J., Yang, L., Liao, C., Chen, H., Bremner, S. P., Nguyen, H. T., Cairney, J. & Ho-Baillie, A. W. Y. (2022). Cation-Diffusion-Based Simultaneous Bulk and Surface Passivations for High Bandgap Inverted Perovskite Solar Cell Producing Record Fill Factor and Efficiency. Advanced Energy Materials 12.

Manwaring, K., Kearnes, M., Morgan, B., Munro, P., Pala, R. & Samarakoon, S. (2022). What does a right to repair tell us about our relationship with technology? Alternative Law Journal 47, 179-186.

Marshall, L., Bruce, A. & MacGill, I. (2022). Market Mechanisms and Technology Transition in Australia's National Electricity Market. Current Sustainable/Renewable Energy Reports 9, 41-51.

Marwick, C. A., Hossain, A., Nogueira, R., Sneddon, J., Kavanagh, K., Bennie, M., Seaton, R. A., Guthrie, B. & Malcolm, W. (2022). Feedback of Antibiotic Prescribing in Primary Care (FAPPC) trial: results of a real-world cluster randomized controlled trial in Scotland, UK. J Antimicrob Chemother 77, 3291-3300.

McMeekin, D. P., Holzhey, P., Fürer, S. O., Harvey, S. P., Schelhas, L. T., Ball, J. M., Mahesh, S., Seo, S., Hawkins, N., Lu, J., Johnston, M. B., Berry, J. J., Bach, U. & Snaith, H. J. (2022). Intermediate-phase engineering via dimethylammonium cation additive for stable perovskite solar cells. Nature Materials.

McPherson, D. J., Dowd, A., Arnold, M. D., Gentle, A. & Cortie, M. B. (2022). Electrochemical energy storage on nanoporous copper sponge. Journal of Materials Research 37, 2195-2203.

Miao, Z., Tian, Y., Li, S., Ding, Z., Chen, X., Ma, W. & Chang, Y. (2022). Photocatalytic degradation of Rhodamine B over popcorn-like ZnFe2O4/CdS–GO ternary composite. Journal of Materials Research and Technology 21, 1863-1877.

Mozaffari, N., Duong, T., Shehata, M. M., Bui, A. D., Pham, H. T., Yin, Y., Mayon, Y. O., Zheng, J., Mahmud, M. A., Tabi, G. D., Andersson, G. G., Black, L. E., Peng, J., Shen, H., White, T. P., Weber, K. & Catchpole, K. R. (2022). Above 23% Efficiency by Binary Surface Passivation of Perovskite Solar Cells Using Guanidinium and Octylammonium Spacer Cations. Solar Rrl 6.

Mozaffari, N., Duong, T., Shehata, M. M., Bui, A. D., Pham, H. T., Yin, Y., Mayon, Y. O., Zheng, J., Mahmud, M. A., Tabi, G. D., Andersson, G. G., Black, L. E., Peng, J., Shen, H., White, T. P., Weber, K. & Catchpole, K. R. (2022). Above 23% Efficiency by Binary Surface Passivation of Perovskite Solar Cells Using Guanidinium and Octylammonium Spacer Cations. Solar RRL 6, 2200355.

Munro, P. G., Samarakoon, S., Hansen, U. E., Kearnes, M., Bruce, A., Cross, J., Walker, S. & Zalengera, C. (2022). Towards a repair research agenda for off-grid solar e-waste in the Global South. Nature Energy 8, 123-128.

Naderi, S., Heslop, S., Chen, D., MacGill, I. & Pignatta, G. (2022). Consumer cost savings, improved thermal comfort, and reduced peak air conditioning demand through pre-cooling in Australian housing. Energy and Buildings 271.

Naderi, S., Pignatta, G., Heslop, S., MacGill, I. & Chen, D. (2022). Demand response via pre-cooling and solar pre-cooling: A review. Energy and Buildings 272.

Nandakumar, N., Rodriguez, J. W., Padhamnath, P., Nampalli, N., Aberle, A. G. & Duttagupta, S. (2022). Large-area monoPoly solar cells on 110 µm thin c–Si wafers with a rear n+ poly-Si/SiOx stack deposited by inline plasma-enhanced chemical vapour deposition. Progress in Photovoltaics: Research and Applications 31, 360-368.

Ng, L. W. T., Lee, S-W., Chang, D-W., Hodgkiss, J. M. & Vak, D. (2022). Organic Photovoltaics' New Renaissance: Advances Toward Roll-to-Roll Manufacturing of Non-Fullerene Acceptor Organic Photovoltaics. Advanced Materials Technology 7, 2101556.

Nie, S., Chin, R. L., Soufiani, A. M., Mehl, T., Theska, F., Haghdadi, N., Primig, S., Chan, C., Trupke, T. & Hameiri, Z. (2022). Temperature sensitivity maps of silicon wafers from photoluminescence imaging: The effect of gettering and hydrogenation. Progress in Photovoltaics: Research and Applications 30, 1298-1311.

Nielsen, M. P., Pusch, A., Sazzad, M. H., Pearce, P. M., Reece, P. J. & Ekins-Daukes, N. J. (2022). Thermoradiative Power Conversion from HgCdTe Photodiodes and Their Current–Voltage Characteristics. ACS Photonics 9, 1535-1540.

O'Neill, A., Jo, E., Choi, E., Park, J., Kim, J. H., Yun, J. S. & Seidel, J. (2022). Enhancing CZTSSe solar cells through electric field induced ion migration. Journal of Materials Chemistry A 10, 5642-5649.

Ostrom, I., Hossain, M. A., Burr, P. A., Hart, J. N. & Hoex, B. (2022). Designing 3d metal oxides: selecting optimal density functionals for strongly correlated materials. Phys Chem Chem Phys 24, 14119-14139.

Othman, M., Zhang, T., McMeekin, D. P., Fürer, S. O., Mao, W., Li, W., Scully, A. D., Chesman, A. S. R., Nakashima, P. N. H., Bach, U. & Etheridge, J. Structural and Photophysical Properties of Guanidinium–Iodide-Treated Perovskite Solar Cells. Solar RRL n/a, 2200852.

Othman, M., Zhang, T., McMeekin, D.P., Fürer, S.O., Mao, W., Li, W., Scully, A.D., Chesman, A.S.R., Nakashima, P.N.H., Bach, U. & Etheridge, J. (2022). Structural and Photophysical Properties of Guanidinium–Iodide-Treated Perovskite Solar Cells. Solar RRL, 2200852.

Othman, M., Zheng, F., Seeber, A., Chesman, A.S.R., Scully, A.D., Ghiggino, K.P., Gao, M., Etheridge, J. & Angmo, D. (2021). Millimeter-sized clusters of triple cation perovskite enables highly efficient and reproducible roll-to-roll fabricated inverted perovskite solar cells. Advanced Functional Materials 32, 2110700.

Pai, N., Chatti, M., Furer, S., Scully, AD., Raga, SR., Rai, N., Tan, B., Chesman A., Xu. Z., Rietwyk. K., Reddy S., Hora, Y., Sepalage, G., Gluck, N., Lira-Cantu, M., Bach, U. & Simonov, A. Solution Processable Direct Bandgap Copper-Silver-Bismuth Iodide Photovoltaics: Compositional Control of Dimensionality and Optoelectronic Properties. Advanced Energy Materials 12,32.

Pai, N., Chatti, M., Fürer, S.O., Scully, A.D., Raga, S.R., Rai, N., Tan, B., Chesman, A.S.R., Xu, Z., Rietwyk, K.J., Reddy, S.S., Hora, Y., Sepalage, G.A., Glück, N., Lira-Cantú, M., Bach, U. & Simonov, A.N. (2022). Solution processable direct bandgap copper-silver-bismuth iodide photovoltaics: Compositional control of dimensionality and optoelectronic properties. Advanced Energy Materials 12, 2201482.

Pan, W., Lin, J., Wu, J., Rong, B., Zhang, X., Chen, Q., Zhang, M., Wang, S., Sun, W., Wang, X. & Lan, Z. (2022). Interface modification by formamidine acetate for efficient perovskite solar cells. Solar Energy 232, 304-311.

Pan, Y., Yan, C., Zhao, X., Chen, W., Sun, K., Wu, Q., Ding, L. & Liu, F. (2022). 11.39% efficiency Cu2ZnSn(S,Se)4 solar cells from scrap brass. SusMat 2, 206-211.

Pearce, P. M., Broderick, C. A., Nielsen, M. P., Johnson, A. D. & Ekins-Daukes, N. J. (2022). Electronic and optical properties of SixGe1−x−ySny alloys lattice-matched to Ge. Physical Review Materials 6.

Pearce, P. M., Camarillo Abad, E. & Hirst, L. C. (2022). Designing transparent nanophotonic gratings for ultra-thin solar cells. Opt Express 30, 4528-4542.

Peerakiatkhajohn, P., Yun, J. H., Butburee, T., Nisspa, W. & Thaweesak, S. (2022). Surface plasmon-driven photoelectrochemical water splitting of a Ag/TiO(2) nanoplate photoanode. RSC Adv 12, 2652-2661.

Peiris, T. A. N., Benitez, J., Sutherland, L., Sharma, M., Michalska, M., Scully, A.D., Vak, D., Gao, M., Weerasinghe, H.C. & Jasieniak, J. (2022). A Stable Aqueous SnO2 Nanoparticle Dispersion for Roll-to-Roll Fabrication of Flexible Perovskite Solar Cells. Coatings, 12, 1948.

Peng, J., Kremer, F., Walter, D., Wu, Y., Ji, Y., Xiang, J., Liu, W., Duong, T., Shen, H., Lu, T., Brink, F., Zhong, D., Li, L., Lee Cheong Lem, O., Liu, Y., Weber, K. J., White, T. P. & Catchpole, K. R. (2022). Centimetre-scale perovskite solar cells with fill factors of more than 86 per cent. Nature 601, 573-578.

Pham, H. T., Weber, K. J., Duong, T. & Wong-Leung, J. (2022). Impact of Halide Anions in CsX (X = I, Br, Cl) on the Microstructure and Photovoltaic Performance of FAPbI3-Based Perovskite Solar Cells. Solar RRL 6, 2200345.

Prakash, A., Bruce, A. & MacGill, I. (2022). Insights on designing effective and efficient frequency control arrangements from the Australian National Electricity Market. Renewable and Sustainable Energy Reviews 161.

Prasad, A. A., Nishant, N. & Kay, M. (2022). Dust cycle and soiling issues affecting solar energy reductions in Australia using multiple datasets. Applied Energy 310.

Purnell, K., Bruce, A. G. & MacGill, I. (2022). Impacts of electrifying public transit on the electricity grid, from regional to state level analysis. Applied Energy 307.

Qian, C., Li, J., Sun, K., Jiang, C., Huang, J., Tang, R., Green, M., Hoex, B., Chen, T. & Hao, X. (2022). 9.6%-Efficient all-inorganic Sb2(S,Se)3 solar cells with a MnS hole-transporting layer. Journal of Materials Chemistry A 10, 2835-2841.

Qian, C., Sun, K. & Bao, W. (2022). Recent advance on machine learning of MXenes for energy storage and conversion. International Journal of Energy Research 46, 21511-21522.

Qian, C., Wang, R., Sun, K. & Bao, W. (2022). Dimensional engineering of anode materials for high performance potassium ion hybrid capacitor—A review. International Journal of Energy Research 46, 17976-17998.

Qian, C., Wang, R., Yu, F., Liu, H., Guo, C., Sun, K., Li, J. & Bao, W. (2022). Conductive Covalent Organic Frameworks Meet Micro-Electrical Energy Storage: Mechanism, Synthesis and Applications—A Review. Crystals 12.

Qiu, T., Akinoglu, E. M., Luo, B., Konarova, M., Yun, J. H., Gentle, I. R. & Wang, L. (2022). Nanosphere Lithography: A Versatile Approach to Develop Transparent Conductive Films for Optoelectronic Applications. Adv Mater 34, e2103842.

Rahaman, M. H., Holland, J., Hossain, M. A., Duan, L., Hoex, B., Mota-Santiago, P., Mitchell, V. D., Uddin, A. & Stride, J. A. (2022). Increased Efficiency of Organic Solar Cells by Seeded Control of the Molecular Morphology in the Active Layer. Solar Rrl 6.

Rahimpour, Z., Verbič, G. & Chapman, A. C. (2022). Can phase change materials in building insulation improve self-consumption of residential rooftop solar? An Australian case study. Renewable Energy 192, 24-34.

Rey, G., Kunz, O., Green, M. & Trupke, T. (2022). Luminescence imaging of solar modules in full sunlight using ultranarrow bandpass filters. Progress in Photovoltaics: Research and Applications 30, 1115-1121.

Rispler, J., Roberts, M. & Bruce, A. (2022). A change in the air? The role of offshore wind in Australia's transition to a 100 % renewable grid. The Electricity Journal 35.

Roberts, M. B., Sharma, A. & MacGill, I. (2022). Efficient, effective and fair allocation of costs and benefits in residential energy communities deploying shared photovoltaics. Applied Energy 305.

Rohr, J. A., Sartor, B. E., Duenow, J. N., Qin, Z., Meng, J., Lipton, J., Maclean, S. A., Romer, U., Nielsen, M. P., Zhao, S., Kong, J., Reese, M. O., Steiner, M. A., Ekins-Daukes, N. J. & Taylor, A. D. (2022). Identifying optimal photovoltaic technologies for underwater applications. iScience 25, 104531.

Sadat, S. A., Hoex, B. & Pearce, J. M. (2022). A Review of the Effects of Haze on Solar Photovoltaic Performance. Renewable and Sustainable Energy Reviews 167.

Safat Dipta, S., Schoenlaub, J., Habibur Rahaman, M. & Uddin, A. (2022). Estimating the potential for semitransparent organic solar cells in agrophotovoltaic greenhouses. Applied Energy 328.

Samadi, A., Ciesla, A., Chan, C. & Juhl, M. (2022). Implications of grain boundaries on quasi-steady-state photoconductance measurements in multicrystalline and cast-mono silicon. Solar Energy Materials and Solar Cells 238.

Samarakoon, S., Munro, P., Zalengera, C. & Kearnes, M. (2022). The afterlives of off-grid solar: The dynamics of repair and e-waste in Malawi. Environmental Innovation and Societal Transitions 42, 317-330.

Santoro, S., Aquino, M., Han Seo, D., Van Der Laan, T., Lee, M., Sung Yun, J., Jun Park, M., Bendavid, A., Kyong Shon, H., Halil Avci, A. & Curcio, E. (2022). Dimensionally controlled graphene-based surfaces for photothermal membrane crystallization. J Colloid Interface Sci 623, 607-616.

Sen, C., Hamer, P., Soeriyadi, A., Wright, B., Wright, M., Samadi, A., Chen, D., Stefani, B. V., Zhang, D., Wu, J., Jiang, F., Hallam, B. & Abbott, M. (2022). Impact of surface doping profile and passivation layers on surface-related degradation in silicon PERC solar cells. Solar Energy Materials and Solar Cells 235.

Sepalage, G.A., Weerasinghe, H., Rai, N., Duffy, N.W., Raga, S.R., Hora, Y., Gao, M., Vak, D., Chesman, A.S., Bach, U. and Simonov, A.N., 2022. Can Laminated Carbon Challenge Gold? Toward Universal, Scalable, and Low-Cost Carbon Electrodes for Perovskite Solar Cells. Advanced Materials Technologies, 7(6), p.2101148.

Shahrokhi, S., Dubajic, M., Dai, Z. Z., Bhattacharyya, S., Mole, R. A., Rule, K. C., Bhadbhade, M., Tian, R., Mussakhanuly, N., Guan, X., Yin, Y., Nielsen, M. P., Hu, L., Lin, C. H., Chang, S. L. Y., Wang, D., Kabakova, I. V., Conibeer, G., Bremner, S., Li, X. G., Cazorla, C. & Wu, T. (2022). Anomalous Structural Evolution and Glassy Lattice in Mixed-Halide Hybrid Perovskites. Small 18, e2200847.

Sharma, A. S., Pusch, A., Nielsen, M. P., Römer, U., Tayebjee, M. J. Y., Rougieux, F. E. & Ekins-Daukes, N. J. (2022). Constraints imposed by the sparse solar photon flux on upconversion and hot carrier solar cells. Solar Energy 237, 44-51.

Sharma, A., Duong, T., Liu, P., Soo, J. Z., Yan, D., Zhang, D., Riaz, A., Samundsett, C., Shen, H., Yang, C., Karuturi, S. K., Catchpole, K. & Beck, F. J. (2022). Direct solar to hydrogen conversion enabled by silicon photocathodes with carrier selective passivated contacts. Sustainable Energy & Fuels 6, 349-360.

Shehata, M. M., Phang, P., Basnet, R., Yin, Y., Kremer, F., Bartholazzi, G., Anderson, G. G., Macdonald, D. H. & Black, L. E. (2022). Outstanding surface passivation for highly efficient silicon solar cells enabled by innovative AlyTiOx-TiOx electron-selective contact stack. Solar RRL 2200550.

Shen, X., Hsiao, P.-C., Wang, Z., Phua, B., Lim, S. & Lennon, A. (2022). Refined nickel nucleation and plated metal adhesion induced by pulsed light-induced plating on picosecond laser-ablated silicon solar cells. Solar Energy Materials and Solar Cells 240.

Sheng, Y., Chen, W., Hu, F., Liu, C., Di, Y., Sheng, C., Chen, Z., Jia, B., Wen, X. & Gan, Z. (2022). Mechanism of Photoinduced Phase Segregation in Mixed-Halide Perovskite Microplatelets and Its Application in Micropatterning. ACS Appl Mater Interfaces 14, 12412-12422.

Shi, K., Zhang, F., Zhang, M., Chen, C., Zhang, W. & Huang, J. (2022). Fluorine-containing organic ammonium salt-doped inverted inorganic perovskite solar cells. Semiconductor Science and Technology 37.

Shin, S. J., Alosaimi, G., Choi, M. J., Ann, M. H., Jeon, G. G., Seidel, J., Kim, J., Yun, J. S. & Kim, J. H. (2022). Strategic Approach for Frustrating Charge Recombination of Perovskite Solar Cells in Low-Intensity Indoor Light: Insertion of Polar Small Molecules at the Interface of the Electron Transport Layer. ACS Applied Energy Materials 5, 13234-13242.

Soufiani, A. M., Lee-Chin, R., Fassl, P., Mahmud, M. A., Pollard, M. E., Zheng, J., Weber, J. W., Ho-Baillie, A., Trupke, T. & Hameiri, Z. (2022). Implied Open-circuit Voltage Imaging via a Single Bandpass Filter Method—Its First Application in Perovskite Solar Cells. Advanced Functional Materials 33.

Stuckelberger, J., Yan, D., Phang, S. P., Samundsett, C., Wang, J., Antognini, L., Haug, F.-J., Wang, Z., Yang, J., Zheng, P., Zhang, X. & Macdonald, D. (2023). Pre-annealing for improved LPCVD deposited boron-doped poly-Si hole-selective contacts. Solar Energy Materials and Solar Cells 251, 112123.

Sun, H., Huang, J., O'Neill, A., Yun, J. S., Young, T. L., Yan, C., Sun, K., Li, J., Nielsen, M. P., Cui, X., Wang, A., Seidel, J., Stride, J. A., Green, M. A. & Hao, X. (2022). Manipulating the Distributions of Na and Cd by Moisture-Assisted Postdeposition Annealing for Efficient Kesterite Cu2ZnSnS4 Solar Cells. Solar Rrl 6.

Sun, H., Huang, J., Young, T. L., Cong, J., Li, J., Sun, K., Yan, C., Soufiani, A. M., Cui, X., Nielsen, M. P., Zhang, X., Stride, J. A., Green, M. A. & Hao, X. (2022). Defect Engineering for Efficient Cu2ZnSnS4 Solar Cells via Moisture-Assisted Post-Deposition Annealing. ADVANCED OPTICAL MATERIALS 10.

Sun, K., Huang, J., Li, J., Yan, C. & Hao, X. (2022). Recent progress in defect engineering for kesterite solar cells. Science China Physics, Mechanics & Astronomy 66.

Sutherland, L. J., Benitez-Rodriguez, J. F., Angmo, D., Peiris, T. A. N., Simon, G. P., Gao M. & Weerasinghe H. (2022). Effect of out-gassing from polymeric encapsulant materials on the lifetime of perovskite solar cells. Solar Energy Materials and Solar Cells 246, 111887.

Tabernig, S. W., Soeriyadi, A. H., Romer, U., Pusch, A., Lamers, D., Juhl, M. K., Payne, D. N. R., Nielsen, M. P., Polman, A. & Ekins-Daukes, N. J. (2022). Avoiding Shading Losses in Concentrator Photovoltaics Using a Soft-Imprinted Cloaking Geometry. IEEE Journal of Photovoltaics 12, 1116-1127.

Tabernig, S. W., Yuan, L., Cordaro, A., Teh, Z. L., Gao, Y., Patterson, R. J., Pusch, A., Huang, S. & Polman, A. (2022). Optically Resonant Bulk Heterojunction PbS Quantum Dot Solar Cell. ACS Nano 16, 13750-13760.

Tabi, G. D., Pham, H. T., Zhan, H., Walter, D., Mayon, A. O., Peng, J., Duong, T., Shehata, M. M., Shen, H., Duan, L., Mozaffari, N., Li, L., Mahmud, M. A., Nguyen, H. T., Weber, K., Catchpole, K. R. & White, T. P. (2022). LiI doping of mixed-cation mixed-halide perovskite solar cells: Defect passivation, controlled crystallization and transient ionic response. Materials Today Physics 27, 100822.

Takamure, N., Caro, L. G., Fukata, N., Ho-Baillie, A. & McKenzie, D. R. (2022). Structural study of hermetic seal formed by water glass at low temperature when trapped between glass plates. Japanese Journal of Applied Physics 61.

Takamure, N., Sun, X., Nagata, T., Ho-Baillie, A., Fukata, N. & McKenzie, D. R. (2022). Thermodynamic Interpretation of the Meyer-Neldel Rule Explains Temperature Dependence of Ion Diffusion in Silicate Glass. Phys Rev Lett 129, 175901.

Tan, V., Dias, P. R., Chang, N. & Deng, R. (2022). Estimating the Lifetime of Solar Photovoltaic Modules in Australia. Sustainability 14.

Tebyetekerwa, M., Truong, T. N., Yan, W., Tang, C., Wibowo, A. A., Bullock, J., Du, A., Yan, C., Macdonald, D. & Nguyen, H. T. (2022). Twist Angle Effects on the Absorbance, Carrier Lifetime, and Diffusion Properties in Low Dimension Type-II MoS2/WS2 Heterobilayers. Advanced Materials Interfaces 2201649.

Teymur, B., Kim, Y., Huang, J., Sun, K., Hao, X. & Mitzi, D. B. (2022). Top Stack Optimization for Cu2BaSn(S, Se)4 Photovoltaic Cell Leads to Improved Device Power Conversion Efficiency beyond 6%. Advanced Energy Materials 12.

Thapa, B., Patterson, R. J., Conibeer, G. & Shrestha, S. (2022). Investigating Electronic, Optical, and Phononic Properties of Bulk gamma-M(2)ON(2) and beta-M(7)O(8)N(4) (M = Hf and Zr) Insulators Using Density Functional Theory. ACS Omega 7, 9196-9205.

Uddin, A. & Yi, H. (2022). Progress and Challenges of SnO2 Electron Transport Layer for Perovskite Solar Cells: A Critical Review. Solar Rrl 6.

Ul Hassan, M., Saha, S., Haque, M. E., Islam, S., Mahmud, A. & Mendis, N. (2022). A comprehensive review of battery state of charge estimation techniques. Sustainable Energy Technologies and Assessments 54.

Underwood, R., Kim, M., Drury, S., Zhang, Y., Wang, L., Chan, C. & Hallam, B. (2022). Abundant Material Consumption Based on a Learning Curve for Photovoltaic toward Net-Zero Emissions by 2050. Solar Rrl.

Vicari Stefani, B., Wright, M., Soeriyadi, A., Chen, D., Kim, M., Wright, B., Andronikov, D., Nyapshaev, I., Abolmasov, S., Wilson, G. & Hallam, B. (2022). Silicon Heterojunction Solar Cells and p-type Crystalline Silicon Wafers: A Historical Perspective. Solar Rrl 6.

Wang, A., He, M., Green, M. A., Sun, K. & Hao, X. (2022). A Critical Review on the Progress of Kesterite Solar Cells: Current Strategies and Insights. Advanced Energy Materials 13.

Wang, G., Lian, Q., Wang, D., Jiang, F., Mi, G., Li, D., Huang, Y., Wang, Y., Yao, X., Shi, R., Liao, C., Zheng, J., Ho-Baillie, A., Amini, A., Xu, B. & Cheng, C. (2022). Thermal-Radiation-Driven Ultrafast Crystallization of Perovskite Films Under Heavy Humidity for Efficient Inverted Solar Cells. Adv Mater 34, e2205143.

Wang, J., Phang, S. P., Samundsett, C., Li, Z., Truong, T. N., Yang, J., Wang , Z., Zheng, P., Zhang, X., Nguyen, H. T., Macdonald, D. & Stuckelberger, J. (2022). Development of Phosphorus-Doped Nanoscale Poly-Si Passivating Contacts via Inkjet Printing for Application in Silicon Solar Cells. ACS Applied Nano Materials.

Wang, R., Li, M., Sun, K., Zhang, Y., Li, J. & Bao, W. (2022). Element-Doped Mxenes: Mechanism, Synthesis, and Applications. Small 18, e2201740.

Wang, R., Li, M., Zhang, Y., Sun, K. & Bao, W. (2022). Atomic surface modification strategy of MXene materials for high-performance metal sulfur batteries. International Journal of Energy Research 46, 11659-11675.

Wang, R., Liu, H., Zhang, Y., Sun, K. & Bao, W. (2022). Integrated Photovoltaic Charging and Energy Storage Systems: Mechanism, Optimization, and Future. Small 18, e2203014.

Wang, R., Sun, K., Liu, H., Qian, C., Li, M., Zhang, Y. & Bao, W. (2022). Integrating a redox-coupled FeSe2/N–C photoelectrode into potassium ion hybrid capacitors for photoassisted charging. Journal of Materials Chemistry A 10, 11504-11513.

Wang, R., Sun, K., Zhang, Y., Li, B., Qian, C., Li, J., Liu, F. & Bao, W. (2022). Nanoscale interface engineering of inorganic Solid-State electrolytes for High-Performance alkali metal batteries. J Colloid Interface Sci 621, 41-66.

Wang, R., Sun, K., Zhang, Y., Qian, C. & Bao, W. (2022). Dimensional optimization enables high-performance capacitive deionization. Journal of Materials Chemistry A 10, 6414-6441.

Wang, R., Zhang, Y., Sun, K., Qian, C. & Bao, W. (2022). Emerging green technologies for recovery and reuse of spent lithium-ion batteries – a review. Journal of Materials Chemistry A 10, 17053-17076.

Wang, S., Scardera, G., Ma, F.-J., Zhang, Y., Payne, D., Abbott, M. & Hoex, B. (2022). Quantifying the Effect of Nanofeature Size on the Electrical Performance of Black Silicon Emitter by Nanoscale Modeling. IEEE Journal of Photovoltaics 12, 744-753.

Wang, S., Xie, T., Liang, R., Zhang, Y., Ma, F.-J., Payne, D., Scardera, G. & Hoex, B. (2022). An Artificial-Intelligence-Assisted Investigation on the Potential of Black Silicon Nanotextures for Silicon Solar Cells. ACS Applied Nano Materials 5, 11636-11647.

Wang, X., Fang, Y., Jin, H., Jiang, W., Gao, M., Burn, P. L. & E Shaw, P. (2022). Using charge collection narrowing to tune from broadband to narrowband all-polymer photodetectors. Physica Scripta. IOP Publishing, 97, 115817.

Wang, Y., Duan, L., Zhang, M., Hameiri, Z., Liu, X., Bai, Y. & Hao, X. (2022). PTAA as Efficient Hole Transport Materials in Perovskite Solar Cells: A Review. Solar Rrl 6.

Wibowo, A. A., Tebyetekerwa, M., Bui, A. D., Kremer, F., Saji, S., Yin, Z., Lu, Y., MacDonald, D. & Nguyen, H. T. (2022). High-Luminescence and Submillimeter-Scale MoS2Monolayer Growth Using Combinational Phase Precursors via Chemical Vapor Deposition. ACS Applied Electronic Materials 4, 5072–5080.

Wright, M., Soeriyadi, A. H., Kim, M., Wright, B., Stefani, B. V., Andronikov, D., Nyapshaev, I., Abolmasov, S., Abramov, A., Bonilla, R. S. & Hallam, B. (2022). On the kinetics of high intensity illuminated annealing of n-type SHJ solar cells: 0.4%abs efficiency gain in one second. Solar Energy Materials and Solar Cells 248.

Wu, Q., Hu, T., Liu, C., Yu, Y., Hou, H., Liu, R., Zhang, M. & Yu, H. (2022). Efficient Energy Level Modulation via Electrophilic KBF4 for High-Performance Inverted Planar Perovskite Solar Cells with Superior Stability. The Journal of Physical Chemistry C 126, 3375-3384.

Wu, Y., Zheng, P., Peng, J., Xu, M., Chen, Y., Surve, S., Lu, T., Bui, A. D., Li, N., Liang, W., Duan, L., Li, B., Shen, H., Duong, T., Yang, J., Zhang, X., Liu, Y., Jin, H., Chen, Q., White, T., Catchpole, K., Zhou, H. & Weber, K. (2022). 27.6% Perovskite/c-Si Tandem Solar Cells Using Industrial Fabricated TOPCon Device. Advanced Energy Materials 12, 2200821.

Xia, J., Wang, R., Qian, C., Sun, K., Liu, H., Guo, C., Li, J., Yu, F. & Bao, W. (2022). Supercapacitors of Nanocrystalline Covalent Organic Frameworks—A Review. Crystals 12.

Xing, Y., Qiao, N., Yu, J., Zhang, M., Dai, J., Niu, T., Wang, Y., Zhu, Y., Bu, L. & Lu, G. (2022). Spectroscopic depth profilometry of organic thin films upon inductively coupled plasma etching. Rev Sci Instrum 93, 073903.

Yamaguchi, M., Dimroth, F., Ekins-Daukes, N. J., Kojima, N. & Ohshita, Y. (2022). Overview and loss analysis of III–V single-junction and multi-junction solar cells. EPJ Photovoltaics 13.

Yang, C., Atwater, H. A., Baldo, M. A., Baran, D., Barile, C. J., Barr, M. C., Bates, M., Bawendi, M. G., Bergren, M. R., Borhan, B., Brabec, C. J., Brovelli, S., Bulović, V., Ceroni, P., Debije, M. G., Delgado-Sanchez, J.-M., Dong, W.-J., Duxbury, P. M., Evans, R. C., Forrest, S. R., Gamelin, D. R., Giebink, N. C., Gong, X., Griffini, G., Guo, F., Herrera, C. K., Ho-Baillie, A. W. Y., Holmes, R. J., Hong, S.-K., Kirchartz, T., Levine, B. G., Li, H., Li, Y., Liu, D., Loi, M. A., Luscombe, C. K., Makarov, N. S., Mateen, F., Mazzaro, R., McDaniel, H., McGehee, M. D., Meinardi, F., Menéndez-Velázquez, A., Min, J., Mitzi, D. B., Moemeni, M., Moon, J. H., Nattestad, A., Nazeeruddin, M. K., Nogueira, A. F., Paetzold, U. W., Patrick, D. L., Pucci, A., Rand, B. P., Reichmanis, E., Richards, B. S., Roncali, J., Rosei, F., Schmidt, T. W., So, F., Tu, C.-C., Vahdani, A., van Sark, W. G. J. H. M., Verduzco, R., Vomiero, A., Wong, W. W. H., Wu, K., Yip, H.-L., Zhang, X., Zhao, H. & Lunt, R. R. (2022). Consensus statement: Standardized reporting of power-producing luminescent solar concentrator performance. Joule 6, 8-15.

Yang, J., He, T., Li, M., Li, G., Liu, H., Xu, J., Zhang, M., Zuo, W., Qin, R., Aldamasy, M. H., Yuan, M., Li, Z., Malekshahi Byranvand, M., Saliba, M. & Abate, A. (2022). π-Conjugated Carbazole Cations Enable Wet-Stable Quasi-2D Perovskite Photovoltaics. Acs Energy Letters 7, 4451-4458.

Yang, Y., Bremner, S., Menictas, C. & Kay, M. (2022). Forecasting error processing techniques and frequency domain decomposition for forecasting error compensation and renewable energy firming in hybrid systems. Applied Energy 313.

Yang, Y., Bremner, S., Menictas, C. & Kay, M. (2022). Modelling and optimal energy management for battery energy storage systems in renewable energy systems: A review. Renewable and Sustainable Energy Reviews 167.

Yang, Z., Krügener, J., Feldmann, F., Polzin, J.I., Steinhauser, B., Le, T.T., Macdonald, D. & Liu, A. (2022). Impurity Gettering in Polycrystalline-Silicon Based Passivating Contacts—The Role of Oxide Stoichiometry and Pinholes. Advanced Energy Materials 2103773.

Yang, Z., Krügener, J., Feldmann, F., Polzin, J.I., Steinhauser, B., Aleshin, M., Le, T.T., Macdonald, D. & Liu, A. (2022). Comparing the Gettering Effect of Heavily Doped Polysilicon Films and Its Implications for Tunnel Oxide-Passivated Contact Solar Cells. Solar RRL 2200578.

Yang, Z., Krügener, J., Feldmann, F., Polzin, J.I., Steinhauser, B., Le, T.T., Macdonald, D. & Liu, A. (2022). Impurity Gettering in Polycrystalline-Silicon Based Passivating Contacts—The Role of Oxide Stoichiometry and Pinholes. Advanced Energy Materials 2103773.

Yang, Z., Krügener, J., Feldmann, F., Polzin, J.I., Steinhauser, B., Aleshin, M., Le, T.T., Macdonald, D. & Liu, A. (2022). Comparing the Gettering Effect of Heavily Doped Polysilicon Films and Its Implications for Tunnel Oxide-Passivated Contact Solar Cells. Solar RRL 2200578.

Yu, W., Liu, C., Sun, X., Hou, T., Yang, X., Wang, X., Yu, Y., Chen, K., Li, H., Huang, Y. & Zhang, M. (2022). Spontaneous relaxation of 2D passivation layer contributes to the aging-induced performance enhancement of perovskite solar cells. Nano Research 16, 521-527.

Yu, Y., Liu, R., Liu, C., Hou, T., Wu, Q., Zhang, M. & Yu, H. (2022). Dimensional Engineering Enables 1.31 V Open-Circuit Voltage for Efficient and Stable Wide-Bandgap Halide Perovskite Solar Cells. Solar Rrl 6.

Yuan, X., Li, J., Huang, J., Yan, C., Cui, X., Sun, K., Cong, J., He, M., Wang, A., He, G., Mahboubi Soufiani, A., Jiang, J., Zhou, S., Stride, J. A., Hoex, B., Green, M. & Hao, X. (2022). 10.3% Efficient Green Cd-Free Cu(2) ZnSnS(4) Solar Cells Enabled by Liquid-Phase Promoted Grain Growth. Small 18, e2204392.

Zeng, Y., Huang, J., Li, J., Sun, K., Shah, U. A., Deng, H., Zhang, X., Sha, C., Qian, C., Song, H. & Hao, X. (2022). Comparative Study of TiO2 and CdS as the Electron Transport Layer for Sb2S3 Solar Cells. Solar Rrl 6.

Zhang, C., Baktash, A., Zhong, J. X., Chen, W., Bai, Y., Hao, M., Chen, P., He, D., Ding, S., Steele, J. A., Lin, T., Lyu, M., Wen, X., Wu, W. Q. & Wang, L. (2022). Dual Metal-Assisted Defect Engineering towards High-Performance Perovskite Solar Cells. Advanced Functional Materials 32.

Zhang, D., Datta, K., Zardetto, V., Veenstra, S., Coletti, G. & Janssen, R. A. J. (2022). Validated Method for Evaluating the Four-Terminal Perovskite/Si Tandem Cell Performance and its Efficiency Potential. Solar Rrl 7.

Zhang, F., Sun, X., Xie, H., Cai, X., Zheng, B., Yu, H., Liu, E., Hao, X. & Zhang, M. (2022). Unraveling the Mechanism of Ion-Migration Suppression by Interstitial Doping for Operationally Stable CsPbI2Br Perovskite Solar Cells. Chemistry of Materials 34, 1010-1019.

Zhang, J., Chang, N., Fagerholm, C., Qiu, M., Shuai, L., Egan, R. & Yuan, C. (2022). Techno-economic and environmental sustainability of industrial-scale productions of perovskite solar cells. Renewable and Sustainable Energy Reviews 158.

Zhang, J., Li, S., Xi, F., Wan, X., Ding, Z., Chen, Z., Ma, W. & Deng, R. (2022). Si@SiO /Ag composite anodes with high initial coulombic efficiency derive from recyclable silicon cutting waste. Chemical Engineering Journal 447.

Zhang, J., Tebyetekerwa, M. & Nguyen, H. T. (2022). Interfacing transition metal dichalcogenides with chromium germanium telluride quantum dots for controllable light-matter interactions. Journal of Colloid and Interface Science. Elsevier Inc. 611, 432–440.

Zhang, J., Tebyetekerwa, M. & Nguyen, H. T. (2022). Interfacing transition metal dichalcogenides with chromium germanium telluride quantum dots for controllable light-matter interactions. Journal of Colloid and Interface Science. Elsevier Inc. 611, 432–440.

Zhang, M. & Lin, Z. (2022). Efficient interconnecting layers in monolithic all-perovskite tandem solar cells. Energy & Environmental Science 15, 3152-3170.

Zhang, M. & Lin, Z. (2022). Monolithic Perovskite Solar Capacitor Enabled by Double-Sided TiO2 Nanotube Arrays. ACS Energy Letters 7, 1260-1265.

Zhang, S. M. F., Seif, J. P., Abbott, M. D., Le, A. H. T., Allen, T. G., Perez-Wurfl, I. & Hameiri, Z. (2022). Illumination-dependent temperature coefficients of the electrical parameters of modern silicon solar cell architectures. Nano Energy 98.

Zhang, S. M. F., Seif, J. P., Abbott, M. D., Le, A. H. T., Allen, T. G., Perez-Wurfl, I. & Hameiri, Z. (2022). Illumination-dependent temperature coefficients of the electrical parameters of modern silicon solar cell architectures. Nano Energy 98.

Zhang, Y., Conibeer, G., Liu, S., Zhang, J. & Guillemoles, J. F. (2022). Review of the mechanisms for the phonon bottleneck effect in III–V semiconductors and their application for efficient hot carrier solar cells. Progress in Photovoltaics: Research and Applications 30, 581-596.

Zhang, Y., Huang, J., Zhang, P., Cong, J., Li, J. & Hao, X. (2022). Formation mechanisms of voids and pin-holes in CuSbS2 thin film synthesized by sulfurizing a co-sputtered Cu–Sb precursor. Journal of Materials Chemistry A 10, 8015-8024.

Zhang, Y., Scardera, G., Wang, S., Abbott, M., Payne, D. & Hoex, B. (2022). Scanning Electron Microscopy Dopant Contrast Imaging of Phosphorus-Diffused Silicon. Advanced Materials Technologies 8.

Zhang, Y., Veeken, T., Wang, S., Scardera, G., Abbott, M., Payne, D., Polman, A. & Hoex, B. (2022). Plasma Focused Ion Beam Tomography for Accurate Characterization of Black Silicon Validated by Full Wave Optical Simulation. Advanced Materials Technologies 7.

Zhang, Y., Zhu, Y., Hu, M., Pai, N., Qin, T., Cheng, Y.B., Bach, U., Simonov, A.N. and Lu, J., 2022. Self-enhancement of efficiency and self-attenuation of hysteretic behavior of perovskite solar cells with aging. The Journal of Physical Chemistry Letters, 13(12), pp.2792-2799.

Zhang, Z., Xi, F., Chen, X., Li, S., Ma, W., Ding, Z., Qu, T., Dai, Y. & Deng, R. (2022). Improved lithium-ion batteries with coral-like anodes made of recycled spherical porous silicon coated with nitrogen-doped carbon. Environmental Chemistry Letters 20, 3377-3385.

Zhang, Z., Xi, F., Ma, Q., Wan, X., Li, S., Ma, W., Chen, X., Chen, Z., Deng, R., Ji, J., Fan, H. J. & Chong, C. M. (2022). A nanosilver-actuated high-performance porous silicon anode from recycling of silicon waste. Materials Today Nano 17.

Zhang, Z., Yang, N., Xi, F., Chen, X., Li, S., Ma, W., Lei, Y. & Deng, R. (2022). Purification of silicon from waste photovoltaic cells and its value-added application in lithium-ion batteries. New Journal of Chemistry 46, 11788-11796.

Zhao, J., Fürer, S. O., McMeekin, D. P., Lin, Q., Lv, P., Ma, J., Tan, W. L., Wang, C., Tan, B., Chesman, A. S. R., Yin, H., Scully, A. D., McNeill, C. R., Mao, W., Lu, J., Cheng, Y.-B. & Bach, U. (2023). Efficient and stable formamidinium–caesium perovskite solar cells and modules from lead acetate-based precursors. Energy & Environmental Science.

Zhao, Y., Yu, Z., Hu, J., Zheng, Z., Ma, H., Sun, K., Hao, X., Liang, G., Fan, P., Zhang, X. & Su, Z. (2022). Over 12% efficient kesterite solar cell via back interface engineering. Journal of Energy Chemistry 75, 321-329.

Zheng, F., Angmo, D., Hall, C. R., Rubanov, S., Yuan, F-F., Laird, J. S., Gao, M., Smith, T. A. & Ghiggino K. P. (2022). Brownian Tree-Shaped Dendrites in Quasi-2D Perovskite Films and Their Impact on Photovoltaic Performance. Applied Materials & Interfaces 9, 2102231.

Zheng, F., Raeber, T., Rubanov, S., Lee, C., Seeber, A., Hall, C., Smith, T. A. , Gao, M., Angmo, D. & Ghiggino K. P. (2022). Spontaneous Formation of a Ligand-based 2D Capping Layer on the Surface of Quasi-2D Perovskite Films. Applied Materials & Interfaces 14, 51910.

Zheng, J., Wang, G., Duan, W., Mahmud, M. A., Yi, H., Xu, C., Lambertz, A., Bremner, S., Ding, K., Huang, S. & Ho-Baillie, A. W. Y. (2022). Monolithic Perovskite–Perovskite–Silicon Triple-Junction Tandem Solar Cell with an Efficiency of over 20%. Acs Energy Letters 7, 3003-3005.

Zhou, S., Sun, K., Toe, C. Y., Yin, J., Huang, J., Zeng, Y., Zhang, D., Chen, W., Mohammed, O. F., Hao, X. & Amal, R. (2022). Engineering a Kesterite-Based Photocathode for Photoelectrochemical Ammonia Synthesis from NO(x) Reduction. Adv Mater 34, e2201670.

Zhou, X., Zhang, W., Wang, S., Wen, F., Chen, Q., Shen, X., Hu, X., Peng, C., Ma, Z., Zhang, M., Huang, Y., Yang, S. & Zhang, W. (2022). Managing interfacial properties of planar perovskite solar cells using Y3N@C80 endohedral metallofullerene. Science China Materials 65, 2325-2334.

Zhou, Z., Juhl, M. K., Vaqueiro-Contreras, M., Rougieux, F. & Coletti, G. (2022). Electronic Properties of Light- and Elevated Temperature-Induced Degradation in Float-Zone Silicon. IEEE Journal of Photovoltaics 12, 1369-1376.

Zhou, Z., Rougieux, F., Siriwardhana, M. & Coletti, G. (2022). Characterisation of striations in n-type silicon wafer processed with polysilicon contacts. Solar Energy Materials and Solar Cells 248.

Zhou, Z., Tkachenko, S., Bahl, P., Tavener, D., de Silva, C., Timchenko, V., Jiang, J. Y., Keevers, M. & Green, M. (2022). Passive PV module cooling under free convection through vortex generators. Renewable Energy 190, 319-329.

Zhou, Z., Vaqueiro-Contreras, M., Juhl, M. K. & Rougieux, F. (2022). Electronic Properties of the Boron–Oxygen Defect Precursor of the Light-Induced Degradation in Silicon. IEEE Journal of Photovoltaics 12, 1135-1141.

Zhu, R., Zhu, Y., Chen, F., Patterson, R., Zhou, Y., Wan, T., Hu, L., Wu, T., Joshi, R., Li, M., Cazorla, C., Lu, Y., Han, Z. & Chu, D. (2022). Boosting moisture induced electricity generation from graphene oxide through engineering oxygen-based functional groups. Nano Energy 94.

Zou, S., Ye, X., Ding, J., Wu, C., Wang, S., Scardera, G., Abbott, M., Zhang, Y., Fan, R., Xu, Y., Wang, X., Shen, M. & Su, X. (2022). A solid strategy to realize heteroface selective emitter and rear passivated silicon solar cells. Progress in Photovoltaics: Research and Applications 30, 1343-1353.

8.5 CONFERENCE PAPERS AND PRESENTATIONS

Abdullah-Vetter, Z., Dwivedi, P., Buratti, Y., Krzywicki, A., Sowmya, A., Trupke, T. & Hameiri, Z. (2022). Automated Analysis of Internal Quantum Efficiency Using Chain Order Regression. 2022 IEEE 49th Photovoltaics Specialists Conference (PVSC), 0476-0478. (Poster Prize)

Abdullah-Vetter, Z., Dwivedi, P., Chin, R. L., Wright, B., Trupke, T. & Hameiri, Z. (2022). Using machine learning to predict the complete degradation of accelerated damp heat testing in just 10% of testing time. 2022 IEEE 49th Photovoltaics Specialists Conference (PVSC), 0472-0474.

Ahmad, V., White, T., Catchpole, K., Weber, K. & Walter, D. (2022). Investigating reverse bias recovery behaviour of perovskite solar cells. Asia Pacific Solar Research Conference 2022. Newcastle: APVI. 29 Nov. – 1 Dec. 2022

Al-Dhahir, I., McNab, S., Yu, M., Shaw, E., Hamer, P. & Bonilla, R. S. (2022). The influence of surface electric fields on the chemical passivation of Si-SiO2 interfaces after firing. SiliconPV 2021, The 11th International Conference on Crystalline Silicon Photovoltaics.

An, N.G. (2022). Fully Printed Organic Photovoltaics to Produce High-Throughput and Reliable Photovoltaic Data. Asia Pacific Solar Research Conference/Australian Centre for Advanced Photovoltaics 2022. Newcastle: APVI. 29 Nov. – 1 Dec. 2022.

Augusto, A., Le, A.H.T., Srinivasa, A., Bowden, S. & Hameiri, Z. (2022). Operation of silicon cells with very high bulk resistivities in relevant field conditions of illumination and temperature. 12th International Conference on Crystalline Silicon Photovoltaics, Konstanz, Germany, April 2022.

Augusto, A., Le, A.H.T., Srinivasa, A., Bowden, S. & Hameiri, Z. (2022). Performance of silicon solar cells and modules using high-resistivity wafers in relevant field conditions of illumination, temperature, and shading, MRS Spring Meeting, 2022.

Bach, U. (2022). The end of traditional manual research, a new era of robotics for rapid energy materials discovery. 10th ACAP Conference 2022. Newcastle. 1 – 2 December 2022

Bartholazzi, G. (2022). Evaporated Cu2O as a hole-selective contact for c-Si solar cells. 8th World Conference on Photovoltaic Energy Conversion (WCPEC). Milan, Italy. 26–30 September 2022.

Bartholazzi, G., Macdonald, D. & Black, L. (2022). Evaporated Cu2O as a hole-selective contact for c-Si solar cells. Asia Pacific Solar Research Conference 2022. Newcastle: APVI. 29 Nov. – 1 Dec. 2022

Benitez, J., Chen, D., Scully, A.D., Easton, C.D., Vak, D., Li, H., Shaw, P.E., Burn, P.L., Caruso, R.A. & Gao, M. (2022). Slot-Die Coating of a Formamidinium-Cesium Mixed-Cation Perovskite for Roll-to-Roll Fabrication. Asia Pacific Solar Research Conference 2022. Newcastle: APVI. 29 Nov. – 1 Dec. 2022

Bing, J., McKenzie, D., Stals, T., Kypriotis, M., Zheng, J. & Ho-Baillie, A. (2022). Total equivalent energy efficiency metric for BIVP and spectrum shifting windows. Asia Pacific Solar Research Conference 2022. Newcastle: APVI. 29 Nov. – 1 Dec. 2022

Black, L. E. (2022). Improved Auger recombination models: Consequences for c-Si solar cells. 12th International Conference on Crystalline Silicon Photovoltaics (SiliconPV). Konstanz, Germany. 28 March – 1 April 2022.

Black, L. E. (2022). Improved Auger recombination models: Consequences for c-Si solar cells. 12th International Conference on Crystalline Silicon Photovoltaics (SiliconPV). Konstanz, Germany. 28 March – 1 April 2022.

Blakers, A. (2022). Rapid, Deep and Cheap Emissions Reductions. 8th World Conference on Photovoltaic Energy Conversion. 26 – 30 September 2022. Milan, Italy.

Broadhurst, G. & Ernst, M. (2022). Low-cost solar irradiance measurement by software-based sun tracking: Pyrheliometer need not apply. 10th ACAP Conference 2022. Newcastle, Australia, 1 – 2 December 2022.

Bui, A.D., Nguyen, K.D.N., Macdonald, D. & Nguyen, H. (2022). Imaging Electrical Properties of Perovskite Solar Cells by Illumination Intensity and Temperature Dependent Photoluminescence. 8th World Conference on Photovoltaic Energy Conversion. 26 – 30 September 2022. Milan, Italy.

Burn, P. L., Mallo, N., Jin, H., McAnally, S., Chu, R., Jiang, L., Gentle, I., Shaw. P. (2022). Tuning dielectric constants for organic semiconductor-based solar cells. The 17th Pacific Polymer Conference.

Burn, P. L., Wang, X., Rakstys, K., Li, H., Ranasinghe, S., Saghaei, J., Jin, H., Zhang, G., Lai. J., Jack, K., Gentle, I., Shaw, P. (2022). 2D or not 2D – that is the perovskite question. 17th Conference of the International Association of Colloid and Interface Scientists.

Burn, P. L., Wang, X., Rakstys, K., Li, H., Ranasinghe, S., Saghaei, J., Jin, H., Zhang, G., Lai. J., Jack, K., Gentle, I., Shaw, P. (2022). 2D or not 2D – that is the perovskite question. International Conference on the Physics of Semiconductors 2022.

Burn, P. L., Wang, X., Rakstys, K., Stephen, M., Gao, M., Ranasinghe, S., Saghaei, J., Jin, H., Zhang, G., Lai. J., Hutchinson, K., Jack, K., Li, H., Gentle, I., Shaw, P. (2022). Manipulating interfaces in inverted perovskite solar cells. National Renewable Energy Agency, USA.

Cai, Y., Soeriyadi, A., Chen, R., Hallam, B. & Rougieux, F. (2022). The fundamental difference in polysilicon crystallinity of p-type and n-type polysilicon contacts. 33rd International Photovoltaic Science and Engineering Conference. Nagoya, Japan. 13-17 November 2022.

Chang, N. & Deng, R. (2022). PP4 Manufacturing Issues summary. 10th ACAP Conference 2022. Newcastle. 1 – 2 December 2022

Chen, Y., Wang, L., Lee, S., Chen, D., Zhang, X., Pietro P. Altermatt, P.P., Feng, Z. & Verlinden, P. (2022). Technology Evolution of PV Industry: Learning from Historical and Recent Progress. 8th World Conference on Photovoltaic Energy Conversion. 26 – 30 September 2022. Milan, Italy.

Chesman, A.S.R. (2022). Material Selection and Modelling for Low-Cost Perovskite Solar Cell Production. Advanced PV30 conference. 13-14 June 2022. Online, Australia.

Chin, R. A. L., Soufiani, A., Zheng, J., Fassl, P., Ho-Baillie, A., Paetzold, U., Trupke, T. & Hameiri, Z. (2022). Photodoping causes inconsistencies in the injection-dependent lifetimes of perovskite thin films. 2022 IEEE 49th Photovoltaics Specialists Conference (PVSC), 0368-0368.

Choi, E., Zhang, Y., Mahboubi Soufiani, A., Lee, M., Webster, R., Pollard, M.E., Reece, P., Lim, J., Lee, W., Seidel, J., Yun, J.-H. & Yun, J. (2022). Exploration of Sub-Bandgap States in 2D Halide 1 Perovskite Single-Crystal Photodetector. 8th World Conference on Photovoltaic Energy Conversion. 26 – 30 September 2022. Milan, Italy.

Ciesla, A., Teymouri, A., Wang, L., Kim, M., Chan, C., Chen, R., Manshanden, P., Van Aken, B., Dijksterhuis, J.J., Hallam, B., & Coletti, G. (2022). LeTID in Real Life: Incoming Cell Qualification for Module Manufacturers. 8th World Conference on Photovoltaic Energy Conversion. 26 – 30 September 2022. Milan, Italy.

Cook, A., Jones, T., Duffy, N., Donne, S. & Wilson, G. (2022). Effect of Lewis Acid, Lewis Base and TOPO Passivation in MAPbI3 and Mixed Perovskites. Asia Pacific Solar Research Conference 2022. Newcastle: APVI. 29 Nov. – 1 Dec. 2022

Corkish, R. (2022). PP5 Education, Training & Outreach summary. 10th ACAP Conference 2022. Newcastle. 1 – 2 December 2022

Corkish, R., & Kumar, S. (2021). Reuse of Deconstructed PV Glass Modules. Asia Pacific Solar Research Conference. Sydney, 16 Dec 2021-17 Dec 2021.

Corkish, R., Leyton, D. & Chang, N. (2022). The Beginnings of R&D and Industrial Development of Solar Module End-of-Life Management in Australia, EnScience 2022, online, 21-22 April 2022

Cui, X., Sun, K., Hoex, B. & Hao, X. (2022). Optical management in enhancing the efficiency of Cd-free CZTS solar cells by wide bandgap oxides. 33rd International Photovoltaic Science and Engineering Conference. Nagoya, Japan. 13-17 November 2022.

Cui, X., Sun, K., Hoex, B. & Hao, X. (2022). Tailoring ZnMgO electro-optical properties for Efficient Kesterite Solar Cells. Asia Pacific Solar Research Conference 2022. Newcastle: APVI. 29 Nov. – 1 Dec. 2022

Dehghanimadvar, M., Chang, N. & Egan, R. (2022). Economic Optimisation of Supportive and Protective Policy Mechanisms for Promoting Local PV Manufacturing in the Global Market. 8th World Conference on Photovoltaic Energy Conversion. 26 – 30 September 2022. Milan, Italy.

Dehghanimadvar, M., Chang, N.L. & Egan, R. (2022). Social and Environmental Impacts of Australian PV Module Production: A Multi-objective Optimization. Asia Pacific Solar Research Conference 2022. Newcastle: APVI. 29 Nov. – 1 Dec. 2022

Dehghanimadvar, M., Egan, R. & Chang, N.L. (2022). A Policy Framework for Promoting Local PV Manufacturing in Australia. Asia Pacific Solar Research Conference 2022. Newcastle: APVI. 29 Nov. – 1 Dec. 2022

Deng, R., Bowen, O., Dias, P. & Egan, R. (2022). Characterising the Composition of End-of-Life Solar Panel Materials in Australia. 8th World Conference on Photovoltaic Energy Conversion. 26 – 30 September 2022. Milan, Italy.

Deng, R., Jose Bilbao, J., Marina Lunardi, M. & Richard Corkish, R. (2022). IEA PVPS Task 12 PV Sustainability: Working progress and Australian Contributions 2021-2022. Asia Pacific Solar Research Conference 2022. Newcastle: APVI. 29 Nov. – 1 Dec. 2022

Deng, S. & Bach, U. (2022). Back-contact perovskite solar cell fabrication via microsphere lithography. Asia Pacific Solar Research Conference 2022. Newcastle: APVI. 29 Nov. – 1 Dec. 2022

Dias, P. R., Kim, M., Lennon, A. & Hallam, B. (2022). What is the Role of Recycling in the Solar Terawatt Future? 2022 IEEE 49th Photovoltaics Specialists Conference (PVSC), 1047-1047.

Drury, S., Kim, M., Dias, P., Zhang, Y., Underwood, R., Wang, L., Altermatt, P.P. & Hallam, B. (2022). Identifying Methods to Reduce Emission Intensity of Centralised PV Deployment: Life Cycle Assessment Case Study of a 30MW PV Plant. 8th World Conference on Photovoltaic Energy Conversion. 26 – 30 September 2022. Milan, Italy.

Duong, T. (2022). Bulk Incorporation with 4-methylphenethylammonium chloride for Efficient and Stable Perovskite Cells. 10th ACAP Conference 2022. Newcastle. 1 – 2 December 2022

Dwivedi, P., Buratti, Y., Abdullah Vetter, Z., Liu, G., Javier, G. M., Trupke, T. & Hameiri, Z. (2022). Accelerating the Solar Energy Transition through Artificial Intelligence. 33rd International Photovoltaic Science and Engineering Conference. Nagoya, Japan. 13-17 November 2022.

Dwivedi, P., Chin, R. L., Trupke, T. & Hameiri, Z. (2022). A deep learning approach to increase luminescence image resolution of solar cells. 2022 IEEE 49th Photovoltaics Specialists Conference (PVSC), 329-329.

Dwivedi, P., Weber, J., Chin, R.L., Trupke, T. & Hameiri, Z. (2022). Super-resolution luminescence imaging of solar cells using deep learning. 33rd International Photovoltaic Science and Engineering Conference, 2022.

Ekins-Daukes, N. (2022). The Quantum Well Solar Cell: The concept to record efficiency. 33rd International Photovoltaic Science and Engineering Conference. Nagoya, Japan. 13-17 November 2022.

Ekins-Daukes, N. J., Nielsen, M. P., Pusch, A., Sazzad, M. H., Pearce, P. M. & Reece, P. J. (2022). Demonstrating the Thermoradiative Diode: Generating Electrical Power Through Radiative Emission. 2022 IEEE 49th Photovoltaics Specialists Conference (PVSC), 0959-0959.

Ekins-Daukes, N.J. Fundamentals of photovoltaics. Tutorial AM1. 2022 IEEE 49th Photovoltaics Specialists Conference (PVSC)

Ernst, M. & Asselineau, C.-A. (2022). Impact of ground albedo surrounding large PV systems on bifacial illumination by ray tracing. 10th ACAP Conference 2022. Newcastle, Australia, 1 – 2 December 2022.

Ernst, M. (2022). Tutorial: Photovoltaic Solar Cell to Module Modelling. 2022 MRS Spring Meeting. Honolulu, USA, 8 – 13 May 2022.

Ernst, M., Black, L., Theeuwes, R., Macdonald, D. & Kessels, E. (2022). High-Efficiency PERL Solar Cells Using Simultaneous Laser Local Contact Opening and n+ Doping from POx/Al2O3 Passivation Stacks. 8th World Conference on Photovoltaic Energy Conversion. Milan, Italy, 26 – 30 September 2022.

Ford, E., Hoex, B. & Peters, I. M. (2022). Impact of the 2019-2020 Australian Black Summer Wildfires on Photovoltaic Energy Production. 2022 IEEE 49th Photovoltaics Specialists Conference (PVSC), 1191-1194. (Plenary)

Ford, E., Hoex, B. & Peters, M. (2022). Impact of the 2019-2020 Australian Black Summer Wildfires on Photovoltaic Energy Production. 8th World Conference on Photovoltaic Energy Conversion. 26 – 30 September 2022. Milan, Italy.

Foti, M., Guillevin, N., Carr, A.J., Van Aken, B., Rametta, F., Sciuto, M., Spampinato, A., Di Matteo, A., Coletti, G. & Gerardi, C. (2022). 1% Absolute Power Gain of Silicon Heterojunction Metal Wrap Through Laminates Produced in Industrial Pilot Line. 8th World Conference on Photovoltaic Energy Conversion. 26 – 30 September 2022. Milan, Italy.

Foti, M., Guillevin, N., Kossen, E., Okel, L., Hoek, E., Carr, A., van Aken, B., Manshanden, P., Rametta, F., Sciuto, M., Spampinato, A., Di Matteo, A., Ragonesi, A., Coletti, G. & Gerardi, C. (2022). High Efficiency Silicon Heterojunction Metal Wrap Through Produced in Industrial Pilot Line. 2022 IEEE 49th Photovoltaics Specialists Conference (PVSC), 1306-1309.

Gaia Maria Javier, G.M., Rhett Evans, R., Priya Dwivedi, P. Yoann Buratti, Y., Thorsten Trupke, T. & Ziv Hameiri, Z. (2022). Evaluation of variations in solar cell production lines using time-series electroluminescence images. Asia Pacific Solar Research Conference 2022. Newcastle: APVI. 29 Nov. – 1 Dec. 2022

Gao, M. (2022). Rollable and Self-Deployable Solar Arrays for Small Satellites. 20th Australian Space Research Conference. 26-28 Sep. 2022. Sydney, Australia.

Gao, M., Vak, D., Angmo, D., Sutherland, L., Scully, A.D., Weerasinghe, H. & Chesman A.S.R.(2022). Roll-to-Roll Compatible Process for Highly Efficient Thin Film Solar Cells. Advanced PV30 conference. 13-14 June 2022. Online, Australia.

Green M. (2022). Cost Projections for Solar PV. Global Smart Energy Summit 2020, Sydney, Australia. 30 Sep 2022

Green, M.A. (2022). 1st China PV Green Supply Chain Conference. Jiaxing, Zhejiang province, 18 August 2022 (virtual, for opening ceremony)

Green, M.A. (2022). SNEC 16th (2022) International Photovoltaic Power Generation and Smart Energy Conference & Exhibition. 26-29 December 2022, Shanghai, China (virtual keynote speech)

Green, M.A. (2022). Ultra-Low Cost Renewables Session, Sydney Energy Forum. 12 July, Sydney 12-13 July 2022 (panel speaker)

Green, M.A. (2022). World Renewable Energy Congress XXI on 5 December, Murdoch University, Perth (keynote speech)

Green, M.A. (2022). Japan Prize Foundation Ceremony, 13 April 2022, Japan

Green, M.A. (2022). keynote speech for PV Magazine virtual annual Award Ceremony, Sydney, Australia, 3 February 2022

Green, M.A. (2022). Photovoltaic visions. Fossil-free electricity production Seminar, the Royal Swedish Academy of Sciences, Sweden, 18 May 2022 (in person)

Green, M.A. (2022). Present status and future developments in photovoltaics. Solar Energy workshop at College de France. Paris, France. 21 April 2022 (invited lecture, recorded virtually)

Green, M.A. (2022). Recent Developments and Future Trends in Solar Photovoltaics. IEEE Latin American Electron Devices Conference. 4-6 July 2022 Cancun, Mexico (virtual)

Green, M.A. (2022). Recent developments in photovoltaics and role in a low-carbon future. Pujiang Innovation Forum 2022, 16 May 2022, Shanghai, China (online)

Green, M.A. (2022). Recent Developments in Photovoltaics. UNSW Engineering Distinguished Seminar Series, UNSW Sydney, 23 November 2022

Green, M.A. (2022). Recent developments in photovoltaics. 2022 Asia-Pacific Solar Research Conference, 29 November 2022, Newcastle, NSW (opening address)

Green, M.A. (2022). Recent Developments in Photovoltaics. Asia Pacific Solar Research Conference 2022. Newcastle: APVI. 29 Nov. – 1 Dec. 2022

Green, M.A. (2022). Recent Developments in Photovoltaics. Carbon Neutrality and Sustainable Environment Conference (I), HKTech Forum, Hong Kong5-7 October 2022

Green, M.A. (2022). Recent developments in photovoltaics. Energy Oceania Global Renewable Energy Meet. Melbourne. 29-31 August 2022 (virtual plenary)

Green, M.A. (2022). seminar Recent Developments in Photovoltaics. Surrey University, UK, 7 October 2022 (online)

Green, M.A. (2022). Silicon Solar cells: Past and Future. World Conference on Photovoltaic Energy Conversion. Milan, Italy, 26 September 2022, (WCPEC-8 Award speech, in person)

Green, M.A. (2022). speech for 2022 Millennium Technology Prize Award, Helsinki, Finland, 25 October 2022

Green, M.A. (2022). speech for Lifetime Achievement for the Advancement of Renewables Award for Abdullah bin Hamad Al-Attiyah International Energy Awards, 12 October; Doha, UAE

Green, M.A. (2022). Toward Commercialisation of Advanced PV 2030. The Advanced PV 2030 Symposium. 14-17 June 2022, Sydney (plenary, pre-recorded virtual)

Guo, Q. & Zhang, T. (2022). Influence of potassium ion incorporation on CsPbIBr2 perovsktite. Asia Pacific Solar Research Conference 2022. Newcastle: APVI. 29 Nov. – 1 Dec. 2022

Gupta, S., Shaw, P., Kumar, S., Burn, P. L., (2022). Investigating the role of fluorinated organic cations in boosting the performance of lead halide perovskite-based solar cells. 2022 Australasian Community for Advanced Organic Semiconductors (AUCAOS) Symposium.

Güsken, N.A., Fu, M., Zapf, M., Nielsen, M.P., Dichtl, P., Roder, R., Ronning, C., Brongersma, M. L. & Oulton, R. F. (2022). Fluorescence enhancement of Er3+-ions using reverse hybrid plasmonic nano-focusing. 2022 Conference on Lasers and Electro-Optics, CLEO 2022. 15- 20 May 2022. San Jose, CA, USA.

Hall, R. N. K., Zhong, H., Kunz, O., Trupke, T. & Rougieux, F. E. (2022). Determining the sensitivity required for fault detection in modules by magnetic field imaging. 33rd International Photovoltaic Science and Engineering Conference. Nagoya, Japan. 13-17 November 2022.

Hallam, B. (2022). Challenges and Opportunities for Terawatt scale deployment of industrial silicon solar cell Technologies. PV Cell Tech (invited)

Hallam, B. (2022). Challenges and Opportunities for Terawatt-Scale Deployment of n-type Solar Cell Technologies. Silicon PV (invited)

Hallam, B. (2022). Heading towards low cost, sustainable TW-scale PV systems . 33rd International Photovoltaic Science and Engineering Conference, 2022.

Hallam, B. (2022). Design and Material Considerations for Sustainable Multi Terawatt PV Manufacturing and Deployment. Terawatt Workshop (keynote)

Hallam, B., Kim, M., Underwood, R., Drury, S., Wang, L. & Dias, P. R. (2022). A Silicon learning curve and polysilicon requirements for broad electrification with photovoltaics by 2050. 2022 IEEE 49th Photovoltaics Specialists Conference (PVSC), 1177-1177.

Hao, X. (2022). Towards High Efficiency Kesterite Solar Cells. 33rd International Photovoltaic Science and Engineering Conference. Nagoya, Japan. 13-17 November 2022.

Herrmann, W., Eder, G.C., Farnung, B., Friesen, G., Koentges, M., Kubicek, B., Kunz, O., Liu, H., Parlevliet, D., Tsanakas, J., Vedde, J. (2022). Review of On-Site Inspection Techniques for the Qualification of PV Power Plants. 8th World Conference on Photovoltaic Energy Conversion. 26 – 30 September 2022. Milan, Italy.

Ho-Baillie, A. (2022). Intrinsic stability of perovskites and meta-stability of perovskite solar cells. Proceedings of the nanoGe Spring Meeting 2022.

Ho-Baillie, A. (2022). Perovskite Tandem Solar Cells (Invited). Proceedings of the Asia-Pacific International Conference on Perovskite, Organic Photovoltaics and Optoelectronics.

Hossain, M., Kubaisi, G. & Mansour, S. (2022). Investigation of different metal contacts for perovskite solar cells. Asia Pacific Solar Research Conference 2022. Newcastle: APVI. 29 Nov. – 1 Dec. 2022

Hossain, M., Kubaisi, K. & Mansour, S. (2022). Alternative p-type metal oxide films as hole transport materials for photovoltaic devices. Asia Pacific Solar Research Conference 2022. Newcastle: APVI. 29 Nov. – 1 Dec. 2022

Hossain, M.A., Sang, B. & Hoex, B. (2022). Electronic Properties of Doped Anatase TiO2: a First-Principles Modelling and Experimental Demonstration. 8th World Conference on Photovoltaic Energy Conversion. 26 – 30 September 2022. Milan, Italy.

Hossain, Md.A., Chen, R., Hoex, B. & Rougieux, F. (2022). Interstitial hydrogen in crystalline silicon: A hybrid DFT investigation. Asia Pacific Solar Research Conference 2022. Newcastle: APVI. 29 Nov. – 1 Dec. 2022

Hsiao, P.-C., Chen, D., Huang, C. Shi, W., Egan, R., Lennon, A. & Allen, V. (2022). Cell-to-Module Analysis of Copper-Plated Silicon Heterojunction Modules with 23.17% Efficiency. Asia Pacific Solar Research Conference 2022. Newcastle: APVI. 29 Nov. – 1 Dec. 2022

Hu, J., Wang, Y., Jia, H., Hu, W., Hassan, M., Uddin, A., Kusy, B. & Youssef, M. (2022). Passive light spectral indoor localization. Proceedings of the 28th Annual International Conference on Mobile Computing And Networking, 832-834.

Isaza, A., Kay, M., Evans, J. P., Bremner, S. (2022). Worldwide photovoltaic potential in climate change scenarios: future projections and associated costs. 33rd International Photovoltaic Science and Engineering Conference. Nagoya, Japan. 13-17 November 2022.

Isaza, A., Kay, M., Evans, J., Bremner, S. & Prasad, A. (2022). Australian Photovoltaic Potential in Different Climate Change Scenarios: Future Projections and Associated Costs. 8th World Conference on Photovoltaic Energy Conversion. 26 – 30 September 2022. Milan, Italy.

Isaza, A.A., Kay, M., Evans, J., Bremner, S. & Prasad, A. (2022). Australian Photovoltaic Potential in Different Climate Change Scenarios: Future Projections and Associated Costs. 8th World Conference on Photovoltaic Energy Conversion. 26 – 30 September 2022. Milan, Italy.

Ismael, M. (2022). 21.9% efficiency achieved by c-Si solar cells with AlyTiOx/TiOx electron-selective contact stack. Asia-Pacific Solar Research Conference. Newcastle. 29 November – 1 December 2022.

Ismael, M. (2022). Outstanding surface passivation and low contact resistivity on c-Si using alumina-titania electron-selective contact. 8th World Conference on Photovoltaic Energy Conversion (WCPEC). Milan, Italy. 26–30 September 2022.

Ismael, M., Macdonald, D. & Black, L. (2022). Outstanding Surface Passivation and Low Contact Resistivity on c-Si Using Alumina-Titania Electron-Selective Contact. 8th World Conference on Photovoltaic Energy Conversion. 26 – 30 September 2022. Milan, Italy.

Javier, G. M. N., Dwivedi, P., Buratti, Y., Trupke, T. & Hameiri, Z. (2022). Fill Factor Prediction of Modern Industrial Cells: Potential Gaps and Improvements. 2022 IEEE 49th Photovoltaics Specialists Conference (PVSC), 0353-0353.

Javier, G.M.N., Dwivedi, P., Buratti, Y., Trupke, T. & Hameiri, Z. (2022). A hybrid empirical and machine learning method to estimate solar cell fill factor from luminescence images. 33rd International Photovoltaic Science and Engineering Conference. Nagoya, Japan. 13-17 November 2022.

Javier, G.M.N., Dwivedi, P., Buratti, Y., Trupke, T. & Hameiri, Z. (2022). A hybrid empirical and machine learning method to estimate solar cell fill factor from luminescence images. 33rd International Photovoltaic Science and Engineering Conference, 2022.

Javier, G.M.N., Evans, R., Dwivedi, P., Buratti, Y., Trupke, T. & Hameiri, Z. (2022). Quality assessment of photovoltaic manufacturing lines through lag-sequential analysis. 33rd International Photovoltaic Science and Engineering Conference. Nagoya, Japan. 13-17 November 2022.

Jiang, J.Y., Liao, Y., Patterson, R., Keevers, M., Ekins-Daukes, N. & Green, M. (2022). Super-efficient coloured photovoltaics: enabling sustainable building and vehicle applications. Asia Pacific Solar Research Conference 2022. Newcastle: APVI. 29 Nov. – 1 Dec. 2022

Jin, H., Jiang W., Mallo, N., Babazadeh, M., Raynor, A., Loch, A., Chu, R., Burn P. L., Gentle, I., Shaw, P. E. (2022). Engineering Organic Semiconductors for Energy. 2022 Royal Australian Chemical Institute (RACI) National Congress.

Jin, H., Jiang, W., Mallo, N., Babazadeh, M., Raynor, A., Loch, A., Chu, R., Burn, P. L., Gentle, I., Shaw, P. (2022). Engineering organic semiconductors for Energy. RACI 2022 National Congress.

Jin, H., Wang, X., Fang, Y, Jiang W., Gao M., Burn P. L., Shaw, P. E. (2022). From Broadband to Narrowband All-Polymer Photodetectors. 2022 Australasian Community for Advanced Organic Semiconductors (AUCAOS) Symposium.

Jones, D. (2022). PP2 Organic Photovoltaics summary. 10th ACAP Conference 2022. Newcastle. 1 – 2 December 2022

Juhl, M., Zhou, Z. Puthen-Veettil, B. & David Payne, D. (2022). Using Low-cost Scanners for Luminescence Imaging of Solar Cells. Asia Pacific Solar Research Conference 2022. Newcastle: APVI. 29 Nov. – 1 Dec. 2022

Juhl, M.K., Puthen-Veettil, B., Khan, M.U., Scardera, G. & David Payne, D. (2022). Using Low Cost Scanners for Optical Inspection of Solar Cells. 8th World Conference on Photovoltaic Energy Conversion. 26 – 30 September 2022. Milan, Italy.

Kampwerth, H. & Pollard, H. (2022). Spectral Filtering for High-Contrast Photoabsorption Measurements. Asia Pacific Solar Research Conference 2022. Newcastle: APVI. 29 Nov. – 1 Dec. 2022

Kean Fong, K. & Moonyong Kim, M. (2022). PP1 Silicon Solar Cells summary. 10th ACAP Conference 2022. Newcastle. 1 – 2 December 2022

Khan, M.U., Chan, C., Sen, C., Wu, Y., Lv, R., Jean-Nicolas, J.-N., Zhang, G. & Hoex, B. (2022). Accelerated solar cell level potential-induced degradation and its impact on solar cell performance. Asia Pacific Solar Research Conference 2022. Newcastle: APVI. 29 Nov. – 1 Dec. 2022

Kim, D., Kim, Y., Im, K., Lee, M., Yun, J. S., Lee, S. H., Cho, Y., Kyung Taek Jeong, K. T., Park, S.,Kang, M.G., Song, M.-E. (2022). Charge Carrier Transport Properties at the Rear Side of TOPCon Solar Cell Structures using P-type and N-type Si Substrates

Kim, J. (2022). Flexible, Light Weight and Highly Efficient Perovskite Solar Modules Manufacturing via High Throughput Roll-to-Roll Process for Space Photovoltaics. Asia Pacific Solar Research Conference 2022. Newcastle: APVI. 29 Nov. – 1 Dec. 2022.

Kim, J.-E., Chantler, R., Scully, A., Weerasinghe, H., Doojin Vak & Gao, M. Flexible, (2022). Light Weight and Highly Efficient Perovskite Solar Modules Manufacturing via High Throughput Roll-to-Roll Process for Space Photovoltaics. 10th ACAP Conference 2022. Newcastle. 1 – 2 December 2022

Kim, M., Ciesla, A., Sun, C., Chen, D., Abbott, M. & Hallam, B. (2022). Application of Δn Normalised Time, β: Linear Injection-Level Dependence on LeTID and the Recovery in Crystalline Silicon. 8th World Conference on Photovoltaic Energy Conversion (WCPEC). Milan, Italy. 26–30 September 2022.

Kim, M., Zhang, Y., Verlinden, P. & Hallam, B. (2022). Towards sustainable silicon PV manufacturing at the terawatt level. SiliconPV 2021, The 11th International Conference on Crystalline Silicon Photovoltaics.

Kim, M., Zhang, Y., Wang, L., Underwood, R. & Hallam, B. (2022). Material Sustainability of Passivating Contact Schemes for Silicon Solar Cells and Modules at the Terawatt Scale. 33rd International Photovoltaic Science and Engineering Conference. Nagoya, Japan. 13-17 November 2022.

Koschier, L. & Egan, R. (2022). Australian PV Market Trends. Asia Pacific Solar Research Conference 2022. Newcastle: APVI. 29 Nov. – 1 Dec. 2022

Kuczynska-Lazewska, A., Chang, N. & Deng, R. (2022). CdTe PV modules recycling step-by-step process – LCA based on own research. Asia Pacific Solar Research Conference 2022. Newcastle: APVI. 29 Nov. – 1 Dec. 2022

Kunz, O., Scott, A., Perez-Wurfl, I., Parlevliet, D., Hameiri, Z. & Trupke, T. (2022). PV system inspection via outdoor luminescence imaging and update on IEA PVPS Task 13. Asia Pacific Solar Research Conference 2022. Newcastle: APVI. 29 Nov. – 1 Dec. 2022

Le, A. H. T., Ochoa, E. P., Bonilla, R. S., Borojevic, N. & Hameiri, Z. (2022). Temperature Dependence of Silicon-Dielectric Interface Recombination. 2022 IEEE 49th Photovoltaics Specialists Conference (PVSC), 0443-0443. (Best Student Presentation Award Finalist)

Le, A. H. T., Srinivasa, A., Bowden, S. G., Hameiri, Z. & Augusto, A. (2022). Silicon Heterojunction Solar Cells with High Bulk Resistivities Over 1,000 Ω·cm in Relevant Field Conditions of Illumination and Temperature. 2022 IEEE 49th Photovoltaics Specialists Conference (PVSC), 1045-1045. (Best Student Presentation Award Finalist)

Le, A.H.T., Pasanen, T., Black, L., Savin, H., Macdonald, D. & Liu, A. (2022). The Impact of Bulk Iron Contamination on the Surface Recombination of Silicon Wafers. 8th World Conference on Photovoltaic Energy Conversion. 26 – 30 September 2022. Milan, Italy.

Le, A.H.T., Srinivasa, A., Bowden, S., Hameiri, Z. & Augusto, A. (2022). Temperature- and Illumination-Dependent Performance of Silicon Heterojunction Solar Cells with Bulk Resistivities over 1,000 Ω.cm. 8th World Conference on Photovoltaic Energy Conversion. 26 – 30 September 2022. Milan, Italy.

Le, T. T. (2022). Industrial Czochralski n-type silicon wafers: gettering effectiveness and possible bulk limiting defects. 8th World Conference on Photovoltaic Energy Conversion (WCPEC). Milan, Italy. 26–30 September 2022.

Le, T. T. (2022). Industrial Czochralski n-type silicon wafers: gettering effectiveness and possible bulk limiting defects. 8th World Conference on Photovoltaic Energy Conversion (WCPEC). Milan, Italy. 26–30 September 2022.

Lee, C. & Jones, D. (2022). Biradical character modification through steric perturbations: a twisted route towards silicon-match. 10th ACAP Conference 2022. Newcastle. 1 – 2 December 2022

Lennon, A. (2022). The ascent of silicon heterojunction technology, but can it be sustainably manufactured at TW annual production levels? 10th ACAP Conference 2022. Newcastle. 1 – 2 December 2022

Leyton D., Chang N. & Corkish, R. (2022). A Reverse Logistics Model for End-of-Life Solar Modules Using Existing Transport Processes. Asia-Pacific Solar Research Conference. Newcastle. 29 November – 1 December 2022.

Leyton, D., Chang, N. & Corkish, R. (2022). Resolving the 'Angefangener' problem using The Solar Reverse Logistics Model (SRLM). Asia Pacific Solar Research Conference 2022. Newcastle: APVI. 29 Nov. – 1 Dec. 2022

Li, G., Toth, P., Mai, L., Conibeer, G. & Hoex, B. (2022). Silicon Solar Cells for Low Earth Orbit Applications – Electron Radiation Stability of TOPCon Solar. Asia Pacific Solar Research Conference 2022. Newcastle: APVI. 29 Nov. – 1 Dec. 2022

Li, H., Burn, P. & Shaw, P. (2022). Fluorinated additives for perovskite solar cells. 10th ACAP Conference 2022. Newcastle. 1 – 2 December 2022

Li, J. (2022). PP2 CZTS summary. 10th ACAP Conference 2022. Newcastle. 1 – 2 December 2022

Li, J., Huang, J., Ma, F. & Hao, X. (2022). Microscopic carrier loss mechanisms in 12% efficient CZTSe thin-film solar cells. 10th ACAP Conference 2022. Newcastle. 1 – 2 December 2022

Li, Y., Vicari-Stefani, B., Jones, T., Fell, C. & Wilson, G. (2022). Developing perovskite-silicon tandem solar cells based on PERC and perovskite CVD technology. Asia Pacific Solar Research Conference 2022. Newcastle: APVI. 29 Nov. – 1 Dec. 2022

Li, Z., Sia, H. C., Liu, A., Basnet, R., Macdonald, D. & Nguyen, H. (2022). Applications of time-resolved photoluminescence decay in characterizing heavily-doped crystalline silicon and amorphous silicon films. 33rd International Photovoltaic Science and Engineering Conference. Nagoya, Japan. 13-17 November 2022.

Liang, W. (2022). Hybrid IBC Solar cells with poly-Si and metal oxide passivating contacts. Asia-Pacific Solar Research Conference. Newcastle. 29 November – 1 December 2022.

Liang, W. (2022). Hybrid IBC Solar cells with poly-Si and metal oxide passivating contacts. Asia-Pacific Solar Research Conference. Newcastle. 29 November – 1 December 2022.

Liang, W., Tong, J., Kho, K., Basnet, R., Narangari, P., Armand, S., Bullock, J. & Fong, K. (2022). Hybrid IBC solar cells with poly-Si and metal oxide passivating contacts. Asia Pacific Solar Research Conference 2022. Newcastle: APVI. 29 Nov. – 1 Dec. 2022

Lim, J., Choi, E., Kim, M., Lee, M., Chen, D., Green, M.A., Seidel, J., Park, J., Hao, X. & Yun, J.S. (2022). Revealing the Dynamics of Thermal Reaction Between Cu and Mixed Halide Perovskite Solar Cells. 8th World Conference on Photovoltaic Energy Conversion. 26 – 30 September 2022. Milan, Italy.

Lima, M., Wright, B. & Hameiri, Z. (2022). Investigating the performance of non-standard cell configurations for reconfigurable solar modules under varying shading conditions, 33rd International Photovoltaic Science and Engineering Conference, 2022.

Liu, D., Bonilla, S., Wright, M., Wilshaw, P. & Hamer,P. (2022). Surface Polarisation of n+ poly Si / SiO2 Passivation Layers: A New Approach to Study Surface Related Degradation in TOPCon. 8th World Conference on Photovoltaic Energy Conversion. 26 – 30 September 2022. Milan, Italy.

Liu, D., Goodarzi, M., Deru, J., Wilshaw, P. R., Hamer, P. & Bonilla, R. S. (2022). Investigating the link between LeTID and hydrogen induced contact resistance in PERC devices. SiliconPV 2021, The 11th International Conference on Crystalline Silicon Photovoltaics.

Liu, G., Dwivedi, P., Trupke, T. & Hameiri, Z. (2022). A Deep Learning Approach to Denoise Electroluminescence Images of Solar Cells. 2022 IEEE 49th Photovoltaics Specialists Conference (PVSC), 0442-0442. (Best Student Presentation Award Finalist)

Liu, G., Dwivedi, P., Trupke, T. & Hameiri, Z. (2022). A deep learning approach to denoise luminescence images of solar cells. Asia Pacific Solar Research Conference 2022. Newcastle: APVI. 29 Nov. – 1 Dec. 2022

Liu, Z., Zhang, P. Li, C., Green, M. & Hao, X. (UNSW), "(2022). A novel method to fabricate transparent conductive adhesive (TCA) intermediate layers for tandem solar cells. 10th ACAP Conference 2022. Newcastle. 1 – 2 December 2022

Lugao de Carvalho, G.B., Macdonald, D. & Black, L. (2022). Evaporated Cu2O as a hole-selective Contact for c-Si Solar Cells. 8th World Conference on Photovoltaic Energy Conversion. 26 – 30 September 2022. Milan, Italy.

Luke Sutherland, L., Hasitha Weerasinghe, H. & George P Simon, G.P. (2022). Printed electrodes for roll-to-roll perovskite solar cells. Asia Pacific Solar Research Conference 2022. Newcastle: APVI. 29 Nov. – 1 Dec. 2022

Macdonald, D., Zheng, P., Phang, P., Yang, J., Wang, E.-C., Stuckelberger, J., Sio, H., Zhang, X. & Jin, H. (2022). Towards industrial poly-silicon contacted solar cells with efficiencies above 26%. Asia Pacific Solar Research Conference 2022. Newcastle: APVI. 29 Nov. – 1 Dec. 2022

Madumelu, C., Underwood, R., Bao, J., Chen, J., Du, Z., Ji, G., Chen, R., Rougieux, F.E., Hoex, B., Hallam, B. & Wright, M. (2022). The Impact of Tunneling Oxide Thickness, Boron Emitter and Polysilicon Doping on the Long-Term Stability of TOPCon Structures. 8th World Conference on Photovoltaic Energy Conversion. 26 – 30 September 2022. Milan, Italy.

Mahmud, Md.A., Zheng, J., Tang, S., Wang, G., Bing, J., Bui, A.D., Liao, C., Chen, H., Bremner, S., Nguyen, H. & Ho-Baillie, A. (2022). Cation-Diffusion-Based Passivation for High Bandgap Perovskite and Pero-Pero Tandem with Record FF. Asia Pacific Solar Research Conference 2022. Newcastle: APVI. 29 Nov. – 1 Dec. 2022

Mallo, N. (2022). Tuning the high frequency dielectric constant of organic semiconductors for organic photovoltaic devices. Australasian Community for Advanced Organic Semiconductors Conference. Tweed Heads. 7 – 10 December 2022

Mallo, N., Burn, P., Gentle, I. & Shaw, P. (2022). Tuning the high frequency dielectric constant of organic semiconductors for organic photovoltaics. 10th ACAP Conference 2022. Newcastle. 1 – 2 December 2022

Mallo, N., Jin, H., McAnally, S. W., Chu, R., Jiang, W., Babazadeh, M., Burn, P. L., Gentle, I. R., Shaw, P. E. (2022). Tuning the high frequency dielectric constant of organic semiconductors for organic photovoltaics. 2022 Asia-Pacific Solar Research Conference (APSRC). Newcastle: APVI. 29 Nov. – 1 Dec. 2022

Mao, W., Hall, C., Bernardi, S., Smith, T., Widmer-Cooper, A. & Bach, U. (2022). Light Induced reversal of ion segregation in mixed-halide perovskite. 10th ACAP Conference 2022. Newcastle. 1 – 2 December 2022

Masoomi-Godarzi, S. Breaking the efficiency limit of perovskite solar cells using singlet fission material. 10th ACAP Conference 2022. Newcastle. 1 – 2 December 2022

McAnally, S. W., Jin, H., Chu, R., Babazadeh, M., Wang, X., Burn, P. L., Gentle, I. R., Shaw, P. E. (2022). More from Less: High efficiency organic solar cells with simple active layers. 2022 Asia-Pacific Solar Research Conference (APSRC). Newcastle: APVI. 29 Nov. – 1 Dec. 2022

McAnally, S. W., Jin, H., Chu, R., Babazadeh, M., Wang, X., Burn, P. L., Gentle, I. R., Shaw, P. E. (2022). More from Less: High efficiency organic solar cells with simple active layers. 2022 Australasian Community for Advanced Organic Semiconductors (AUCAOS) Symposium.

Michel, J.D.J.I., Yan, D., Phang, P., Zheng, T., Johnson, B.C., Yang, J., Zhang, X., Chen, W., Wan, Y., Truong, T.N., Stuckelberger, J., Pan, Y., Macdonald, D. & Bullock, J. (2022). Poly-Si passivating contacts prepared via phosphorus spin-on-doping: a comparison between different …. Asia Pacific Solar Research Conference 2022. Newcastle: APVI. 29 Nov. – 1 Dec. 2022

Mo, A. C.-H., Baldacchino, A., Nielsen, M., Tayebjee, M. & Hoex, B. (2022). Optimisation of passivating exciton transport layer for singlet fission sensitised silicon solar cell. 33rd International Photovoltaic Science and Engineering Conference. Nagoya, Japan. 13-17 November 2022.

Mohamed Ismael, M., Daniel Macdonald, D. & Lachlan Black, L. (2022). 21.9% efficiency achieved by c-Si solar cells with AlyTiOx/TiOx electron-selective contact stack. Asia Pacific Solar Research Conference 2022. Newcastle: APVI. 29 Nov. – 1 Dec. 2022

Na Gyeong An, N.G., Mei Gao, M., Leonard Ng Wei Tat, L.N.W., Udo Bach, U. & Vak, D. (2022). Fully Printed Organic Photovoltaics for Producing High-Throughput and Reliable Photovoltaic Data. Asia Pacific Solar Research Conference 2022. Newcastle: APVI. 29 Nov. – 1 Dec. 2022

Nadolny, A. & Cheng, C. (2022). A bluefield atlas for lower cost pumped hydro energy storage. Asia Pacific Solar Research Conference 2022. Newcastle: APVI. 29 Nov. – 1 Dec. 2022

Najafi, M., Veenstra, S., Zardetto, V., Simurka, L., Verhees, W., Fledderus, H., Gorter, H., Lucarelli, G., Dogan, I., Bakker, K., Zhang, D., Hadipour, A., Lammar, S., Theelen, M., Janssen, R., Aernouts, T., Weeber, A., Geerligs, B., Coletti, G. & Manshanden, P. (2022). Highly Efficient Perovskite/Silicon Four-Terminal Tandem Solar Cells and Modules. Proceedings of the International Conference on Hybrid and Organic Photovoltaics.

Ng, L.W.T. (2022). Machine Learning for Printable Photovoltaics: Ever-Increasing Efficiencies By Single Experiment Optimisation Via a Microfactory. Asia Pacific Solar Research Conference 2022. Newcastle: APVI. 29 Nov. – 1 Dec. 2022.

Nguyen, H. (2022). Optical and electrical properties of photovoltaic materials via luminescence. The 3rd International Conferences on Material Science and Engineering. Gold Coast. 5 – 8 December 2022.

Nguyen, H. (2022). Optical and electrical properties of photovoltaic materials via luminescence. 3rd International Conferences on Material Science and Engineering. Gold Coast. 5 – 8 December 2022.

Nguyen, K.D.N., Bui, A.D., Truong, T.N., Macdonald, D. & Nguyen, H. (2022). Correlative Imaging of Optical Properties for Perovskite Materials in Single-Junction and Tandem Solar Cells. 8th World Conference on Photovoltaic Energy Conversion. 26 – 30 September 2022. Milan, Italy. (Student Awards Finalist Presentation)

Nguyen, N. D. K. (2022). Correlative imaging of optical properties for perovskite materials in single-junction and tandem solar cells. 8th World Conference on Photovotaic Energy Conversion (WCPEC-8). Milan, Italy. 26 – 30 September 2022.

Nguyen, T.D. (2022). Simulating Proton Radiation Tolerance of Perovskite Solar Cells for Space Applications. 2022 International Symposium on Clean Energy Materials 30 Jun – 2 July 2022

Nie, S., Zhu, Y., Kunz, O., Trupke, T. & Hameiri, Z. (2022). Photoluminescence Imaging Using Non-Uniform Excitation: Recent Progress. 8th World Conference on Photovoltaic Energy Conversion. 26 – 30 September 2022. Milan, Italy. (Student Awards Finalist Presentation)

Nielsen, M. P., Pusch, A., Sazzad, M. H., Pearce, P. M., Reece, P. J., Ekins-Daukes, N. J., Sood, A. K., Wijewarnasuriya, P. & D'Souza, A. I. (2022). Demonstrating the thermoradiative diode: generating electrical power through radiative emission. Infrared Sensors, Devices, and Applications XII.

Nielsen, M., Pusch, A., Sazzad, M.H., Pearce, P., Reece, P., Ekins-Daukes, N. (2022). Generation of Electrical Power Through Radiative Emission from a Thermoradiative Diode. 8th World Conference on Photovoltaic Energy Conversion. 26 – 30 September 2022. Milan, Italy.

Oestroem, I., Kasim, S., Hossain, Md. A., Burr, P., Hoex, B. (2022). Low-Cost Catalysts for Next-Generation Fuel Cells, 6th Catalysis and Chemical Engineering Conference 2022 (online).

Olivia Bowen, O. & Rong Deng, R. (2022). Characterising the composition of photovoltaic panels for recycling in Australia. Asia Pacific Solar Research Conference 2022. Newcastle: APVI. 29 Nov. – 1 Dec. 2022

Oulton, R. F., Fu, M., Gusken, N., Nielsen, M. P., Jacassi, A., Mota, M., Dichtl, P. M., Xiao, X., Maier, S. A., Lu, Y.-J., Tanaka, T. & Tsai, D. P. (2022). Enhanced light matter interaction in waveguides with extreme nanofocussing. Plasmonics: Design, Materials, Fabrication, Characterization, and Applications XX.

Pai, N., Chatti, M., Scully, A.D., Raga, S.R., Chesman, A.S.R., Xu, Z., Lira-Cantú, M., Bach, U. & Simonov, A.N. (2022). Compositional Control of Solution-Processable Direct Bandgap Bismuth- Based Perovskite-Inspired Materials for Photovoltaics. 8th World Conference on Photovoltaic Energy Conversion. 26 – 30 September 2022. Milan, Italy.

Phoebe Pearce, P. & , Ekins-Daukes, N. (2022). RayFlare: A Powerful and Flexible Open-Source Modelling Tool for Solar Cells. 8th World Conference on Photovoltaic Energy Conversion. 26 – 30 September 2022. Milan, Italy.

Poddar, S., Kay, M., Evans, J., Bremner, S. & Prasad, A. (2022). Analysis of Future Solar Power Generation Feasibility in Australia Using High-Resolution Regional Climate Model Projections. 8th World Conference on Photovoltaic Energy Conversion. 26 – 30 September 2022. Milan, Italy.

Poddar, S., Rougieux, F., Kay, M., Bremner, S., Prasad, A. & Jason Evans, J. (2022). Analysis of degradation rates in PV modules and prospective future changes due to climate change33rd International Photovoltaic Science and Engineering Conference. Nagoya, Japan. 13-17 November 2022.

Poduval, G., Ji, D., Bremner, S., Joshi, R. & Hoex, B. (2022). Direct Chemical vapour deposition of graphene on atomic layer deposited functional nickel oxide. ALD/ALE 2022, 26-29 June, 2022, Ghent, Belgium.

Pusch, A. (2022). Thermodynamics of emerging photovoltaic concepts. 33rd International Photovoltaic Science and Engineering Conference. Nagoya, Japan. 13-17 November 2022.

Qian, C., Li, J., Sun, K., Jiang, C., Huang, J., Tang, R., Green, M., Hoex, B., Chen, T. & Hao, X. (2022). Amorphous Manganese Sulfide Enables Efficient and Stable All-Inorganic Antimony Selenosulfide Solar Cells. 2022 IEEE 49th Photovoltaics Specialists Conference (PVSC), 1126-1126. (Best Student Presentation Award Finalist)

Reddy, S., Rai, N. & Bach, U. (2022). A new class of passivating polymers for perovskite solar cells. 10th ACAP Conference 2022. Newcastle. 1 – 2 December 2022

Rougieux, F. (2022). Battle of the dopants: Challenges and opportunities for n-TOPCon vs Ga-PERC technologies. Asia Pacific Solar Research Conference 2022. Newcastle: APVI. 29 Nov. – 1 Dec. 2022

Rougieux, F., Hossain, Md. H. & Hoex, B. (2022). Density Functional Theory to Calculate Accurate Defect Energy Levels in Silicon. 12th International Conference on Crystalline Silicon Photovoltaics, Konstanz, Germany, April 2022.

Rougieux, F., Sen, C., Abbott, M. & Hoex, B. (2022). Surface Passivation with a-Si: Determining the Role of Interface Defects and Field-Effect Using Modeling of Lifetime Curves. 8th World Conference on Photovoltaic Energy Conversion. 26 – 30 September 2022. Milan, Italy.

San Jose L, Vallerotto G, Abdullah-Vetter Z, Herrero R, Hameiri Z. & Anton, Ignacio. (2022). On the effect of misalignment distributions on the I-V curve of micro-CPV modules. 18th International Conference on Concentrator Photovoltaic Systems, Miyazaki, Japan (Online), 25-27 Apr 2022.

Saripally, S.R., Rai, N. & Bach, U. (2022). A New Class of Passivating Polymers for Perovskite Solar Cells. Asia Pacific Solar Research Conference 2022. Newcastle: APVI. 29 Nov. – 1 Dec. 2022

Scott, A., Hameiri, Z., Trupke T., Perez-Wurfl, I. & Kunz, O. (2022). Outdoor Photoluminescence Imaging from Unmanned Aerial Vehicles. Asia-Pacific Solar Research Conference. Newcastle. 29 November – 1 December 2022.

Sen, C., Chan, C., Mao, L., Jaubert, J.-N., Jiang, F., Zhang, G., Khan, M.U., Wu, X., Wang, H. & Hoex, B. (2022). The role of Na+ contamination in humidity-induced degradation in silicon HJT cells. Asia Pacific Solar Research Conference 2022. Newcastle: APVI. 29 Nov. – 1 Dec. 2022

Shaw, P. (2022). PP3 Optics & Characterisation summary. 10th ACAP Conference 2022. Newcastle. 1 – 2 December 2022

Shi Tang, S. & Anita Wing Yi Ho-Baillie, A.W.Y. (2022). Doping of hole transport materials on the stability and recoverability of on very thin substrate PSC. Asia Pacific Solar Research Conference 2022. Newcastle: APVI. 29 Nov. – 1 Dec. 2022

Shim, H. & Yun, J.S. (2022). Integrating Perovskite Photovoltaics and Nickel Cobalt Sulfide Catalysts for Efficient Hydrogen Evolution Reaction. 8th World Conference on Photovoltaic Energy Conversion. 26 – 30 September 2022. Milan, Italy.

Shrestha, B., Subedi, I., Collins, R. W. & Podraza, N. J. (2022). External Quantum Efficiency and Device Reflectance of CIGS PV for Terrestrial and Space Based Applications. 2022 IEEE 49th Photovoltaics Specialists Conference (PVSC), 0833-0835.

Sinton, R., Wilterdink, H., Sainsbury, C., Dobson, W., Dinger, J., Dapprich, K., Zhang, X., Xu, G., Hu, Y., Wang, Y., Chen, D., Feng, Z. Q., Chen, Y., Altermatt, P. & Verlinden, P. (2022). Characterization of a cell process from IV cell-test data. SiliconPV 2021, The 11th International Conference on Crystalline Silicon Photovoltaics.

Soeriyadi, A. H., Hollemann, C., Madumelu, C., Haase, F., Römer, U., Brendel, R., Peibst, R. & Hallam, B. J. (2022). Impact of firing and capping layers on long-term stability of doped poly-Si passivating contact layers. SiliconPV 2021, The 11th International Conference on Crystalline Silicon Photovoltaics.

Soeriyadi, A.H., Wright, M., Vicari-Stefani, B., Zhang, S., Nyapshaev, I., Abolmasov, S., Andronikov, D. & Hallam, B. (2022). 1% Efficient SHJ Using Compensated and Intentionally Contaminated p- Type Wafer with Defect Engineering Pre-Fabrication Process. 8th World Conference on Photovoltaic Energy Conversion. 26 – 30 September 2022. Milan, Italy.

Song, N., Zeng, Y., Jiang, Y., Chang, N., Gentle, A., Zhou, Z., Keevers, M., Ekins-Daukes, N., Egan, R. & Green, M. (2022). Revolutionizing anti reflection coatings for solar module glass. 33rd International Photovoltaic Science and Engineering Conference. Nagoya, Japan. 13-17 November 2022.

Subbiah, J. (2022). Halogen functionalized solid additives for morphology control in high-efficiency organic solar cells. Australasian Community for Advanced Organic Semiconductors Conference. Tweed Heads. 7 – 10 December 2022

Sun, K., Zhou, S., Amal, R. & Hao, X. S. (2022). Kesterite-based photocathode for photoelectrochemical CO2 reduction and NH3 production33rd International Photovoltaic Science and Engineering Conference. Nagoya, Japan. 13-17 November 2022.

Sun, Z., Lei, F., Hallam, B., Zhang, X. & Wang, L. (2022). Application of Advanced Hydrogenation Process on SiGe/Si Solar Cells. 8th World Conference on Photovoltaic Energy Conversion. 26 – 30 September 2022. Milan, Italy.

Sun, Z., Zhou, Z., Luo, H., Hallam, B. & Wang, L. (2022). Hydrogen passivation on SiGe solar cells grown on silicon substrates using amorphous silicon layers. 33rd International Photovoltaic Science and Engineering Conference. Nagoya, Japan. 13-17 November 2022.

Surmiak, A. (2022). The end of traditional manual research, a new era of robotics for rapid energy materials discovery. Asia Pacific Solar Research Conference 2022. Newcastle: APVI. 29 Nov. – 1 Dec. 2022

Sutherland, L. (2022). R2R Perovskite Solar Cells with Solvent-free Printed Electrodes. Australian Centre for Advanced Photovoltaics conference 2022. Newcastle: APVI. 1-2 Dec. 2022.

Sutherland, L., Benitez-Rodriguez, J., Angmo, D., Peiris, N., Gao, M., Simon, G. & Tan, B., Chesman, A. & Bach, U. (2022). Back Contact Perovskite Solar cells with a stabilized power output up to 10.9%. Asia Pacific Solar Research Conference 2022. Newcastle: APVI. 29 Nov. – 1 Dec. 2022

Sutherland, L., Benitez-Rodriguez, J., Angmo, D., Peiris, N., Gao, M., George Simon, Weerasinghe, H. (2022). Perovskite solar cell encapsulation: The subtle influence of moisture outgassing from encapsulation. 10th ACAP Conference 2022. Newcastle. 1 – 2 December 2022

Sutherland, L., Weerasinghe, H. & George Simon, G. (2022). Printed electrodes for roll-to-roll perovskite solar cells. 10th ACAP Conference 2022. Newcastle. 1 – 2 December 2022

Tabernig, S.W., Soeriyadi, A.H., Römer, U., Pusch, A., Lamers, D., Nielsen, M., Polman, A. & Ekins-Daukes, N. (2022). Shading Losses in Concentrator Photovoltaics Using a Soft-imprinted Cloaking Geometry. 8th World Conference on Photovoltaic Energy Conversion. 26 – 30 September 2022. Milan, Italy.

Tabi, G.D. (2022). Simulation of nanohole point contacts for perovskite solar cells with insulating passivation layers. 10th ACAP Conference 2022. Newcastle. 1 – 2 December 2022

Tan, B. (2022). Back Contact Perovskite Solar cells with a stabilized power output up to 10.9%. 10th ACAP Conference 2022. Newcastle. 1 – 2 December 2022

Tan, V., Deng, R. (2022). Solar panel waste projection in Australia, 2022-2035. Asia Pacific Solar Research Conference 2022. Newcastle: APVI. 29 Nov. – 1 Dec. 2022

Tan, V., Dias, P., Deng, R., Chang, N. (2022). Estimating the Lifetime of Solar Photovoltaic Modules in Australia. 8th World Conference on Photovoltaic Energy Conversion. 26 – 30 September 2022. Milan, Italy.

Tat, L.N.W., An, N.G. & Vak, D. (2022). Breakthrough Efficiencies for Printable PVs Using High-Throughput Methods and achine-Learning. Asia Pacific Solar Research Conference 2022. Newcastle: APVI. 29 Nov. – 1 Dec. 2022

Tayebjee, M. (2022). Coaxing Triplets into Silicon. Australasian Community for Advanced Organic Semiconductors Conference. Tweed Heads. 7 – 10 December 2022

Thapar, E., Lunardi, M., Dias, P. & Brett Hallam, B. (2022). Evaluating the Feasibility & Environmental Impacts of EoL Management Strategies for PV Modules. Asia Pacific Solar Research Conference 2022. Newcastle: APVI. 29 Nov. – 1 Dec. 2022

Tong, J. (2022). Improved Thermal Stability of Metal Oxide Passivated Contacts for Si Solar Cells, 8th World Conference on Photovotaic Energy Conversion (WCPEC-8). Milan, Italy. 26 – 30 September 2022.

Tong, J., Tien Le, T., Liang, W., Hossain, Md.A., Mcintosh, K., Narangari, P., Armand, S., Kho, T., Khoo, K., Zakaria, Y., Abdallah, A.A., Surve, S., Ernst, M., Hoex, B. & Fong, K.C. (2022). Improve Thermal Stability of Metal Oxide Passivated Contacts for Si Solar Cells. 8th World Conference on Photovoltaic Energy Conversion. 26 – 30 September 2022. Milan, Italy.

Truong, T., Kang, D., Wang, E.-C., Phang, P., Macdonald, D. & Stuckelberger, J. (2022). Ex-situ phosphorus-doped poly-Si passivating contacts for high efficiency solar cells by PVD. Asia Pacific Solar Research Conference 2022. Newcastle: APVI. 29 Nov. – 1 Dec. 2022

Truong, T., Young, M., Al-Jassim, M., Macdonald, D., Nguyen, H. & Stuckelberger, J. (2022). Gallium-Boron Spin-on co-Doping for Polycrystalline Silicon Passivating Contacts. 2022 IEEE 49th Photovoltaics Specialists Conference (PVSC), 0075-0075. Philadelphia, USA (2022). 5 – 10 June 2022.

Underwood, R., Kim, M., Zhang, Y., Wang, L., Drury, S., Dias, P., Altermatt, P.P. & Hallam, B. (2022). Estimates of Material Consumption for PV Towards Net-Zero Emissions by 2050. 8th World Conference on Photovoltaic Energy Conversion. 26 – 30 September 2022. Milan, Italy.

Vak, D. (2022). Reliable Fabrication and Testing of Roll-To-Roll Printed PV For Digital Revolution In PV Research. Australian Centre for Advanced Photovoltaics conference 2022. Newcastle: APVI. 1-2 Dec. 2022.

Vicari Stefani, B. (2022). Light-induced degradation in p-type silicon heterojunction solar cells. Asia Pacific Solar Research Conference 2022. Newcastle: APVI. 29 Nov. – 1 Dec. 2022

Wallwork, N. R., McAnally, S., Jin, H., Babazadeh, M., Shaw, P., Burn, P. L., (2022). Effect of Conjugation Length on Absorption and Dielectric Constant of Organic Photovoltaic materials. 2022 Australasian Community for Advanced Organic Semiconductors (AUCAOS) Symposium.

Wang, A., Sun, K., Huang, J., Green, M. & Hao, X. (2022). 10. 7% efficient Cd-free Cu2ZnSnS4 solar cells with over 800 mV open-circuit voltage enabled by Ge incorporation. 33rd International Photovoltaic Science and Engineering Conference. Nagoya, Japan. 13-17 November 2022.

Wang, G., Zheng, J. & Ho-Baillie, A. (2022). Hole-selective contact engineering for perovskite single-junction and tandem solar cell. Asia Pacific Solar Research Conference 2022. Newcastle: APVI. 29 Nov. – 1 Dec. 2022

Wang, J. (2022). Inkjet printing for boron-doped polycrystalline silicon passivating contacts. 33rd International Photovoltaic Science and Engineering Conference (PVSEC-33). Nagoya, Japan. 13 – 17 November 2022.

Wang, J. (2022). Inkjet printing for boron-doped polycrystalline silicon passivating contacts. Asia-Pacific Solar Research Conference. Newcastle. 29 November – 1 December 2022.

Wang, J., Phang, S.P., Li, Z., Truong, T., Nguyen, H., Macdonald, D. & Stuckelberger, J. (2022). Inkjet printing for boron-doped polycrystalline silicon passivating contacts. 10th ACAP Conference 2022. Newcastle. 1 – 2 December 2022

Wang, J., Phang, S.P., Samundsett, C., Li, Z., Truong, T.N., Yang, J., Wang, Z., Zheng, P., Zhang, X., Nguyen, H.T., Macdonald, D. & Stuckelberger, J. (2022). Inkjet printing for polycrystalline silicon passivating contacts. 10th ACAP Conference 2022. Newcastle. 1 – 2 December 2022

Wang, J., Truong, T., Sieu Pheng Phang, Li, Z., Yang, J., Wang, Z., Zheng, P., Zhang, X., Nguyen, H., MacDonald, D. & Stuckelberger, J. (2022). Inkjet printing for boron-doped polycrystalline silicon passivating contacts. 33rd International Photovoltaic Science and Engineering Conference. Nagoya, Japan. 13-17 November 2022.

Wang, L., Koh, D., Hamer, P., Pollard, M. & Chan, C. (2022). Suppression of LeTID in p-type multi-crystalline PERC silicon solar cells by biased annealing process. SiliconPV 2021, The 11th International Conference on Crystalline Silicon Photovoltaics.

Wang, L., Sun, Z., Luo, H. & Hamer, P. (2022). Hydrogen passivation of low temperature deposited amorphous silicon layers on SiGe solar cells grown. Asia Pacific Solar Research Conference 2022. Newcastle: APVI. 29 Nov. – 1 Dec. 2022

Wang, L., Zhang, Y., Kim, M., Underwood, R., Drury, S. & Hallam, B. (2022). Sustainability Evaluations on Material Consumption for Terawatt Scale Manufacturing of Silicon based Tandem Solar Cells. 8th World Conference on Photovoltaic Energy Conversion. 26 – 30 September 2022. Milan, Italy.

Wang, S., Dwivedi, P. & Buratti, Y. (2022). Extracting the parameters of two-energy-level defects in silicon wafers using machine learning model. Asia Pacific Solar Research Conference 2022. Newcastle: APVI. 29 Nov. – 1 Dec. 2022

Weerasinghe, H. (2022). Perovskite Solar Cell Encapsulation: The Subtle Influence of Moisture Outgassing from Encapsulation. Asia Pacific Solar Research Conference 2022. Newcastle: APVI. 29 Nov. – 1 Dec. 2022

Weerasinghe, H. (2022). Perovskite Solar Cell Encapsulation: The Subtle Influence of Moisture Outgassing from Encapsulant Materials. Australian Centre for Advanced Photovoltaics conference 2022. Newcastle: APVI. 1-2 Dec. 2022.

Wibowo, A. A. (2022). High-Quality Large-Area Growth of MoS2 Monolayers using Combinational Phase Precursors based Chemical Vapor Deposition. European Material Research Society (E-MRS) Conferences. 30 May - 3 June 2022.

Wibowo, A. A. (2022). High-Quality Large-Area Growth of MoS2 Monolayers using Combinational Phase Precursors based Chemical Vapor Deposition. 38th International Conferences on the Physics of Semiconductor (ICPS). Sydney. 27 - 30 June 2022

Wibowo, A. A. (2022). Large-size, High-quality 2D Transition Metal Dichalcogenides Lateral Heterostructures by Mixed Molten-salt-supported Chemical Vapour Deposition. 3rd International Conferences on Material Science and Engineering. Gold Coast. 5- 8 December 2022.

Wright, B. & Hallam, B. (2022). Unsupervised machine learning for photovoltaic systems: Modelling LID dynamics in SHJ solar cells. SiliconPV 2021, The 11th International Conference on Crystalline Silicon Photovoltaics.

Wright, B. & Hameiri, Z. (2022). Machine learning-powered module end-of-life decisions from luminescence images. Asia Pacific Solar Research Conference 2022. Newcastle: APVI. 29 Nov. – 1 Dec. 2022

Wright, B. & Hameiri, Z. (2022). Machine learning-powered module end-of-life decision making based on luminescence images, 33rd International Photovoltaic Science and Engineering Conference, 2022.

Wright, B. (2022). Kinetics of Light-Induced Instability in Bifacial N-Type Silicon Heterojunctions. 11th International Workshop on Crystalline Silicon for Solar Cells & 4th Silicon Materials Workshop. Lisbon 20-22 April 2022.

Wright, B., Hameiri, Z. & Mozer, A. (2022). Modelling the dynamics of charge extraction transients from organic photovoltaic devices using generative representation learning. 33rd International Photovoltaic Science and Engineering Conference. Nagoya, Japan. 13-17 November 2022.

Wright, M., Chen, R., Wright, B., Soeriyadi, A., Stefani, B. V., Zhang, X. & Hallam, B. (2022). 0.3% efficiency improvement for n-PERT solar cells with illuminated hydrogenation process. SiliconPV 2021, The 11th International Conference on Crystalline Silicon Photovoltaics.

Wright, M., Madumelu, C., Soeriyadi, A.H., Vicari- Stefani, B., Andronikov, D. Bonilla, S. & Hallam, B. (2022). High Intensity Illuminated Annealing of Silicon Heterojunction Solar Cells: a Stability Study. 8th World Conference on Photovoltaic Energy Conversion. 26 – 30 September 2022. Milan, Italy.

Xie, T., Wan, Y., Hoex, B. & Chunyu, K. (2022). Deep learning accelerated material discovery for Si-based solar cells passivating contact layers material discovery & synthesis. 33rd International Photovoltaic Science and Engineering Conference. Nagoya, Japan. 13-17 November 2022.

Xinyuan Wu, X., Borong Sang, B., Baochen Liao, B. & Bram Hoex, B. (2022). Industrial Batch-type Tube ALD Reactor Enables TiO2 and Al-doped TiO2 Deposition on Large-scale Solar. Asia Pacific Solar Research Conference 2022. Newcastle: APVI. 29 Nov. – 1 Dec. 2022

Yamaguchi, M., Dimroth, F., Geisz, J., Ekins-Daukes, N., Nobuaki Kojima, N. & Ohshita, Y. (2022). Overview and Loss Analysis of III-V Single-Junction and Multi-Junction Solar Cells. 8th World Conference on Photovoltaic Energy Conversion. 26 – 30 September 2022. Milan, Italy.

Yang, Z. (2022). Investigating the Impurity Gettering Effect in Polycrystalline-Silicon Based Passivating Contacts. Asia-Pacific Solar Research Conference. Newcastle. 29 November – 1 December 2022.

Yang, Z. (2022). Investigating the Impurity Gettering Effect in Polycrystalline-Silicon Based Passivating Contacts. 8th World Conference on Photovoltaic Energy Conversion (WCPEC). Milan, Italy. 26–30 September 2022.

Yang, Z. Krügener, J., Feldmann, F., Polzin, J.-I., Steinhauser, B., Aleshin, M., Le, T.T., Macdonald, D. & Liu. A.Y. (2022). Impurity gettering by polysilicon/oxide passivating contacts. Asia Pacific Solar Research Conference 2022. Newcastle: APVI. 29 Nov. – 1 Dec. 2022

Yang, Z., Krügener, J., Feldmann, F., Polzin J.-I., Steinhauser, B., Le, T., Macdonald, D. & Liu, A. (2022). (2022). Investigating the Impurity Gettering Effect in Polycrystalline-Silicon Based Passivating Contacts. 8th World Conference on Photovoltaic Energy Conversion. 26 – 30 September 2022. Milan, Italy.

Yang, Z., Krügener, J., Feldmann, F., Polzin, J. I., Steinhauser, B., Le, T. T., MacDonald, D. & Liu, A. (2022). Investigating the impurity gettering rate in polycrystalline-silicon based passivating contacts. 2022 IEEE 49th Photovoltaics Specialists Conference (PVSC), 0369-0369.

Yu, M., Wright, M., Chen, J., Shi, Y., Hallam, B., Hwu E.-T., Murphy, J., Grant, N., Wilshaw, P. & Bonilla, S. (2022). (2022). Towards High Efficiency Inversion Layer Cells Based on Ion-Charged Dielectric. 8th World Conference on Photovoltaic Energy Conversion. 26 – 30 September 2022. Milan, Italy.

Yuan, X., Li, J., Huang, J., Cui, X., Yan, C., Sun, K., Cong, J., He, M., Wang, A., He, G., Mahboubi Soufiani, A., Jiang, J., Zhou, S., Stride, J., Hoex, B., Green, M., Hao, X. (2022). 10.3% Efficient Green Cd-free Cuz2nSnS4 Solar Cells Enabled by Liquid-phase Promoted Grain Growth. 33rd International Photovoltaic Science and Engineering Conference. Nagoya, Japan. 13-17 November 2022.

Zeng, Y., Song, N., Green, M. & Jiang, Y. (2022). Comparative durability study of commercial inner-pore antireflection coatings and alternative dense coatings. 33rd International Photovoltaic Science and Engineering Conference. Nagoya, Japan. 13-17 November 2022.

Zhang, S. M. F., He, G., Yan, C., Sun, K., Hao, X., Perez-Wurfl, I. & Hameiri, Z. (2022). Temperature- and Illumination-Dependent Characterization of Wide Bandgap Sulfide CIGS and CZTS Solar Cells. 2022 IEEE 49th Photovoltaics Specialists Conference (PVSC), 352-352.

Zhang, T. & Chesman, A. (2022). PP2 Perovskites summary. 10th ACAP Conference 2022. Newcastle. 1 – 2 December 2022

Zhang, T., Guo, Q. & Yan, J. (2022). Vacuum-assisted quenching and soft-cover annealing for low bandgap Sn/Pb mixed perovskite solar cell. Asia Pacific Solar Research Conference 2022. Newcastle: APVI. 29 Nov. – 1 Dec. 2022

Zhang, T., Guo, Q. & Yan, J. (2022). Vacuum-assisted quenching and soft-c over annealing for low bangap Sn/Pb mixed perovskite solar cell. 10th ACAP Conference 2022. Newcastle. 1 – 2 December 2022

Zhang, Y., Chang, N., Kim, M., Wang, L., Drury, S., Underwood, R., Woodhouse, M. & Hallam, B. (2022). The Role of Silver Usage in Manufacturing Costs of Silicon Solar Cells. 8th World Conference on Photovoltaic Energy Conversion. 26 – 30 September 2022. Milan, Italy.

Zhang, Y., Wang, L., Chen, R., Chan, C. & Brett Hallam, B. (2022). Low-area Laser-doped Selective Contacting Scheme for Industrial Solar Cells. 8th World Conference on Photovoltaic Energy Conversion. 26 – 30 September 2022. Milan, Italy.

Zhang, Y., Wang, L., Kim, M., Teymouri, A., Chen, R., Chan, C. & Hallam, B. (2022). Low-area Selective Screen-printed Contacts for High-efficiency PERC and TOPCon Solar Cells. 33rd International Photovoltaic Science and Engineering Conference. Nagoya, Japan. 13-17 November 2022.

Zheng, J., Wang, G. & Ho-Baillie, A. (2022). Efficient Monolithic Perovskite/Perovskite/Silicon Triple Junction Tandem Solar Cells. 33rd International Photovoltaic Science and Engineering Conference. Nagoya, Japan. 13-17 November 2022.

Zheng, J., Wang, G., Duan, W., Mahmud, Md.A., Ding, K., Huang, S. & Ho-Baillie, A. (2022). Efficient Monolithic Perovskite/Perovskite/Si Triple-Junction Tandem Solar Cells. Asia Pacific Solar Research Conference 2022. Newcastle: APVI. 29 Nov. – 1 Dec. 2022

Zheng, P., Yang, J., Wang, Z., Chen, J., Jiang, C., Guo, Y., Sun, H., Chen, S., Zhang, X., Jin, H., Phang, S. P., Wang, E.-C., Stuckelberger, J., Sio, H. & Macdonald, D. (2022). Pathways for above 26% efficiency polysilicon contacted solar cells in mass production. 33rd International Photovoltaic Science and Engineering Conference. Nagoya, Japan. 13-17 November 2022.

Zhongshu Yang, Z., Krügener, J., Feldmann, F., Polzin, J.-I., Steinhauser, B., Le, T., Macdonald, D. & Liu, A. (2022). Investigating the Impurity Gettering Effect in Polycrystalline-Silicon Based Passivating Contacts. 8th World Conference on Photovoltaic Energy Conversion. 26 – 30 September 2022. Milan, Italy.

Zhou, Z., Juhl, M. K., Vaqueiro-Contreras, M., Rougieux, F. & Coletti, G. (2022). Deep level transient spectroscopy study of float-zone silicon degradation under light and elevated temperature. SiliconPV 2021, The 11th International Conference on Crystalline Silicon Photovoltaics.

Zhu, Y., Trupke, T. & Hameiri, Z. (2022). Contactless Determination of Emitter Sheet Resistance for Diffused Silicon Wafers. 2022 IEEE 49th Photovoltaics Specialists Conference (PVSC), 0367-0367.

Ziheng Liu, Z., Pengfei Zhang, P., Caixia Li, C. & Xiaojing Hao, X. (2022). Transparent conductive adhesive (TCA) intermediate layers for tandem solar cells. Asia Pacific Solar Research Conference 2022. Newcastle: APVI. 29 Nov. – 1 Dec. 2022

8.6 THESES

Al-Farsi, M.S. 2022. Computational materials discovery: Ab initio modelling of new, high-performance semiconductors for top cells in multi-junction tandems on silicon solar cells. PhD UNSW

Caixia, L. 2022. High-Efficiency Si-Based III-V Tandem Solar Cells. PhD UNSW

He, M. 2021. Cation doping/alloying in kesterite solar cells. PhD UNSW

Hhan, M.U. 2022. The impact of silicon nano-texture morphology on solar cell integration, performance, and degradation. PhD UNSW

Li, C. 2022. High-Efficiency Si-Based III-V Tandem Solar Cells. PhD UNSW

Li, Y. 2021. Material Engineering for High Performance Perovskite Solar Cells. PhD UNSW

McGoldrick, S. 2022. Linking Morphology with Device Performance in Organic Photovoltaics. Honours Thesis, The University of Queensland

Nguyen, M. 2022. Toward Singlet Fission Enhanced Photovoltaic Devices. PhD UNSW

Nie, S. 2022. Advanced Characterisation of Silicon Wafers and Solar Cells under Different Operating Conditions. PhD UNSW

Phua, B. 2022. Plated Metallisation for Silicon Solar Cells: A Deeper Dive into the Importance of Contact Adhesion. PhD UNSW

Poduval, G. 2022. Indium-free transparent conductive oxides for improved solar cell performance and reliability. PhD UNSW

Sang, B. 2022. Transition Metal Oxides as Passivating Contacts for High-Efficiency Solar Cells. PhD, UNSW

Smyth, J. 2022. Charge transport in novel organic semiconducting materials. Honours Thesis, The University of Queensland

Sun, H. 2021. Developing Efficient Cu2ZnSnS4 (CZTS) Thin Film Solar Cells by Heterojunction Engineering. PhD UNSW

Tabari-Saadi, Y. 2022. Fabrication and characterization of AgBiS2 and BiSI light harvesting materials for thin film solar cell application. PhD UNSW

Tebyetekerwa, M. 2022. Photovoltaic Properties of Monolayer 2D Transition Metal Dichalcogenides. PhD ANU

Truong, T. N. 2022. Characterisation and defect engineering of poly-Si passivating contacts in silicon solar cells. PhD ANU

Vicari Stefani, B. 2022. Understanding light-induced degradation in p-type silicon heterojunction solar cells. PhD UNSW

Wang, S. 2022. On Electrical Properties of Black Silicon for Photovoltaic Applications. PhD UNSW

Zhang, Y. 2022. Advanced Characterisation of Black Silicon by Electron Microscopy Techniques. PhD UNSW

Zhou, Z. 2022. The Electronic Properties of Defects in Silicon Solar Cells. PhD UNSW

8.7 REPORTS

Komoto, K., Held, M., Agraffeil, C., Alonso_Garcia, C., Danelli, A., Lee, J.-S., Lyu , F., Bilbao, J., Deng, R., Heath , G., Ravikumar, D. & Sinha, P. (2022). Status of PV Module Recycling in Selected IEA PVPS Task12 Countries. IEA-PVPS Task 12. https://iea-pvps.org/key-topics/status-of-pv-module-recycling-in-selected-iea-pvps-task12-countries/

AUSTRALIAN CENTRE FOR ADVANCED PHOTOVOLTAICS

UNSW SYDNEY NSW 2052 AUSTRALIA

Tel: +61 2 9385 4018
Email: acap@unsw.edu.au
Website: acap.org.au

Director: Scientia Professor Martin Green